An ATM and ATR dependent checkpoint inactivates spindle assembly by targeting CEP63

BY

ELOISE AME SMITH

University College London

**Undertaken at
Clare Hall Laboratories, Cancer Research UK**

October 2009

I, Eloise Ame Smith, confirm that the work presented in this thesis is my own. Where information has been derived from other sources, I confirm that this has been indicated in the thesis.

…………………………………..

Abstract

The effects of ATM and ATR signalling induced by chromosomal breakage have been described extensively in modulating cell cycle progression up to the onset of mitosis. However, DNA damage checkpoint responses in mitotic cells are not well understood. This thesis reports on the effects of double strand breaks on the progression of mitosis.

We found ATM and ATR activation can occur in mitotic *Xenopus laevis* egg extract and the induction of ATM and ATR by chromosomal breakages inhibits spindle assembly in both *Xenopus* egg extract and somatic cells. The delay in mitotic progression induced by ATM and ATR was found not to involve major spindle assembly factors activities such as, Cdk1, Plx1 and RCC1/Ran-GTP. However, normal anastral spindles formation around linear DNA coated beads, which can activate ATM and ATR, linked centrosome-driven spindle assembly to ATM and ATR dependent spindle defects. cDNA expression library screening was undertaken to identify novel ATM and ATR targets in this mitotic checkpoint pathway, through which the novel centrosomal protein XCEP63 was identified as a likely candidate. Data obtained from depletion and reconstitution of XCEP63 in *Xenopus* egg extract established that normal centrosome-driven spindle assembly requires XCEP63. Moreover, ATM and ATR phosphorylates XCEP63 on serine 560 and promotes delocalisation from the centrosome. ATM and ATR inhibition or addition of non-phosphorylable XCEP63 recombinant protein mutated at serine 560 prevents spindle assembly abnormalities. These findings suggest that ATM and ATR regulate mitotic events by targeting XCEP63 and centrosome-dependent spindle assembly. This pathway may provide support for DNA repair processes or regulate cell survival in the presence of mitotic DNA damage.

Table of Contents

List of Figures

List of Tables

Abbreviations

α	Alpha
A	Adenine
A (Ala)	Alanine
APC	Anaphase promoting complex
A-T	Ataxia Telangiectasia
ATM	Ataxia Telangiectasia-mutated
ATP	Adenosine-5'-triphosphate
ATR	ATM- and Rad3-related
ATRIP	ATR interacting partner
β	Beta
Biotin-dATP	Biotin-14-2'-deoxyadenosine-5'-triphosphate
Biotin-dUTP	Biotin-16-2'-deoxyuridine-5'-triphosphate
bp	Base pairs
BSA	Bovine serum albumin
BRAC1	Breast cancer 1
BRCT	Breast cancer C-terminus repeat
Bub	Budding uninhibited by benomyl
C	Cytosine
CAK	Cdk activating kinase
Caprin-1	Cytoplasmic activation/proliferation-associated protein-1
Cdc6	Cell division cycle 6
Cdk	Cyclin dependent kinase
cDNA	Complementary DNA
Cdt1	Cdc10-dependent transcript
Ci	Curie
Cip	Cdk interacting protein
CKI	Cdk inhibitory subunit
CnBr	Cyanogen bromide
cps	Counts per second
CRUK	Cancer Research UK
CSF	Cytostatic factor
° C	Degrees centigrade
da	Dalton
DISC1	Disrupted-In-Schizophrenia 1
DNA	Deoxyribonucleic acid
DNA-PK	DNA-dependent protein kinase
dNTPs	Deoxynucleotide
Drosophilia	*Drosophila melanogaster*
DSB	Double strand break
dsDNA	Double stranded DNA
DTT	Dithio-DL-threitol
E (Glu)	Glutamate
ECL	Enhanced **c**hemi**l**uminescence
E. coli	*Escherichia coli*
EDTA	Ethylenediaminettracetic acid
EGTA	Ethylene glyco-bis (2-aminoethyl ether) N',N',N',N' tetraacetic acid

et al.	et alii (and others)
FANCD2	Fanconi's anemia complex D2
γ	Gamma
γ-tubulin	Gamma tubulin
γ-TuRC	γ-tubulin ring complex
G	Guanine
G0	Gap 0 of the cell cycle
G1	Gap 1 of the cell cycle
G3BP-1	RasGAP SH3 domain binding protein
GDP	guanosine diphosphate
GFP	Green Fluorescent Protein
G.gallus/ Gallus	*Gallus gallus*
GTP	guanosine triphosphate
Gy	Gray
HEPES	N-[2-Hydroxyethyl] piperazine-N'-[2-ethanesulphonic acid
His	Histidine
HR	Homologous recombination
HRP	Horseradish peroxidase
H.Sapiens/ human	*Homo sapiens*
HU	Hydroxyurea
IgG	Immunoglobulin
Ink4	Inhibitors of CDK4
IPTG	Isopropyl-β-D-thiogalactopyranoside
IR	Ionising radiation
IRF-6	Interferon regulatory factor-6
kb	Kilobases
KDa/kD	Kilodaltons
KLH	Keyhole Limpet Haemocyanin
Kip	Kinase inhibitory protein
kpsi	Knots per square inch
L (Leu)	Leucine
LB	L-Broth
LC/MS/MS	Liquid Chromatography/Tandem Mass Spectrometry
LPC	Leupeptin trifluoroacetate salt, Pepstatin A, Chymostatin
μg	Microgram
μl	Microlitre
μM	Micromolar
mA	Milliamp
Mad	Mitosis arrest deficient
Maspin	Mammary serine protease inhibitor
MBP	Maltose binding protein
MCC	Mitotic checkpoint complex
MCM	Mini chromsome maintenance
MDC1	Mediator of DNA damage checkpoint 1
MEM	Modified eagle's medium
mg	Milligram
ml	Millilitre
mM	Millimolar
M phase	Mitosis phase of the cell cycle
MPF	M-Phase promoting factor /maturation-promoting factor /mitosis-

	promoting factor
Mps1	Multipolar spindle-1
Mr	Molecular weight
MRM	Multiple reaction monitoring
MRN	Mre11-Rad50-Nbs1
mRNA	Messenger RNA
MTOC	Microtubule-organising centres
Mus musculus	*M.Musculus*
m/z	Mass to charge ratio
Nbs1	Nijmegen breakage syndrome 1
NCBI	National centre for Biotechnology Information
ng	Nanogram
nM	Nanomolar
nm	Nanometer
NuMA	Nuclear mitotic apparatus protein
OD	Optical density
ORC	Origin recognition complex
ORF	Open reading frame
%	Percentage
P	Phosphorylated/phosphate
PAGE	Polyacrylamide gel electrophoresis
pA/pT	Annealed poly-deoxy-(A)70 and poly-deoxy-(T)70 oligomers
PBS	Phosphate buffer saline
PBST	PBS supplemented with Tween 20
PCNA	Proliferating cell nuclear antigen
PCR	Polymerase chain reaction
pH	Power of hydrogen
PIKK	Phosphatidylinositol 3'-kinase related kinase
PIPES	Piperazine-N,N'-bis [2-ethanesulfonic acid]
Plk/Plx	Polo-like kinase (human/*Xenopus*)
pRb	Retinoblastoma tumour suppressor gene product
Pre-RC	Pre-replication complex
Q (Gln)	Glutamine
Ran	Ras like nuclear protein
RanBP1	Ran-GTP binding protein-1
RanGEF	Ran guanine nucleotide exchange factor
RanGP1	Ran-GTP hydrolysis-activating protein-1
RCC1	Regulator of chromosome condensation-1
rcf	Relative centrifugal force
RFC	Replication factor c
RNA	Ribonuclei acid
RPA	Replication Protein A
Rpm	Revolutions per minute
S (Ser)	Serine
SAC	Spindle assembly checkpoint
S.cerevisiae	*Saccharomyces cerevisiae*
s.d.	Standard deviation
SDS	Sodium dodecyl sulphate
SMC	Structural maintenance of chromatin
S phase	Synthesis phase of the cell cycle

S.Pombe	*Schizosaccharomyces Pombe*
ssDNA	Single stranded DNA
T	Thymine
T (Thr)	Threonines
TAE	Tris/acetate/EDTA
TBS	Tris-buffered saline (Tris/borate/EDTA)
TBS-TX	TBS supplemented with Triton X-100
TCA	Trichloroacetic acid
TE	Tris/EDTA
TEMED	Tetramethylethylenediamine
Thio-dCTP	2'Deoxycytidine-5'-O-(1-Thiotriphosphate)
Thio-dGTP	2'-Deoxyguanosine-5'-O-(Thiotriphosphate)
TnT	Coupled transcription and translation system
topBP1	Topisomerase binding protein 1
Tris	Tris[hydroxymethyl]aminomethane
Tween-20	Polyoxyethylene-sorbitan monolaurate
U	Units of enzyme activity, defined by supplier)
UV	Ultra violet
V	Voltage
v/v	Volume per volume
v/w	Volume per weight
w/v	Weight per volume
Xenopus	*Xenopus laevis*
XGEMC1	Gemmin coiled-coil containing protein
XIRF-6	Interferon regulatory factor-6
XTC	*Xenopus* tissue culture
Y (Tyr)	Tyrosine
9-1-1	Rad9, Rad1 and Hus1
53BP1	P53 binding protein 1

Acknowledgements

I am so appreciative to Vincenzo Costanzo, my supervisor, for his understanding, compassion, patience, support, encouragement and help. Vincenzo has been an absolutely amazing supervisor to me and I could not have wished for better. I am thankful for having had this great opportunity and I am very grateful for my stipend from Cancer Research UK.

I would like to thank Simon Boulton, my second supervisor, and Debbie Barnes, my thesis committee member, for all their constructive comments, support and encouragement. Thank you also to all past and present members of the DNA Damage and Genome Stability Laboratory: Sarah Smith, Alessia Balestrini, Yoshi Hashimoto, Simona Fiorani, Claudia Costentino, Francesco Merolla, Elizabeth Garner, Kristina Trenz, Nicola Brown and Ali Jazayeri for answering all my many questions, and for making the laboratory a brilliant and friendly environment in which to work. I wish to thank Tim Hunt and his laboratory members for all their help, in particular Jane Kirk for the proofreading of this work. Thank you also to Nicola Brown and Rachel Coulthard who also kindly proofread parts of this thesis. Many thanks to Hiro Mahbubani, Laurett Egbuniwe and Jane Kirk for taking care of the frogs and providing me with eggs to work with. So many others at Cancer Research UK supported me, it is impossible to thank each individually. A collective thank you to all those in the research service facilities and my friends at Clare Hall Laboratories.

I am eternally indebted to my father, who has been my rock through extremely tough personal times and helped me to find my way through my Ph.D. research. Not only did he capture my interest in science at a young age, but his support in many forms throughout my studies has helped me immensely.

I am also very grateful to my sister, my mother and good friends Miriam Kirby, Jennie Holloway and Chris Page. They have believed in me, listened to me and put up with me. A medal is deserved by Jon Hilliard: the extent of his patience and understanding in the last year has been endless.

I would like to dedicate this thesis to my Chris Mahon (1978-2006),
my uncle John Stevens (1954-2006) and my grandmother Beryl Stevens (1915-2006),
who are missed deeply.

1   Chapter 1 Introduction

1.1   Cell cycle phases

The cell cycle is an orderly progression through phases in which biochemical processes and cellular events of cell reproduction take place. The process of cell proliferation involves the replication of **d**eoxyribo**n**ucleic **a**cid (DNA) followed by the segregation of synthesized DNA to form two identical daughter cells. The schematic representation shown in figure 1.1 illustrates the cell cycle. The cycle is consists of two main stages: synthesis phase also know as S phase and mitosis, which is also termed M phase. S and M cell cycle phases are separated by gaps, G1 and G2 respectively. The schematic representation of the cell cycle illustrated in figure 1.1 shows the four sequential stages, G1 gap phase follows M phase and G2 gap phase follows S phase in preparation for entry into mitosis. G1, S and G2 cell cycle phases are collectively referred to as interphase. Cells reversibly enter G0 phase when they are non-proliferating, fully differentiated, quiescent or senescent (Planas-Silva and Weinberg, 1997). Cells can remain in this "resting phase" for lengthy periods of time before re-entering G1 phase.
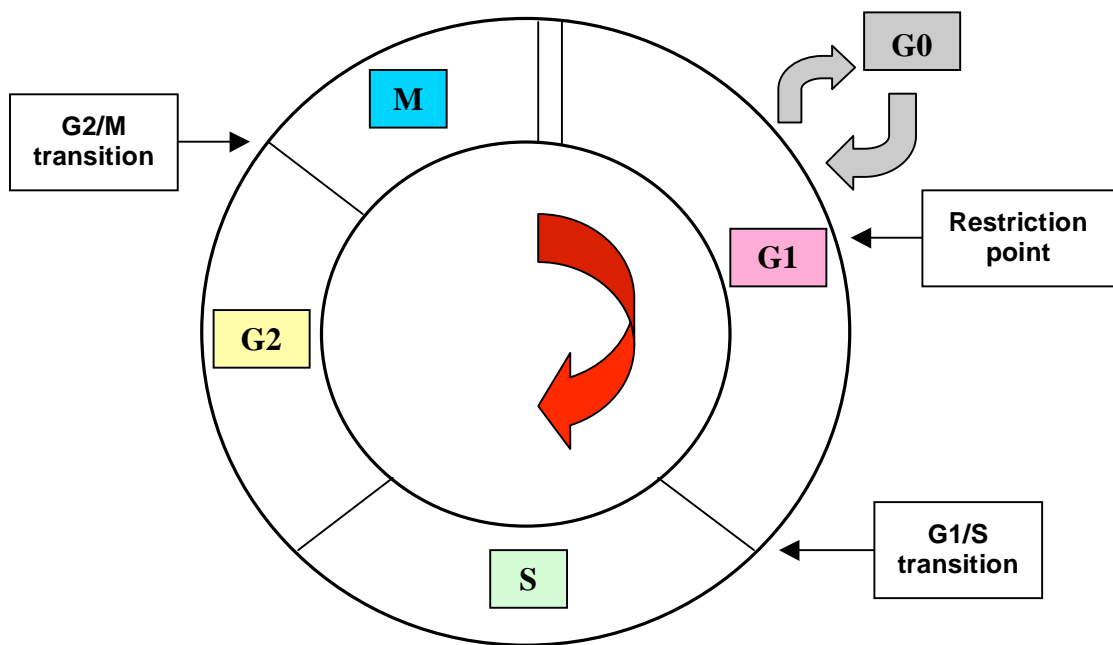
Figure 1.1 Simplified schematic illustration of the vertebrate cell cycle

The cell cycle is an ordered series of events subdivided into phases. The cell cycle begins at G1, following the satisfaction of the G0 restriction point the cell cycle continues into S phase, then G2 and completes at the end of M phase. Relative durations of cell cycle phases are represented in the diagram. The red arrow indicates the direction of cell cycle progression.

The protein family of serine/threonine **Cyclin-d**ependent **k**inases (Cdk) essentially regulate the cell cycle by dictating the timing and order of cellular events. Primarily, Cyclins activate Cdks, which are central to the orchestration of specific cell cycle phases (Morgan, 1997; Murray, 2004). Cdk control of cellular events relies on oscillating Cyclin levels, which are regulated mainly through gene transcription and protein degradation by ubiquitin-dependent proteolysis (King *et al.,* 1996; Peters *et al.,* 2002). **C**d**K a**ctivating **k**inase (CAK) complexes complete Cdk activation by phosphorylating conserved Cdk sites (Nigg, 1996; Morgan, 1997). The activities of Cdks in association with Cyclins are further modulated by interactions with other proteins and phosphorylation modifications. For instance, Cdks can be inactivated or activated by **C**dk **i**nhibitory **s**ubunits (CKIs), which are grouped into protein families Cip/Kip (**C**dk **i**nteracting **p**rotein/ **k**inase **i**nhibitory **p**rotein, factors include p21, p27 and p57) and Ink4 (**in**hibitors of Cdk**4**, factors include p15, p16, p18 and p19) (Sherr and Roberts, 1999). Further influence on substrate reactions corresponds to cellular positioning and activation timing of Cdks (Murray, 2004). Overall, Cdk regulatory mechanisms are fast, persistent and heavily reliant on positive feedback. These Cdk controls ensure the irreversible commitment to cell cycle transitions. The interdependency of Cdk and Cyclin oscillations dictates cellular processes in which the completion of an earlier event is dependent on initiation of the later event. Table one summarizes the cell cycle specific Cdk and Cyclin associations, these will be discussed further in the following cell cycle descriptions.

Cell cycle function	Cdk	Cyclin partner
G1	Cdk4	Cyclin D
G1	Cdk6	Cyclin D
G1/S transition	Cdk2	Cyclin E
S and G2 phase	Cdk1/Cdk2	Cyclin A
M phase	Cdk1	Cyclin B

Table 1 A summary of the Cdk and Cyclin pairing and relative functions in regulating cell cycle phases

The table shows the preferred Cdk-Cyclin associations in the cell cycle. Both Cdck4 and Cdk6 bind Cyclin D and regulate events in G1 phase. Cdk2 paired with Cyclin E initiates entry into S phase from G1 phase. Cdk1 and Cdk2 bind Cyclin A and regulates the progression of S phase into G2 phase. Cdk1 in association with Cyclin B functions in mitosis (Murray, 2004).

1.2   A brief description of cell cycle progression from G1 and S phase

On completion of the previous cell cycle, the resulting daughter cells enter the first phase of a new cycle, G1. Early G1 progression is regulated through the combination of positive and negative extracellular signals. At the G1 'restriction point' cells either commit to the cell division cycle or alternatively cells in the absence of certain growth factor triggers enter a non-proliferate state in G0 phase (Pardee, 1989). Extracellular mitogenic activated signalling pathways activate Cyclin D promoters leading to the rapid synthesis of Cyclin D subunits during G1 phase (Matsushime *et al.,* 1991; Won *et al.,* 1992; Sherr, 1993). Active c-Myc is an example of a Cyclin D promoter binding factor, which has been proven to induce Cyclin D expression and is required for cell cycle progression (Bouchard *et al.,* 1999; Perez-Roger *et al.,* 1999). Positive growth factor signaling is also required in Cyclin D1 mRNA stabilization (Guo *et al.,* 2005). Synthesized Cyclin D subunits associate with and activate both Cdk4 and Cdk6 (Matsushime *et al.,* 1992; Meyerson and Harlow, 1996). Mitogenic signalling pathways have also been demonstrated to mediate Cyclin D assembly with Cdk4/Cdk6 and prevent Cyclin D degradation (Diehl *et al.,* 1997; Matsushime *et al.,* 1994). Cdk4/Cdk6-Cyclin D association is thought to be assisted by CIP/KIP CKI interaction and consequently Cdk4/Cdk6-Cyclin D mediates G1 progression by sequestering CKIs, such as p21 and p27, preventing their inhibition of Cdk2 (Sherr and Roberts, 1999). Cdk4/Cdk6-Cyclin D complexes are also critical for entry into S phase by preventing the anti-proliferate effect of the retinoblastoma tumour suppressor gene product (pRb) (Harbour and Dean, 2000). Cdk4/Cdk6-Cyclin D interacts with, and hyperphosphorylates pRb, which leads to the release of tightly bound transcription factors belonging to the E2F family (Dowdy *et al.,* 1993; Ewen *et al.,* 1996; Meyerson and Harlow, 1996). Inactivation of pRb repression of E2F results in the transcription of Cyclin E, and Cyclin A, as well as E2F itself prior to the G1/S transition stage (Woo and Poon, 2003). At the onset of S phase, Cdk2 (Cdc28 in yeast) is activated by expressed Cyclin E subunits, which then continues the phosphorylation of pRb (Koff *et al.,* 1991; Koff *et al.,* 1992). Accumulating Cyclin A generated from the pRb/E2F positive feedback pathway also activates Cdk2 and induces S phase onset (Girard *et al.,* 1991; Pagano *et al.,* 1992; Ninomiya-Tsuji *et al.,* 1991). In addition, active Cdk2-Cyclin A can inhibit E2F-dependent transcription by phosphorylating E2F (Dynlacht *et al.,* 1994; Krek *et al.,* 1994; Dynlacht *et al.,* 1997).

In the most part, control mechanisms and initiation of DNA replication are conserved from yeast to human. DNA replication firing initiates from DNA chromosomal replication origins loaded with **pre**-**r**eplication **c**omplexes (pre-RC). Pre-RC consist of regulatory factors that are assembled in G1 including the **o**rigin **r**ecognition **c**omplex (ORC), **c**ell **d**ivision **c**ycle 6 (Cdc6), **C**dc10-**d**ependent **t**ranscript (Cdt1) and **m**ini **c**hromosome **m**aintenance (MCM) proteins (Bell and Dutta, 2003; Takeda and Dutta 2005). Cdk2-Cyclin E triggers the recruitment and the assembly of pre-RC components. The induction of pre-RC factors requires Cdk2 and Cdc7 activities (Woo and Poon, 2003). However, it has been shown in *Saccharomyces cerevisiae* (*S. cerevisiae*) that replication initiation requires Cdk activation by Cdc28p catalytic subunit and Cyclin B subunits, Clb5,6p (Schwob and Nasmyth, 1993). In turn, Cdc45 is recruited to the pre-RC, which triggers DNA replication origins. Cdc45 directs DNA helix unwinding and RPA (**r**eplication **p**rotein **A**) association stabilizes the resulting single stranded DNA (Walter and Newport, 2000). At origin sites, polymerase α binds and a bi-directional replication fork is generated, to which other polymerases are then recruited to elongate DNA.

Once DNA replication origins have been fired, the pre-replication complexes are removed and are not reformed until the next round of the cell cycle at G1 phase (Prasanth *et al.,* 2004). Therefore, DNA replication is only permitted in cells that have already undergone mitosis. Such S-M phase interdependency ensures that the cycle events follow in the correct order and DNA is duplicated only once per cell cycle (Rao and Johnson, 1970). An example of one regulatory mechanism preventing re-replication is the phosphorylation of Cdc6 by Cdk2-Cyclin A, which leads to the displacement of Cdc6 from the nucleus to the cytoplasm (Petersen *et al.,* 1999). Once DNA replication is completed cells enter G2 phase, during which time cells continue to accumulate Cyclin A and B subunits (expression also promoted by E2F transcription factor), which prepares the cell for mitosis onset. However, mitotic Cdk-Cyclin complexes are maintained in an inactive state until the onset of mitosis (refer to mitosis section below).

1.2.1 M phase finalises the cell cycle: A focus on the progression and regulation of mitotic events

The last stage of the cell cycle encompasses both mitosis and cytokinesis. Mitosis is the process of segregating duplicate chromosomes into two separate nuclei and cytokinesis is the process of dividing the mother cell into two daughter cells. Mitosis is a series of structural and molecular changes. As shown in figure 1.2, mitotic progression has been subdivided into stages: prophase, prometaphase, metaphase, anaphase and telophase according to cell morphology. Mitosis begins with prophase in which chromosomes become condensed. In prometaphase the nuclear envelope disintegrates, in metaphase chromatids are first aligned along the methapse plate and then segregated in anaphase. Mitosis ends with telophase in which nuclear envelope re-forms around the separated daughter nuclei. The correct progression of mitotic events ensures the proficient execution of cell division and ultimately the integrity of the genome. For instance, the mis-segregation of sister chromatids can lead to an incorrect number of chromosomes in a cell (aneuploidy) (Chi and Jeang, 2007). Cancer cells often display aneuploidy, a phenotype that is considered both to drive and to result from Tumourigenesis.

Prophase:

- **Nuclear envelope breakdown**
- **Chromosome condensation**
- **Centrosome separation**
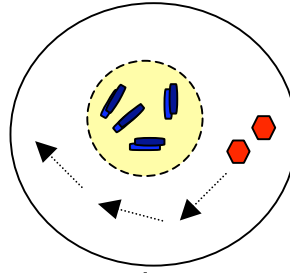
Prometaphase:

- **Chromosome capture**
- **Chromosome congression**
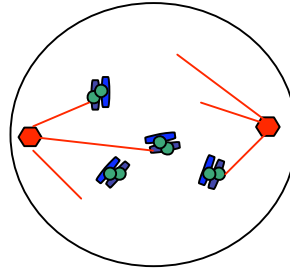
Metaphase:

- **Chromosome alignment along the metaphase plate**
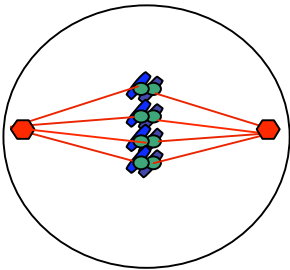
Anaphase:

- **Sister chromatid separation**
- **Spindle pole separation**

Telophase:

- **Nuclear envelope re-forms**

Legend:
- Centrosome
- Sister Chromatid
- Kinetochore
- Microtubule (spindle)
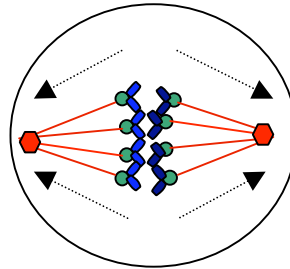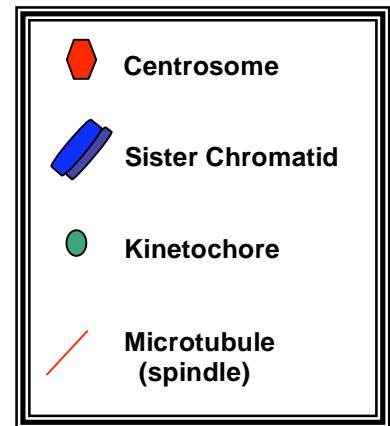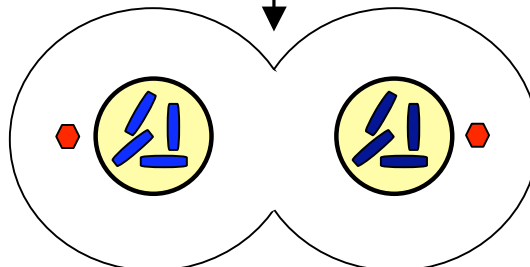
Figure 1.2 The stages of mitosis

During prophase chromosomes condense, the nuclear envelope breaks down and centrosomes separate to opposite sides of the cell. At prometaphase, kinetochores capture microtubules connecting chromosomes to the spindle. At metaphase, chromosomes are bi-orientated and have congressed to the metaphase plate in the centre of the spindle. During anaphase, sister chromatids are separated and are segregated towards opposite poles, which are moving further apart. At telophase, nuclear envelope re-forms around separated sets of chromosomes. Adapted from Gadde and Heald, 2004 (Gadde and Heald, 2004).

The accurate separation of chromosomes is dependent on the correct assembly and functioning of bipolar spindles (Gadde and Heald, 2004). Centrosomes are described as **m**icro**t**ubule-**o**rganising **c**entres (MTOC), acting as dominant sites in spindle assembly (by regulating the formation of spindle poles, which orientates the mitotic bipolar spindle) (Schatten, 2008). Centrosomes are small cytoplasmic organelles made up of a pair of perpendicular centrioles embedded in pericentriolar material. The pericentriolar material within centrosomes is a scaffolding lattice made up numerous coiled-coiled proteins and includes the ring complex around centrioles consisting of 13 γ-tubulin molecules (**γ-tu**bulin **r**ing **c**omplexes, γ-TuRC) (Zheng *et al.,* 1995; Anderson *et al.,* 2003). Further pericentriolar factors are recruited to centrosomes in preparation for mitotic spindle assembly (centrosome maturation). Many of the centrosomal core proteins, in addition to γ-tubulin, have been shown to function in spindle formation, which includes pericentrin and ninein with roles in microtubule organisation and anchoring respectively (Doxsey *et al.,* 1994; Mogensen *et al.,* 2000). Whereas, other non-centrosomal proteins involved in spindle assembly associate only temporary to centrosomes during mitosis, such as **Nu**clear **M**itotic **A**pparatus protein (NuMA), which has multiple functions in spindle assembly including cross-linking microtubules (bundling) into the correct organization (Sun and Schatten, 2006). Particularly noteworthy is the presence of Cdk1–Cyclin B, Plk1 (**P**olo-**l**ike **k**inase-**1**) and Aurora A mitotic cell cycle regulatory proteins within mitotic centrosomes (Jackman *et al.,* 2003; Golsteyn *et al.,* 1995; Tsvetkov *et al.,* 2003; Barr and Gergely 2007). These centrosomal factors play important roles in spindle formation.

It has been well documented that abnormal centrosomes structure and number leads to aberrant spindle formation that can lead to genetic instability. Within normal cells, tight control mechanisms across the cell cycle ensure the correct duplication of centrosomes. The centrosome cycle itself also has control over cell cycle progression (Hinchcliffe and Sluder, 2001; Rieder *et al.,* 2001; Stearns, 2001). During S phase, centrosome duplication takes place and at the onset of mitosis centrosomes separate forming two centrosomes, containing one mother and one daughter centriole (Crasta and Surana, 2006). However, the process of segregating centrosomes to opposite ends of the polarized cell is not well understood.

After the separation of centrosomes, nuclear envelope breakdown and chromosome

condensation, microtubule spindles begin to form in prometaphase. Within centrosomes, the γ-TuRC nucleates microtubules promoting polymerisation of α and β tubulin subunits; the formed microtubule prolifaments are then bundled together into the tubular microtubule fibre (Zheng *et al.,* 1995; Moritz *et al.,* 2000; Job *et al.,* 2003; Desai and Mitchison, 1997; Nogales, 2000). Microtubule fibres are polar, the negative ends reside at centrosomes and the positive ends project outwards. In association with microtubules are a vast number of proteins, which are thought to facilitate microtubule regulation. Microtubules constantly shrink (depolymerise) and grow (polymerise). Such microtubule dynamics provide the continuous movement of microtubules towards the pole known as "Microtubule flux" (Mitchison, 1989). In addition, motor proteins associated with microtubules, which include minus-end directed dynein and negative and positive-end directed kinesins, drive microtubule movements by utilizing ATP hydrolysis. The functions of microtubule associated motor proteins are massively diverse, these include the promotion spindle bi-polarity (Heald and Walczak, 1999; Gadde and Heald, 2004). Further spindle bi-polarity arises from overlapping antiparallel microtubule fibres derived from the cytoplasm and the interaction of centrosomal aster microtubules with the cell cortex (Tulu *et al.,* 2003; Gadde and Heald, 2004).

In prometaphase, kinetochores, a protein structure formed at the centromere of each sister chromatid, 'capture' and interact with microtubules projecting from centrosomes (search and capture model) (Rieder and Salmon, 1998; Hayden *et al.,* 1990; Tanaka *et al.,* 2005; Tanaka *et al.,* 2008). Kinetochores are then moved along the length of the attached microtubules toward the spindle pole promoted by kinetochore associated minus-end motor proteins (dynein in metazoans and kinesin-14 in budding yeast) (Rieder and Alexander, 1990; Yang *et al.,* 2007b; King *et al.,* 2000; Tanaka *et al.,* 2007). Finally, chromosome bi-orientation is achieved when kinetochores on both sister chromatids are attached to microtubules originating from opposite spindle poles. At this point, kinetochores are attached to the positive ends of microtubules and chromosome movement is thought it be coupled directly with microtubule dynamics. The turnover of kinetochore-microtubule interactions promoted by Aurora B has been proposed as a mechanism to ensure chromosome bi-orientation (Tanaka *et al.,* 2002; Hauf *et al.,* 2003; Dewar *et al.,* 2004; Lampson *et al.,* 2004). It is generally thought that only when bi-orientation is achieved, the process that is referred to as chromosome congression takes place, in which chromosomes are directed towards the central metaphase plate (Rieder and Salmon, 1994). Although, it has been shown in metazoans that kinetochore

localized CENP-E (kinesin) can transport mono-orientated chromosomes away from spindle poles along microtubules with already bi-orientated/congressed chromosomes (Kapoor *et al.,* 2006).

Metaphase is the stage where kinetochores are all attached to microtubules and chromosomes are centrally aligned along the metaphase plate. Anaphase onset is not only dependent on spindle assembly checkpoint inactivation, but also on reliant on the completion of DNA decatenation (disentanglement of chromomsomes), which is performed predominantly by Topisomerase II (Nasmyth *et al.,* 2002; Damelin and Bestor, 2007; Nitiss, 2009). At this stage, cohesin connecting the two sister chromatids is cleaved. Following which, the combined mechanisms of microtubule shortening by depolymerisation at kinetochores and utilisation of "microtubule flux" are thought to separate chromatids towards opposite spindle poles in anaphase (Nasmyth, 2002; Maddox *et al.,* 2002). In late anaphase, both positive and negative end-directed motors proteins are proposed to force the centrosomes further apart by pulling and pushing non-spindle microtubules. Following the separation of sister chromatids, a nuclear envelope re-assembles around each set of segregated chromatin (telophase). The cell cycle is terminated after the evolutionally conserved process of cytokinesis, which comprises the following major events (Guertin *et al.,* 2002; Barr and Gruneberg, 2007). Cytokinesis begins with the formation of a contractile ring, which provokes the growth of the cleavage furrow assembled from recruited membrane proteins. On the completion of cleavage furrow formation the contractile ring disintegrates. Finally, the cleavage of the plasma membrane (abscission) at the adjoining midbody structure separates the two daughter cells.

Mitotic entry, progression and exit are controlled by complex mechanisms. The mitotic entry mechanism consists of interconnected positive feedback mechanisms, shown in figure 1.3. Mitotic entry is dependent on activation of **Cyclin**-**d**ependent **k**inase **1** (Cdk1, also alternatively named Cdc2), in association with Cyclin B (Nurse, 1990). Cdk1-Cyclin B complex is also known as **M**-phase **p**romoting **f**actor (MPF). During G2, Cyclin B accumulates leading to the assembly of Cdk1-Cyclin B complex (Murray and Kirchner, 1989). At this time, Cdk1-Cyclin B is maintained in an inactive state by inhibitory phosphorylation additions by Wee1 and Myt1 (Dunphy, 1994; Parker and Piwnica-Worms, 1992; Liu *et al.,* 1997; Mueller *et al.,* 1995). Towards the end of G2 phase, Cdk1 in association with Cyclin B is activated following Cdc25 phosphatase

dependent removal of these inhibitory phosphorylations (Lee *et al.,* 1992). The elimination of Cdk1 phosphorylation modifications at threonine (Thr) 14 and tyrosine (Tyr) 15 enables CAK complex to phosphorylate Cdk1 at Thr161 (Fesquet *et al.,* 1993; Poon *et al.,* 1993; Solomon *et al.,* 1993; Fisher and Morgan, 1994). In the G2/M transition, Cdk1-Cyclin B essentially promotes its own activation. Induced Cdk1-Cyclin B activates Cdc25, which in turn promotes Cdc25 dephosphorylation of Cdk1 at Thr14 and Tyr15. Consequently, this Cdk1-Cyclin B/Cdc25 positive feedback loop leads to the rapid rise in active Cdk1-Cyclin B levels (Hoffmann *et al.,* 1993). This mechanism promotes the full activation of Cdk1-Cyclin B, which is required in order to enter mitosis (Izumi and Maller, 1993). In *Xenopus*, active Plx1 has been shown to participate in the Cdk1-Cyclin B amplification loop by activating Cdc25 (Kumagai and Dunphy, 1996). At the onset of mitosis, Cdk1-Cyclin B activates Plk1, which suggests Cdk1 and Plk1 mutually sustain one another through the Cdk1-Cyclin B/Cdc25 positive feedback amplification loop (Abrieu *et al.,* 1998; Qian *et al.,* 1998). In addition, both active Cdk1 and Plk1 kinases have been shown to promote Wee1 degradation, thus depleting Cdk1 inhibitory phosphorylation at Thr14 (Watanabe *et al.,* 2004).
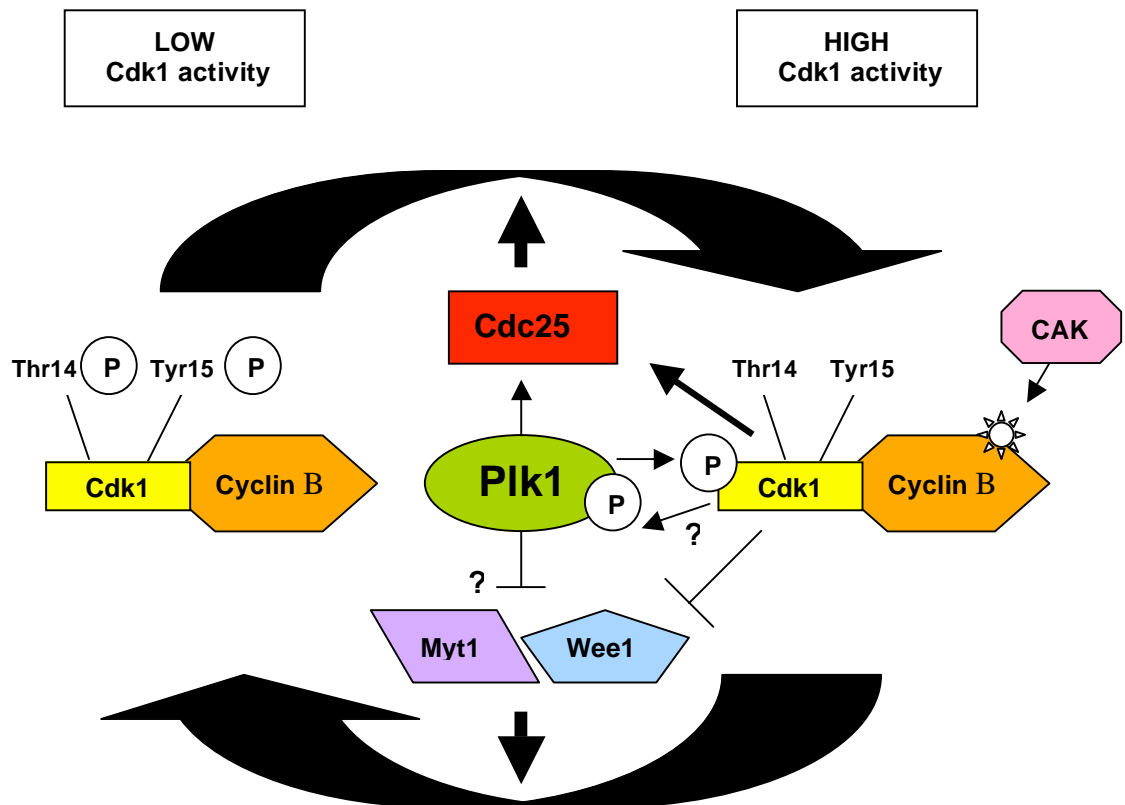
Figure 1.3 Cdk1 activation pathway

Cdk1 in association with Cyclin B is maintained in an inactivated state by Wee1 and Myt1 inhibitory phosphorylations at Thr14 and Thr15. Activated Cdc25 phosphatase then removes Cdk1 inhibitory phosphorylations, following which, CAK complex activates Cdk1-Cyclin B. Activation of Cdk1(-Cyclin B) initiates a positive feedback amplification loop by phosphorylating Cdc25. Active Cdk1 activates Plk1, which leads to further activation of Cdc25. In this mechanism of Cdk1 activation, it is thought that both active Plk1 and Cdk1 prevent Wee1 and Myt1 inhibitory phosphorylations on Cdk1. Adapted from Barr *et al.,* 2004 and van Vugt and Medema, 2005 (Barr *et al.,* 2004; van Vugt and Medema, 2005).

Mitosis onset is signified by active Cdk1-Cyclin B translocation from the cytoplasm to the nucleus, which is regulated by a phosphorylation event on Cyclin B (Li *et al.,* 1997; Hagting *et al.,* 1999). It is postulated that nuclear translocation is mediated by Plk1 phosphorylation of Cyclin B (Toyoshima-Morimoto *et al.,* 2001; Yuan *et al.,* 2002). Nuclear Cdk1-Cyclin B activities aid chromosome condensation and nuclear envelope breakdown, required for mitosis progression. Centrosomal Cdk1-Cyclin B activation has a role in the process of centrosome separation (Blangy *et al.,* 1997; Crasta *et al.,* 2006; Jackman *et al.,* 2003; Lindqvist *et al.,* 2005). Interestingly, Kramer *et al.,* determined that Cdk1 is prevented from premature activation by Chk1 at centrosomes (Kramer *et al.,* 2004). The increasingly popular hypothesis is that controlled activation of Cdk1-Cyclin B at centrosomes ensures the timely initiation of cytoplasmic Cdk1-Cyclin B activation and therefore mitosis onset.

From the G2/M transition both Plk1 and Cdk1-Cyclin B kinase activity escalates during mitosis (Golsteyn *et al.,* 1995). As well as mitotic entry, active centrosomal Plk1 also functions in the formation of spindle arrays (van Vugt and Medema, 2005; Golsteyn *et al.,* 1995). Early *Drosophila melanogaster (Drosophilia)* polo-like kinase (gene product *polo*) mutation studies showed embryos with irregular spindle formation resulting from aberrant centrosomes (Sunkel and Glover, 1988). Investigations into human Plk1 have described Plk1 functions in centrosome maturation and separation in late G2/early prophase, which is required for normal spindle formation (Lane and Nigg, 1996; van Vugt *et al.,* 2004b). Importantly, Plk1 role in centrosome maturation includes the recruitment of additional γ-tubulin to centrosomes (Lane and Nigg, 1996; Feng *et al.,* 1999). Further studies have shown that Plk1 regulates many factors involved in microtubule nucleation and microtubule stabilization (Casenghi *et al.,* 2003; Budde *et al.,* 2001; do Carmo Avides *et al.,* 2001; Yarm, 2002). Plk1 is important in normal mitotic progression as shown by the interference of Plk1 function, which leads to abnormal spindle formation and mitotic arrest (refer to section 1.4.1 on the spindle assembly checkpoint) (Lane and Nigg, 1996; van Vugt *et al.,* 2004b; Seong *et al.,* 2002). However, the understanding of how mitotic progression is driven by rising Cdk1-Cyclin B activity is limited. Several studies have indicated that Cdk1-Cyclin B regulates microtubule dynamics (Verde *et al.,* 1990; Fourest-Lieuvin *et al.,* 2006). It is proposed that the gradual increase in Cdk1-Cyclin B activity prepares the cell to exit mitosis and the absence of high Cdk1-Cyclin B activity levels are thought to cause a

delay in mitosis (Lindqvist *et al.,* 2007).

Ran, (Ras-like nuclear protein) a small GTPase, also functions in spindle assembly and regulating mitotic progression (Ciriarello *et al.,* 2007). Ran associated GTP (**g**uanosine **trip**hosphate) molecules are hydrolysed to GDP (**g**uanosine **dip**hosphate) by RanGP1 (**Ran**-**G**TP hydrolysis-activating **p**rotein-**1**) (Bischoff *et al.,* 1994). Ran bound GDP is replaced with GTP by RanGEF (**Ran g**uanine nucleotide **e**xchange **f**actor), RCC1 (**r**egulator of **c**hromosome **c**ondensation-**1**) (Bischoff and Ponstingl, 1991a; Bischoff and Ponstingl, 1991b). RanBP1 (**Ran**-GTP **b**inding **p**rotein-**1**) prevents GTP dissociation from Ran and regulates Ran-GTP/GDP turnover (Bischoff *et al.,* 1995). Ran-GTP is thought to competitively bind to importin α and β, which in turn leads to an increase in unbound aster/spindle promoting factors, TPX2 and NuMA respectively (Gruss *et al.,* 2001; Wiese *et al.,* 2001). Research has determined that a Ran-GTP/GDP concentration gradient exists, which is proposed to drive chromatin induced spindle assembly (Carazo-Salas *et al.,* 1999; Kalab *et al.,* 2002). Chromatin bound RCC1 concentrates Ran-GTP in the proximity of chromatin, the amount of Ran-GTP lessens with distance away from chromatin. It is thought that this Ran-GTP gradient restricts the initiation of aster assembly around the chromosomes and hence helps positioning of asters (Hetzer *et al.,* 2002; Quimby and Dasso, 2003). However, Ran-GTP is also required in centrosome-driven spindle assembly and functions in microtubule stabilization and dynamics (Carazo-Salas *et al.,* 2001). Mitotic progression and exit has been proposed to rely on mechanisms directed by Ran, including the regulation of spindle assembly checkpoint factor localization at kinetochores, sister chromatid separation and nuclear envelope re-formation (Ciriarello *et al.,* 2007).

The E3 type ubiquitin ligase, **A**naphase-**P**romoting-**C**omplex or cyclosome (APC/C), plays a fundamental role in driving mitotic progression, exit and cytokinesis (van Leuken *et al.,* 2008). Active APC adds poly-ubiquitin chains on targets, these are recognised by proteasomes leading to rapid proteolysis of mitotic factors (Peters, 2006; King *et al.,* 1996). From prometaphase until the end of metaphase, APC activity is induced by associated co-factor Cdc20 (Fizzy) and from anaphase onwards APC is activated by associated co-factor Cdh1 (Visintin *et al.,* 1997; Fang *et al.,* 1998; Kramer *et al.,* 1998). Association of Cdc20 or Cdh1 alters APC substrate specificity, the switch involves the dephosphorylation of Cdh1 and APC/Cdh1 targeting of Cdc20, which in turn inactivates APC/Cdc20 (Peters, 2002). Furthermore, APC activity is enhanced by a number of phosphorylation events, Cdk1-Cyclin B phosphorylations are established to

be most important, whereas Plk1 phosphorylations are of secondary importance (Golan *et al.,* 2002; Kraft *et al.,* 2003). Active APC/Cdc20 operates in the process of separating sister chromatids (Nasmyth, 2002). APC ubiquitylates securin and the resulting degradation of securin releases the associated protease, separase (Peters, 2006). Separase cleaves cohesin, which breaks the link between sister chromatids (Uhlmann *et al.,* 1999; Hauf *et al.,* 2001). Plk1 is also thought to play a role in priming sister chromatids for separase cleavage by phosphorylating the SCC1 cohensin subunit after spindle assembly checkpoint inactivation (van Gugt and Medema, 2005). During metaphase APC/Cdc20 also ubiquitylates Cyclin B, the following destruction of Cyclin B inactivates Cdk1 (Glotzer *et al.,* 1991; Sudakin *et al.,* 1995; Peters, 2006). Phosphatases dephosphorylate many Cdk1 targets, these factors then participate in processes such as chromosomes segregation, spindle disassembly and nuclear envelope re-formation (Sullivan and Morgan, 2007). In addition, preparation for the next cell cycle, such as for the re-loading of Pre-RC on DNA replication origins requires low Cdk1 activity (Prasanth *et al.,* 2004; Noton and Diffley, 2000; King *et al.,* 1996). In late anaphase, Plk1 localized to the centre of the spindle array phosphorylates a number of substrates, which function in cytokinesis (Golsteyn *et al.,* 1995; van Yugt and Medema, 2005). Active APC/Cdh1 during anaphase promotes Plk1 degradation, which mediates cytokinesis execution (Lindon and Pines, 2004). Mitotic progression is reliant on secruin and Cyclin B destruction, however, activation of APC by Cdc20 or Cdh1 targets different mitotic factors in a timely and orderly fashion, which contributes to the progression of mitotic exit (Sullivan and Morgan, 2007; Pines, 2006). The order of APC directed substrate degradation is illustrated in figure 1.4. Firstly, APC/Cdc20 targets Cyclin A in prometaphase, Cyclin A destruction is thought to be a required step in the onset of anaphase (Geley *et al.,* 2001; Sigrist *et al.,* 1995; den Elzen and Pines, 2001). However, it still remains unclear how APC/Cdc20 targets Cyclin A as the active spindle assembly checkpoint blocks APC. The last APC/Cdh1 target is Aurora B at the anaphase to telophase transition, which continues into G1 of the next cell cycle (Lindon and Pines, 2004). It has been proposed that ubiquitylated Aurora B, which promotes chromosome decondensation and nuclear envelope re-assembly, is displaced from kinetochores (Ramadan *et al.,* 2007). APC/Cdh1 remains active during G1 phase, and then downregulated in S phase by an autonomous mechanism, which is thought not only to mediate the accumulation of mitotic Cyclins A and B, but also factors required for DNA replication (Petersen *et al.,* 2000; Araki *et al.,* 2003; Rape and Kirschner, 2004).
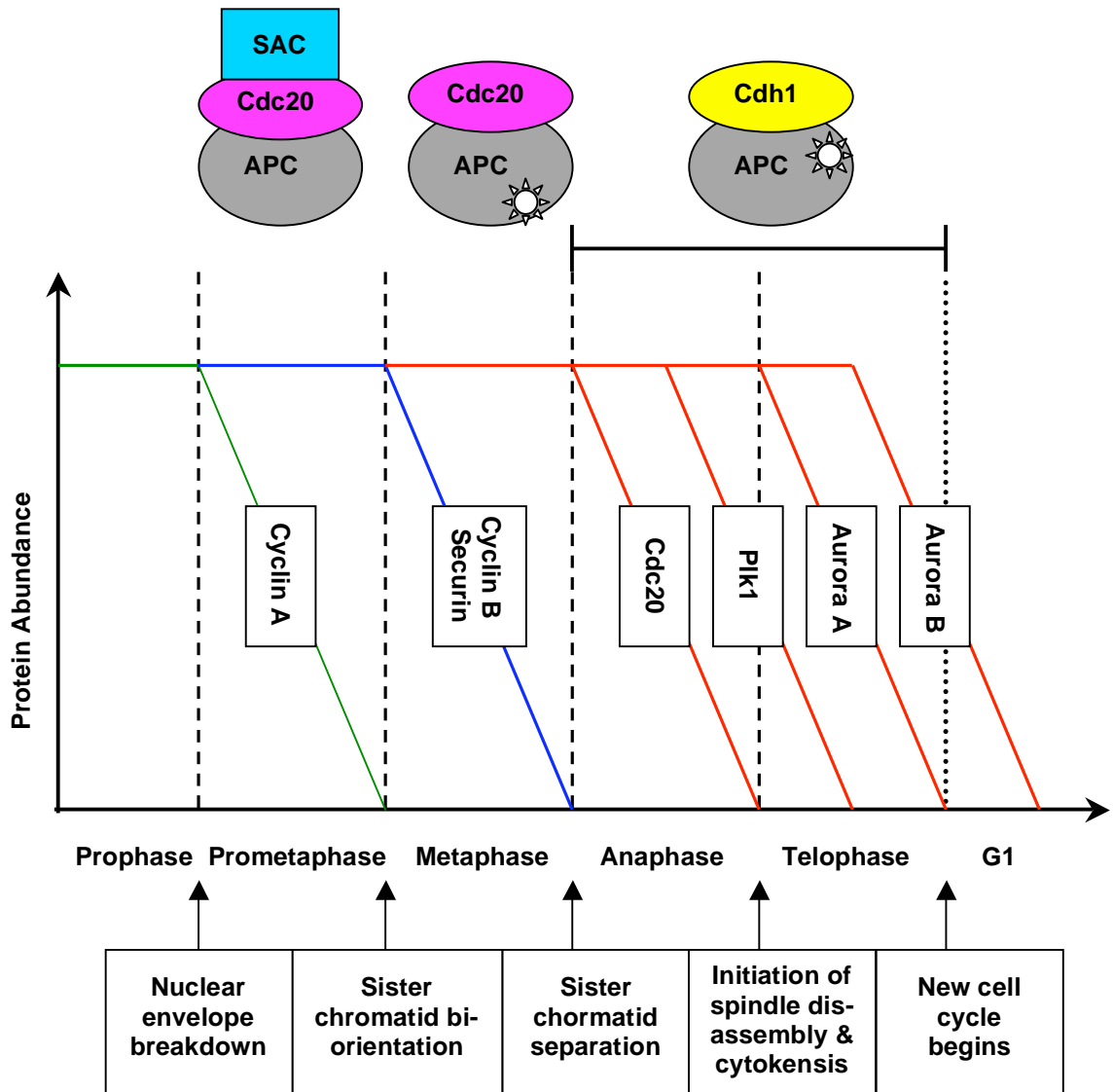
Figure 1.4 APC directed destruction in mitosis

The order in which APC targets mitotic proteins for degradation is shown. APC/Cdc20 during prometaphase directs Cyclin A proteolyisis, which is not subject to spindle assembly checkpoint (SAC) inhibition. Once sister chromatids are bi-orientated (metaphase), the SAC is satisfied and APC/Cdc20 is activated. During metaphase APC/Cdc20 activity promotes securin and Cyclin B destruction. Following chromatid separation and Cdk1 inactivation, APC association switches to Cdh1. APC/Cdh1 directs the orderly destruction of Cdc20, Plk1, Aurora A and Aurora B providing the mechanism to exit mitosis and re-entry into the next cell cycle. The dashed lines signify the stage transitions. Adapted from Sullivan and Morgan, 2007 (Sullivan and Morgan, 2007).

1.3 Signalling networks in response to DNA damage

Genomic DNA damage can occur through a variety of sources, including intercellular metabolic by-products, incomplete replication, or exposure to radiation and chemicals. DNA damage is detected and mechanisms are activated that maintain genomic stability and preserve the genetic material transferred into progeny cells. Failures or defects in DNA damage signalling pathways may lead to genetic instabilities that are frequently found in cancer cells (Lengauer *et al.,* 1998). As summarised in figure 1.5, DNA damage signalling pathways have been traditionally organised into the following classifications; sensors, mediators (adaptors), transducers and effectors (Niida and Nakanishi, 2006). DNA damage response pathways provoke downstream effectors that regulate specific cellular endpoints, cell cycle arrest, DNA repair and apoptotic cell death (Zhou and Elledge, 2000). The signalling pathways that regulate cell cycle progression are termed 'checkpoint responses'. Checkpoints are vital in supporting DNA repair processes and initiating apoptosis when DNA damage is extensive and irreparable. Checkpoints will be discussed in more detail in section 1.4.
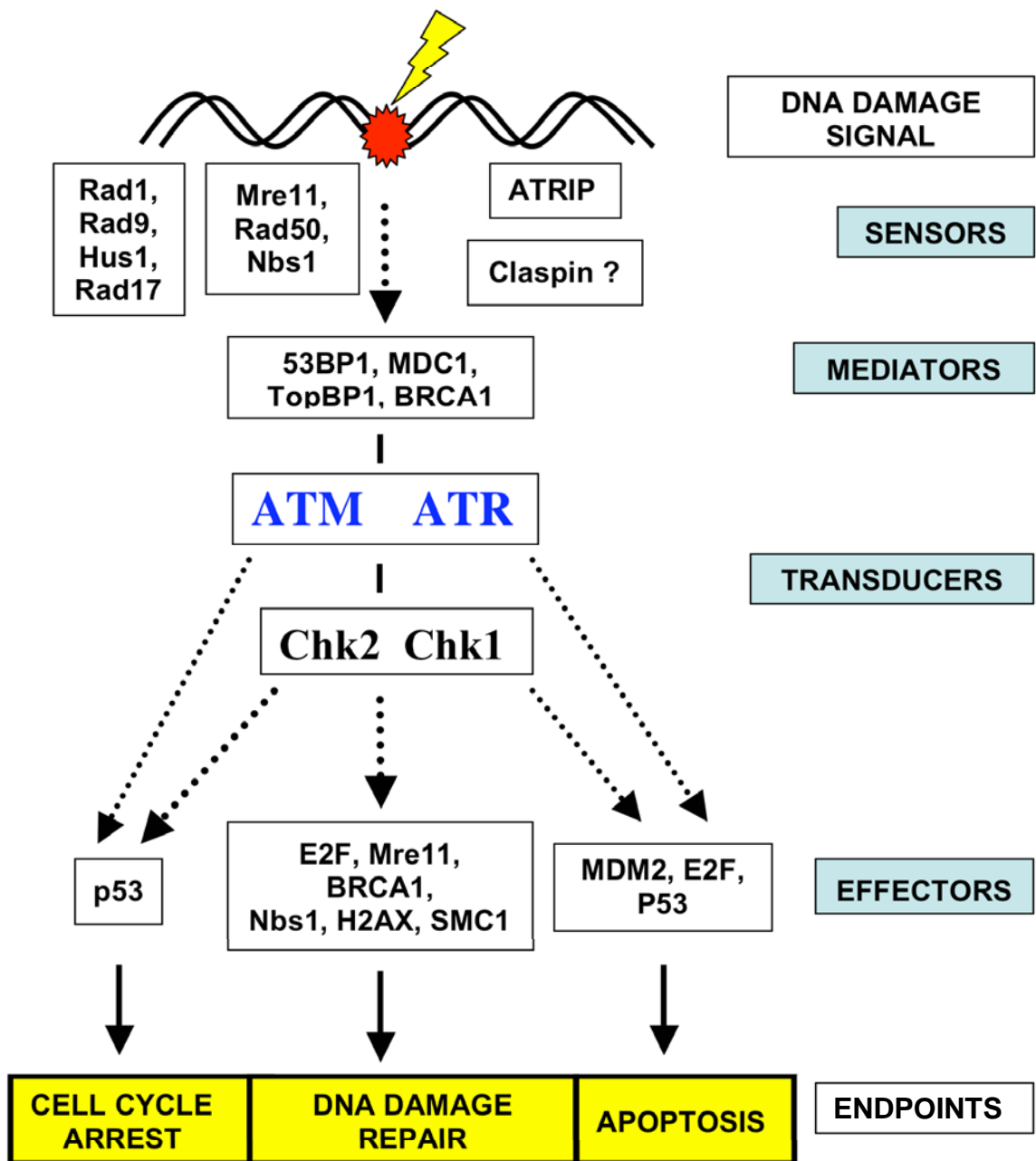
Figure 1.5 Schematic representation of vertebrate DNA damage induced signalling networks

The DNA damage response pathway is organised into sensors, mediators, transducers and effectors. Sensor proteins recognise DNA damage, which then activate transducers ATM and ATR and downstream checkpoint response kinases, Chk1 and Chk2. Mediator proteins facilitate transducer activation. Once transducers are active they target downstream effector substrates, which lead to the cellular endpoints: Cell cycle arrest, DNA damage repair and apoptosis. Adapted from Niida and Nakanishi, 2006 and Zhou and Elledge, 2000 (Niida and Nakanishi, 2006; Zhou and Elledge, 2000).

Signalling cascades are orchestrated through DNA damage recognition by DNA surveillance sensory proteins. The recruitment of sensor complex 9-1-1 (consisting of Rad**9**, Rad**1** and Hus**1**) to **s**ingle **s**trand DNA (ssDNA) damage is mediated by Rad17 (associated with **r**eplication **f**actor **c** (RFC) subunits) (Jones *et al.,* 2003). Whereas, at the sites of **d**ouble **s**trand **b**reaks (DSB) the DNA damage sensor complex, MRN (**M**re11-**R**ad50-**N**bs1) assembles (van den Bosch *et al.,* 2003; Petrini and Stracker, 2003). In addition, there is evidence that supports ATRIP (**ATR i**nteracting **p**artner) being a DNA damage sensory protein, which specifically recognises RPA coated ssDNA independently of Rad17 and 9-1-1 complexes (Zou and Elledge, 2000; Cortez *et al.,* 2001). Another proposed sensory protein is Claspin (although it shows mediator properties), which is also found to associate with ssDNA created by stalled replication forks independently of RPA and Rad17 (Kumagai and Dunphy, 2000; Lee *et al.,* 2003).

Sensor protein accumulation at sites of DNA damage leads to signalling to downstream transducer proteins. Mediator proteins facilitate the initiation of transducer activities. A number of mediator proteins in human cells can be distinguished by consensus **br**east **ca**ncer **1** (BRCA1) C-terminus repeat (BRCT) protein-protein interaction domain (Bork *et al.,* 1997; Niida and Nakanishi, 2006). Examples of mediator proteins include: p**53 b**inding **p**rotein **1** (53BP1) **m**ediator of **D**NA **d**amage **c**heckpoint **1** (MDC1) and **Top**isomerase **b**inding **p**rotein **1** (TopBP1) (Schultz *et al.,* 2000; Wang *et al.,* 2002; Stewart *et al.,* 2003; Yamane *et al.,* 2002). BRCA1, H2AX and **s**tructural **m**aintenance of **c**hromatin **1** (SMC1) have important roles in DNA damage repair or chromosome segregation, but they also function in activating transducers (Sancar *et al.,* 2004; Niida and Nakanishi, 2006).

Within DNA damage response networks there are two main conserved protein kinase transducers, **A**taxia-**T**elangiectassia-**m**utated (ATM) and **AT**M and **R**ad3- related (ATR). These conserved protein kinases will be described in more detail in section 1.3.1. **DNA**-dependent **p**rotein **k**inase (DNA-PK) is also a transducer kinase that responds less stringently to the presence of DSB DNA damage and is thought to be involved in early response signalling that, in turn, orchestrates DNA damage repair and cell cycle arrests (Lee and Kim, 2002; Gottlieb and Jackson, 1993). Active ATM and ATR trigger downstream effector kinases Chk2 and Chk1 respectively, which are essential to DNA damage checkpoint responses (Chaturvedi *et al.,* 1999; Rhind and Russel, 2000; Capasso *et al.,* 2002). Furthermore, ATM/ATR transducer kinases

phosphorylate a vast number of effector proteins, which provoke the DNA damage cellular endpoints. Some of the extensively investigated key ATR/ATM targets include p53, BRCA1 and Nbs1 (**N**ijmegen **b**reakage **s**yndrome **1**) (Banin *et al.,* 1998; Tibbetts *et al.,* 1999; Cortez *et al.,* 1999; Tibbetts *et al.,* 2000; Lim *et al.,* 2000). There is growing evidence to suggest that DNA damage response pathways are extremely complex and are not constrained to this linear organisation. Instead, it is proposed that spatial and temporal restrictions order DNA damage signal transductions (Lukas *et al.,* 2004; Bekker-Jensen *et al.,* 2006). However, it is clear within these extensively branched complex DNA damage response signalling networks that key roles are played by ATM and ATR, which are conserved from yeast to humans.

1.3.1   ATM and ATR are key regulators of DNA damage response networks

ATM and ATR are well-documented signalling regulators of DNA damage response networks that are fundamental to checkpoint control of the cell cycle (Shiloh, 2003; Abraham, 2001; Cimprich and Cortez, 2008). ATM (350 KDa) and ATR (303 KDa) both belong to the Phosphatidylinositol 3'-kinase (PI3K) related kinase (PIKK) family of proteins (Savitsky *et al.,* 1995; Cimprich *et al.,* 1996). Similarly, ATM and ATR associate with DNA and preferentially phosphorylate target substrates on serine/threonine-glutamine (S/T-Q) consensuses motifs (Abraham, 2001; Kim *et al.,* 1999; Matsuoka *et al.,* 2007). In the literature ATM and ATR have been separated by their response to different types of DNA damage lesion and by the difference between in protein related disease states.

1.3.1.1   ATM activation in response to double strand break DNA damage

Primarily, ATM reacts to DSBs resulting from exposure to **I**onising **R**adiation (IR) or chemotoxic agents, such as etoposide, camptothecin or doxorubicin (Canman *et al.,* 1998; Banin *et al.,* 1998; Shiloh, 2003). The presence of a DSB causes distal chromatin structure alterations that activate ATM by means that are not completely understood. ATM exists under normal circumstances as a homodimer, in a confirmation that obscures the kinase domain. ATM activation causes a conformational change that leads to autophosphorylation of serine 1,981 and dissociation of the dimer (Bakkenist and Kastan, 2003). Phosphorylation of Histone H2X variant H2AX, is implicated as a very

early response to DNA damage. Followed by the formation of γH2AX foci at damage sites within 1 minute and continuing to increase for 10 to 30 minutes (Rogakou *et al.,* 1998). γH2AX foci disappear in a comparable rate to repair of DNA damage. γH2AX is thought to aid the assembly and retention of other repair factors at sites of DNA breaks, such as 53BP1, MRN complex, MDC1 and BRCA1 (Celeste *et al.,* 2003). Targeting of activated ATM to sites of damage is thought to be dependent on the signalling generated by the sensory MRN complex (Niida and Nakanishi, 2006; Costanzo *et al.,* 2004a). It has been shown that the MRN complex not only regulates ATM activity, but also enhances ATM substrate phosphorylations (Lee and Paull, 2004). ATM is connected to DNA repair processes by MRN complex functions in unwinding the DNA helix and cleaving the hairpin loop in preparation for repair (Paull and Gellert, 1999).

In humans, ATM mutations leads to the condition **A**taxia-**T**elangiectasia (A-T), a rare autosomal recessive human disorder hallmarked by hypersensitivity to IR (Savitsky *et al.,* 1995; Lavin and Shiloh, 1997; Shiloh, 1997). Clinical manifestations of A-T include: cereberalller degeneration (ataxia), dilation of blood vessels (telangiectasia), growth retardation and immune deficiency (Jason and Gelfand, 1979). A-T is described as a 'genomic/chromosome instability syndrome', patients show signs of premature aging and predisposition to cancers. On a cellular level, A-T leads to a failure of G1 and G2 checkpoint induced cell cycle arrest (described in more detail in section 1.4) and sensitises cells to the cytotoxic effects of DNA damage (Shiloh, 1997; Kastan *et al.,* 1992; Paules *et al.,* 1995). Interestingly, A-T sufferers retain intact mechanisms to repair single strand breaks, to remove base damage and perform DSB end joining (Fornace and Little, 1980; Shiloh, 1997). The lack of cell cycle arrest does not allow for the appropriate repair mechanisms to correct DNA lesions. Therefore, A-T cells undergo radio-resistant DNA synthesis leading to chromosomsal instability (Painter and Young, 1980; Kojis *et al.,* 1991).

1.3.1.2   ATR activation in response to single strand DNA damage

It has been well established that ATR (Mec1 in *S.cerevisiae*) signalling is activated in the presence of single stranded DNA resulting from replication stress, such as replication fork stalling (Abraham, 2001). ATR signalling is also induced by bulky DNA adducts, lesions resulting from ultraviolet radiation (UV), such as pyrimidine dimers   and   the   6-(1,2)-dihydro-2-oxo-4-pyrimidinyl-5-methyl-2,4-(1H,3H)-

pyrimidinediones (Unsal-kacmaz *et al.,* 2002). In humans, ATR is stably associated with ATRIP (ATR/ATRIP), this is also the case in yeast (Mec1/Dcd2 in *S.cerevisiae* (budding yeast) and Rad3/Rad56 in *Schizosaccharomyces Pombe* (*S.pombe,* fission yeast) (Cortez *et al.,* 2001; Unsal-kacmaz and Sancar, 2004; Paciotti *et al.,* 2000; Edwards *et al.,* 1999). ATR is thought to be constitutively active during unstressed DNA replication, thus it is believed that during S phase substrate reactions are reliant on cellular localisation (Niida and Nakanishi, 2006). It is thought that ATR-ATRIP, as part of the DNA replication machinery, associated with RPA, monitors single stranded DNA damage during the progression of DNA replication fork elongation (Niida and Nakanishi, 2006; Shechter *et al.,* 2004b). In addition, ATR functions in both S and M phases include regulating late DNA replication origin firing, replication fork elongation, restarting stalled replication forks and involvement in centrosome stability (Shechter *et al.,* 2004a; Cha and Kleckner, 2002; Sorensen *et al.,* 2004; Friedel *et al.,* 2009; Alderton *et al.,* 2004; Smith *et al.,* 1998).

ATR is essential in development and somatic cell growth. ATR indispensability is thought to revolve around ATR's multifaceted roles in monitoring the progression of DNA replication (Brown and Baltimore, 2000). Similarly, Chk1 (ATR downstream target) knockout mice are embryonic lethal (Takai *et al.,* 2000; Liu *et al.,* 2000). Seckel syndrome is an heterogenous rare genetic disorder associated with impaired ATR function and defects in downstream ATR DNA damage response signalling pathways. The basis of Seckel syndrome remains largely undefined, many susceptibility loci have been identified, however, only one specific ATR hypomorphic mutation has been uncovered (O'Driscoll *et al.,* 2003). Seckel syndrome is clinically characterised by dwarfism, abnormal brain development and microcephaly (Majewski and Goecke, 1982). Seckel cells show higher sensitivity to replication fork stalling agents and illustrate defects in downstream ATR DNA damage responses exemplified by impaired H2AX, Rad17, Nbs1 P53, and Chk1 phosphorylation (O'Driscoll *et al.,* 2003; Alderton *et al.,* 2004). In addition, Seckel cells exposed to UV were unable to execute the G2/M checkpoint (the G2/M checkpoint is described in section 1.4.3) (Alderton *et al.,* 2004).

1.3.1.3 The interconnectivity between ATM and ATR DNA damage response kinases

Specific types of DNA damage have been shown to activate either ATM or ATR. A growing number of studies are demonstrating that ATM and ATR work in a partnership (Hurley and Bunz, 2007). Complementary functions of ATM and ATR redefine the long-lived paradigm of distinctly separate molecular functions. S and G2/M phase ATM and ATR independent Chk1 checkpoint signalling was disregarded through the discoveries made by Jazayeri *et al.*, (Jazayeri *et al.*, 2006). In this study, it was unveiled that the reaction convergence occurs through ATM processing of DBSs (end resection) mediated by Mre11 to form ssDNA. The resulting ssDNA coated by RPA, then initiates ATR signalling (Jazayeri *et al.*, 2006). Studies by Cuadrado *et al.*, Yoo *et al.*, and Adams *et al.*, have provided further experimental evidence to support ATM dependent activation of ATR is required in double strand break DNA repair (Cuadrado *et al.*, 2006; Yoo *et al.*, 2007; Adams *et al.*, 2006). Importantly, ATR has also been shown to activate ATM in response to the presence of ssDNA damage (Stiff *et al.*, 2006). It is becoming clear that ATM and ATR activation as well as function, are connected in response to DNA damage.

1.4 DNA damage checkpoint responses control cell cycle progression into mitosis

ATM and ATR signal transductions are critical in maintaining genomic stability by arresting cells that are progressing through the cell cycle with damaged DNA (Abraham, 2001). These cell cycle checkpoints are feedback mechanisms induced by genotoxic stress that govern the pace of cell cycle progression, ensuring the timely and precise completion of critical cell phase events (Hartwell and Weinert, 1989). Overall, checkpoints are surveillance pathways that ensure the success and fidelity of important cellular processes and prevent cells from entering mitosis with DNA damage. The in depth understanding of checkpoints has come about through extensive studies in a number of species, particularly in *S.pombe, S.cerevisiae* and *Xenopus laevis.* The importance of checkpoint integrity is highlighted by checkpoint defects in a number of cancers (Kastan and Bartek, 2004). DNA damage induced checkpoints relate to G1/S, S and G2/M cell cycle phases, which are described in the following sections (1.4.1-1.4.3). Following which, the spindle assembly checkpoint and the potential of M phase DNA

damage induced checkpoints are then discussed in section 1.5. Figure 1.6 summarises the checkpoint targets that provoke cell cycle delay/arrest at the different phase transitions. It should be noted at this point that the discussed checkpoint factors, in many cases, have more than one function within DNA damage induced checkpoints.
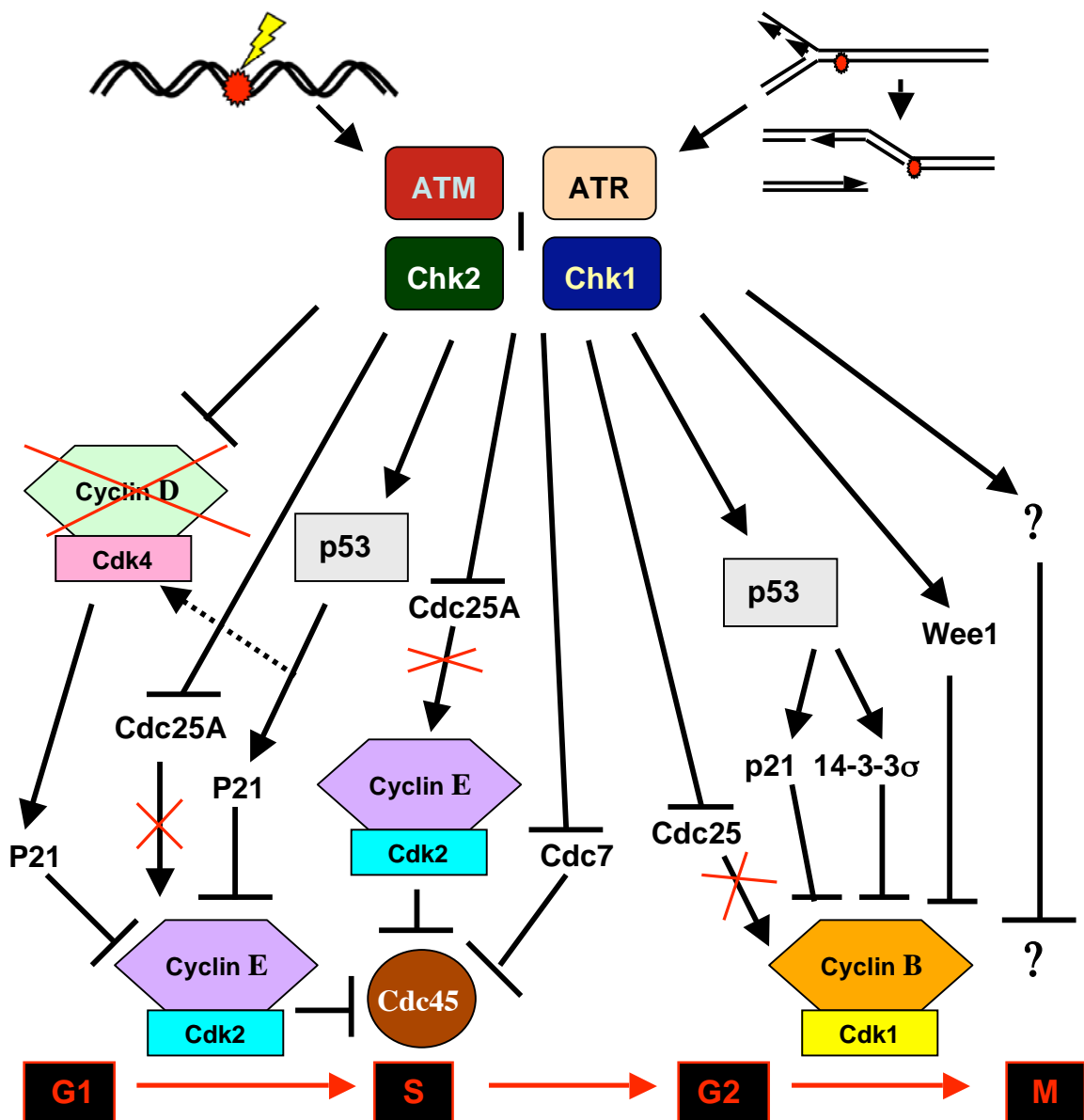
Figure 1.6 Mammalian G1/S transition, S and G2/M transition DNA damage checkpoints

In the G1/S checkpoint response to DNA damage, active ATM and ATR phosphorylate downstream Chk1/Chk2 and p53. Checkpoint initiation involves down-regulation of Cdc25A, which leads to the accumulation of inactive Cdk2, which cannot induce Cdc45 required for replication initiation. p53 phosphorylation induces expression of p21, which then maintains the checkpoint by preventing Cdk4-Cyclin D from provoking release of pRb bound S phase transcription factor, E2F. Cdk4-Cyclin D destruction provoked by ATM/ATR facilitates the inhibition of S phase Cyclin transcription and releases p21, which inhibits Cdk2-Cyclin E. The S phase checkpoint is dependent on ATM/ATR (Chk2/Chk1) initiation of Cdc25A degradation, resulting in Cdk2-Cyclin E inactivation, which prevents Cdc45 loading onto replication origins. Alternative pathways prevent replication origin firing, including ATM phosphorylation of SMC1 (not shown) and ATR down-regulation of Cdc7. The G2/M checkpoint involves Chk1 phosphorylation of Cdc25 phosphatases leading to their nuclear export and degradation, which in turn increases the levels inhibitory phosphorylations on Cdk1-Cyclin B. The G2/M checkpoint also involves Chk1/Chk2 stabilisation of p53, which leads to Cdk1-Cyclin B activity inhibition through p21 and by increasing expression of 14-3-3σ. Furthermore, Wee1 is up-regulated, which increases Cdk1-Cyclin B inhibitory phosphoryation levels. Adapted from Sancar *et al.,* 2004 (Sancar *et al.,* 2004).

1.4.1   G1/S transition checkpoint

DNA damage induced G1/S checkpoint prevents damaged genetic templates from being replicated until the defects have been resolved. The initiation of the G1/S checkpoint involves Cyclin D degradation, inhibition of Cdk2 through phosphorylation, CKI interaction and Cdc25 phosphatase inactivation (Agami and Bernards, 2000). In the presence of DNA damage, ATM or ATR phosphorylates Cyclin D at Thr286, which promotes Cyclin D proteasomal degradation (Hitomi *et al.,* 2008). In cells with proficient p53 activation, between 30 % and 50 % of G1 cell cycle arrest is related to Cyclin D1 suppression in response to ATM activation (Hitomi *et al.,* 2008; Agami and Bernards, 2000). It is possible that if DNA damage is incurred prior to the G1 phase "restriction point", ATM/ATR activation suppression may lead to entry into G0 phase. This would potentially allow for a longer period of DNA damage repair before re-entering the cell cycle and committing to cell proliferation (Hitomi *et al.,* 2008). It has been postulated that ATM and ATR can indirectly aid DNA repair by promoting Cyclin D destruction, leading to the release of PCNA (**p**roliferating **c**ell **n**uclear **a**ntigen), thus increasing the availability of PCNA for repair processes (Hitomi *et al.,* 2008; Pagano *et al.,* 1994; Xiong *et al.,* 1992).

An additional pathway is initiated by the destruction of Cyclin D; CDK inhibitor p21 (CIP) is released, preventing Cdk2-Cyclin E activity. In addition, the destruction of Cyclin D inactivates Cdk4, which is then unable to phosphorylate pRb required to release the associated S phase Cyclin transcription factor E2F. Furthermore, active ATM-Chk2/ATR-Chk1 targeting of Cdc25A leads to the rapid destruction of phosphatase activity and consequently the levels of Cdk2 inhibitory phosphorylation increase (Molinari *et al.,* 2000; Falck *et al.,* 2001; Mailand *et al.,* 2000). In combination, the negative regulation of Cdk2 contributes to G1 cell cycle arrest by preventing Cdk2 phosphorylation of Cdc45 and therefore, its loading onto orgins, which is required in the initiation of DNA replication (Costanzo *et al.,* 2000; Broderick and Nasheuer, 2009).

The initiation of G1/S phase cell cycle arrest is rapid, but a slower increase in p53 stability within the nucleus maintains the arrest (Agami and Bernards, 2000). Many studies have demonstrated that G1/S checkpoint arrest in response to DNA damage requires functioninal p53 (Kuerbitz *et al.,* 1992; Lakin and Jackson, 1999). ATM and ATR directly, or indirectly through Chk2/Chk1, phosphorylate p53 (Hirao *et al.,* 2000;

Kuerbitz *et al.,* 1992). Phosphorylation of p53 at Ser20 (Chk1/Chk2) leads to the release of associated Mdm2 ubiquitin E3 ligase, which then renders p53 stable (Ashcroft and Vousden, 1999). The resulting P53 up-regulation in turn activates transcription of genes involved in maintaining the cell cycle arrest. For example, p53 increases the expression of factors including p21, which continues the inhibition of Cdk2-Cyclin E that prevents S phase onset (Harper *et al.,* 1993).

1.4.2   S phase checkpoint

The S phase checkpoint is activated in response to DSBs created by collapsed replication forks or the presence of DNA lesions that block DNA replication. S phase checkpoint slows cell cycle progression to mitosis by controlling the DNA replication machinery at stalled replication forks (Nyberg *et al.,* 2002; Sancar *et al.,* 2004). In contrast to the G1/S transition checkpoint, S phase checkpoint activation does not lead to a full cell cycle arrest (Rowley *et al.,* 1999). Instead, the S-phase checkpoint decreases the rate of DNA synthesis by preventing the elongation of replication forks and inhibits late replication origin firing. S phase checkpoint initiation relies on both ATM and ATR kinase activities (Yoo *et al.,* 2004b). ATM and ATR targets include BRCA1 and Nbs1, these and many more coordinate the replication fork inhibition, DNA repair and also replication fork recovery (Flack *et al.,* 2001; Sancar *et al.,* 2004).

In the event of stalled replication forks, partially repaired DSBs or replicated DNA damage, the primary signal for checkpoint activation is thought to be the coating of RPA on exposed ssDNA (Branzei and Foiani, 2005). ATR binds to RPA and promotes factors that stabilize the halted replication forks. Furthermore, the RPA-ATR-Chk1 signaling pathway prevents the replication of damaged DNA by blocking the initiation of replication origins. RPA-ATR-Chk1 signalling inhibits Cdk2 (-CyclinE) activity by inactivating and down-regulating Cdc25A phosphatase (Sancar *et al.,* 2004). Another ssDNA induced ATR checkpoint has also been described in which ATR targets Cdc7 activity and thus prevents Cdc45 loading onto replication origins (Costanzo *et al.,* 2003). In response to DSBs, two ATM dependent mechanisms delay S phase; the ATM-Chk2-Cdc25A-Cdk2 pathway and ATM phosphorylation of **s**tructural **m**aintenance of **c**hromosomes protein, SMC1 (aided by BRCA1/FANCD2 (**F**anconi's **an**emia **c**omplex **D2**) and Nbs1) (Yazdi *et al.,* 2002).

1.4.3   G2/M phase transition checkpoint

The G2/M checkpoint prevents cells that have damage DNA or that have not completed replication, from entering mitosis and segregating their chromosomes. Original data obtained from *S.pombe* revealed that blocking replication through **H**ydroxy**u**rea (HU) treatment led to the maintenance of the Tyr15 phosphorylation on Cdc2, which prevents the progression of S phase and entry into mitosis (Gould and Nurse, 1989; Nurse, 1990) It has also been shown that unphosphorylatable Cdc2 mutants inappropriately enter mitosis in the presence of unreplicated DNA (Gould and Nurse, 1989). This G2/M checkpoint is an important mechanism in maintaining the S-M cell cycle phase interdependence.

As previously mentioned in section 1.2.1, Cdc25 phosphatases dephosphorylate Cdk1 (Cdc2) required for full Cdk1-Cyclin B activation. Mitosis onset is prevented in response to DNA damage through the stabilisation of the inhibitory phosphorylation on Cdk1-Cyclin B (Dasso and Newpot, 1990; Jin *et al.,* 1996). Activated ATM and ATR induce Chk1 and Chk2, which initiates Cdc25 inhibition and/or degradation (Matsuoka *et al.,* 1998; Sanchez *et al.,* 1997; Kastan and Bartek, 2004). For example, in fission yeast, Chk1 kinase phosphorylation of Cdc25C at Ser216 enables 14-3-3 proteins to bind, which leads to nuclear displacement of Cdc25C, preventing dephosphorylation of Cdk1-Cyclin B1 (Peng *et al.,* 1997). The maintenance of the G2/M checkpoint is thought to involve p53 activities. It has been shown that p53 levels are up-regulated, which can inhibit Cdk1 activity in two ways, by inducing p21 (CIP) and by increasing expression of 14-3-3σ protein (Bunz *et al.,* 1998; Chan *et al.,* 1999). P21 can specifically inhibit nuclear activity of Cdc2-Cyclin B, whereas 14-3-3σ sequesters Cdc2-Cyclin B preventing it from entering the nucleus. The G2/M checkpoint also up-regulates Wee1, which leads to an increase in inhibitory phosphorylation on Cdk1-Cyclin B (Yarden *et al.,* 2002). Furthermore, ATM and ATR dependent Plk1 inactivation has been shown, which most likely prevents activation of Cdc25C by phosphorylation (Smits *et al.,* 2000; van Vugt *et al.,* 2001).

The resulting arrest allows for the proficient repair of DSBs in cells by utilizing the duplicated chromatid as a template in **h**omologous **r**ecombination (HR) (Haber, 2000). Once DNA damage response signaling discontinues after DNA has been repaired, Plk mediates the recovery of cell cycle, potentially through inducing degradation of Wee1

(van Vugt *et al.,* 2004a). In addition, active Plk1 is also thought to participate in Cdk1-Cyclin B activation after checkpoint inactivation (Watanabe *et al.,* 2004).

1.5 The current understanding of mitotic checkpoints

As described in the previous section, the presence of DNA damage provokes an ATM and ATR dependent checkpoint, which delays the onset of mitosis. However, if DNA damage is left unchecked in mitosis this could potentially lead to the loss of genetic information or alternatively chromosome rearrangement. Ultimately, the presence of mitotic DNA damage could jeopardise the next generation of cells. Research efforts are now being directed towards determining the cellular responses to DNA damage exposure during mitosis. There is relatively little data in this field compared with other stages of the cell cycle.

1.5.1 The spindle assembly checkpoint

During mitosis, the **s**pindle **a**ssembly **c**heckpoint (SAC) monitors the proper alignment of chromosomes along the central metaphase plate. This checkpoint pathway is intrinsically active and prevents anaphase onset until the last kinetochore attaches to the spindle (Musacchio and Salmon, 2007). Studies undertaken in yeast have contributed vastly to SAC understanding. *S.cerevisiae* mutation screens originally uncovered SAC proteins **m**itosis **a**rrest **d**eficient (Mad1, Mad2 and Mad3 (or BubR1 in humans)) and **b**udding **u**ninhibited by **b**enomyl (Bub1) as essential factors in maintaining normal cell division and preventing mitotic progression in the presence of abnormal spindle assembly (Li and Murray, 1991; Hoyt *et al.,* 1991). These identified yeast SAC genes are highly conserved in all eukaryotes and studies have shown that they are universally essential for SAC function. Similarly to yeast, the loss of SAC function in higher eukaryotes leads to inaccurate chromosome segregation (Wassmann and Benezra, 2001). It is widely considered that SAC proficiency is strongly involved in preventing errors in chromosome segregation leading to aneuploidy (Kops *et al.,* 2005). The importance of the SAC to the integrity of the genome has been made evident by cancer links to defects in the spindle assembly checkpoint mechanism. As illustrated by Bub1 and BubR1 mutations identified in colon and colorectal cancers respectively (Cahill *et al.,* 1998).

The current basic model describing the complex SAC pathway activation and inactivation is illustrated in figure 1.7. Prior to chromatin attachment, after nuclear envelope breakdown, SAC factors including Mad1, Mad2, Mps1 (**m**ulti**p**olar **s**pindle-**1**), Aurora B, Bub1, BubR1 and Bub3 as well as APC cofactor Cdc20 are recruited to phosphorylated kinetochores. In higher eurakoyotes other SAC regulatory elements including motor proteins CENP-E (kinesin) and dynein are also concentrated at kinetochores (Musacchio and Salmon, 2007; Cheeseman and Desai, 2008). Following the recruitment of factors to kinetochores, the **m**itotic **c**heckpoint **c**omplex (MCC) forms, consisting of activated Mad2, activated BubR1 and Bub3, which associates strongly with APC co-factor Cdc20 (Sudakin *et al.,* 2001). MCC-Cdc20 binds to APC and blocks its activation, therefore preventing securin and Cyclin B degradation, necessary for sister chromatid separation and mitotic exit respectively (refer to section 1.2.1) (Yu, 2002; Hagting *et al.,* 2002). The additional SAC components also recruited to kinetochores have multiple functions including aiding the assembly and signal transmission of MCC, recruiting SAC factors to kinetochores and regulating SAC activity (Musacchio and Salmon, 2007). In turn, the bi-orientation of chromosomes along the central metaphase plate, made possible by microtubule-kinetochore attachment, satisfies the SAC. At which point MCC releases sequestered Cdc20, which enables APC activation. The mechanism that discontinues the checkpoint is subject to ongoing discussion, the checkpoint inactivation pathways proposed involve dynein transportation of SAC proteins away from kinetochores, CENP-E "silencing" of BubR1 or instead p31^{Comet} blocks Mad2 activity (Howell *et al.,* 2001; Mao *et al.,* 2005; Xia *et al.,* 2004; Yang *et al.,* 2007a).
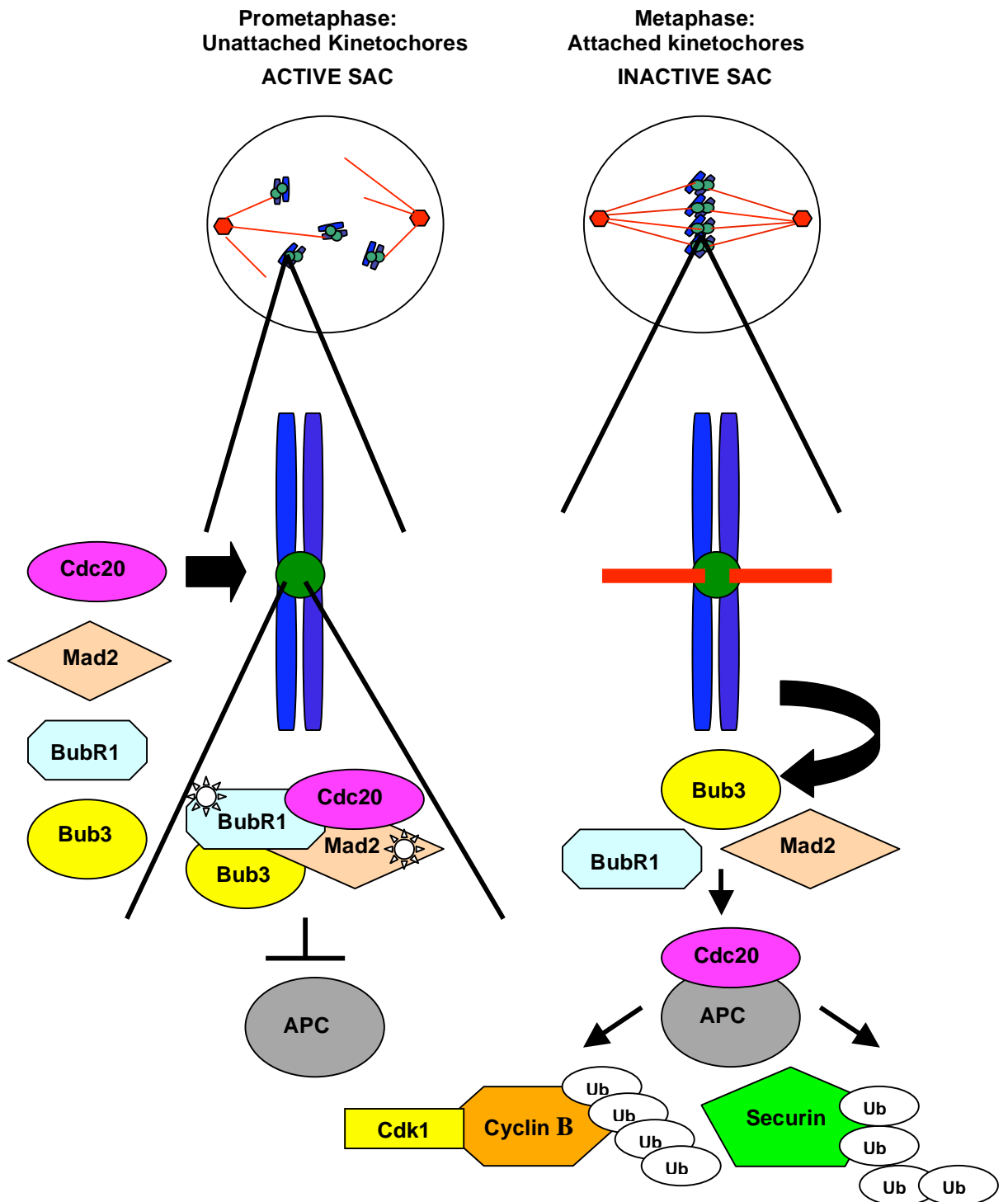
Figure 1.7 The spindle assembly checkpoint prevents mitosis progression with unattached kinetchores by regulating APC activity

Spindle assembly checkpoint (SAC) is activated by unattached kinetochores in prometaphase. SAC factors are recruited to kinetochores, activated BubR1, activated Mad2, Bub3 assemble to form the mitotic checkpoint complex (MCC), which associates with Cdc20 and blocks APC activation. SAC inactivation occurs when chromosome bi-orientation is achieved in metaphase (both sister kinetochores are attached to microtubules from opposite poles). MCC complex disassembles releasing Cdc20, which then associates with and activates APC. Ubiquination of securin and Cyclin B by active APC leads to their degradation required for sister chromatin separation and mitosis exit respectively. Adapted from Kops *et al.,* 2005 (Kops *et al.,* 2005).

SAC activity is "switched on" with the treatment of microtubule inhibiting agents, which cause errors in chromatin attachment to microtubule spindles and the failure in spindle tension (Zhou *et al.,* 2002). In this situation, SAC activity is retained and inhibition of Cdc20 is prolonged, thus continuing the block on APC activity required in the metaphase to anaphase transition. The maintenance of SAC activity leads to a delay in mitosis progression that allows for chromosome realignment through microtubule kinetochore re-attachment and spindle tension correction.

Early investigations into the effects of UV radiation described a mitotic arrest resulting from spindle assembly abnormalities and chromatin-kinetochore attachment failure or dis-attachment (Carlson, 1950; Zirkle, 1970). These early studies, and many others since, have shown that mitotic DNA damage mediates a slowing of phase progression by activating, or delaying the inactivation, of the SAC. Recent research in a number of species has determined that the incorporation of mitotic DNA damage leads to the activation of SAC component BubR1, which is thought to be vital in the mitotic delay (Royou *et al.,* 2005; Fang *et al.,* 2006; Choi and Lee, 2008). It is generally believed that widespread DNA damage or structural changes to chromatin affect the centromere region, which results in the disruption of kinetochore structure/function (Garber and Rine, 2006). Mikhailov *et al.,* demonstrated that extensive DNA damage incurred by laser microbeam treatment led to a mitotic arrest in cells specifically through damage acquired in the kinetochore region. However, the presence of DNA damage at kinetochores was found to prolong SAC activity by a pathway independent of ATM (Mikhailov *et al.,* 2002). Interestingly, Kim and Burke very recently demonstrated in yeast that DNA damage away from the proximity of kinetochores can initiate a Mec1 (ATR) and Tel1 (ATM) dependent pathway that elicits the SAC and consequentially restrains anaphase onset (Kim and Burke, 2008). This potential cross over of DNA damage response signalling with SAC is supported further by the identification of essential SAC components in the recent large-scale proteomic analysis of ATM and ATR substrates (Matsuoka *et al.,* 2007). It has been postulated that downstream of the SAC, a post mitotic checkpoint prevents DNA reduplication in the next cell cycle. The trigger of this checkpoint is thought to be the failure of p53 localisation to centrosomes in association with active ATM during mitosis (Tritarelli *et al.,* 2004; Oricchio *et al.,* 2006).

1.5.2 The potential existence of DNA damage mitotic checkpoints

In the field of mitotic research there is much controversy over whether mitotic delay can also be caused by DNA damage checkpoints. To date there is contradicting research, which indicates that mitotic DNA damage induces no affect on mitotic progression versus that which shows a delay in mitosis exit.

Within the previously mentioned studies undertaken by Mikhailov *et al.,* (section 1.4.3) it was found that early mitotic human cells treated with low levels of DNA damage progressed and successfully completed cell division (Mikhailov *et al.,* 2002). Similarly, research undertaken by Skoufias *et al.,* established no detectable mitotic delay in human cells in response to DNA DSBs induced during metaphase, although cells presented abnormalities in chromatin separation and a phenotype similar to mitotic catastrophe (Skoufias *et al.,* 2004). This study contributed to the uncertainty of whether DNA damage can induce a durable mitotic arrest and instead concluded DNA decatenation rather than DNA damage was the cause. Interestingly, DNA decatenation invoked a prolonged mitotic delay that was directly associated with Mad2 with Cdc20 spindle assembly checkpoint factors away from kinetochores (Skoufias *et al.,* 2004). In contrast, Smits *et al.* showed that Polo-like kinase activity is inhibited in the response to DNA damage during mitosis (Smits *et al.,* 2000). Importantly, this investigation showed that mammalian cells have mitotic DNA damage checkpoints as well as yeast (Yang *et al.,* 1997; Tinker-Kulberg and Morgan, 1999; Liang and Wang, 2007).

It has been made clear by the consistent observations of γH2AX foci formation that ATM and ATR DNA damage response kinases can be activated in mitosis. There is insufficient evidence to support the notion that G2 DNA damage checkpoints also function during mitosis (Morrison and Rieder, 2004). However, other potential mechanisms have been proposed which describe DNA damage checkpoints that slow the progression of mitosis independently from the activation of the SAC. For instance, Smits *et al.* showed that DNA damage induces Plk1 inhibition, which prevents APC activation required in mitotic exit (Smits *et al.,* 2000). This pathway was substantiated as a specific DNA damage response by a subsequent report by van Yugt *et al.,* which showed ATM/ATR dependent Plk1 inactivation in mitosis (van Yugt *et al.,* 2001). In agreement, there is growing evidence for Plk1 and Chk2 interaction in this mitotic checkpoint response (Tsvetkov *et al.,* 2003; Seo *et al.,* 2003; Jang *et al.,* 2007). A report

by Chow *et al.* showed exposure of mitotic cells to DNA damage leads to ATM dependent destruction of Cdc25A phosphatase, inactivatation of Cdk1-Cyclin B and cell cycle reversal into G2 phase (Chow *et al.*, 2003). An alternative mitotic DNA damage checkpoint mechanism was devised from studies in *Drosophila* embryos in which ATM (Mei-41 in the fly) induction is thought to cause a mitotic delay by stabilising Cyclin A, which prevents anaphase onset (Su and Jaklevic, 2001; Laurencon *et al.*, 2003). It has also been shown in *Drosophila* embryos that DSBs, away from kinetochore regions, retard mitosis progression through activation of a Chk1 signalling pathway (Royou *et al.*, 2005). Works by Huang *et al.*, have demonstrated that DNA damage in human cells elicits a mitotic exit blockade dependent on BRCA1 and Chk1 (Huang *et al.*, 2005). This checkpoint mechanism was proposed to prevent cells from dividing normally and also to take part in terminating mitosis by inducing mitotic catastrophe. Further to these mentioned findings, there are several studies that are now implicating centrosomes as an organelle that monitors DNA damage and regulates mitosis progression.

1.5.3   Growing evidence of centrosomal checkpoints responding to DNA damage

As previously described in section 1.2.1 centrosomes key regulators for mitotic spindle organisation. However, mitotic spindles can form in the absence of centrosomes through actions of motor proteins and structural elements (Theirkauf and Hawley, 1992; Bartolini and Gundersen, 2006; Walczak *et al.*, 1998; Compton, 1998; McKim and Hawley, 1995; Matthies *et al.*, 1996; Heald *et al.*, 1997). It is commonly believed that centrosome functions have not been fully elucidated. The interconnection between cell cycle progression and the centrosome cycle is substantiated by the centrosomal presence of cell cycle and checkpoints proteins. Furthermore, connections have lately been made between DNA damage response S and G2/M checkpoint elements and their control over the centrosome cycle and centrosome integrity (Löffler *et al.*, 2006). This relationship was confirmed in a recent study, which demonstrated DNA damage response elements MDC1 and BRIT1 localise at centrosomes and have respective roles in centrosome duplication and mitotic spindle assembly (Rai *et al.*, 2008).

It has already been made clear that centrosomes act as "command centres for cellular control", which does not exclude their direct involvement in checkpoint responses to DNA damage (Doxsey, 2001; Doxsey *et al.*, 2005; Reider *et al.*, 2001; Löffler *et al.*,

2006). For instance, G2/M transition checkpoint activation in response to the incorporation of DNA damage in S phase is regulated by centrosomes. It is thought that active Chk1 accumulation at centrosomes prevents mitosis onset by inhibiting Cdc25B and Cdc2 activation, in addition to which, centrosomal Chk1 activity correlates to centrosome amplification (Cazales 2005; Löffler *et al.,* 2007; Bourke *et al.,* 2007). Centrosome structural protein pericentrin could be part of this G2/M arrest pathway, as suggested from the identification pericentrin mutations causing Seckel-syndrome (Griffith *et al.,* 2008). Although the function of pericentrin in this checkpoint mechanism has not been established, it was posited that either pericentrin could aid Chk1 recruitment to centrosomes or alternatively assist in downstream signalling to centrosome components involved in the arrest.

There is mounting evidence within the context of mitosis that the presence of DNA damage perturbs centrosome integrity (Sibon, 2003). These DNA damage invoked pathways interfere with centrosome-dependent mitotic processes, which can prevent the division of cells with damaged DNA. Originally, a report by Sibon *et al.,* showed that unreplicated DNA or incorporation of DNA damage can induce the loss of centrosome function in *Drosophila* embryos in mitosis. This loss of centrosome function was associated with the displacement of γ-TuRCs, which led to the formation of insufficient spindle structures that were unable to segregate chromosomes (Sibon *et al.,* 2000). In this situation centrosome inactivation occurs after checkpoint failure in response to DNA damage at the point of mitosis onset. These findings were followed by another study in *Drosophila* embryos, which showed Chk2 dependent destruction of centrosome function induced by the presence of DNA damage (Takada *et al.,* 2003). It is generally thought that defective mitotic cells undergo mitotic catastrophe, which in turn leads to their elimination from the cell population by cell death (Schatten *et al.,* 1999; Roninson *et al.,* 2001). This promotion of mitotic catastrophe could be a means of rendering cells non-viable in order to avoid aneuploidy. However, mitotic cells have been described to respond differently to incomplete DNA replication. Research performed by Hut *et al.,* described the induction of centrosome fragmentation leading to the formation of aberrant multipolar spindle structures that inappropriately divide chromosomes (Hut *et al.,* 2003). The abnormal cells derived from failed mitosis can arrest in G1 in the next cell cycle, or alternatively die following mitotic catastrophe. It is possible, however, that this process may be detrimental to the cell population by causing the formation of viable aneuploid cells. It is believed that this proposed DNA damage induced pathway of

inhibiting normal mitosis progression is also likely to be controlled by checkpoint factors.

It has been noted that many DNA damage response factors and cell cycle checkpoint proteins co-localise with centrosomes specifically during mitosis in addition to Chk1 and Chk2. Particularly of interest is the proposal that in human mitotic cells ATM and ATR kinases are found at centrosomes (Shen *et al.,* 2006; Zhang *et al.,* 2007). In the research performed by Zhang *et al.,* DNA damage led to ATM and ATR delocalisation from centrosomes. Interestingly, this shift in localisation was shown to coincide with an increase in γ-tubulin nucleation (Zhang *et al.,* 2007). However, it is possible that these ATM/ATR observations could be related to the SAC induced activated by perturbed mitotic spindle assembly. At this point, there is no clear model for ATM/ATR activation status, localisation or potential movement away from centrosomes in mitosis. Tumour suppressor proteins including BRCA1 and p53 have also been found to co-localize with centrosomes in mitosis, although how these proteins participate in centrosome regulation it is not known. It is also unknown if they impact on centrosome stability in the context of mitotic DNA damage (Hsu and White, 1998; Kais and Parvin, 2008; Shinmura *et al.,* 2007; Fukasawa, 2007).

As the mitotic responses to DNA damage are poorly elucidated, it is feasible that the mentioned checkpoint factors and potentially others could participate in these described mechanisms of enhancing chromosome instability through provoking centrosome instability. This process of orchestrating mitotic errors could be representative of a safety net for mitotic cells with persistent DNA damage. Alternatively, compartmentalisation of cell cycle machinery, for example within centrosomes, may provide a platform in which checkpoint reactions can occur (Löffer *et al.,* 2006). This is in alliance with the hypothesis that complex DNA damage response networks are organised temporally and spatially rather than a linear orientation (Lukas *et al.,* 2004). Within the confinement of centrosomes DNA damage checkpoint components could plausibly regulate mitosis without imposing on centrosome integrity by pathways that were discussed in section 1.5.2. Furthermore, this proposed model for inducing mitotic arrest provides a possible explanation to why Plk1, Cdk1-Cyclin B and other mitosis regulation factors are also found at centrosomes during mitosis (Jackman *et al.,* 2003; Golsteyn *et al.,* 1995; Tsvetkov *et al.,* 2003). The two posited mitotic arrests pathways

orchestrated by centrosomal checkpoint signalling in response to DNA damage are depicted below in figure 1.8.

Mitotic DNA damage

Checkpoint interactions with centrosomal structural /regulatory elements

Chk1

Chk2

?

Mitotic arrest

Cdk1 Cyclin B

Centrosome inactivation or fragmentation

Inhibition of mitotic cell cycle events
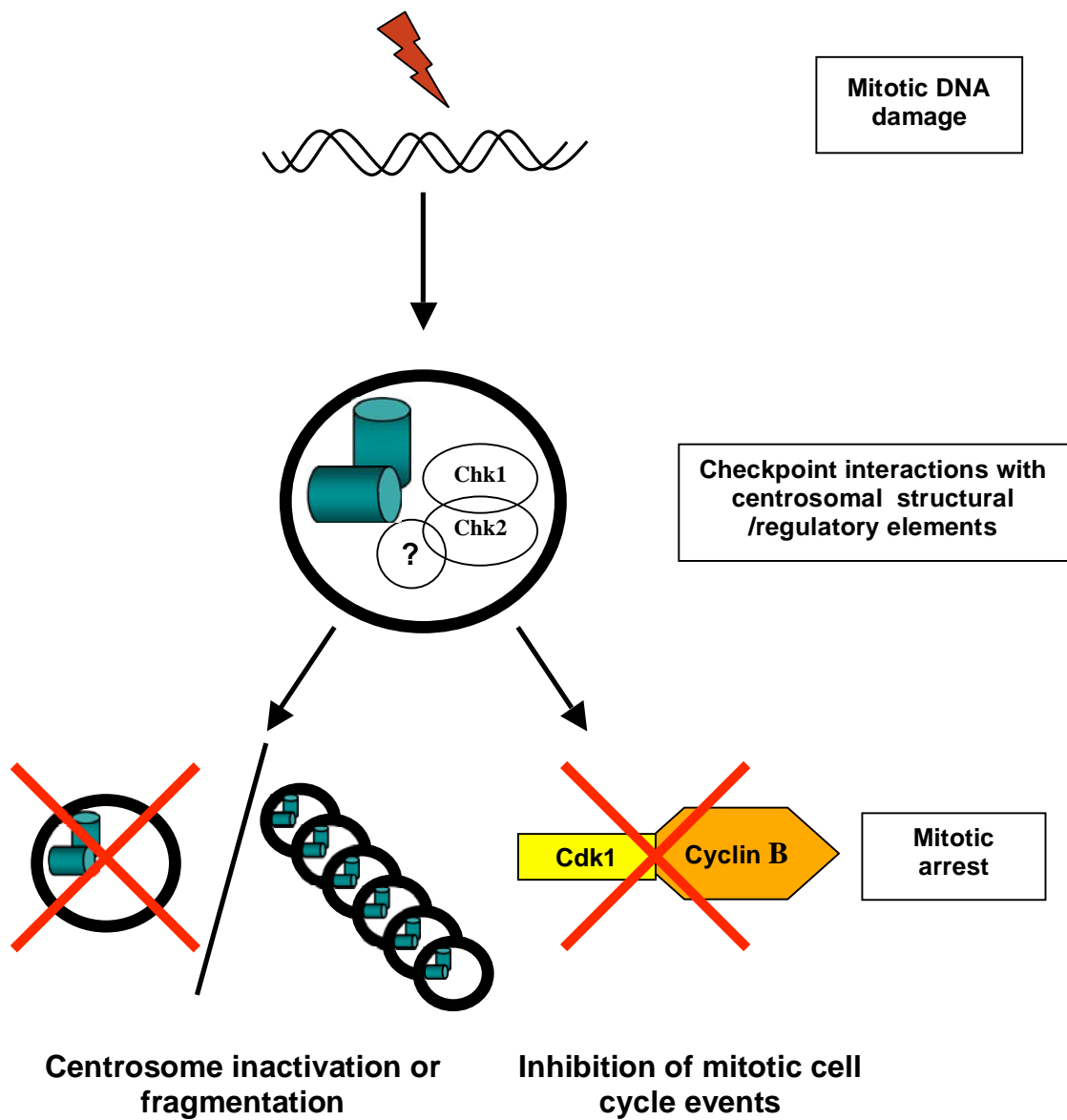
Figure 1.8 The proposed mitotic arrest models involving centrosomal checkpoint signalling elicited in the presence of DNA damage

This diagram illustrates the two potential centrosome related pathways that affects mitotic progression in cells containing damaged DNA. The presence of mitotic DNA damage could induce checkpoint interactions within centrosomes that target centrosome integrity leading to their inactivation. Alternatively, checkpoint interactions within centrosomes may in turn regulate factors such as Cdk1-Cyclin B involved in mitotic transit. Adapted from Löffler *et al.,* 2006 (Löffler *et al.,* 2006).

1.6 *Xenopus laevis* as a model system

The amphibian *Xenopus laevis* is a popular research model that has proven very useful to a wide variety of structural and functional analyses. *Xenopus* shows a good homology with human genes and the knowledge gained through using this system has contributed vastly to the understanding of complex biochemical processes. The *Xenopus* egg contains an abundance of components required for rapid cell divisions without the requirement for transcription (Smythe and Newport, 1991; Laskey *et al.,* 1977; Lohka *et al.,* 1983). *Xenopus* eggs crushed by centrifugation provide a cytoplasmic extract that can be used as a cell-free biochemical system. *Xenopus* egg extract allows investigations into cellular mechanism outside the limitation of the cell environment, which often hinders experiments. A particularly useful quality of *Xenopus* egg extract is the synchronous progression through multiple rounds of the cell cycle, driven by oscillations in Cdk activities (Murray, 1991). In addition, *Xenopus* egg extract has been shown to recapitulate cellular processes including semiconservative DNA replication and mitotic spindle assembly (Blow and Laskey 1986; Blow *et al.,* 1987; Lohka and Maller 1985). This extract system is also enhanced by the ease of protein depletions and reconstitutions. The examination of biochemical reactions are straightforward, avoiding the limitations often found associated with other systems. For these reasons, *Xenopus* extracts are widely considered as a useful biochemical tool.

Research focussing on DNA damage response signalling has been mostly performed in yeast and mammalian cells. Genetic mutant screens in yeast have been critical to the identification of important DNA checkpoint response genes including *Rad* family and *Mec1-3, mad1-3 and bub1-3* (Murray, 1995; Longhese *et al.,* 1998). However, more complex mechanisms functioning in vertebrates are absent in yeast (Zhou and Elledge, 2000). The extensive mammalian cell based research has provided much information on DNA damage responses (Sancar *et al.,* 2004). However, the use of mammalian cells is disadvantaged by cell line diversity and the complexity of DNA damage response defects (Beamish *et al.,* 1996). Furthermore, yeast and mammalian cell research can be limited by the intricate biochemistry behind cellular endpoints. Typically, *Xenopus* egg extract has been applied in developmental and cell cycle control studies, in recent years it is being used increasingly to investigate DNA damage responses (Murray *et al.,* 1989; Murray and Kirschner 1989; Gautier *et al.,* 1990; Costanzo *et al.,* 2004b; Garner and Costanzo, 2009). It has been shown that *Xenopus* egg extract can reproduce several

aspects of DNA damage response and has provided significant insights into checkpoint mechanisms (Costanzo *et al.,* 2000; Costanzo *et al.,* 2003). Importantly, ATM/ATR have been isolated and found to function in regulating DNA damage checkpoint pathways within *Xenopus* egg extract (Robertson *et al.,* 1999; Costanzo *et al.,* 2000; Hekmat-Nejad *et al.,* 2000; Guo *et al.,* 2000). In using this system, chemicals can be added to interfere with biochemical processes. For example, extract can be supplemented with aphidicolin, which is a DNA polymerase inhibitor that blocks DNA replication enabling investigations into the effects of incomplete DNA replication (Dasso and Newport, 1990; Guo *et al.,* 2000). In the most part, DNA damage checkpoint studies in *Xenopus* egg extracts have concentrated on control of DNA replication and entry into mitosis.

A very useful aspect of *Xenopus* egg extract is the ability to undertake experiments at isolated cell phases. *Xenopus* egg extract is maintained in an arrested state through the activity called **C**yto**s**tatic **F**actor (CSF) (Masui and Markert, 1971). The presence of sperm during fertilisation, triggers a calcium spike that is required in inducing events that lead to CSF and Cyclin degradation required to drive entry into mitosis (Maller *et al.,* 2002). In *Xenopus* egg extract calcium is required to provoke mitosis exit, mimicking sperm entry into the egg (Lindsay *et al.,* 1995). CSF arrested *Xenopus* egg extract has been extensively applied to understanding mitotic processes, such as spindle assembly and microtubule dynamics (Sawin and Mitchison, 1991; Verde, 1990; Belmont *et al.,* 1990). The amount of detail gained from vertebrate studies is unlikely to have been unveiled in lower eukaryotes. In combining the two areas of research, DNA damage and mitosis, investigations centred on mammalian cells have provided a limited understanding of this field. Due to *Xenopus* extract attributes and its ability to recapitulate cellular events this system is appropriate to study the effects of DNA damage during the cell cycle stage of mitosis.

1.7 This Thesis

This introduction has described the mechanisms of cell cycle control and the cellular process during each phase of the cell cycle. It was emphasised that in response to chromosomal breakages there are complex signalling networks in which ATM and ATR kinases play key roles. Then described are the DNA damage induced checkpoints that maintain genome stability by regulation of the cell cycle during interphase and

preventing progression up to the point of mitosis. The focus of this thesis is on the cell phase of mitosis and determining the effects of DNA damage during this stage of the cell cycle. Mitosis, although short lived, is the finial stage in the process of cell reproduction and may have DNA damage checkpoint controls to maintain genome stability. Although the mitotic spindle assembly checkpoint is activated in the presence of DNA damage that breaks the spindle tension or causes the detachment of chromatin from spindles, it seems likely that other mechanisms exist to sense DNA damage away from the kinetochores. As reviewed, the investigations undertaken so far, have been insufficient to fully understand the effects of DNA damage and the checkpoint mechanism(s) activated during mitosis. The contradictory lines of evidence have led to much controversy in this field and therefore further works are required in a system other than in cultured mammalian cells.

Firstly, we addressed whether ATM and ATR can be activated in mitosis by the presence of DNA damage in *Xenopus* egg extract. We then continued by investigating whether spindle assembly is perturbed in the presence active ATM and ATR. Strikingly we found that ATM/ATR activation leads to inhibition of centrosome-dependent spindle assembly. Instead, spindles assembled in the absence of centrosomes were resistant to ATM/ATR activation. Upon finding that ATM and ATR activation leads to inhibition of normal spindle formation, we then tried to identify the substrate responsible for the observed phenotype. We tested the major mitotic pathways such as Cdk1-Cyclin B, Plx1 and Ran-GTP/GDP and found the chosen candidates were not the target of this ATM and ATR pathway. We next applied a *Xenopus* cDNA library screening procedure to identify candidates for ATM and ATR targets within the physiological context of *Xenopus* egg extract. We identified a likely substrate XCEP63, which was in line with experimental evidence that suggested the ATM and ATR target lies within centrosome-driven spindle assembly. In characterisation studies we unveiled the role of XCEP63 in regulating normal spindle assembly. Finally, we identified XCEP63 phosphorylation at serine 560 by ATM and ATR and found that this phosphorylation correlates with XCEP63 displacement from the centrosome. XCEP63 phosphorylation, upon ATM/ATR activation, corresponds to abnormal spindle formation.

2 Chapter 2 Materials and Methods

2.1 General reagents and enzymes

General reagents were of the highest grade available, commonly purchased from Sigma–Aldrich or Fisher Scientific unless otherwise stated. All enzymes used were obtained from New England BioLabs unless otherwise stated.

Ultra-pure Acrylagel Acrylamide (30 %) and ultra-pure Bis-Acrylagel (2 %) were 'electrophoresis grade' and obtained from National Diagnostics. Acrylamide solution (40 %), Bis-acrylamide solution (2 %) and 40 % Acrylamide/Bis-acrylamide Solution (37:5:1) were from Bio-Rad Laboratories. Stacking buffer (0.5 M Tris-HCl pH 6.8) and Resolving Gel buffer (1.5 M Tris-HCl pH 8.8) were also purchased from Bio-Rad.

Nitrocellulose membrane for immunoblotting was Protran Nitrocellulose with 0.2 µM and 0.45 µM pore size manufactured by Whatman, supplied by GE Healthcare. 'Marvel' dried skimmed milk used in immunoblotting protocols was made by 'Premier Beverages'. Immunoblots were exposed to ECL (**e**nhanced **c**hemi**l**uminescence) Western-Blot detection reagents from GE Healthcare. ELC chemiluminescence and MP autoradiograph hyperfilms were from GE Healthcare.

2.2 Donated reagents

ATM Inhibitor, Ku55933 was initially donated by KuDOS pharmaceuticals and later supplied by Calbiochem. *Xenopus laevis* cDNAs expression library was a gift from Tony Hyman (Max Planck Institute of Molecular and Cellular Biology and Genetics, Dresden, Germany). Histidine-tagged *Xenopus* Plx1 recombinant protein, as described in Trenz *et al.,* 2008, was kindly provided by Kristina Trenz within the DNA Damage and Genomic Stability Laboratory, CRUK Clare Hall Laboratories (Trenz *et al.,* 2008). Flag-ATM and Flag-ATR purified recombinant proteins, described in Trenz *et al.,* 2006, were also provided by Kristina Trenz (Trenz *et al.,* 2006). Simon Boulton (DNA Damage Response Laboratory, CRUK Clare Hall Laboratories) kindly provided the pMAL vector.

2.3   Donated antibody

Howard Lindsay (University of Lancaster) kindly donated anti-Cds1 (Chk2). *Xenopus* Plx1 polyclonal antibody for egg extract immunoprecipitions was provided by Kristina Trenz (Trenz *et al.,* 2008). Polyclonal antibody recognizing **g**reen **f**luorescent **p**rotein (GFP) was a gift from Julian Gannon (Cell Cycle Control Laboratory, CRUK Clare Hall Laboratories).

2.4   Oligonucleotides

Oligonucleotides used for molecular biology techniques were synthesised and purified by Sigma–Aldrich custom oligonucleotides service.

2.5   Buffers, solutions and media

Commonly used buffers, solutions and media were prepared by CRUK Clare Hall Laboratories in house research services as described here. More specialized buffers, solutions and media will be described in corresponding methods.

TBE:	90 mM Tris-borate, 2 mM **E**thylene **D**iamine**t**etraacetic **a**cid (EDTA)
TAE:	40 mM Tris-acetate, 2 mM EDTA
TBS:	10 mM Tris-HCl pH 8.0, 150 mM EDTA
TE:	10 mM Tris-HCl pH 8.0, 1 mM EDTA
PBSA:	170 mM NaCl, 3 mM KCl, 10 mM Na_2HPO_4, 2 mM KH_2PO_4
L-broth (LB):	10 g Bactotryptone, 5 g yeast extract, 10 g NaCl per litre
SOC:	20 g Bactotryptone, 5 g yeast extract, 0.6 g NaCl, 0.2 g KCl, 2 g $MgCl_2$, 2.5 $MgSO_4$, 3.6 g D-glucose per litre

2.6 Antigen preparations and polyclonal antisera production

2.6.1 XCEP63 recombinant protein for antibody production

Histidine (6xHis) tagged XCEP63 fusion recombinant protein was generated for antibody production using the following protocol. Full-length XCEP63 **o**pen **r**eading **f**rame (ORF) was amplified by PCR (polymerase chain reaction) from cDNA contained within pCS2 library expression vector. XCEP63 PCR amplification used the following oligonucleotides: forward primer 5' CAACCCGTAGCCTCACGCTTCCTC 3' and reverse primer 5' **CTA**AAATGTGCAGAACATTTC 3' (incorporating a stop codon shown in bold). XCEP63 ORF was cloned into Invitrogen Gateway ® pDEST™17 vector via pENTR™/D-TOPO® as described in manufacturers manual using Gateway® LR Clonase™ II Enzyme Mix. The resulting amino-terminal (N-terminal) 6xHis tagged XCEP63 plasmid construct was transformed into BL21-AI™ One Shot® cells (Invitrogen) and then grown in LB medium at 37 ℃ with shaking for one hour. Cells were spread onto LB plates supplemented with 100 µg/ml ampicillin (prepared by CRUK Clare Hall Laboratories in house research services). Individual colonies were used to inoculate ampicillin-supplemented LB medium and these cultures were grown at 37 ℃ overnight with shaking. Small glycerol (30 %) stocks were made, and plasmid DNA from the remainder of the culture was isolated by Qiaprep Spin Miniprep kit (Qiagen). The XCEP63 DNA insert sequence was then checked by DNA sequencing (2.9.8.3).

XCEP63-GFP was grown up from glycerol stocks in ampicillin-supplemented LB medium at 37 ℃ until the optical density at 600 nm (OD600) reached approximately 0.4. 6xHisXCEP63 recombinant protein expression was induced with 0.2 % w/v L-arabinose at 37 ℃ for four hours with shaking. Cells were lysed in denaturing buffer (8 M Urea, 10 mM Tris-HCl pH 8.0, 100 mM NaH_2PO_4) supplemented with 5 mM imidazole for 40 minutes at room temperature with gentle vortexing. Cell lysate was then clarified by centrifuging at 10,000 x g for 20–30 min at room temperature. Recombinant XCEP63 was purified using Nickel (Ni) agarose beads (Qiagen) based on descriptions in manufacturers handbook. In brief, clarified cell lysate was incubated with nickel agarose beads for one hour at 4 ℃ with rotation. The lysate- Ni Bead mix was transferred to a column and washed with denaturing buffer supplemented with

increasing concentrations of 5 mM to 10 mM imidazole. Purified XCEP63 was eluted from the Nickel beads by 250 mM imidazole. Purified protein was then boiled in Bio-Rad sample buffer and loaded onto 10 % polyacrylamide with a large sample well. The polyacrylamide gel was stained with Coomassie Blue (2.10.2) and the band corresponding to recombinant 6xHisXCEP63 protein was sliced into ten pieces for polyclonal antibody generation.

2.6.2   Peptide synthesis for antibody production

Lyophilised peptides powders were produced by CRUK in-house protein and peptide chemistry service using a solid phase standard synthesis protocol suitable for antibody production. A 20 mer XCEP63 peptide with an N-terminal cysteine residue and containing a phosphorylated serine at position 10, corresponding to XCEP63-S560 (XCEP63-PS560), was prepared by the protein and peptide chemistry service for antibody production by coupling to **K**eyhole **L**impet **H**aemocyanin (KLH) (Pierce). Equivalent non-phosphorylated XCEP63-S560 peptide was also produced for affinity purification of XCEP63-PS560 antibodies (2.6.4).

2.6.3   Antibody production

Four rabbits were injected with purified 6xHisXCEP63 full-length recombinant protein to obtain XCEP63 whole protein antibodies. XCEP63 phosphorylated serine 560 specific antibodies were raised by injecting eight rabbits with KLH conjugated XCEP63-PS560 peptide. Antigens were given to Del Watling in the Biological Resources Unit within CRUK to be injected into New Zealand white rabbits (HsdIF:NZW) at Harlan UK, Hillcrest (Harlan Serum) following standard protocol as described by Harlow and Lane (Harlow and Lane, 1988). Whole protein 6xhisXCEP63 antibody was used at 1/1000 v/v dilution for immunoblotting in PBS (**p**hosphate **b**uffer **s**aline), 0.1 % Tween 20 v/v with 5 % **b**ovine **s**erum **a**lbumin (BSA) and used at 1/300 v/v for immunofluorescence in standard blocking buffer (2.10.6). XCEP63-PS560 peptide raised antisera were affinity purified as follows.

2.6.4 Affinity purification of XCEP63-PS560 antibodies

Affinity chromatography procedure was performed as outlined in GE healthcare CnBr (**c**ya**n**ogen **br**omide)-sepharose 4B product handbook. Dry CnBr-sepharose was suspended and pre-activated with 1 mM HCl for 30 minutes and packed into Econo-Pac Columns (Bio-Rad). The resulting swollen sepharose was washed with 200 ml of cold 1 mM HCl. XCEP63-PS560 peptide (5 mg), was dissolved in 5 ml of coupling buffer (100 mM NaHCO$_3$, 500 mM NaCl pH 8.3) and rotated with prepared resin at room temperature for two hours. Excess peptide was removed from the beads by washing with 30 ml of coupling buffer. CnBr uncoupled beads were blocked by washing with 200 ml of 100 mM Tris-HCl pH 8.0.

Peptide coupled to CnBr-sepharose resin was washed with 200 ml of wash buffer containing 100 mM Tris-HCl pH 8.0 and 500 mM NaCl. Rabbit sera were filtered through 0.22 um Millex GP filter unit (Millipore). 20 ml of filtered sera was then applied to the column and reloaded ten times. The resin was then washed with 200 ml of wash buffer (100 mM Tris-HCl pH 8.0, 500 mM NaCl). Bound antibodies were eluted from the column with 100 mM glycine, 500 mM NaCl pH 2.5 and collected in 500 µl fractions in Eppendorf tubes containing 50 µl of 1 M Tris-HCl pH 8.0. The fractions containing antibodies were determined by Nanodrop ND-1000 spectrophotometer at OD280 nm. Non-phospho-specific IgGs were eliminated from antibodies fraction(s) by passing them through a non-phospho XCEP63-S560 peptide column. Affinity purified XCEP63-PS560 antibody was used at 1/1000 v/v dilution in PBS, 0.1 % Tween 20 v/v with 5 % BSA w/v for immunoblotting and used at 1/300 v/v in standard blocking buffer for immunofluorescence.

2.7 Other antibodies used for immunoblotting

ATM (phospho S1,981) antibody was obtained from Abcam and used at the concentration of 0.2 µg/ml in **T**ris-**b**uffered **s**aline (TBS), 0.1 % Tween 20 v/v with 5 % milk w/v. Anti-ATM/ATR substrate, phospho-serine/threonine antibody (L(S*/T*)Q) was purchased from Cell Signaling Technology and used as suggested by the manufacturers at a 1/1000 v/v dilution in TBS, 0.1 % Tween 20 v/v with 5 % milk w/v. Chk1 antibody was purchased from Santa Cruz Biotechnology and used at a

concentration of 0.2 µg/ml in TBS, 0.1 % Tween 20 v/v with 5 % milk w/v. *Xenopus* Cds1 (Chk2) antibody (kindly given by Howard Lindsay) was used at an approximate concentration of 0.8 µg/ml in PBS, 0.1 % Tween 20 v/v with 5 % milk w/v anti-RanGEF (RCC1) antibody was obtained from Millipore and used at a suggested dilution of 1/1000 in PBS, 0.1 % Tween-20 v/v and 3 % milk w/v. Histone H3 antibody was purchased from Millipore and used at suggested concentration of 0.5 µg/ml in PBS, 0.1 % Tween 20 v/v with 5 % milk w/v.

Secondary immunoblotting antibodies were anti-rabbit or anti-mouse IgG **H**orse**r**adish **p**eroxidase (HRP) linked to whole antibody from sheep (compatible with ECL detection reagents) obtained from GE Healthcare. In general, secondary antibodies were used at recommended dilution of 1/10,000.

2.8 Other antibodies used for immunofluorescence

Anti-gamma (γ) tubulin and anti-alpha (α) tubulin antibodies were obtained from Sigma–Aldrich and used in cell and spindle immunofluorescence at an approximate concentration of 3 µg/ml in blocking buffer. Anti-phospho Histone-H3 (phospho-serine 10) mitosis marker was acquired from Abcam and used in cell immunofluorescence at approximate concentration of 3 µg/ml in blocking buffer. GFP recognizing antibody was at a diluted as recommended at 1/400 in blocking buffer.

Secondary anti-mouse and anti-rabbit IgG (H + L) antibodies Alexa Fluor® red-fluorescent dye (594) and Alexa Fluor® green-fluorescent dye (488) obtained from Invitrogen were used at an approximate concentration of 5 µg/ml.

2.9 Standard Molecular Biology Techniques

Most protocols followed methods published by Sanbrook *et al.,* 1989 and Ausubel *et al.,* 1991 (Sanbrook *et al.,* 1989; Ausubel *et al.,* 1991). More details are given if modifications were undertaken and for more specialised methods.

2.9.1 Preparation of Plasmid DNA

Plasmid DNA was purified using Qiaprep Spin Miniprep kit (Qiagen) and using Eppendorf table-top microcentrifuge as described in kit protocol. In general, plasmid DNA was prepared from transformed *Escherichia coli* (*E. coli*) grown from a single colony overnight at 37 °C in 1ml of supplemented LB medium. DNA was eluted from spin column by 50 µl of provided EB buffer (10 mM Tris·HCl, pH 8.5). XCEP63-GFP fusion DNA was isolated by Qiagen plasmid midi kit according to the provided protocol. DNA concentration was measured using Nanodrop ND-1000 spectrophotometer at OD260 nm. Samples were blanked against EB buffer provided in Qiagen miniprep kit.

2.9.2 DNA analysis by agarose gel

Horizontal agarose gels (Invitrogen, electrophoresis grade) containing 0.4 µg/ml ethidium bromide solution (Bio-Rad) were run in TAE (**T**ris/**a**cetate/**E**DTA) electrophoresis buffer as based on descriptions in Maniatis *et al.,* 1982 (Maniatis *et al.,* 1982). DNA markers were from New England BioLabs (50 bp ladder, 1 kb ladder and/or lambda DNA) and samples were mixed with Gel loading buffer from Calbiochem. Within Bio-Rad Gel doc system, DNA was visualised and images were acquired with ultra violet (OD302 nm) illumination. Alternatively, agarose gels were fixed in 30 % v/v **tri**chloroacetic **a**cid (TCA) for 20 minutes, prepared for and then exposed by autoradiography phosphoimaging (2.10.4).

2.9.3 Purification of DNA from agarose gels

DNA fragments of interest were excised from the agarose gel and underwent Qiaquick gel extraction as described in Qiagen Kit manual.

2.9.4   DNA Digestion with restriction enzymes

Typically 100 µg/ml DNA was treated with the presence of an excess of enzyme, generally 1-2 units of enzyme were applied per µg of DNA. Samples were incubated with corresponding recommended reaction buffer for one to two hours usually at 37 ºC. Enzyme treatments included, *BamHI* and *SalI* digestion linearised pMal–c2X vector and created compatible blunt ends of amplified XCEP63 DNA insert (2.11.2). PcDNA3 plasmid was prepared for association with chromatin beads by digesting with *NotI* and *EcoRI* (2.9.4). PcDNA3 plasmid DNA was linearised with *EcoRI* as a control for chromatin-coated bead investigations into ATM and ATR activity (2.15.1). XCEP63 fusion/tagged plasmids constructs were also restriction enzyme digested and then separated by agarose gel (2.9.2), from which the presence and orientation of XCEP63 DNA insert were determined. XCEP63 mutant DNA was digested with 1 µl of 10 U/µl *DpnI* after PCR site directed mutagenesis procedure (2.9.8.4).

2.9.5   Ligation of DNA fragments

For 'blunt end' ligations, 20 ng of prepared DNA fragments were mixed with 40 ng of digested vector and heated for five minutes at 45 ºC. DNA was then ligated by T4 DNA Ligase in provided T4 DNA ligase buffer at 16 ºC for two hours or overnight.

2.9.6   Screening *E. coli* colonies for the presence of plasmid DNA

Following transformation of *E. coli* with plasmid DNA, a number of colonies were picked and grown in supplemented LB at 37 ºC overnight with shaking. DNA was extracted as previously described with Qiagen miniprep kit (2.9.1). DNA was sequenced (2.9.8.3) to check the presence and quality of plasmid DNA. Bacterial stocks were made by addition of 30 % glycerol and stored at – 80 ºC.

2.9.7   Preparation of chromatin-coated beads

Chromatin coated beads were prepared for anastral spindle assembly in *Xenopus* egg extract (2.14.4.5). Biotinylated pcDNA3 plasmid DNA (Invitrogen) was coupled to

streptavidin beads through Dynal Kilobinder kit (Invitrogen) incorporating a few modifications to protocol described by Heald *et al.,* (Heald *et al.,* 1996). In more detail, pcDNA3 5.4 kb plasmid DNA was prepared by digesting with *NotI* and *EcoRI* creating GC and AT overhanging ends respectively. DNA was ethanol precipitated and resuspended in TE buffer. DNA was subjected to a fill-in reaction performed in 80 μl volume containing 35 μg DNA, 50 μM biotin-dATP, 50 μM biotin-dUTP (Invitrogen), 50 μM thio-dCTP, 50 mM thio-dGTP (Tebu-Bio) and 20 U Klenow (Roche Diagnostics) in supplied Klenow buffer. Reactions were incubated for two hours at 37 °C and then applied to G-25 spin columns (Pharmacia) to remove unincorporated nucleotides.

Biotinylated pcDNA3 plasmid DNA was coupled to streptavidin Dynal beads using Kilobase Binder kit (Invitrogen) according to manufacturer instructions. In brief, 4 μl beads per μg of DNA were coupled in 1 ml final volume of binding buffer overnight at 16°C with rotation. The approximated amount of DNA immobilized was determined by comparing the concentration of DNA in the buffer before and after coupling. The beads were washed with washing solution (Invitrogen) and then with bead buffer (1.5 M NaCl, 10 mM Tris pH 7.6, 1 mM EDTA). Beads were re-suspended in bead buffer at a final concentration of 1 μg DNA/10 μl beads.

2.9.8   Polymerase Chain Reaction (PCR) based techniques

All PCR reactions were carried out on a Peltier Thermal Cycler, DNA engine Tetrad 2 manufactured by MJ Research, USA. Primer annealing temperatures were calculated using the formula described by Baldino (Baldino *et al.,* 1989). When oligonucleotide pairs annealing temperatures differed significantly, the lower one was applied.

2.9.8.1   Amplification of DNA by PCR

PCR reactions usually performed as outlined by Stratagene with 2.5 U of Pfu/Pfu Ultra/Pfu Turbo DNA polymerase. In a volume of 50 μl reactions contained provided reaction buffer with 200 ng of each oligonucleotide primer, 100 ng of DNA template,

25 mM of each deoxynucleotide (dNTPs, purchased as a set from GE Healthcare). The usual PCR program applied followed this three step program.

1) Denaturing step: 95 °C for 1 minute
2) Annealing step: 44 °C to 60 °C depending on annealing temperature of individual
                        primers for 30 seconds
3) Elongation step: 75 °C for 1 minute

Product was usually amplified for 30 cycles and finally incubated at 4 °C.

2.9.8.2   Annealing of poly A and poly T (pA/pT) oligomers

Annealed poly-deoxy-(A)70 and poly-deoxy-(T)70 oligomers formed DNA linear molecules (pA/pT), which were applied to *Xenopus* egg extract experiments. 3 µg/µl poly A and 3 µg/µl poly T oligomers were annealed in PK buffer provided by New England BioLabs either by incubating at a constant 16 °C for one hour or alternatively underwent the following PCR program (Costanzo *et al.,* 2000; Guo and Murphy, 2000; Kumagai and Durphy, 2000).

1) Denaturing step: 95 °C for 3 minutes
2) Annealing steps: 65 °C for 10 minutes
                        37 °C for 10 minutes
                        23 °C for 10 minutes

2.9.8.3   DNA sequencing

Plasmid DNA for automatic cycle sequencing was prepared using the Bigdye® terminator v1.1 cycle sequencing kit as outlined in the manufacturer's protocol (Applied Biosystems (Applera UK). Dye terminators were introduced into the DNA sequence during repeated cycles of linear PCR. In short, 8 µl terminator ready reaction made up of BigDye® terminator sequencing mix and BigDye® terminator reaction mix was mixed with 3.2 pmole of primer, and 500 ng of plasmid DNA template in a total volume of 20 µl. Samples were subjected to the following PCR program:

1) Initial denaturing step: 96 $^{\circ}$C for one minute

2) Denaturing step: 96 $^{\circ}$C for ten seconds

3) Annealing step: 44 $^{\circ}$C to 60 $^{\circ}$C depending on annealing temperature of individual primers for five seconds

4) Elongation step: 60 $^{\circ}$C for four minutes

In general, the product was amplified for 25 cycles from step two and then finally incubated at 4 $^{\circ}$C.

PCR extension products were purified through Qiagen DyeEx™ 2.0 spin kit as outlined in the DyeEX handbook. Drying of samples and DNA capillary sequencing (Applied Biosystems 3730 DNA analyser) was undertaken by the CRUK in house sequencing service.

2.9.8.4   Quickchange Site Directed Mutagenesis

XCEP63 mutants were generated using PCR based Stratagene Quickchange Site Directed Mutagenesis Kit. XCEP63 serines (S) and threonines (T) of candidate and speculative ATM and ATR phosphorylation sites were converted to alanines (A) in XCEP63 cDNA contained within pCS2 library expression vector. Mutagenesis was performed as outlined by the manufacturer protocol. In brief, XCEP63 oligonucleotide primers were designed with a melting temperature of greater than or equal to 78 $^{\circ}$C between 25 and 45 bases in length with base change corresponding to the alanine mutation in the centre. The oligonucleotide sequences described in XCEP63 ATM and ATR phosphorylation site investigations are shown in table two.

Serine/ Threonine Mutation	Mutagenic Oligonucleotide (5'to 3')	Coordinates	Direction (-/+)
S41	ATGCTGGATCACAAGAGGGCACAGTGGGAAGCAGAGACAG	103-142	+
S41	CTCTGTCTCTGCTTCCCACTGTGCCCTCTTGTGATCCAGC	1977-2016	-
S135	GAGGAGGAAAGAGCCGAGGTCAGCCGTCTG	391-420	+
S135	CAGACGGCTGACCTCGGCTCTTTCCTCCTC	1701-1730	-
S202	CCTAGTCGGCCGTGCTGAACTTCAGAACCTCAG	591-623	+
S202	CTGAGGTTCTGAAGTTCAGCACGGCCGACTAGG	1498-1530	-
S353	AGTGTTGAGTCTGTGACAGCCCAGTGTCAACTGCTGGCAAAG	1039-1080	+
S353	CTTTGCCAGCAGTTGACACTGGGCTGTCACAGACTCAACACT	1041-1082	-
S391 *	CTGAAAGGCCAGCTCGCACAGGCTGAGCTGACCCAC	1156-1191	+
S391 *	GTGGGTCAGCTCAGCCTGTGCGAGCTGGCCTTTCAG	930-965	_
S409 and T412	AGGAAGGAGATCGCACAGCTCGCTCAGGAGTTACACCAG	1211-1253	+
S409 and T412	CTGGTGTAACTCCTGAGCGAGCTGTGCGATCTCCTTCCT	868-910	-
T471	GTTATCGGAACTCCTTCAGGCGCAAGAGCCGGATGTGGCG	1392-1431	+
T471	CGCCACATCCGGCTCTTGCGCCTGAAGGAGTTCCGATAAC	609-729	-
S497	GCAGAGGGAGCTGCTACAGGCACAGGAGAAACTGGAGCTGATAGCG	1470-1515	+
S497	CGCTATCAGCTCCAGTTTCTCCTGTGCCTGTAGCAGCTCCCTCTGC	606-651	-
S520	CCAGAATGCAGTGGATAGTATAGCTCAAGAGCTGTTGAATAAACAGG	1536-1582	+
S520	CCTGTTTATTCAACAGCTCTTGAGCTATACTATCCACTGCATTCTGG	539-585	-
S550	CAGGAGATGCAGACTTTTAGGGCCCAACAAGATGCAGCTTCAAGTGG	1627-1673	+
S550	CCACTTGAAGCTGCATCTTGTTGGGCCCTAAAAGTCTGCATCTCCTG	488-494	-
S560 (1) *	TGCAGCTTCAAGTGGAAGCGCACTGGAGTCTATATTCTCTG	1659-1699	+
S560 (1) *	CAGAGAATATAGACTCCAGTGCGCTTCCACTTGAAGCTGCA	422-462	-
S560 (2) *	TGCAGCTTCAAGTGGAAGCGATCTGGAGTCTATATTCTCTG	1659-1699	+
S560 (2) *	CAGAGAATATAGACTCCAGATCGCTTCCACTTGAAGCTGCA	422-462	-
S603 *	TTCCACCCACCGCCCCAGCAAATGC	1796-1820	+
S603*	GCATTTGCTGGGGCGGTGGGTGGAA	301-325	-

Table 2. A list of Oligonucleotides used in examples of XCEP63 serine/threonine site directed mutagenesis

Mutated base residues are shown in red (refer to Appendix one for XCEP63 amino acid sequence). XCEP63 DNA sequence primer coordinates are also indicated, as well as the direction of the primers (+ indicates binding to coding strand and – indicates binding to complementary strand). Serine 560 requires two oligonucleotides (1 and 2) in order to convert amino acid to alanine. * indicates the potential phosphorylation sites identified by Mass Spectrometry analysis.

In general, 50 µl of reaction mixtures contained provided reaction buffer supplemented with 20 ng of XCEP63 plasmid DNA, 125 ng of both primers, 1 µl of provided dNTP mix and finally 1 µl of PfuTurbo DNA polymerase 2.5 U/µl. Samples were applied to the following PCR Cycling parameters.

1) Initial denaturing step: 95 ^{o}C for 30 seconds
2) Denaturing step: 95 ^{o}C for 30 seconds
3) Annealing step: 55 °C for one minute
4) Elongation step: 68 ^{o}C for ten minutes

Amplification reactions were cycled in general 18 times from step two and then cooled. Reactions then proceeded to enzyme digestion with *DpnI* (2.9.4). The mutated XCEP63 plasmid DNA was transformation into *E. coli* cells (DH5α or One Shot® TOP10 cells (Invitrogen) following manufactures guidelines. Cells were grown at 37 ^{o}C in LB medium for one hour and then spread on LB plates supplemented with 100 µg/ml ampicillin which were inverted overnight at 37 ^{o}C. Colonies were picked and grown at 37 ^{o}C in LB medium with 100 µg/ml ampicillin for one hour. Plasmid DNA was isolated by Qiaprep spin miniprep kit (2.9.1) and incorporation of alanine mutation was checked by DNA sequencing (2.9.8.3). Mutants were then screened following the procedure described in 2.15.5.

2.10   Separation and detection of proteins

2.10.1 SDS polyacrylamide gel electrophoresis (SDS-PAGE)

Standard polyacrylamide resolving gels was based on descriptions by Laemmli, which were outlined within Bio-Rad solution manual (Laemmli, 1970). Unless otherwise stated standard 10 %, resolving SDS (Sodium dodecyl sulphate) gels were usually used, made up with Bio-Rad 37:5:1 Bis-Acrylamide solution, 375 mM Tris-HCl pH 8.8 and 0.1 % SDS (**S**odium **d**odecyl **s**ulphate) w/v. For assessment of Chk1 in treated *Xenopus* egg extract, samples underwent electrophoresis on an 8 % SDS ultra pure Bis-Acrylamide gel. The ratio of acrylamide to bisacrylamide was 37.5.1 made from 30 % Acrylagel Acrylamide and 2 % ultra pure Acrylagel Bis-Acrylamide in 375 mM Tris-HCl pH 8.8 with 0.1 % SDS w/v.

Anderson SDS-PAGE was also used to resolve proteins, particularly in *Xenopus* egg extract shift assays. Anderson gels were prepared based on descriptions by Anderson (Anderson *et al.,* 1973). 10 % Anderson resolving gels were prepared with 40 % Acrylamide solution (with a finial of 10 v/w) and 2 % Bis-Acrylamide solution (with a finial of 0.13 % v/v), 375 mM Tris-HCl resolving buffer and 0.1 % w/v SDS.

Typically, acrylamide gels were made up using Bio-Rad stacking buffer (0.5 M Tris-HCl pH 6.8) and resolving gel buffer (1.5 M Tris-HCl pH 8.8). Stacking gels topping resolving gels were 4 % acrylamide and made up with Bio-Rad 37:5:1 Bis-Acrylamide solution in 120 mM Tris-HCl pH 6.8. Ammonium persulphate (0.05 % w/v) and N,N,N′,N′-**Te**tra**m**ethyl**e**thylene**d**iamine (TEMED, 0.05 % v/v) were used to polymerise acrylamide. Gels were made up and assembled within the Bio-Rad mini system apparatus or in Sigma–Aldrich vertical electrophoresis unit for medium or large gels. As indicated in the figure legends, Bio-Rad medium Criterion 4-12 % pre-cast gels were also used to separate proteins, samples underwent electrophoresis in Bio-Rad XT-MOPS running buffer within Bio-Rad Criterion gel apparatus.

Reaction samples were prepared for electrophoresis by addition of Bio-Rad sample buffer prepared with 5 % β-mercaptoethanol, which were then boiled for four minutes unless otherwise stated. Bio-Rad Precision plus dual colour marker was loaded adjacent to samples. Electrophoresis was performed in 1 x running buffer (24 mM Tris base, 193 mM glycine and 0.1 % w/v SDS). In general, small and medium gels underwent electrophoresis at a constant voltage of 200 V and for larger gels a constant voltage of 280 V (Bio-Rad power pack) was applied. Electrophoresis was stopped once the front dye had reached the bottom of the gel or alternatively gels were left running for longer if a greater protein separation was required.

2.10.2 Detection of proteins by Coomassie Blue staining

Polyacrylamide gels were rotated for one to two hours with Coomassie Blue stain at room temperature or alternatively incubated for a few minutes in pre-warmed staining solution. Coomassie Blue stain contained 0.1 % w/v Coomassie Blue, 30 % v/v methanol, 10 % v/v acetic acid. The stain was removed from gels in a destain solution

containing 30 % v/v ethanol, 10 % v/v acetic acid rotating for a minimum of one hour at room temperature.

2.10.3 Detection of proteins by SYPRO® Ruby staining

All fixation and staining steps were performed with gentle agitation at room temperature following the long procedure described in Invitrogen manufacturers protocol. In summary, polyacrylamide gels were fixed twice for 30 minutes with 100 ml of 50 % v/v methanol, 7 % v/v acetic acid solution at room temperature. SYPRO® Ruby stain was applied overnight and finally washed with 100 ml of 10 % v/v methanol, 7 % v/v acetic acid. Fluorescent images of gels were acquired on GE Healthcare Typhoo Trio variable mode imager using florescence excited by Green laser source at 532 nm and emission recorded at 610 nm. Gel were visualised on a blue light transilluminator (Clare Chemical Research, Dark Reader) and protein bands of interest were excised with clean scalpel.

2.10.4 Autoradiography

Gels to be fluorographed were dried on Whatman 3MM Chromatography paper in a Bio-Rad gel dryer for two hours with heat curve cycle program reaching 90 °C. Radioactive gels were placed in intensifying exposure cassettes (Sigma–Aldrich) and exposed to Kodak biomax MR-1 film or MP autoradiography hyperfilm for between one and three days (^{35}S radioactive labelling) stored at -80 °C as specified by Laskey (Laskey, 1980). Alternatively, ^{32}P radioactive labelling gels were exposed to a phosphoscreen (GE Healthcare) for approximately 12 hours or for a longer time depending on radioactive signal. The recorded radioactive signal was monitored within a phosphoImager (GE Healthcare, Typoon Trio variable mode imager) and measured by ImageQuant software.

2.10.5 Immunoblotting

Immunoblotting or Western blotting was based on procedure outlined by Towbin *et al.,* 1979 (Towbin *et al.,* 1979). Polyacrylamide gels were stacked between 3 M Whatman

filter paper, 3 mM Chromatography paper and nitrocellulose transfer membrane (Protran® 0.45 or 0.2 µM pore size). All constituents were pre-soaked in transfer buffer (24 mM Tris base, 193 mM glycine, 10 % v/v methanol, 0.01 % v/v SDS), then assembled in the Bio-Rad mini or larger gel blot transfer system, which was filled with transfer buffer. In the mini system, proteins were transferred at 30 mA (milliamp) overnight or 200 mA for two hours. For larger blots proteins were transferred at 200 mA overnight or 400 mA for two hours. All transfer systems were prevented from overheating by stirring at 4 °C.

Nitrocellulose membranes were blocked with 5 % BSA w/v or 5 % milk w/v in PBS with 0.1 % TWEEN 20 v/v (PBST) for one hour rotating at room temperature or overnight at 4 °C. An appropriate dilution of antibody was prepared in PBS or TBS, BSA or milk and 0.1 % TWEEN 20 v/v (refer to 2.6.3, 2.6.4 and 2.7). Antibody solution immersed the membrane and was rotated at room temperature for one hour or 4 °C overnight. The membrane was rinsed once briefly with PBS and three times for 20 minutes with PBST to remove unbound primary antibody. HRP conjugated anti-rabbit or anti-mouse secondary antibody (2.7) was applied generally in 3 % BSA or 3 % milk w/v PBST for one hour rotating at room temperature. The membrane was rinsed as previously to remove non-specifically bound antibody. ECL detection reagents were mixed and applied to the blot for one minute and chemiluminescence was detected by exposure to ECL hyperfilms.

2.10.6 Immunofluorescence

Cells were cultured or spun on precoated poly-L-lysine 12 mm^2 coverslips and then fixed with room temperature 3 % paraformaldehyde for 10 minutes. *Xenopus* egg extract assembled spindle assembly reactions were spun onto poly-L-lysine–coated coverslips as described in 2.14.4.6 and then fixed with –20 °C methanol for two minutes. Coverslips were processed essentially as described by Walczak (Walczak *et al.,* 1996). Fixed coverslips were rehydrated twice for five minutes in TBS-TX (TBS, 0.1 % Triton X-100 v/v) and then blocked for 30 minutes at room temperature in a standard blocking buffer containing TBS-TX and 2 % BSA w/v. Coverslips were rinsed three times with TBS-TX and immersed in an appropriate dilution of primary antibodies (2.8) in blocking buffer for one hour at room temperature. Unbound antibody was

removed in three five-minute washes with TBS-TX. Secondary Alexa Fluor® fluorescent antibodies in blocking buffer were applied for one hour at room temperature. Coverslips were rinsed again three times with TBS-TX and then immersed in 2 μg/ml Hoechst 33342 or DAPI in TBS-TX. Coverslips were mounted onto microscope slides using ProLong® Gold antifade reagent (Invitrogen) or 90 % glycerol, 1 mg/ml *p*-phenylenediamine, 20 mM Tris-HCl, pH 8.8 and sealed with nail varnish. All images were acquired at room temperature using a DeltaVision RT Olympus 1 x 70 (DV 41040) microscope from Applied Precision® using softWoRx suite 3.5 software.

2.11   XCEP63 construct fusions

2.11.1   GFP tagged XCEP63: XCEP63-GFP

XCEP63 ORF was amplified by PCR from cDNA contained within pCS2 library expression vector by forward oligonucleotide 5' CAAC**ATG**GAAGCTTTGTT ACAAGG 3' (incorporation start codon shown in bold) and reverse oligonucleotide 5' AAATGTGCAGAACATTTCTTC 3'. XCEP63 DNA was cloned into Invitrogen Gateway® pcDNA™-DEST47 vector via pENTR™/D-TOPO® to incorporate carboxyl-terminal **G**reen **F**luorescence **P**rotein (GFP) fusion as described in manufacturers manual using Gateway® LR Clonase™ II Enzyme Mix. XCEP63-GFP DNA was transformed into One Shot® TOP10 *E. coli* (Invitrogen) grown in LB at 37 ºC with shaking for one hour. Cells were spread onto LB plates supplemented with 100 μg/ml ampicillin and inverted overnight at 37 ºC. Clones were checked by restriction enzyme digestion (2.9.4) and DNA sequencing (2.9.8.3) for the presence of plasmid DNA and XCEP63 DNA insert orientation and quality.

XCEP63-GFP plasmid DNA was transfected into *Xenopus* Tissue Culture (XTC) cells (2.16.3) or alternatively transcribed and translated in TnT® T7 Quick Control Coupled translation/transcription System (Promega) in the absence of [^{35}S]-methionine as described in 2.12 for use in *Xenopus* egg extract spindle assembly assay (2.14.4.1).

2.11.2 MBP fused XCEP63: XCEP63-MBP

XCEP63-MBP (**M**altose **b**inding **p**rotein) fusion was constructed following the procedure outlined by New England BioLabs instruction manual for pMAL™ protein fusion and purification system. pDEST-MAL (pMAL–c2X) construct was originally custom made and donated by Simon Boulton, which then became commercially available as pMAL-c2X. XCEP63 was amplified by PCR using Pfu Ultra DNA polymerase purchased from Stratagene. The forward primer was 5' GGATCCGAAGCTTTGTTACAAGGGCTTCAACG 3' incorporating *BamHI* restriction enzyme digestion site (shown in red). The reverse primer 5' GTCGAC**CTA**AAATGTGCAGAACATTTCTTCTTTG 3' contained a stop codon (shown in bold) and incorporated a *SaI1* restriction digestion site (shown in red). Both pMAL–c2X vector and XCEP63 PCR product were digested by *BamHI* and *SalI* restriction endonucleases (2.9.4). Digestion products were checked by separating on an agarose gel, then excised and isolated using Qiaquick Gel Extraction Kit (2.9.3). 40 ng of prepared vector and 20 ng of XCEP63 insert were ligated. 5 µl of the ligation reaction was transformed into OneShot® BL21 Star™ (DE3) chemically competent *E. coli,* which was then spread on a LB plate containing 100 µg/ml ampicillin as described in Invitrogen product manual. Plates were inverted overnight at 37 °C. A number of clones were checked for the presence of plasmid, and the orientation and quality of the XCEP63 insert by restriction enzyme digestion (2.9.4) and DNA sequencing analysis (2.9.8.3). For mutant studies, XCEP63-MBP construct at serine 560 was converted to alanine (XCEP63-MBP- S560A) by site directed mutagenesis (2.9.8.4).

2.11.2.1 Expression and purification of XCEP63-MBP recombinant proteins

E. coli transformed with XCEP63 pMAL-c2X vector construct were grown in LB supplemented with 50 µg/ml carbenicillin and 0.2 % v/v glucose at 37 °C. Once the OD600 nm measured 0.5-0.7, the expression of XCEP63-MBP recombinant protein was induced with addition of 0.3 mM **i**so**p**ropyl-beta-D-**t**hio**g**alactopyranoside (IPTG) obtained from Promega at 25 °C for five hours. *E. coli* were harvested at 4,000 rcf (**r**elative **c**entrifugal **f**orce) for 15 minutes in Beckman J6-MC in JS-4.2 swing bucket rotor at 4 °C, washed with PBS and then re-pelleted under the same conditions.

Purification of XCEP63-MBP fusion protein was undertaken as follows. Pelleted *E. coli* were re-suspended in column buffer (20 mM Tris-HCl, 200 mM NaCl, 1mM EDTA pH7.4) containing a complete protease inhibitor cocktail tablet (Roche Diagnostics). Lysate was passed through a pressurised Cell Disruptor from Constant System Ltd at 25 kpsi (**K**nots **p**er **s**quare **i**nch). Lysate was clarified at 20,000 rpm (**r**evolutions **p**er **m**inute) for 30 minutes in a Sorvall fixed angle rotor SS-34 at 4 °C. The supernatant was transferred to fresh tubes and then centrifuged at the same conditions for a further 20 minutes. MBP amylose bead slurry obtained from New England Biolabs was equilibrated three times by column buffer and spun at 4,000 rpm for five minutes in a Sorvall RT7 centrifuge. Clarified extract and equilibrated amylose beads were coupled by rotating for a minimum of two hour or 4 °C overnight. The extract/beads mix was then transferred to a column and unbound lysate was drained. The column was washed with 12 column volumes of column buffer and then eluted with 25 ml of elution buffer (20 mM Tris-HCl, 200 mM NaCl, 1 mM EDTA pH 7.4 and 10 mM maltose) collected in 500 µl fractions. Fractions containing XCEP63 protein MBP fusion were pooled and concentrated in Amicon ultra centrifugal filter device from Millipore. XCEP63-MBP protein was transferred to Dialysis cassette purchased from Perbio and dialysed in 150 mM KCl, 20 mM Hepes pH 7.5, 1 mM 1,4-**Di**thio-DL-**t**hreitol (DTT) at 4 °C overnight.

2.12 Coupled transcription and translation of cDNAs

cDNAs from pooled expression library (2.14.5) and XCEP63 site directed phosphorylation mutants (2.9.8.4) were transcribed and translated by TnT® SP6 Quick Control Coupled Translation/Transcription System (rabbit reticulocyte lysate) obtained from Promega following the protocol provided. In brief, 20 µl reactions contained 1 µl (100 ng/µl) of cDNA pool, 19 µl of translation mix diluted with provided nuclease free water and 0.5 µCi/µl of [^{35}S]-methionine (Promix, GE Healthcare). Translation was allowed to proceed for 90 minutes at 30 °C. Translated cDNAs were then exposed to *Xenopus* egg extract. XCEP63-GFP construct was also transcribed and translated similarly but within TnT® T7 Quick Control Coupled Translation/Transcription System (Promega) in the absence of [^{35}S]-methionine. Translated XCEP-GFP was used in *Xenopus* egg extract spindle assembly (2.14.4.4).

2.13   *Xenopus* laevis egg and sperm nuclei preparation

Cytostatic factor (CSF) arrested *Xenopus* egg extract and sperm nuclei were prepared in the most part as described by Murray, 1991 (Murray, 1991).

2.13.1   *Xenopus* egg extract

Female *Xenopus* were injected with 50 units of pregnant mare serum gonadotrophin within six days prior to requirements. On the day before (ideally day six) egg collection, females were induced to ovulate by injection of 400 units of human chorionic gonadotrophins. Eggs were laid and collected in MMR buffer (100 mM NaCl, 2 mM KCl, 1 mM $MgCl_2$, 0.1 mM EDTA and 5 mM Hepes pH 7.8). Some alterations were made to CSF egg extract protocol described by Murray 1991, changes to method are detailed in chapter 3, section 3.3 and the procedure used is described below. Throughout the procedure, eggs and extracts from different frogs remained separated. In short, eggs were de-jellied by washing two to three times in 2 % w/v L-cysteine in salt solution (100 mM KCl, 5 mM **e**thylene **g**lycol-bis (2-aminoethyether)-N,N,N',N'-**t**etraacetic **a**cid (EGTA), 0.1 mM $CaCl_2$, 2 mM $MgCl_2$ at pH 7.8) for approximately five minutes in total. Eggs were washed three to four times in chilled XB containing salt solution with 10 mM HEPES pH 7.8 and 50 mM sucrose. Eggs were transferred to 14 ml polypropylene tubes (Falcon 2059) in minimal volume buffer with 10 µg/ml LPC protease inhibitor mix (leupeptin trifluoroacetate salt, pepstatin A, chymostatin) and 10 µg/ml cytochalasin B. Eggs were packed at 1,200 rpm in Sorvall RT7 centrifuge at 4 °C for 1 minute and excess XB buffer was removed from above the eggs. Eggs were then crushed at 4 °C by centrifuging for 20 minutes at 12,000 rpm in a Sorvall swing out HB-4 rotor. The cytoplasmic layer was collected into a tube at 4 °C using a syringe and needle through the side of the tube avoiding top lipid layer and debris pellet. Collected extract was supplement with energy mix (7.5 mM creatine phosphate (Calbiochem), 1 mM ATP, 0.2 mM EGTA, 1 mM $MgCl_2$), 10 µg/ml LPC protease inhibitor mix and 10 µg/ml cytochalasin B, then transferred into 5 ml polypropylene tube (Falcon, 2063) inserted into a 14 ml polypropylene tube (Falcon, 2059) containing 1 ml of water. In the same conditions of the first spin, extract was clarified to remove residual debris for a further 10 minutes. The cytoplasmic fraction was again collected and used immediately for spindle assembly assays. Alternatively, extract was supplemented with 200 mM

sucrose and then aliquoted in liquid nitrogen for long-term storage in liquid nitrogen cryostats. In some experiments, CSF egg extracts were induced to enter interphase by a final concentration of 0.4 mM $CaCl_2$ and supplemented further with 0.2 mg/ml Cycloheximide (Calbiochem).

2.13.2 *Xenopus* **sperm nuclei**

Male frogs were primed with 50 units of Folligon five to nine days before the testes are removed. Testes were cleaned in EB buffer (50 mM KCl, 50 mM Hepes KOH pH 7.6, 5 mM $MgCl_2$, 2 mM β-mercaptoethanol) and finely chopped with a scalpel. The EB buffer and testes suspension was homogenised, then filtered through 25 μM Nitex membrane (Nybolt, UK) and centrifuged at 3,400 rpm for five minutes at 4 °C in a HB-4 Sorvall swing out rotor. The pellet was resuspended in 2 ml of SuNaSp (250 mM sucrose, 75 mM NaCl, 0.5 mM spermidine, 0.15 mM spermine) and recentrifuged as previously. Again, the pellet was resuspended in SuNaSp to give a total volume of 2 ml to which 40 μg/ml lysolecithin was added and incubated for five minutes at room temperature. The integrity of sperm membranes were checked by Hoescht staining (1 μl/ml). Sperm preparations with greater than 95 % demembranation proceeded, otherwise pelleting and lysolecithin treatments were continued. Demembraned sperm suspension was centrifuged at 3,000 rpm for five minutes. Pelleted sperm was resuspended in 2 ml of SuNaSp containing 3 % BSA and then centrifuged as previously. The pellet was washed with EB buffer twice and finally resuspended in 500 μl EB buffer supplemented 30 % glycerol. Small aliquots of prepared sperm nuclei at a density of 1-5 x 10^7 were frozen in liquid nitrogen and stored at -80 °C.

2.14   **Techniques involving *Xenopus* egg extract**

2.14.1 **ATM and ATR activation and inhibition**

CSF egg extract were then treated with 5 ng/μl linear DNA (pA/pT) usually for 30 minutes at 20 °C as described in Costanzo *et al.,* 2004 (Costanzo *et al.,* 2004a). Alternatively, extract was supplemented with 1,000 sperm nuclei/μl and treated with 0.25 U/μl *EcoRI* to induce chromosomal breakage usually for 30 minutes at 20 °C based

on descriptions by Grandi *et al.,* 2001 and Yoo *et al.,* 2004 (Grandi *et al.,* 2001; Yoo *et al.,* 2004b). ATM and ATR were inhibited by the addition of 2 mM caffeine or 20 µM Ku55933 (ATM inhibitor) (Hickson *et al.,* 2004). Investigations into XCEP63 phosphorylation by ATM and ATM, extracts were supplemented with 50 ng/µl recombinant XCEP63-MBP recombinant protein (2.11.2.1) or left un-supplemented (endogenous XCEP63).

2.14.2 Chromatin binding

Chromatin isolation was based on previous description in Costanzo *et al.,* 2003 with some modifications (Costanzo *et al.,* 2003). CSF egg extracts were treated in 50 µl aliquots in the absence or presence of 3,000 sperm nuclei/µl. Samples with sperm nuclei were treated with and without 0.25 U/µl of *EcoRI*. At time points, 0, 30, 60 and 90 minutes after incubation at 23 °C, extracts were mixed with 500 µl of cold buffer (100 mM KCl, 50 mM HEPES pH 7.5, 2.5 mM $MgCl_2$) with 0.25 % Ipegal v/v and kept at 4 °C. The control sample without sperm nuclei was diluted at 90 minutes. Reactions were under-layered with 200 µl of buffer with 20 % w/v sucrose and spun at 10,000 rpm for five minutes at 4 °C in a Sorvall adapted HB-6 rotor. Supernatants were removed leaving approximately 100 µl, washed with 500 µl of buffer and spun in a table-top Eppendorf centrifuge at 13,000 rpm for five minutes at 4 °C. Supernatants were removed leaving approximately 20 µl and Bio-Rad sample buffer was added. Samples were boiled for 4 minutes and then underwent SDS-PAGE (2.10.1).

2.14.3 Immunoprecipitation of Plx1

Trenz *et al.,* 2008 previously described Plx1 antibody and application in precipitating Plx1 (Trenz *et al.,* 2008). Plx1 was precipitated from 20 µl of pre-treated extract by incubation with 5 µl of anti-Plx1 serum in 200 µl of PBS. Reactions were rotated for one hour at 4 °C and then protein A sepharose beads were added. After an additional hour of incubation, Plx1 immunoprecipitates were washed in PBS containing 0.2 % Ipegal v/v. Immunoprecipitates proceeded to Plx1 activity assessment with Caesin recombinant protein (2.15.2).

2.14.4 Spindle assembly in *Xenopus* egg extract

Spindle assembly assays were performed in manipulated fresh CSF *Xenopus* egg extracts. The procedure of spindle assembly in *Xenopus* egg extract was essential as described by Sawin and Mitchison, 1991 and reviewed in more detail by Desai *et al.,* 1999 (Sawin and Mitchison, 1991; Desai *et al.,* 1999). Spindle assembly and the isolation of samples onto coverslips were originally described by Evans *et al.,* 1985 (Evans *et al.,* 1985).

2.14.4.1 Half spindle assembly

CSF extract was supplemented with 1,000 sperm nuclei/μl and, unless otherwise stated, further supplemented with 50 μg/ml rhodamine labeled tubulin (Universal Biologicals Ltd). Extracts were subdivided into 20 μl and incubated for 90 minutes at 20 ℃. Spindles were then isolated as described in 2.14.4.6.

2.14.4.2 Bipolar spindle assembly

CSF extract was supplemented with 1,000 sperm nuclei/μl and induced into interphase with addition of $CaCl_2$ to a finial concentration of 0.4 mM and further supplemented with Cycloheximide (0.2 mg/ml). Extract was incubate for two hours at 20 °C and after which a half volume of CSF extract was added. Extracts were supplemented with 50 μg/ml rhodamine-labeled tubulin and incubated for 60 minutes at 20 °C in 20 μl reactions. Similarly spindles were then isolated as described in 2.14.4.6.

2.14.4.3 Spindle assembly in the presence of active ATM and ATR

ATM and ATR activation was induced in spindle assembly extracts by introducing *EcoRI* (0.25 U/μl), *NotI* (0.25 U/μl), linear DNA (pA/pT 5 ng/μl) or doxorubicin (5 μM). To inhibit ATM and ATR, caffeine (2 mM) or Ku55933 (ATM inhibitor 20 μM) were added. CSF-XB extract preparation buffer was used to compensate for volume changes.

2.14.4.4 Protein additions to spindle assembly

In spindle assembly assays with or without ATM and ATR activating treatments, proteins were added as follows (2.14.4.3). Again, CSF-XB extract preparation buffer was used to compensate for volume changes. As described by Carazo-Salas *et al.,* 1999, 2.5 μl of constitutively active RanQ69L recombinant protein (Jena Bioscience) was added to spindle assembly assay (Carazo-Salas *et al.,* 1999). Excess Plx recombinant protein was introduced at 80 ng/μl. XCEP63-GFP transcribed/translated protein (2.12) from DNA construct (2.11.1) was added to extracts at a ratio of 1/5 respectively. XCEP63 immunodepleted spindle assembly extracts were reconstituted with 50 ng/μl XCEP63-MBP (WT) or XCEP63- MBP-S560A recombinant proteins (2.11.2.1).

2.14.4.5 Anastral spindle assembly

Anastral spindles formation in *Xenopus* egg extract was undertaken as essentially described by Heald *et al.,* (Heald *et al.,* 1996). CSF extract was supplemented with 5 ng/μl chromatin-coated bead (2.9.7) or beads alone and induced into interphase with addition of $CaCl_2$ to a finial concentration of 0.4 mM and further supplemented with cycloheximide (0.2 mg/ml). Extracts were incubated for two hours at 20 °C and after which a half volume of CSF extract and 50 μg/ml rhodamine-labeled tubulin were added. Extracts were incubated for 45 minutes at 20 °C in 20 μl reactions. Spindles were then isolated for analysis as described below (2.14.4.6).

2.14.4.6 Isolation of spindles onto coverslips

5 ml snap-cap tubes (Falcon) were prepared with 1 ml of dilution buffer containing BRB80 (80 mM Pipes (Piperazine-N,N'-bis [2-ethanesulfonic acid]), pH 6.8, 1 mM $MgCl_2$, 1 mM EGTA) supplemented with 30 % glycerol and 1 % Triton X-100 and spindles assembly extract reactions were transferred then mixed gently. Samples are further mixed and incubated for five minutes at room temperature with 1 ml of fixation buffer containing BRB80 with 30 % glycerol, 1 % v/v Triton X-100 and 4 % formaldehyde solution. Adapted Corex centrifuge tubes were assembled with a 12 mm^2 coverslip pre-coated with poly-L-lysine placed on top of a removable plastic disc at the

bottom of the tube. 5 ml of 40 % glycerol BRB80 cushion was added to tubes onto which the fixed samples were layered. Samples were centrifuged in a HB-6 Sorvall rotor at 5500 rpm for 20 minutes at 18 °C. Samples were aspirated below the sample-cushion interface and rinsed with BRB80. The remaining solution was aspirated and the coverslip was removed. As described in 2.8, coverslips were methanol fixed and were either mounted face downwards in mounting medium onto microscope slides or alternatively underwent immunofluorescence (2.10.6).

2.14.5 *Xenopus* cDNA library screening for ATM/ATR substrates

A screen based on a *Xenopus* cDNA expression library was developed from methodology described by (Lustig *et al*, 1997) to identify novel ATM/ATR targets (Lustig *et al.,* 1997). The cDNA library, kindly donated by Tony Hyman, consisted of full-length normalized *Xenopus laevis* egg cDNAs containing 7296 clones within a modified pCS2 expression vector arrayed individually into 384-well plates. cDNAs were pooled in rows and columns from plates, then transformed into *E. coli*, which were then cultured. DNA pools were obtained by Qiagen miniprep kit and then transcribed and translated by TnT® SP6 Quick Control Coupled translation/transcription System (Promega) in the presence of [^{35}S]-methionine (2.12). *Xenopus* interphase egg extract pre-treated for 30 minutes at 20 °C with and without 50 ng/μl pA/pT. Translated cDNA pools (2 μl) were mixed with 2 μl of pre-treated extract and incubated for 30 minutes at 20 °C. Reactions were mixed with Bio-Rad sample buffer and then boiled for one minute and then separated on a standard large 10 % SDS-PAGE gel (2.10.1). Polyacrylamide gels were incubated with fixative (20 % v/v methanol, 15 % v/v acetic acid) for 20 minutes and then 100 mM sodium saliatate for ten minutes with agitation. Gels then underwent autoradiography (2.10.4).

Shifts in gel migration patterns in the presence of pA/pT were pursued as possible candidates for ATM/ATR substrates. Intersecting rows and columns of cDNA arrayed in 384 well-plates were pooled, and transformed in into *E. coli* strain DH5α (Invitrogen). In order to isolate the clone of interest, DNA from cultures was purified using Qiagen Miniprep kit, then translated as previously and re-screened. Each cDNA was represented twice, comparisons were made between 'row' and 'column' of translated cDNAs to isolate the well with the clone containing the cDNA encoding the

protein of interest. The proteins were then identified by DNA sequencing (2.9.8.3). Isolated translated proteins of clones were then re-tested with *Xenopus* egg extract in the absence and presence of 5 ng/µl pA/pT with and without 5 mM caffeine.

2.14.6 Immunodepletion of XCEP63

Depletion of XCEP63 from *Xenopus* egg extracts was undertaken with polyclonal antibody sera raised against full-length 6xHisXCEP63 based on protocol detailed in Desai *et al.,* (Desai *et al.,* 1999). Anti-XCEP63 sera (100 µl) and 25 µl Protein A sepharose beads (GE Healthcare) were coupled in EB buffer (25 mM Hepes pH 7.8, 15 mM MgCl$_2$, 20 mM EGTA, 10 mM DTT, 80 mM beta-Glycerophosphate) at room temperature for two hours or overnight at 4 ℃ with rotation. Unbound IgGs were removed by washing twice with 400 µl of EB buffer and twice with 400 µl of CSF egg extract XB preparation buffer (100 mM KCl, 0.1 mM CaCl$_2$, 10 mM HEPES (N-[2-Hydroxyethyl] piperazine-N'-[2-ethanesulphonic acid] pH 7.7, 50 mM sucrose, 5 mM EGTA, 2 mM MgCl$_2$). 50 µl of extracts were rotated at 4 ℃ for one hour in the presence of prepared IgG-resins. XCEP63 extract depletions were preformed with one or two incubations with coupled beads. Mock depletion was performed using Protein A sepharose alone. Samples (2 µl) were mixed with Bio-Rad sample buffer, boiled and separated by SDS-PAGE (2.10.1) and the remaining sample was used in DNA replication experiment (2.14.7) or spindle assembly assay (2.14.4.1).

2.14.7 DNA replication

DNA replication was monitored in *Xenopus* egg extract as described in Costanzo *et al.,* 2001 and more recently in Trenz *et al.,* 2008 (Trenz *et al.,* 2008; Costanzo *et al.,* 2001). In short, mock and XCEP63 depleted interphase egg extracts were supplemented with 2,000 nuclei/µl and 10 µCi of [α^{32}P]-dATP. Samples were treated in the absence or in the presence of 0.1 U/ µl *EcoRI* or 0.1 U/ µl *EcoRI* with 3 mM caffeine and incubated for two hours at 23 °C. Reactions were stopped with stop buffer (8 mM EDTA, 80 mM Tris pH 8. 0, 1 % w/v SDS), supplemented with 1 mg/ml Proteinase K and incubated at 37 ℃ for one hour. Genomic DNA was extracted by phenol-chloroform-isoamyl alcohol mixture and precipitated with ethanol. Samples were mixed with gel loading

dye and then separated on agarose gels. Radioactivity incorporation was analysed by autoradiography phosphoimaging (2.10.4).

2.15 Protein phosphorylation

2.15.1 Histone H2AX Kinase assay

Monitoring phosphorylation of human Histone H2AX carboxyl-terminal peptide containing serine 139 (Sigma-Genosys) was performed as described by Costanzo *et al.,* 2004 with some modifications (Costanzo *et al.,* 2004a). CSF *Xenopus* egg extract were left untreated or were treated with pA/pT or sperm nuclei with 0.25 U/µl *EcoRI* in the absence and presence of 2 mM caffeine or 20 µM Ku55933. Alternatively, anastral spindle assembly extracts were treated with Dynal streptavidin beads, or 5 ng/µl pcDNA3 plasmid linearised with *EcoRI* 5 ng/µl biotinylated DNA bound to straptavidin beads (chromatin beads) in absence and presence of 2 mM caffeine or 20 µM ku55933 (2.14.4.5).

In order to eliminate DNA-PK activity pre-treated egg extracts were pre-incubated twice with Dynal streptavidin-coated beads (Invitrogen) coupled to 5' biotinylated linear DNA for 20 minutes at 4 °C. After which 2 µl of extract was mixed with 20 µl of EB kinase buffer (20 mM HEPES pH 7.5, 50 mM NaCl, 10 mM $MgCl_2$, 1 mM DTT, 1 mM NaF, 1 mM Na_3VO_4, and 10 mM $MnCl_2$) supplemented with 50 µM ATP, 1 µl of [γ-^{32}P]-ATP 10 mCi/µl (greater than 3,000 Ci/mmol) and 0.5 mg/ml of Histone H2AX peptide. Samples were incubated for 20 minutes at 30 °C. Reactions were spotted on p81 phosphocellulose filter paper (Upstate) and then air-dried. Unincorporated [γ-^{32}P]-ATP was removed by washing three times with 5 % orthophosphoric acid. Radioactivity was quantified in a scintillation counter (Perkin-Elmer, Tri-Carb 1500 Liquid Scintillation Analyzer)

2.15.2 Monitoring Cdk1 and Plx1 activity

Histone H1 and Caesin kinase assays were performed based on descriptions by Costanzo *et al.,* 2004 (Costanzo *et al.,* 2004a). Fresh CSF extract was supplemented

with 1,000 sperm nuclei, then treated with 0.25 U/µl EcoRI, 5 ng/µl pA/pT, CSF-XB preparation buffer or left untreated. Extract was incubated for 180 minutes at 23 °C, 2 µl or 20 µl were taken every 30 minutes. At 90 minutes $CaCl_2$ was added to a finial concentration of 0.4 mM to induce mitosis exit.

For monitoring Cdk1 activity 2 µl samples were mixed with 20 µl EB kinase buffer (20 mM HEPES pH 7.5, 50 mM NaCl, 10 mM $MgCl_2$, 1 mM DTT, 1 mM NaF, 1 mM Na_3VO_4, and 10 mM $MnCl_2$) supplemented with 50 µM ATP, 1 µl of [γ-^{32}P]-ATP 10 mCi/µl (greater than 3,000 Ci/mmol) and 0.5 mg/ml histone H1 recombinant protein (Sigma–Aldrich). Reactions were incubated for 20 minutes at 30 °C and then spotted onto p81 phosphocellulose filter paper (Upstate). Papers were air-dried, washed three times with 5 % orthophosphoric acid and then measured by a scintillation counter.

For monitoring of Plx1 activity, Plx was immunoprecipitated from the 20 µl aliquots of treated extracts (2.14.3). Imunoprecipitates were mixed with 20 µl of EB kinase buffer supplemented with 50 µM ATP, 1 µl of [γ-^{32}P]-ATP 10 mCi/µl (greater than 3,000 Ci/mmol) and 0.5 mg/ml Caesin recombinant protein (Sigma–Aldrich). Samples were incubated for 20 minutes at 30 °C and then separated on a standard SDS-PAGE. Gels were stained with Coomassie Blue (2.10.2), dried and underwent autoradiography (2.10.4). Radioactive bands corresponding to Casein were excised and radioactivity monitored with a scintillation counter.

2.15.3 XCEP63 dephosphorylation

Lambda protein phosphatase treatment was performed following New England BioLabs guidelines. In brief, 2 µl of pA/pT treated extract was incubated at 30 ℃ for 30 minutes with provided reaction buffer alone or supplemented with 2 µl (16 U/µl) of Lambda phosphatase. Samples then underwent SDS-PAGE (2.10.1).

2.15.4 XCEP63-MBP recombinant protein phosphorylation

Amylose beads (40 µl) were pre-bound with 5 µg MBP recombinant protein or 5 µg XCEP63–MBP recombinant protein in 250 µl EB buffer (25 mM Hepes pH 7.8, 15 mM

MgCl$_2$, 20 mM EGTA, 10 mM DTT, 80 mM beta-glycerophosphate) rotating at 4 ℃ for two hours. Beads were washed three times with 500 µl of EB buffer. Beads were supplemented with 50 µl of *Xenopus* egg extract, 50 µl of EB buffer, 1µl [γ-^{32}P]-ATP 10 mCi/µl (greater than 3,000 Ci/mmol) in the absence and presence of 5 ng/µl pA/pT. Extract was gently agitated at 23 ℃ for 60 minutes. Beads were washed three times with EB buffer supplemented with 0.2 % Ipegal v/v. Reactions were boiled in 30 µl of Bio-Rad sample buffer for four minutes. Eluted proteins were run on a large 10 % Anderson SDS-PAGE gel (2.10.1). Gels were stained with Coomassie Blue (2.10.2) and then underwent autoradiography (2.10.4).

2.15.5 Screening for XCEP63 ATM and ATR phosphorylation site

XCEP63 cDNA within original library expression vector underwent site directed mutagenesis at candidate and speculative ATM and ATR phosphorylation sites as described in 2.9.8.4. XCEP63 mutated DNA was transcribed and translated as described in 2.12. Similarly to cDNA expression library screening (2.14.5), translated XCEP63 mutants were exposed to *Xenopus* egg extract in absence and presence of 5 ng/µl pA/pT and then underwent SDS-PAGE analysis. Isolation of the correct XCEP63 phosphorylation site would result in abolished changes in gel migration pattern in the presence of pA/pT. Similarly, potential XCEP63 phosphorylation sites identified by Mass Spectrometry analysis underwent a similar mutation screening process.

2.15.6 Mass Spectrometry identification of XCEP63 ATM/ATR phosphorylation site

The identification of XCEP63 ATM/ATR phosphorylation site was undertaken by Alessandro Vindigni and Martin Hampel at ICGEB (International Centre for Genetic Engineering and Biotechnology) Padriciano 9934012 Trieste, Italy and Christof Lenz at Applied Biosystems, Frankfurter Darmstadt, Germany Strasse 129 B, 64293.

2.15.6.1 Treatment of XCEP63-MBP for Mass Spectrometry analysis

Samples for Mass Spectrometry were prepared as follows: 20 µl of 1 mg/ml MBP or XCEP63-MBP recombinant proteins were incubated at 23 °C for 60 minutes with 50 µl of CSF egg extract with and without 5 ng/µl pA/pT. Samples were diluted with 1:2 with EB buffer (25 mM Hepes pH 7.8, 15 mM $MgCl_2$, 20 mM EGTA, 10 mM DTT, 80 mM beta-glycerophosphate) and 50 µl of amylose resin was added. Reactions were incubated for two hours at 4 ºC with rotation. Beads were washed three times with 400 µl EB buffer 0.2 % Ipegal v/v and XCEP63-MBP was eluted from beads by boiling with Bio-Rad sample buffer. Samples were separated on a Bio-Rad 4-12 % Criterion XT 4-12 % Bis Tris pre-cast gel (2.10.1). The gel was subsequently stained with SYPRO® Ruby stain (2.10.3) and protein bands were made visible by a blue light transilluminator. Protein bands corresponding to MBP and XCEP63-MBP were excised with a clean scalpel. Samples were then sent to Alessandro Vindigni for Mass Spectrometry analysis.

2.15.6.2 Trypsin digestion of XCEP63-MBP

Excised gel bands were cut roughly into 1 mm pieces, washed with distilled water and then 50 % CH_3CN, 20 mM NH_4HCO_3. The resulting dehydrated gel pieces were reduced in 10 mM DTT, 100 mM NH_4HCO_3 for 60 minutes at 56 °C and then alkylated in 55 mM iodoacetamide, 100 mM NH_4HCO_3 for 45 minutes at room temperature in the dark. The gel pieces were washed with 50 % CH_3CN, 20 mM NH_4HCO_3 and dehydrated with CH_3CN. Sequencing grade porcine trypsin (Promega) was added at a concentration of 10 µg/µl in 20 mM NH_4HCO_3 and incubated at 4 °C for 45 minutes. The excess buffer and trypsin was discarded and the gel pieces were covered with 20 mM NH_4HCO_3 and incubated overnight at 37 °C. The supernatant was collected and additional peptides were extracted from the gel pieces with 50 % CH_3CN / 0.1 % TFA. Gel extraction and collected supernatant were pooled together and dried in a Speedvac (Eppendorf concentrator).

2.15.6.3 Mass Spectrometry analysis on XCEP63-MBP

The ATM phosphorylation site on XCEP63 was determined using the following strategy. Tryptic peptides were separated by reversed phase-C18 chromatography on a Tempo 1D nanoLC system (Applied Biosystems, Foster City, CA, USA). The eluted peptides were analysed on a 4,000 Q TRAP hybrid triple quadrupole/linear ion trap Mass Spectrometer equipped with a nanoDCI source (Applied Biosystems) in an information-dependent acquisition mode. An electrospray voltage of 2800/-2800, an interface heater temperature of 150 ºC was used for positive mode analysis and a cone voltage of 60/-85 was used for negative ion mode analysis. Depending on to the charge state and molecular weight (Mr) of the precursors, the collision energy was extensively adjusted.

Three different types of LC/MS/MS Mass Spectrometry (Liquid Chromatography/ Tandem Mass Spectrometry) XCEP63 phosphorylation investigations were performed as follows. Firstly, standard LC/MS/MS analysis was performed to establish protein identity at high sequence coverage. A linear ion trap MS full scan, a high resolution linear ion trap experiment of the five most abundant MS precursors determined the charge state and molecular weight, and up to five linear ion trap product ion spectra per cycle (in positive ion mode).

Secondly, in order to selectively identify phosphorylated peptides LC/MS/MS analysis was undertaken consisting of a Precursor Ion Scan for mass to charge ratio (m/z) 79 (in negative ion mode) followed by a high-resolution linear ion trap experiment on the two most abundant precursors (in negative ion mode). After a polarity switch, up to two linear ion trap product ion spectra per cycle were undertaken (Williamson *et al.,* 2006).

Thirdly, the identified phosphopeptide candidates were confirmed or rejected by semiquantitative LC/MS/MS analysis consisting of Multiple Reaction Monitoring (MRM) (Cox *et al.,* 2005; Unwin *et al.,* 2005). Experiments for both observed and predicted ion fragmentation reactions were performed in positive ion mode and followed by up to two linear ion trap product ion spectra in positive ion mode per cycle.

2.15.7 ATM and ATR *in vitro* XCEP63 phosphorylation

We proceeded with ATM and ATR *in vitro* XCEP63 phosphorylation assay based on description by Costanzo *et al.,* 2004 as follows (Costanzo *et al.,* 2004a). XCEP63 peptides (50 mer) wild type (XCEP63-S560) or XCEP63 serine 560 mutated to alanine (XCEP63-S560A) at position 25 were produced by CRUK in house protein and peptide chemistry service. Kindly donated recombinant Flag-ATM and Flag-ATR proteins were and purified as described in Trenz *et al.,* 2006 (Trenz *et al.,* 2006). XCEP63-S560 and XCEP63-S560A at 0.5 mg/ml were incubated with and without Flag-ATM or Flag-ATR in 20 µl of EB kinase buffer (20 mM HEPES pH 7.5, 50 mM NaCl, 10 mM $MgCl_2$, 1 mM DTT, 1 mM NaF, 1 mM Na_3VO_4, and 10 mM $MnCl_2$) supplemented with 50 µM ATP and 1 µl of $[\gamma\text{-}^{32}P]$-ATP 10 mCi/µl (greater than 3, 000 Ci/mmol). Samples were incubated at 30 °C for 20 minutes and then spotted onto P81 phosphocellulose filter paper. Papers were air-dried and then washed three times with 5 % orthophosphoric acid. Radioactivity was quantified in a scintillation counter.

2.16   Techniques involving *Xenopus* tissue culture

2.16.1 XTC cell culture

XTC (*Xenopus* Tissue Culture), adherent *Xenopus* fibroblast cell line was kindly provided by CRUK Clare Hall Laboratories cell culture facility and maintained as they advised. Cells were grown as monolayers at 24 °C in 70 % Leibovitz L-15 medium (Gibco) or modified eagle's medium (MEM) with 10 mM Hepes (prepared by cell culture facility). Media was supplemented with antibiotics (100 U/ml penicillin, and 100 µg/ml streptomycin) and 10 % fetal bovine serum (FBS) (Gibco).

2.16.2 XTC cell passage

XTC cells were detached by trypsin EDTA (versene) solution containing 0.25 % w/v trypsin and 0.02 % w/v versene was provided by CRUK Clare Hall Laboratories cell culture facility. After less than one minute cells were detached and then growth medium

was added. Cells were passaged at a 1:2 dilution every three days in order to maintain ideal growth conditions.

2.16.3 XTC transient transfection with XCEP63-GFP construct

XTC cell culture were transfected with XCEP63-GFP fusion plasmid DNA by lipid-based FuGENE® 6 Transfection Reagent (Roche Diagnostics) as described in manufacturers protocol. In brief, asynchronous XTC cells were plated at 50 % confluency and cultured on sterilised pre-coated poly-L-lysine 12 mm^2 coverslips for 24 hours. For each well, 2 ml of medium and 1.8 µl FuGENE® 6 reagent were mixed and incubated at room temperature for five minutes. 0.4 µg of XCEP63-GFP fusion plasmid DNA was mixed with transfection reaction and incubated for a further 30 minutes at room temperature. The transfection reaction was added to XTC culture well and incubated at normal conditions for 24 hours. Coverslips were recovered and proceed to immunofluorescence as described in 2.10.6.

2.16.4 XTC Synchronization

XTC cells were synchronized in mitosis by a double-thymidine block (Rao and Johnson, 1970). XTC cells at 50 % confluency were seeded and incubated for 24 hours. Cells were treated for 12 hours in medium supplemented with 2 mM thymidine (first block) and released into normal medium without thymidine for nine hours. Cells were treated again with medium supplemented with 2 mM thymidine for an additional 12 hours (second block) and then released for eight hours into medium with 25 µM MG-132 (Potapova *et al.,* 2006). Mitotic cells then underwent treatments as described below.

2.16.5 XTC cells treatments activating ATM and ATR

XTC cells synchronized in mitosis by a double-thymidine block entered mitosis were left untreated or irradiated with 10 Gy (Grays) performed with a source of ^{137}Cs (CIS Biointernational, 1BL 437C) in the absence or in the presence of 5 mM caffeine. XTC cells were spun onto coverslips and immunofluorescence was performed as described in 2.10.6.

In general, asynchronous XTC cells were seeded at 4 x10^5 onto sterile poly-L-lysine coated 12 mm^2 coverslips and allowed to adhere overnight and reach sub-confluency. In localisation studies of XCEP63, cells were untreated, incubated with 400 nM camptothecin (CPT) with and without 5 mM caffeine. Cells were treated for four hours under normal growth conditions. Coverslips were recovered and underwent immunofluorescence as described in 2.10.6.

3 Chapter 3 ATM and ATR activation in mitosis

DNA damage, such as double strand breaks (DSBs) and various DNA lesions, induce ATM and ATR kinase phosphorylation of downstream factors. Complex ATM and ATR checkpoint signalling prevent the initiation of DNA replication (G1/S phase transition), inhibit DNA replication progression (S phase) and halt cells at mitosis transition (G2/M phase transition) (Abraham, 2001). In addition to cell cycle arrests, ATM and ATR response networks coordinate the repair of damaged DNA or induce apoptotic cell death (Sancar *et al.,* 2004). It has been shown extensively that ATM and ATR DNA damage response mechanisms ensure genomic stability (Shiloh *et al.,* 2003; Cimprich and Cortez, 2008). However, there is little understanding of DNA damage responses during the mitotic cell phase. It seems a likely hypothesis that ATM and ATR kinases are also triggered during mitosis in response to DNA damage. We suspect that ATM and ATR responses play an additional role in maintaining genomic stability at the mitotic cell phase. This chapter focuses on establishing the status of ATM and ATR activity with the occurrence of DNA damage during mitosis in the *Xenopus laevis* model system. In this context, we aimed to examine the effects of mitotic DNA damage on spindle assembly and consequently identify a possible mechanism targeted.

3.1 ATM and ATR activation in mitotic *Xenopus* egg extracts

Xenopus egg extract as a biochemical system recapitulates several physiological aspects of DNA damage responses (Garner and Costanzo, 2009). This cell free system has been applied extensively to research ATM and ATR response networks. However, these works have mainly furthered the understanding of ATM and ATR checkpoint signalling in the setting of DNA replication. Typically, ATM and ATR activation has been prompted in egg extracts by the addition of DNA linear molecules mimicking DSBs (Costanzo *et al.,* 2000; Guo and Murphy, 2000; Kumagai and Durphy, 2000; Costanzo *et al.,* 2004a). ATM and ATR induction (as well as DNA-PK induction) in egg extract are sensitive to the presence of caffeine (Sarkaria *et al.,* 1999; Blasina *et al.,* 1999; Zhou *et al.,* 2000). Alternatively, a novel ATM inhibitor, 2-morpholin-4-yl-6-thianthren-1-yl-pyran-4-one termed Ku55933, specifically inhibits *Xenopus* ATM activation in egg extract (Hickson *et al.,* 2004). The addition of restriction endonucleases induce **d**ouble **s**trand **b**reak**s** (DSBs) in sperm chromatin as indicated by the localisation of **R**eplication

Protein A (RPA) foci (Grandi *et al.,* 2001). ATM and ATR activation has also been illustrated in the presence of restriction endonuclease treatment by the detection of replication protein substrate, Mcm2 phosphorylation (Yoo *et al.,* 2004b).

Under specific conditions *Xenopus* egg extracts are capable of maintaining a specific cell cycle status rather than Cycling from interphase to metaphase. *Xenopus* eggs are naturally arrested in metaphase of meiosis II through CSF activity (Masui and Markert, 1971; Maller *et al.,* 2002). In calcium chelating conditions the cytoplasm from crushed eggs retains this CSF arrest, (Murray, 1991), CSF arrest can be monitored by checking sperm morphology in the nuclear disassembly assay, in which mitosis is defined as combined events of nuclear envelope breakdown and chromosome condensation (data not shown) (Lohka and Maller, 1985; Smythe and Newport, 1991). Or alternatively, CSF arrest can be determined through the detection of Cyclin B (data not shown). The presence of low calcium concentration activates Cyclin B destruction driving mitosis exit (Murray *et al.,* 1989; Kobayashi *et al.,* 1992; Lorca *et al.,* 1993). It is worth reiterating at this point that CSF arrested extracts are meiotic (meiosis II), but enable relevant insights by mimicking mitosis. Moreover, due to the ability of CSF arrested extract to induce mitosis when mixed with interphase extracts, CSF egg extracts are commonly described as mitotic (Sawin and Michison, 1991). *Xenopus* CSF arrested extracts have been widely used to examine many of the events involved in cell division and provide in depth understanding of numerous vertebrate mitotic processes and morphological changes. However, little investigation has been undertaken to determine the effects of DNA damage during mitosis.

In order to investigate ATM and ATR activity in arrested *Xenopus* egg extracts, we introduced linear DNA molecules or added restriction endonuclease *EcoRI* together with sperm nuclei. Synthetic linear DNA fragments consisted of annealed poly-deossi-T and poly-deossi-A 70 mer oligonucleoides (pA/pT) (Costanzo *et al.,* 2000; Guo and Murphy, 2000; Kumagai and Dunphy, 2000). We applied restriction endonuclease and pA/pT to *Xenopus* egg extract based on previous findings, at doses that efficiently induce ATM and ATR activation (data not shown).

We firstly analysed whether ATM and ATR are activated in CSF *Xenopus* egg extract by measuring Histone H2AX serine 139 carboxyl-terminal peptide phosphorylation (Costanzo *et al.,* 2004a). In figure 3.1a, we show strong incorporation of radiolabelled

phosphate into H2AX peptide treated with egg extracts in the presence of pA/pT and *EcoRI*. Treatments with pA/pT and *EcoRI* indicate an approximate 12 and 9 fold higher extent of H2AX phosphate labelling, respectively, compared to the absence of treatments. H2AX radiolabelled phosphate incorporation was abolished by the addition of caffeine and by ATM inhibition. We found the phosphate incorporation in inhibition treatments remained at similar levels to the extract without DNA damage conditions. These initial findings suggest that ATM and ATR kinases activate within the context of mitosis, stringently in the presence of pA/pT treatment and highly with *EcoRI* treatment. The evidence is substantiated by caffeine and ATM inhibitor sensitivity, abolishing ATM and ATR response to DNA damage conditions.

Through determining the changes in H2AX modification levels, we had a basis on which to continue research into mitotic ATM and ATR activation. Figure 3.1b is an immunoblot detection with antibodies recognising ATM 1,981 phosphorylation. Within CSF egg extract we directly confirm ATM activation by pA/pT addition, which is not detectable in the presence of inhibition or in absence of treatment. Figure 3.1c shows an immunoblot detection with antibodies recognising ATM and ATR substrate phosphorylation on consensus SQ/TQ motif. The immunoblot shows strong bands detected in the presence of pA/pT, which are absent in untreated extract and attenuated by inhibitors, caffeine and Ku55933. The occurrence of downstream ATM and ATR substrate phosphorylation suggests active DNA damage responses regulated by ATM and ATR inductions.

A) Quantification of Histone H2AX kinase assay
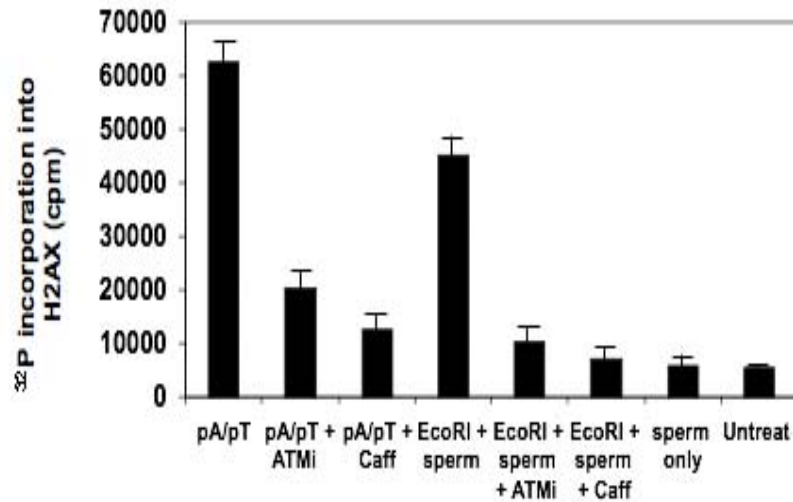
B) Immunoblot detection of ATM serine 1,981 phosphorylation
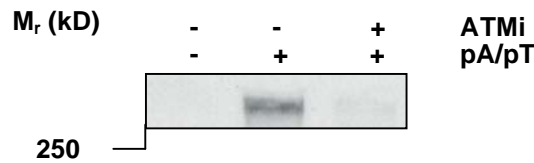
C) Immunoblot detection of ATM and ATR substrate SQ/TQ site phosphorylation
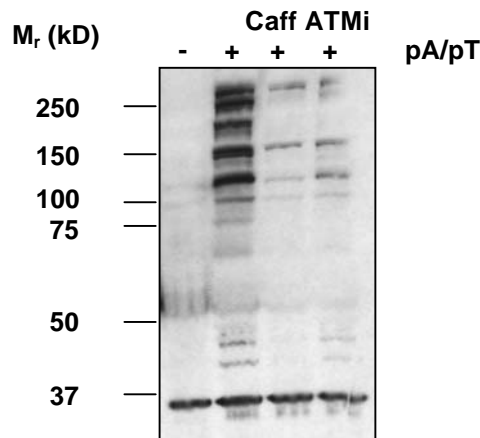
Figure 3.1 ATM and ATR activation in mitotic *Xenopus* egg extract

(a) CSF egg extracts were supplement as indicated and incubated at 20 °C for 30 minutes. Treatments included, linear DNA (pA/pT) at 5 ng/μl, sperm at 1,000 nuclei/μl, *EcoRI* at 0.25 U/μl, Ku55933 (ATMi) at 20 μM and caffeine (Caff) at 2 mM. Extracts were pre-cleared twice with 5' biotinylated linear DNA coupled streptavidin beads. Kinase assays were performed at 30 °C for 20 minutes with treated extracts (2 μl) and 0.5 mg/ml histone H2AX carbossi-terminal peptide in 20 μl of EB kinase buffer supplemented with 50 μl ATP and 1 μl of [γ-^{32}P]-ATP (10 mCi/μl). Labeled samples were spotted on phosphocellulose filter paper, washed and then quantified by a scintillation counter. The amount of radioactivity incorporated on H2AX peptide was reported in the graph. Error bars indicate standard deviation (s.d.). (b) CSF arrested egg extract was treated in the absence (-) and presence of 5 ng/μl linear DNA (+ pA/pT) with (+) or without (-) 20 μM ATMi (Ku55933). Samples were incubated at 20 °C for 30 minutes, 1 μl was then boiled in Bio-Rad sample buffer and separated by electrophoresis on a standard 7 % SDS-PAGE gel. Immunoblot detection was performed with antibody recognizing ATM phospho serine 1,981. (c) CSF arrested egg extract was treated and processed as in part b, with an additional extract treatment with 5 ng/μl linear DNA (+ pA/pT) and caffeine (Caff) at 2 mM. Samples were separated on a standard 10 % SDS-PAGE gel. Immunoblot detection was performed with antibody recognizing ATM/ATR substrates SQ/TQ phosphorylation. Data shown is representative of three separate experiments.

3.2   Downstream Chk1 and Chk2 activation in mitotic *Xenopus* egg extract

We continued by ascertaining whether ATM and ATR activation orchestrates the induction of downstream DNA damage checkpoint effector kinases, Chk1 and Cds1 (Chk2). In vertebrates, active ATM and ATR directly phosphorylates Cds1 and Chk1 respectively which contribute to cell cycle arrests (Abraham, 2001; Zhou and Elledge, 2000) Within *Xenopus* interphase egg extract Chk1 phosphorylation has been described in response to DNA replication blocks or UV irradiation (Hekmat-Nejad *et al.,* 2000), Guo *et al.,* 2000). Whilst, Cds1 rapid phosphorylation and activation within *Xenopus* interphase egg extract has been shown in response to DNA molecules with double strand ends (Guo *et al.,* 2000). However, in interphase *Xenopus* egg extracts it has been found that Cds1 full activation requires sequential phosphorylations by DNA-PK, ATR and ATM (McSherry and Mueller, 2004).

In order to gain more information on ATM and ATR responses in the presence of activating conditions in CSF arrested *Xenopus* egg extract, we performed immunoblots with antibodies detecting the targets, Chk1 and Cds1 (figure 3.2a and figure 3.2b respectively). Both Chk1 and Cds1 immunoblots show band mobility shifts indicative of phosphorylation in the presence of pA/pT. Chk1 and Cds1 phoshorylation is not apparent on the addition of caffeine or in the absence of any treatment.

In figure 3.2a, the data shows that DNA linear molecules induce Chk1 phosphorylation, indirectly inferring ATR induction. However, the caffeine sensitive nature of the Chk1 phosphorylation does not discount a possible interconnecting role of ATM kinase in contributing to Chk1 modification in the setting of mitotic egg extract. Outside the context of DNA replication checkpoint responses, these data suggests that perhaps ATM, but most likely ATR kinase phosphorylates Chk1 in response to DSBs. In figure 3.2b, Cds1 phosphorylation in the presence of linear DNA molecules, indirectly suggests ATM activation. However, ATM inhibition affected Cds1 phosphorylation only partially. The caffeine sensitive nature of Cds1 phosphorylation suggests a possible activation of alternative DNA damage response kinases, such as ATR and/or DNA-PK. In the context of mitosis, it remains unclear if Cds1 phosphorylation is dependent on ATM kinase activation in response to DSBs. Taken together, these data show a contribution of ATM and ATR with respect to downstream DNA damage response activation in phosphorylating Chk1 and Cds1.

A) Immunoblot detection of Chk1

M$_r$ (kD) | - | - | + | Caff |
| - | + | + | pA/pT |

50
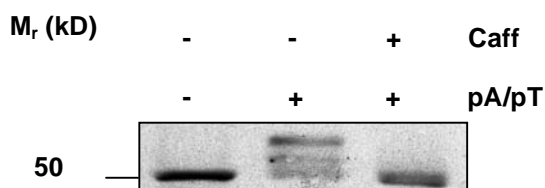
B) Immunoblot detection of Chk2 (Cds1)

M$_r$ (kD)
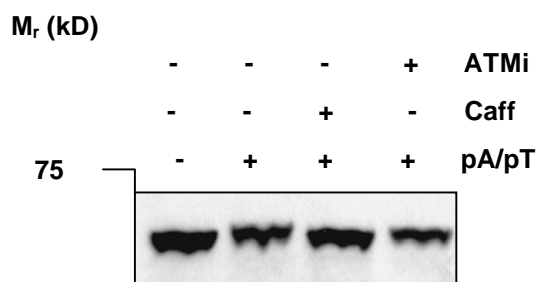
| - | - | - | + | ATMi |
| - | - | + | - | Caff |
75 | - | + | + | + | pA/pT |

Figure 3.2 Downstream Chk1 and Chk2 phosphorylation in the presence of ATM and ATR activation in mitotic *Xenopus* egg extract

CSF egg extracts untreated and treated with 5 ng/µl linear DNA (pA/pT) in the absence or presence of 20 µM Ku55933 (+ ATMi) or 2 mM caffeine (+ Caff) as indicated. Extracts were incubated at 20 °C for 30 minutes and 1 µl of extracts were boiled in Bio-Rad sample buffer. **(a)** Samples underwent electrophoresis on a small 8 % ultrapure bisacrylamide gel. Immunoblot detection was performed using Chk1 specific antibodies. **(b)** Samples underwent electrophoresis on a small 10 % Anderson gel. Immunoblot detection was performed using Cds1 (Chk2) specific antibodies. Data shown is representative and typical findings of three separate experiments.

3.3   Spindle assembly in *Xenopus* egg extract

To investigate the effects of ATM and ATR activation during mitosis we analysed spindle assembly. Half spindle arrays form in CSF arrested extract with the addition of sperm nuclei. The process of spindle assembly occurs as follows: each sperm nucleus drives aster formation, from which half spindles then assemble and finally two half spindles fuse to form a polar mitotic spindle (Sawin and Mitchison, 1991; Desai *et al.,* 1999). Figure 3.3a is a schematic representation illustrating the progression of spindle assembly in *Xenopus* egg extracts.

Unfortunately, frozen extracts were found to be inefficient in spindle assembly. Therefore, all assays were performed in fresh extract. The quality of *Xenopus* eggs determined the ability of extracts to form spindles. We encountered egg quality differences associated with batch-to-batch variations. Extracts that failed to progress into mitosis and self-activating, non-arrested extracts were discarded. Poor performing extracts arose from eggs that were not uniform in appearance, showed some spontaneous activation or any degree of lysis during preparation. We also established that isolating batches of eggs from individual frogs rather than pooling led to a higher probability of obtaining a good extract (data not shown). We reduced variability further by optimising the preparation of CSF arrested extracts in several ways. We exchanged the egg laying buffer to MMR, eliminated the mineral oil packing of eggs before crushing and ensured meticulous collection of cytoplasmic layers by syringe needle extraction. In addition, the final extract clarification spin was reduced from a lengthy high-speed ultra centrifugation to that of the first clarification centrifugation conditions. Other factors also strongly influenced the proficiency of spindle assembly, including the length of time before extracts were used, avoidance of vigorous physical perturbations, the quality of and freeze-thawing of sperm nuclei. It was noted that more spindles were assembled after longer incubation times, therefore we extended incubation from 60 to 90 minutes.

The technique applied to isolate assembled spindle in CSF *Xenopus* egg extract was first described by Evan et al, 1985 (Evan *et al.,* 1985). Figure 3.3b shows a schematic representation illustrating Evan's devised protocol. We have modified the procedure in order to isolate spindle formations in the presence of ATM and ATR activation.

A) Schematic representation of spindle assembly in CSF *Xenopus* egg extract

Time (minutes)

0	5-15	15-30	30-60	60-90

CSF extract + Sperm chromatin | Centriole (centrosome) driven aster formation | Microtubule-Chromatin interaction | Half spindle assembly | Half spindle fusion

KEY: ● Centriole   / Microtubules   ■ Assembled chromosome
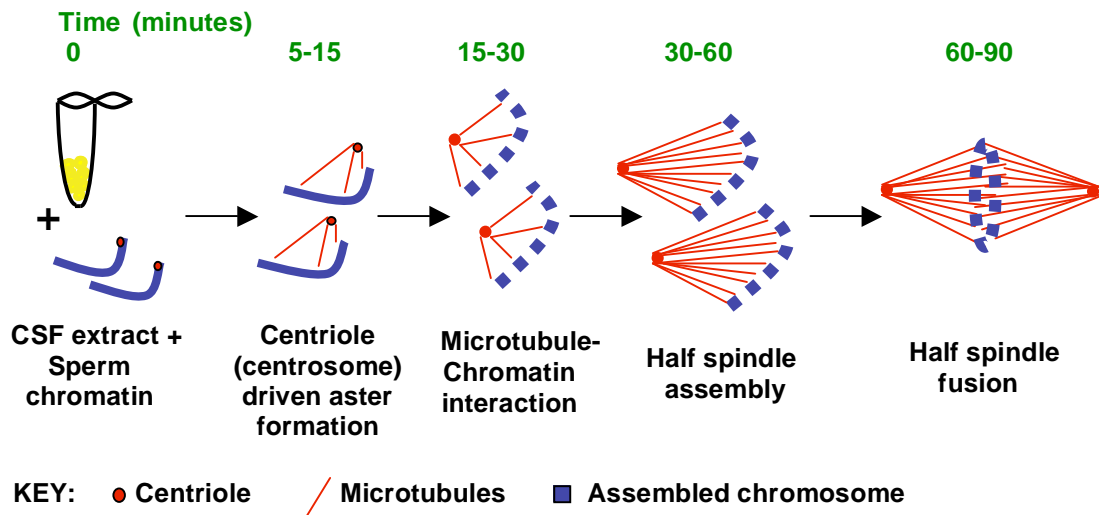
B) Schematic representation of spindle assembly assay and isolation for analysis

Sperm nuclei + Rhodamine tubulin

CSF egg extract

CSF-XB buffer   EcoRI + caff ← EcoRI → EcoRI + ATMi

90 minutes 20 °C

BRB80 dilution /Formaldehyde Fix

BRB80 Glycerol cushion
Coverslip
Plastic disc
Silcon bottom

Load onto glycerol cushion in specialised corex tubes

Centrifuge 5,500 rpm 20 minutes 18°C

Methanol fix spindles DNA DAPI/Hoechst stain Mount onto slide
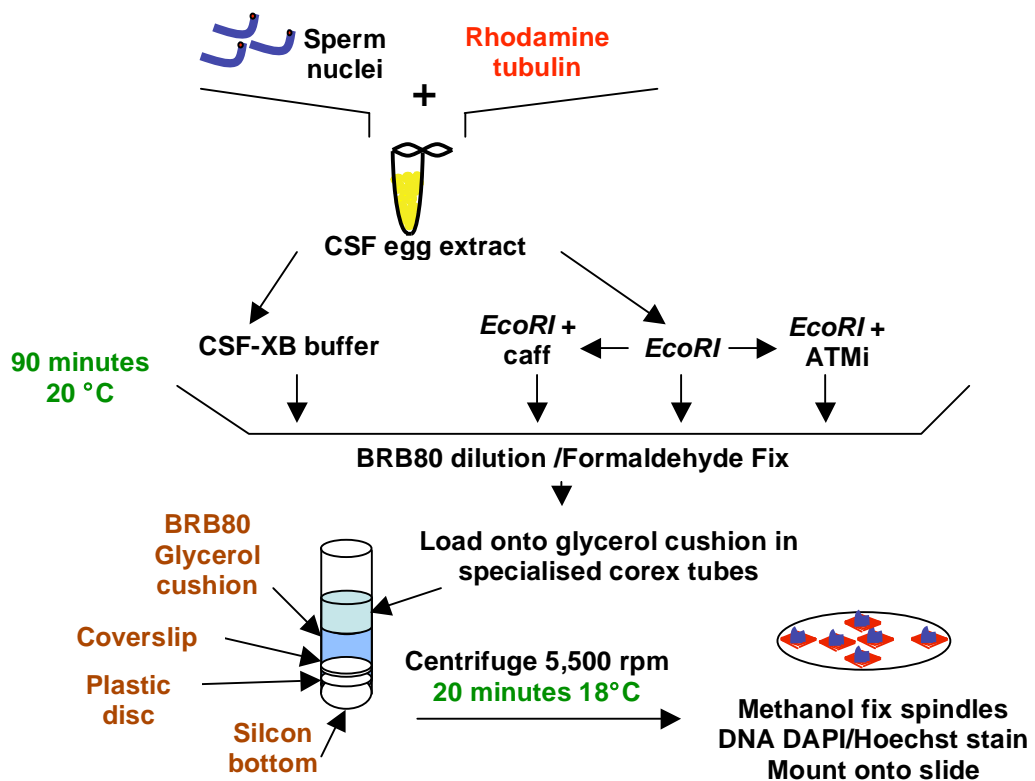
Figure 3.3 Schematic representations of mitotic *Xenopus* egg extract spindle assembly and procedure of ATM and ATR activation in spindle assembly with isolation onto coverslips

(a) Sperm nuclei addition to CSF arrested *Xenopus* egg extract drives centrosome dependent aster formation, over time microtubules attach to assembled chromosome, half spindles form, two of which fuse together forming a bipolar spindle. (b) Sperm nuclei and rhodamine tubulin were added to CSF egg extract. Extracts were supplemented with CSF-XB buffer or treated with *EcoRI* in the absence and presence of caffeine (Caff) or ATM inhibitor (ATMi). Samples were incubated at 20 °C for 90 minutes, diluted in BRB80 buffer and then fixed with BRB80 formaldehyde solution. Spindles were centrifuged onto coverslips in a specialised corex tube through a BRB80 glycerol cushion. Retracted coverslips were fixed in methanol, DNA stained and then mounted onto slides for microscopic analysis.

3.4   ATM and ATR activation inhibits spindle assembly in *Xenopus* egg extract

Optimisation of the *Xenopus* egg extract spindle assay allowed us to investigate the effects of chromosomal breakage induction of ATM and ATR on spindle assembly. Strikingly, we observe ATM and ATR activation leads to the formation of large aggregated microtubule structures with chromosomes associated throughout (figure 3.4a). Normal spindle formation, demonstrated by pole orientation and DNA centrally aligned along the metaphase plate, is observed in extracts left untreated and in *EcoRI* treated extracts supplemented with inhibitors, caffeine or ATM inhibitor (Ku53933) (figure 3.4a). Images of aster morphology also shown in figure 3.4a, illustrate normal aster assembly and microtubules polymerization in the presence of *EcoRI*. These data suggests we can rule out ATM and ATR checkpoint induction impeding regulation or processes involved in aster formation.

Figure 3.4b shows the quantification of the microtubule structures observed in samples. Spindle assembly defects are observed at high levels in *EcoRI* supplemented extracts. An approximate 30 % increase in aggregated microtubule structures occurs in DNA damaging *EcoRI* conditions compared to untreated extracts. Spindle assembly rescue is observed in the presence ATM inhibitor or to a higher extent with caffeine addition, returning normal spindle formation to similar levels of untreated extract. The reversal of spindle aberrancies suggests that ATM and ATR are responsible for checkpoint induction leading to spindle morphology changes. We observe an increase in aster number with ATM and ATR activation, which suggests spindle assembly is abolished. Aster frequency returns to normal levels by incorporation of ATM and ATR inhibitors. Again, high aster abundance suggests that spindle defects result from perturbation of aster maturation to spindles.

A) Fluorescent images of spindle assembly in *Xenopus* egg extract
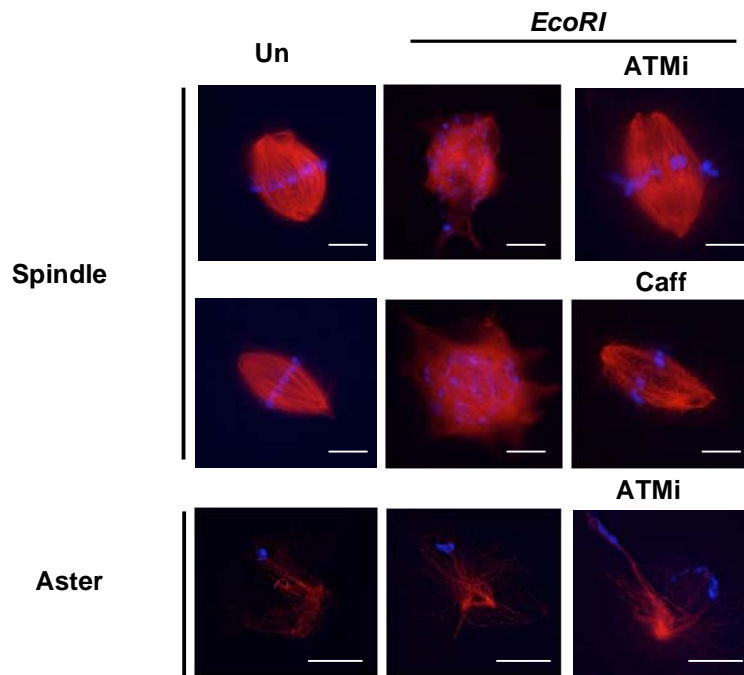
B) Quantification of spindle assembly structures observed in treatments
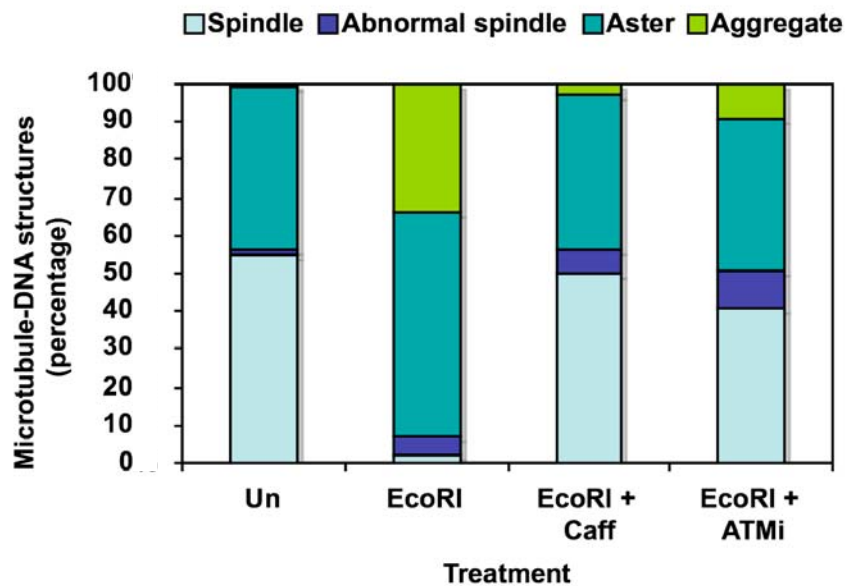
Figure 3.4 ATM and ATR activation perturbs spindle assembly in *Xenopus* egg extract

Spindles and asters were formed in mitotic arrested CSF extract incubated at 20 °C for 90 minutes with the addition of 1,000 sperm nuclei/μl and 50 μg/ml rhodamine tubuin. Extracts were treated with CSF-XB buffer (Un) or supplemented with 0.25 U/μl *EcoRI* (*EcoRI*) with and without 20 μM Ku55933 (*EcoRI* + ATMi) or 2 mM caffeine (*EcoRI* + Caff). Extracts were diluted in BRB80 buffer and fixed in BRB80 formaldehyde solution and then spun onto polylisine coverslips through a glycerol cushion as described in material and methods. DNA was stained with DAPI. Images were acquired and quantification performed on a Deltavision microscope. Data is representative and typical findings of three separate experiments **(a)** Images of spindle assembly, microtubules are shown red and DNA in blue. Scale bars indicate 10 μm. **(b)** Quantification of DNA associated microtubule structures with treatments as above. Microtubule structures were qualified as bipolar spindles, asters, abnormal spindles (spindles without poles + spindles with dispersed chromosomes) and aggregates (large disorganized microtubules with DNA dispersed throughout). Percentages are relative to 100 structures counted for each treatment.

3.5 Activation of ATM and ATR perturbs spindle assembly at all stages of formation in *Xenopus* egg extract

On showing that ATM and ATR activation severely perturbs spindle assembly from the onset of spindle formation, we then asked whether checkpoint activation by ATM and ATR during spindle assembly also leads to spindle defects. As shown in 3.3a, the schematic representation of spindle formation in CSF arrested *Xenopus* egg extract, asters form between 5-15 minutes after sperm addition, half spindle assembly at 30 minutes and fusion occurs at 60 minutes onwards. To determine whether the spindle assembly defects dependent on ATM and ATR induction correlate with aster formation, half spindle assembly or fusion, we introduced treatments at specific time points during mitotic progression.

The *EcoRI* time course in figure 3.5, shows chromosomal breakage introduction at each time point leads to the formation of aggregated microtubule structures with DNA dispersed throughout. Consistent spindle assembly irregularities suggests ATM and ATR signaling affects a spindle formation in early and late stages. These data, in combination with normal aster morphology determined previously in figure, 3.4a, suggests a dissociation of ATM and ATR induction specifically affecting aster formation. Furthermore, observations of defective spindle formation in extracts with introduction of ATM and ATR activation at later time points 30 and 60 minutes, suggests that ATM and ATR target mechanism involves processes of spindle maturation, microtubule dynamics or array maintenance.

Un

EcoRI

| **0 minutes** | **7 minutes** | **30 minutes** | **60 minutes** |
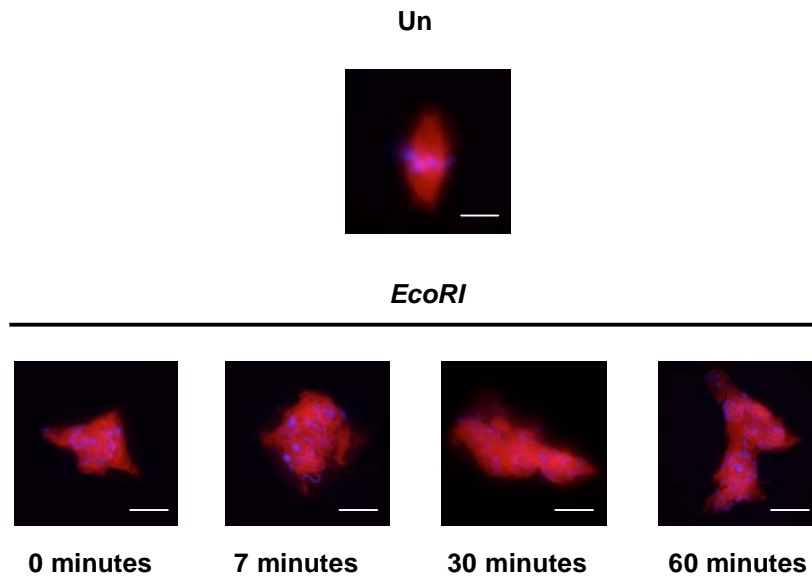
Figure 3.5 ATM and ATR activation perturbs spindle formation during assembly in *Xenopus* egg extract

Spindles were formed in CSF extract with 1,000 nuclei/μl and supplemented with 50 μg/ml rhodamine tubulin. Extracts were treated with *EcoRI* at 0.25 U/μl added at times points: 0, 7, 30 and 60 minutes (*EcoRI*) and untreated (Un) supplemented with CSF-XB buffer at 60 minutes. Extracts were incubated at 20 °C for 90 minutes, then diluted and fixed in formaldehyde in BRB80 buffer. Samples were spun onto polylysine coverslip through a glycerol cushion as described in material and methods. DNA was stained with DAPI, shown in blue and microtubules are shown in red. Images were acquired on a Deltavision microscope, scale bar indicates 10 μm. Data is representative of three separate experiments.

3.6 Abnormal spindle assembly is dependent on active ATM and ATR signaling in *Xenopus* egg extract

In the previous figures, we show evidence that ATM and ATR activation mediated by the addition of *EcoRI* to spindle assembly samples leads to spindle defects. Since *EcoRI* restriction endonuclease frequently induces DNA double strand breaks, we questioned whether the involvement of physical chromatin damage or kinetochore disruption plays a role in the disruption of normal spindle formation. Primarily to eliminate these factors, we induced ATM and ATR by supplementing extracts with linear DNA (pA/pT) (figure 3.1). To further extend this analysis, alternative ATM and ATR activating DNA damaging agents were also applied: restriction endonuclease *NotI*, which induces fewer DNA cuts and therefore is less likely to impact kinetochores and Doxorubucin, a topoisomerase poison producing DSBs (Grandi *et al.,* 2001; Zunino *et al.,* 1977; Cliby *et al.,* 2002; Siu *et al.,* 2004).

In figure 3.6, we show that DNA associated microtubule aggregates form in response to alternative ATM and ATR activating agents, pA/pT, *NotI* and Doxorubicin. We observe spindle assembly inhibition is similar to that after ATM and ATR activation induced by *EcoRI* restriction endonuclease treatment. Consistently, spindle assembly defects in the presence of DNA damaging conditions were rescued by caffeine addition, indicating a reliance on ATM and ATR signal induction. Taken together, these data suggest defective spindle assembly is independent of physical perturbation of chromatin and/or kinetochores and dependent on ATM and ATR checkpoint induction.
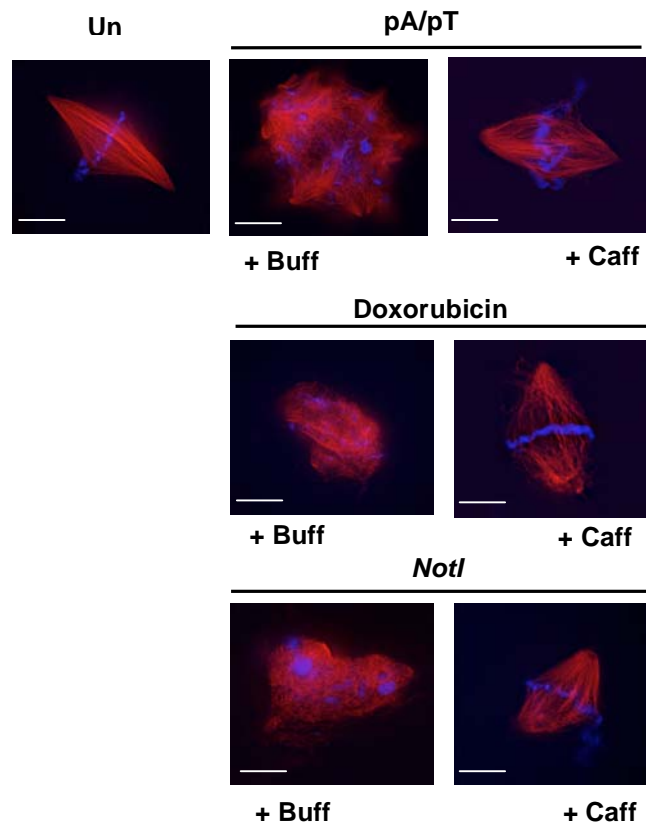
Figure 3.6 Alternative DNA damage ATM and ATR activating conditions perturb spindle assembly in *Xenopus* egg extract

Spindles were formed in CSF extract with 1,000 nuclei/μl in the presence of 50 μg/ml rhodamin tubulin. Extract was left untreated (Un), supplemented with 5 ng/μl linear DNA (pA/pT), 5 mM Doxorubicin or 0.25 U/μl restriction endonuclease, *NotI* (*NotI*). Extracts were also treated with CSF-XB buffer (Buff) or 2 mM caffeine (+ Caff). Samples were incubated at 20 °C for 90 minutes, then diluted and formaldehyde fixed in BRB80 buffer. Spindles were spun onto coverslips through a glycerol cushion as described in materials and methods. Images were acquired on a Deltavision microscope and represent a typical finding of three separate experiments. DNA was stained with DAPI, shown in blue and microtubules are shown in red. Scale bar indicates 10 μm.

3.7 ATM and ATR activation perturbs bipolar spindle assembly in *Xenopus* egg extract

To this point of investigations, we have established that ATM and ATR activation affects normal half spindle assembly in mitotic extracts. The question arose whether bipolar spindle assembly, formed in the presence of replicated DNA, is similarly disrupted in the presence of ATM and ATR activation. Bipolar spindle assembly in cycled (interphase-to-mitosis) extract, differs distinctly from previously the described CSF egg extract half spindle assembly (figure 3.3a). Within *Xenopus* interphase egg extracts sperm nuclei undergo one round of DNA replication, after which the addition of CSF arrested extract drives extract into mitosis and bipolar spindles assemble. The process of cycled bipolar spindle assembly in *Xenopus* egg extract is illustrated in figure 3.7a schematic representation (Sawin and Mitchison, 1991; Desai *et al.,* 1999).

Images of cycled bipolar spindle assembly are shown in figure 3.7b. As expected, we find abnormal bipolar spindle formation in the presence of ATM and ATR activation and rescue of normal bipolar spindle assembly with caffeine addition. These data indicate ATM and ATR dependent induction of bipolar spindle assembly defects. Irregularities in bipolar spindle assembly closely resemble abnormalities in half spindle formation around non-replicated DNA. Therefore these results suggest bipolar spindle assembly around replicated DNA also undergo active ATM and ATR checkpoint inhibition.

A) Schematic representation of bipolar spindle assembly in cycled *Xenopus* egg extract

B) Fluorescent images of bipolar spindle assembly in cycled *Xenopus* egg extract

Figure 3.7 Defects in cycled bipolar spindle assembly in the presence of ATM and ATR activation

(a) Schematic representation of bipolar spindle assembly in *Xenopus* egg extract. Sperm nuclei undergo DNA replication in CSF egg extract supplemented with calcium, then subsequently driven into metaphase with addition CSF arrested egg extract, forming bipolar spindles around replicated chromosomes. (b) Bipolar spindle assembly obtained by incubation at 20 °C for 120 minutes of 20 µl untreated CSF *Xenopus* egg extracts with 1,000 sperm nuclei/µl, 0.2 mg/ml Cyclohexamide and 0.4 mM CaCl$_2$ followed by incubation at 20 °C for 60 minutes with 10 µl addition of CSF egg extracts supplemented with 50 µg/ml rhodamine tubulin. On CSF addition extracts were untreated (un) and supplemented with CSF-XB buffer (+ Buff), or treated with 0.25 U/µl *EcoRI (EcoRI)* in the absence or presence of 2 mM caffeine (+ Caff). Extracts were diluted and formaldehyde fixed in BRB80 buffers, then spun onto coverslips as described in materials and methods. DNA was stained DAPI, shown in blue and microtubules shown in red. Images were acquired on a Deltavision microscope. Scale bar indicates 10 µm. Images shown are representative and typical findings of three separate experiments.

3.8   ATM and ATR activation inhibits spindle assembly in XTC cells

To further the evidence shown in *Xenopus* egg extracts, although such a cell free system is representative of intact cells, we investigate the effects of ATM and ATR activation on spindle assembly in somatic *Xenopus* tissue culture (XTC) cells. We tested the effects of Ionizing Radiation during mitosis. Immuno-staining for a mitotic marker, Histone H3 phosphorylation at serine 10, identifies cells in M phase, whilst alpha tubulin staining allows the visualization of microtubules and elucidates the morphology of spindle assembly. Cells are typically synchronized through antimitotic agents, such as nocodozol, which block cells at M phase by inhibiting microtubule dynamics (Jordan *et al.,* 1992; Vasquez *et al.,* 1997). Such synchronization methodology may influence microtubules organization observations in the context of ATM and ATR activation. Instead, we achieved XTC cells synchronization through a double thymidine treatment, an inhibitor of DNA synthesis. Cells were released from early S phase thymidine arrest and in turn coordinately entered mitotic phase (Rao and Johnson, 1970). Subsequently, we prevented exit from mitosis through addition of a proteasome inhibitor, MG-132 which inhibits proteasome-dependent Cyclin B degradation transition from M phase to G1 (Potapova *et al.,* 2006). Without preventing mitotic exit, the detection of ATM and ATR activation effects on spindle formation would potentially be masked. The mitotic index in figure 3.8a shows cells released from thymidine treatments are synchronized in S phase, which then enter into mitosis and subsequently exit shortly. We observe that the cell population is retained in mitosis when treated with MG-132. Preventing cells from exiting mitosis with MG-132 treatment ensures cells are specifically held in mitosis for investigations into the effects of ATM and ATR on spindle assembly.

Mitotic XTC cells maintained in the presence of MG-132, were treated in the absence and presence of Ionizing Radiation (IR) with and without caffeine. The results obtained from this experiment are shown in figure 3.8b. Representative fluorescent images show abnormal spindle assembly in the presence of IR, compared to normal spindle assembly in untreated cells. Spindles structures in cells exposed to IR show a lack of pole orientation and DNA dispersed away from the central metaphase plate. Spindle defects in IR treated cells were abolished by caffeine addition. These data suggests that severe perturbation of spindle assembly in cells is dependent on the presence of active ATM and ATR.

Quantification of experiment in figure 3.8c indicates a 7-fold increase in abnormal

spindle assembly in the presence of IR compared to the absence of treatment. We observe that normal spindle formation is rescued in treated cells supplemented with caffeine. These data suggest spindle assembly inhibition is dependent on active ATM and ATR also in XTC cells. These findings are in agreement with *Xenopus* egg extract data, once again highlighting the striking disruption of spindle assembly by an ATM and ATR checkpoint induction.

A) Mitotic index of XTC cells
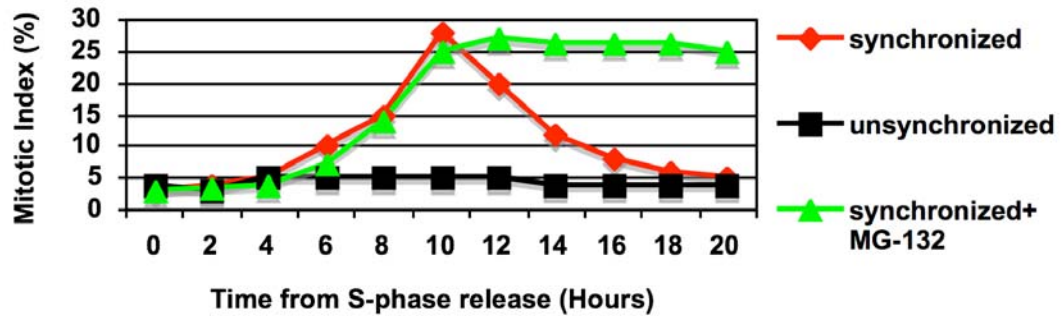
B) Fluorescent images of spindle assembly in XTC cells
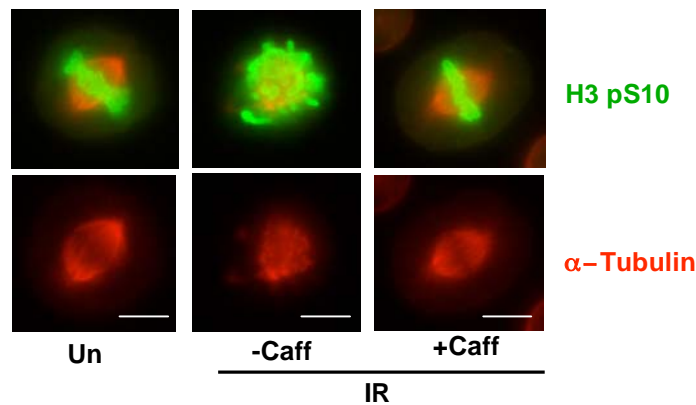
C) Quantification of observed aberrant spindle assembly in XTC cells
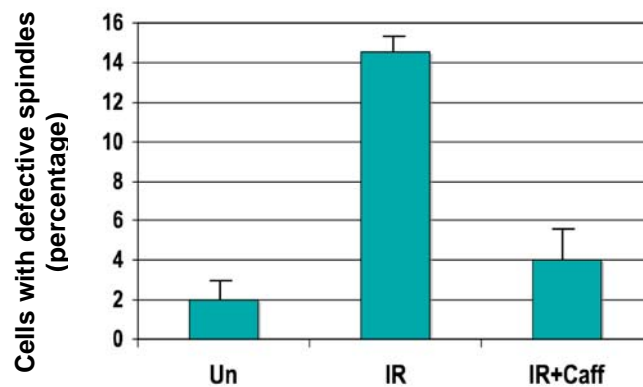
Figure 3.8 Spindle assembly defects in the presence ATM and ATR activation *in vivo*

XTC cells were synchronized in mitosis with 25 μM MG-132 for eight hours following a double 2 mM thymidine S-phase block for 12 hours with a nine hours interim release. Immunofluorescence staining was performed on collected cells as described in material methods with antibodies detecting alpha tubulin (α-tubulin) and mitotic chromosome marker histone H3 phospho serine 10 (H3 pS10). Cells were counted and images were acquired on a Deltavision microscope. **(a)** Mitotic index of XTC cells with and without thymidine synchronization released in the presence or in the absence of MG-132. Mitotic index graph shows the percentage of mitotic cells (positive for H3 pS10 staining). **(b)** MG-132 treated synchronised XTC cells were untreated (Un) or irradiated with 10 Gy (IR) in the absence (- Caff) or in the presence (+ Caff) of 5 mM caffeine. Images show immunofluorescence antibody detection, H3 pS10 in green and α-tubulin in red. Images of spindle assembly are representative of three separate experiments. Scale bar indicates 10 μm. **(c)** Quantification of defective spindle morphology determined by α-tubulin staining, 200 mitotic H3 pS10 positive cells were counted for each indicated treatments. Percentages represent the average number of defective spindles observed from three independent experiments. Error bars indicate standard deviation (s.d.).

3.9 Activation of ATM and ATR shows no affect on Cdk1 and Plx1 mitotic kinase activities

After ascertaining that ATM and ATR activation inhibits spindle assembly in both *Xenpous* egg extract and XTC somatic cell, we went about identifying the corresponding target mechanism. We monitored the mitotic status of *Xenopus* egg extract in the presence of ATM and ATR activation by measuring the activities of two major mitotic kinases, Cdk1-Cyclin B and Plx1, described in chapter one (1.2.1). Cdk1-Cyclin B (MPF) functions in mitosis onset and mitotic events, whilst Cdk1 inactivation promotes mitotic exit (Murray *et al.,* 1989; Nurse *et al.,* 1990; Verde *et al.,* 1990; Fourest-Lieuvin *et al.,* 2006; Glotzer *et al.,* 1991; Sullivan and Morgan, 2007). Plx1 kinase also displays multiple functions in entry, progression and exit from mitosis (Qian *et al.,* 1998; van Yugt and Medema, 2005; Liu *et al.,* 2005). Plx1 and Cdk1-Cyclin B sustain one another through a Cdc25 amplification feedback loop (Hoffmann *et al.,* 1993; Kumagai and Dunphy 1996; Abrieu *et al.,* 1998; Qian *et al.,* 1998). Cdc25 phosphatase, is essential in initiating the transition from G2 phase to M phase, which is down-regulated by ATM and ATR checkpoint targeting (Sancar *et al.,* 2004).

Mitotic *Xenopus* egg extracts samples were tested to establish Cdk1 and Plx1 kinase activities in the presence of activated ATM and ATR. We performed kinase reactions with substrates of Cdk1 and Plx1 kinases, Histone H1 and Caesin respectively. We show in figure 3.9a and figure 3.9b that ATM and ATR activation introduced by *EcoRI* or linear DNA (pA/pT) did not impose any detectable disruption of Cdk1 and Plx1 activities. These data show Cdk1 and Plx1 kinases, in mitotic egg extract, do not undergo ATM and ATR checkpoint inhibition. Within mitotic *Xenopus* egg extracts, calcium addition inactivates Cdk1-Cyclin B which promotes mitotic exit (Maller *et al.,* 2002). These data also suggests, the presence of ATM and ATR activation has no affect on calcium inactivation of Cdk1 or interconnected Plx1. Mitotic exit consequentially was induced in a similar manner to extract without ATM and ATR induction. In conclusion, figure 3.9a and 3.9b results show neither Cdk1 nor Plx1 mitotic kinase activities are target mechanisms of the ATM and ATR dependent defects in spindle assembly.

A) Quantification of Histone H1 *in vitro* kinase assay
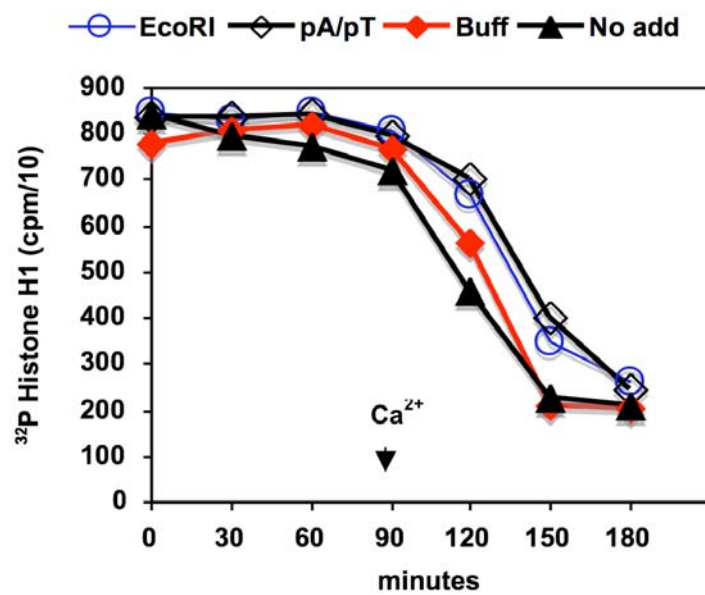
B) Quantification of Casein *in vitro* kinase assay
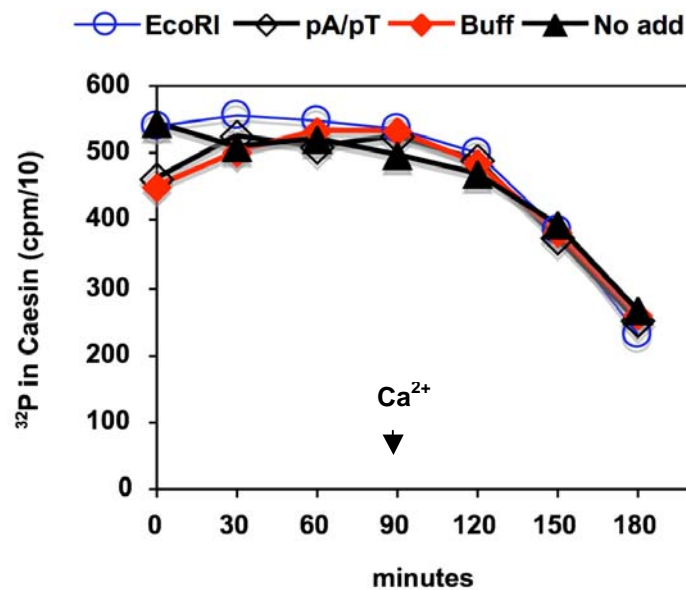
Figure 3.9 ATM and ATR induction shows no affects on mitotic kinases, Cdk1 and Plx1 activities

CSF extracts were supplemented with 1,000 sperm nuclei/μl and treated with CSF-XB buffer (Buff), 0.25 U/μl *EcoRI (EcoRI)*, 5 ng/μl linear DNA (pA/pT) or left untreated (No add). After 90 minutes incubation at 23 °C, CaCl$_2$ was added to samples and incubated for a further 90 minutes. Kinase reactions were performed at 30 °C for 20 minutes in 20 μl of EB kinase buffer supplemented with 50 μM ATP and 1 μl of [γ-32P]-ATP (10 mCi/ml). Radioactivity incorporated was quantified by a scintillation counter and reported as a mean of three separate experiments in the graphs. **(a)** Cdk1 kinase assay was performed with 2 μl of extracts taken at indicated times in kinase reaction supplemented with 0.5 mg/ml histone H1 recombinant protein. Labeled samples were spotted on phosphocellulose filter paper, washed and then quantified. **(b)** Plx1 was immunoprecipitated from 20 μl of extracts taken at indicated times, as described in materials and methods. Plx1 kinase assay was performed in kinase reaction supplemented with 0.5 mg/ml Casein recombinant protein. Reactions were separated by electrophoresis on a small standard SDS-PAGE gel, stained with Coomassie Blue and then underwent autoradiography. Bands corresponding to Casein were excised and radioactivity quantified.

3.10 Plx1 kinase activity elimination from ATM and ATR spindle assembly inhibition in *Xenopus* egg extract

We observe in the previous figure (3.9), endogenous Plx1 kinase activity in mitosis is unaffected by the presence of active ATM and ATR. We extended Plx1 investigations by attempting to rescue ATM and ATR dependent abnormal spindle formation by addition of excess Plx1 recombinant protein. Potentially, a higher abundance of Plx1 kinase could overcome possible ATM and ATR inhibition affects.

Spindle assembly in *Xenopus* egg extract after the introduction of Plx1 recombinant protein and *EcoRI* treatment is shown in figure 3.10. We observe excess Plx1 has no affect on ATM and ATR dependent spindle abnormalities. The quantification shown in figure 3.10b, confirms ATM and ATR disrupted spindle formation is not prevented by supplementing with excess recombinant Plx1.

Taken together with figure 3.9, these data consistently suggest the activity of Plx1 kinase is not contributing to ATM and ATR dependent spindle defects. These data indicate that ATM and ATR are not inhibiting Plx1 mechanisms in spindle assembly. The ATM and ATR checkpoint target in spindle assembly inhibition still requires identification.

A) Fluorescent images of *Xenopus* egg extract spindle assembly
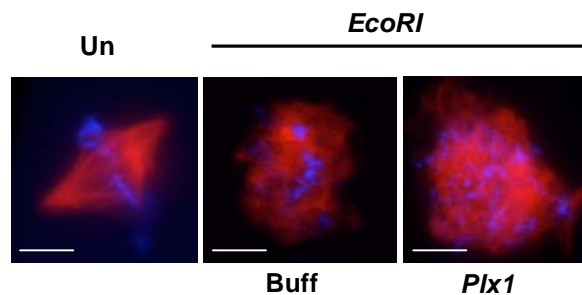
B) Quantification of observed spindle structures
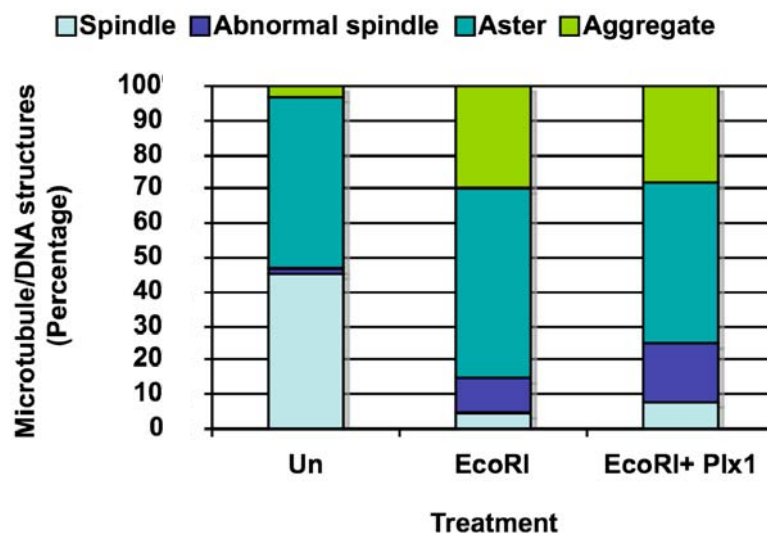
Figure 3.10 Absence of Plx1 role in ATM and ATR induced spindle assembly defects

Spindle assembly was obtained in CSF egg extract supplemented with 1,000 sperm nuclei/μl and rhodamine tubulin 50 μg/ml incubated at 20 °C for 90 minutes. Extracts were untreated (Un) with recombinant protein buffer and CSF-XB buffer, or supplemented with 0.25 U/μl *EcoRI* (*EcoRI*) and recombinant protein buffer or with 0.25 U/μl *EcoRI* and 80 ng/μl purified recombinant *Xenopus* Plx1 (Plx1). Spindles were spun onto coverslips as described in materials and methods. Spindle assembly images were acquired and quantified on a Deltavision microscope, data is representative of three separate experiments. **(a)** Images of spindle assembly, DNA is shown in blue and microtubules shown in red. Scale bar indicates 10 μm. **(b)** Quantification of different DNA associated microtubule structures found in treatments. Microtubule structures were identified as bipolar spindles, asters, abnormal spindles (spindles without poles + spindles with dispersed chromosomes) and aggregates (large disorganized microtubules with DNA dispersed throughout). Percentages are relative to 100 structures counted for each treatment.

3.11 RCC1 chromatin association remains unchanged by ATM and ATR activation in *Xenopus* egg extract

Following the elimination of both mitotic kinase, Plx1 and Cdk1, the target in ATM and ATR spindle assembly disruption remains unidentified. Further experiments were necessary to attempt to isolate the ATM and ATR checkpoint mechanism involved in the spindle assembly abnormalities. As discussed in chapter one (1.2.1), it has been shown that RCC1 is the guanine-nucleotide exchange factor for RanGTPase required for Ran-GDP conversion to Ran-GTP (Bischoff and Ponstingl, 1991a). Carazo-Salas, *et al.* proposed that Ran-GTP is an essential factor in microtubule nucleation regulation, with additional functions in spindle array organisation and dynamics (Carazo-Salas *et al.,* 2001). Initiation of spindle assembly has been determined to be dependent on concentrated RCC1 chromatin association leading to the generation of localised Ran-GTP (Carazo-Salas *et al.,* 1999). RCC1 has been implicated in regulating the amount of microtubule nucleation through controlling the conversion of Ran-GDP to Ran-GTP (Carazo-Salas *et al.,* 1999). ATM and ATR inhibition of RCC1 chromatin association would consequently affect RCC1 capacity in localised Ran-GDP conversion to Ran-GTP. Potentially ATM and ATR targeting of RCC1 function may disturb control mechanisms of spindle assembly.

Due to the major contribution of RCC1 function in the spindle assembly pathway described, we next carried out an investigation into the effects of ATM and ATR activation on RCC1 binding to chromatin. In figure 3.11 (top panel) we show RCC1 immunoblot detection of isolated chromatin at time points across mitosis progression, in the absence and presence of *EcoRI* within *Xenopus* egg extract. RCC1 immunoblot detection reveals that ATM and ATR induced by chromosomal breakage appears not to impair endogenous RCC1 binding to sperm chromatin compared to the absence of DNA damage. Histone H3 immunoblot detection of the time course is shown below in figure 3.11 (bottom panel) as a loading control.

These findings indicate RCC1 chromatin binding, necessary for initiation of spindle formation, is not perturbed by ATM and ATR activation. We therefore can argue that RCC1 mechanism is not the target of ATM and ATR in generating spindle assembly abnormalities.

M$_r$ (kD)

50 —	RCCI
15 —	HISTONE H3

No nuclei	-	+	-	+	-	+	*EcoRI*
	30		60		90		minutes
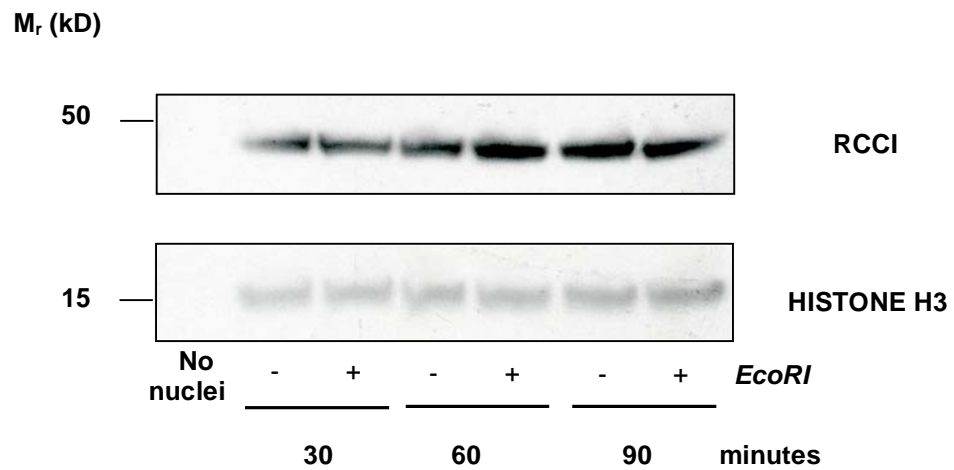
Figure 3.11 Unperturbed RCC1 association with chromatin in the presence of ATM and ATR activation in mitotic *Xenopus* egg extract

Chromatin binding was performed in 50 μl of CSF arrested *Xenopus* egg extracts, left untreated (no nuclei) or supplemented with 3,000 nuclei/μl. Extracts were treated with (+) or without (-) of 0.25 U/ml *EcoRI* and incubated for 90 minutes at 20 °C. At indicated time intervals, extracts reactions were stopped by addition of cold EB buffer. Samples underwent chromatin isolation through a series of centrifugation steps and washed as described in materials and methods. Finally, samples were boiled in Bio-Rad sample buffer, separated by electrophoresis on a standard 10 % SDS-PAGE gel and proceeded to immunoblot detection with antibodies recognising RCC1 (top panel) and Histone H3 (bottom panel).

3.12 Absence of Ran-GTP role in ATM and ATR dependent spindle assembly inhibition in *Xenopus* egg extract

As we have previously described in figure 3.11, an important pathway of spindle assembly involves initiation by localised RCC1 chromatin association, which in turn gives rise to localised generation of Ran-GTP. Ran-GTP gradient generation in proximity to chromatin is required for coordinating regulation of microtubule nucleation and dynamics of spindle formation (Carazo-Salas *et al.,* 1999). In the previous figure, we found RCC1 association to chromatin was unaffected by ATM and ATR activation. We continued by exploring the possibility that ATM and ATR targets a downstream factor, Ran within the spindle assembly pathway. For this purpose, we obtained constituently active RanQ69L recombinant protein, a mutant form of Ran loaded with GTP and unable to hydrolyse GTP (Bischoff *et al.,* 1994; Carazo-Salas *et al.,* 1999). We performed the spindle assembly in the absence and presence of ATM and ATR activation, with and without the addition of RanQ69L. Fluorescent images in figure 3.12a show in the presence of RanQ69L and absence of *EcoRI* treatment spindles form with and without associated chromatin (panel one and three). These findings are in agreement with those of Carazo-Salas *et al.,* 1999, where they demonstrated that excess Ran-GTP induced a partial uncoupling of spindle assembly from chromatin (Carazo-Salas *et al.,* 1999). We also show in figure 3.12a that addition of constitutively active Ran to *EcoRI* also generates not only typical DNA associated aggregated abnormal spindle (panel two), but also spindle-like-structure independent of DNA (panel four). This observation suggests Ran-GTP displays some degree of ATM and ATR dependent spindle assembly defect rescue, whilst being unable to fully recapitulate normal spindle assembly. Further confirmation of Ran-GTP insufficiency in restoring normal spindle assembly is highlighted by figure 3.12b. The quantification of structures associated with DNA revealed that supplementing RanQ69L in the presence of *EcoRI* does not rescue defective spindle structures compared with *EcoRI* treatment alone.

In light of these data and previous findings of preserved RCC1 chromatin binding (figure 3.11), we draw the conclusion that RCC1/Ran-GTP spindle assembly pathway is unaffected by active ATM and ATR. We can state that ATM and ATR do not target RCC1 and Ran-GTP spindle assembly mechanisms. Therefore, at this point, the ATM and ATR checkpoint inactivating spindle assembly remains undetermined.

.

A) Fluorescent images of spindle assembly in *Xenopus* egg extract

Figure 3.12 ATM and ATR dependent spindle defects in the presence of Ran-GTP

Spindle assembly was obtained in CSF egg extract supplemented with 1,000 sperm nuclei/μl and 50 μg/ml rhodamine tubulin. Extract was treated with CSF-XB buffer (Buff) or 0.25 U/μl *EcoRI* (*EcoRI*) both in the absence and presence of 2.5 μM recombinant RanQ69L (Ran-GTP). Samples were incubated at 20 °C for 90 minutes, diluted and formaldehyde fixed in BRB80 buffer and spun onto coverslips through a glycerol cushion as described in materials and methods. DNA was stained with DAPI. Images were acquired and counting was undertaken on a Deltavision microscope. Data is representative and shows typical findings of three separate experiments. **(a)** Images of treatments show DNA in blue and microtubules in red, scale bar indicates 10 μm. Fields showing DNA associated microtubule structures (panels one and two) and DNA independent spindle structures (panels three and four). **(b)** Quantification of different DNA associated microtubule structures found in isolated treatments: (Un), extracts treated with 0.25 U/μl *EcoRI* (*EcoRI*) or 0.25 U/μl *EcoRI* + 2.5 μM recombinant RanQ69L (*EcoRI* + Ran-GTP). Microtubule structures were identified as bipolar spindles, asters, abnormal spindles (spindles without poles + spindles with dispersed chromosomes) and aggregates (large disorganized microtubules with DNA dispersed throughout). Percentages are relative to 100 structures counted for each treatment.

3.13 Chromatin-coated bead in anastral spindle assembly induce ATM and ATR activation in *Xenopus* egg extract

In figures 3.9-3.12, we investigated some of the central factors involved in mitosis progression and spindle assembly pathways in the context of ATM and ATR activation. Research undertaken so far suggests a lack of ATM and ATR influence on functions and activities of the major spindle assembly elements tested. Through these studies, we had gained no further insight into the basis of spindle inhibition nor did we ascribe a mechanism engaged in spindle perturbation. Previous experiments have been based on centrosome-directed spindle assembly. To determine the pathway corresponding to defective spindle assembly, we turned our focus to acentrosomal or anastral self-ordering spindle assembly mechanism. An important distinction between spindle assembly mechanisms is that the presence of sperm nuclei promotes the formation of aster/centrosome structures, which act as dominant sites for spindle assembly and organization (Heald *et al.,* 1997). Whereas, anastral spindles formation relies on self-assembly. Anastral spindle assembly is prevalent in higher plants, meiotic cells and in some other cell types (Theirkauf and Hawley, 1992; Bartolini and Gundersen, 2006). In the process of spindle self-assembly, chromatin promotes microtubule polymerisation and actions of motor proteins aid sorting and organisation of microtubules into a bipolar spindle array (McKim, and Hawley, 1995; Heald *et al.,* 1997; Theurkauf and Hawley, 1992; Matthies *et al.,* 1996; Khodjakov and Rieder, 2001).

In *Xenopus* egg extract, chromatin-coated beads can promote the assembly of spindles in the absence of centrosomes and kinetochores (Heald *et al.,* 1996). Figure 3.13a, a schematic representation illustrates anastral spindle assembly in *Xenopus* egg extract. It was very apparent that the platform of anastral spindle assembly is based on linear DNA molecules, which potentially could activate ATM and ATR. We tested the capability of spindle promoting chromatin-coated beads in inducing ATM and ATR through monitoring downstream H2AX phosphorylation. We observe an approximate 11-fold increase in H2AX radiolabelled phosphate incorporation in the presence of chromatin-coated beads compared to beads alone. Figure 3.13b also shows similarly high levels of H2AX phosphate incorporation in the presence of chromatin-coated beads to that of linear DNA plasmid (DSB) alone. Moreover, we observe H2AX modification levels in the presence of chromatin-coated beads were reduced by over 2-fold with incorporation

of ATM and ATR inhibitors. As expected, we determined the presence of DNA beads does indeed induce ATM and ATR activation (figure 3.13b).

We examined the formation of anastral spindles and questioned whether chromatin-coated bead induction of ATM and ATR inhibits their assembly. In agreement with previous published data, we show polar spindles correctly assemble in *Xenopus* egg extracts around the platform of chromatin-coated beads (Heald *et al.,* 1996). We counted an average number of 16 anastral spindles in the three microscope fields examined from three separate experiments. This is a remarkable phenomenon, as in these conditions active ATM and ATR do not perturb anastral spindle assembly. These experiments indicate that in contrast to sperm driven spindle assembly DNA beads induced spindle are insensitive to DNA damage response pathways. A major difference between beads and sperm induced spindles is that the former lack centrosomes and mostly rely upon pathways emanating from chromatin induced gradients to coordinate microtubule polymerization and spindle formation. Since the basic mechanisms are the same for the two spindle assembly pathways we thought that the effect of ATM and ATR on centrosome-driven spindle assembly was due to a target present on centrosomes. Therefore we set out to investigate possible centrosome targets of ATM and ATR. This strategy will be described in the next chapter.

A) Anastral spindle assembly in *Xenopus* egg extract

Time (minutes)   0   120   135   165

Chromatin-coated beads in CSF extract + Calcium   Interphase DNA replication   + CSF extract   Microtubule polymerisation and sorting   Anastral spindles

KEY: ○ Chromatin-coated beads   / Microtubules

B) Quantification of Histone H2AX kinase assay

Bar chart: x-axis categories DSB, DNA beads, DNA beads + ATMi, DNA beads + Caff, Beads, Un. y-axis ^{32}P in H2X peptide (cpm) from 0 to 70000.

C) Fluorescent image of Anastral spindle formation in *Xenopus* egg extract

Figure 3.13 Anastral spindle assembly in *Xenopus* egg extract in the presence ATM and ATR activating chromatin-coated beads

(a) A schematic representation of anastral spindle assembly in *Xenopus* egg extract. Chromatin-coated beads undergo interphase DNA replication in CSF egg extract with calcium addition. Subsequently driven into metaphase with CSF extract addition, microtubule polymerise and organise into anastral spindles around chromatin-coated beads. (b) Chromatin-coated beads were prepared as described in materials and methods. CSF extracts were supplemented with 0.4 mM CaCl, 0.2 mg/ml Cyclohexamide in the presence of beads alone (Beads) or 5 ng/μl DNA-coated beads (DNA beads) or 5 ng/μl linear plasmid DNA (DSB). Extracts were incubated for two hours at 20 °C, then supplemented with half volumes of CSF extract supplemented with 50 μg/ml rhodamine tubulin. Extracts in the presence of chromatin-beads were left untreated (DNA beads), or treated with 20 μM Ku55933 (DNA beads + ATMi) or 2 mM caffeine (DNA beads + Caff). Samples were incubated for a further 45 minutes at 20 °C. Kinase assay was performed at 30 °C for 20 minutes with 2 μl of extracts and 0.5 mg/ml histone H2AX peptide in 20 μl of EB kinase buffer containing 50 μl ATP and 1 μl of [γ-^{32}P]-ATP (10 mCi/μl). Labeled samples were spotted on phosphocellulose filter paper, washed and then quantified by a scintillation counter. The mean values radioactivity incorporated on H2AX peptide from three separate experiments reported in the graph. Error bars indicate standard deviation (s.d.). (c) Untreated anastral spindles extracts were diluted and formaldehyde fixed and spun onto coverslips through a glycerol cushion as described in material and methods. Image was acquired on a Deltavison microscope and representative of anastral spindle assembly. Microtubules shown in red and DNA in blue. Scale bar indicates 10 μm.

3.14 Summary

In this chapter, we have demonstrated that ATM and ATR activate in mitotic *Xenopus* egg extract in response to linear DNA molecules (pA/pT) and restriction endonucleases (*EcoRI*) together with sperm nuclei (figures 3.1 and 3.2). Strikingly, we found spindle assembly was perturbed following ATM and ATR activation in CSF and cycled *Xenopus* egg extracts and in somatic XTC cells (figure 3.4, 3.7 and 3.8). Consistently, spindle assembly abnormalities were directly associated with ATM and ATR activation, as spindle defects were prevented in the presence of ATM and ATR inhibitors (figure 3.4, 3.6 and 3.7). Furthermore, we showed the application of alternative DNA damage conditions such as pA/pT, Doxorubicin and restriction endonuclease *NotI* similarly resulted in perturbed spindle assembly in *Xenopus* egg extract (figure 3.6). These treatments discounted the involvement of chromosomal or kinetochore physical damage in spindle assembly abnormalities. Collectively, these data showed ATM and ATR dependent checkpoint signalling leads to spindle formation defects.

Interestingly, in the presence of ATM and ATR activation in *Xenopus* egg extracts the number of asters increased, although their morphology remained normal (figure 3.4). We propose that activated ATM and ATR targets a pathway involved in aster maturation into maintained spindle arrays. This idea was further supported by the observation of spindle assembly aberrancies induced by the induction of ATM and ATR activation during spindle assembly progression and once spindles were formed (figure 3.5). We then aimed to identify the corresponding ATM and ATR target mechanism. In contrast to its effect on mitotic onset, ATM and ATR activation did not influence mitotic kinases, Cdk1-Cyclin B or Plxl activities in mitotic progression or mitosis exit (figure 3.9). Furthermore, Plx1 excess was unable to rescue ATM and ATR spindle assembly inhibition (figure 3.10). We also eliminated spindle assembly dependent pathway RCC1 and Ran(GTP) as targets of active ATM and ATR. We found that RCC1 binding to chromatin was not impaired (figure 3.11) and inhibition of spindle assembly remained in extracts supplemented with constitutively active excess Ran-GTP (figure 3.12).

In attempts to uncover the mechanism responsible for spindle assembly abnormalities, we investigated the formation of anastral spindles induced by chromatin-coated beads in *Xenopus* egg extract. We established that chromatin-coated beads, made up of linear

DNA molecules, activate ATM and ATR. However, we showed normal anastral spindle assembly occurs (figure 3.13). These observations were crucial to this research, as anastral spindle formation and centrosome-driven spindle assembly depend on many common mechanisms, excluding their potential as ATM and ATR targets. Normal anastral spindle assembly in the presence of ATM and ATR activation indirectly elucidates the ATM and ATR checkpoint target to centrosome-driven spindle assembly. We posit that ATM and ATR target a spindle assembly regulatory element within functional centrosomes. On this basis, we concentrated on isolating ATM and ATR target candidates.

4 Chapter 4 Identification of ATM and ATR target in spindle assembly

In the previous chapter, we showed ATM and ATR activation in mitotic *Xenopus* egg extract strongly impairs normal spindle assembly. Through testing the major mechanisms required for spindle assembly we eliminated these spindle formation pathways as targets of mitotic ATM and ATR activation. Importantly, we observed anastral spindle formation around linear DNA coated beads that activate ATM and ATR. These data uncovered a possible dependency of abnormal spindle formation on the presence of sperm nuclei and subsequent aster-centrosome driven assembly. On this basis, we proceeded by directing research towards discovering a novel centrosome related target mechanism. In this chapter, we address the identification of ATM and ATR targets by developing a screening method utilizing a *Xenopus* cDNA expression library.

4.1 Isolation of ATM and ATR substrates by screening *Xenopus* cDNA expression library

We deviated from traditional methods of isolating substrates, which utilized direct *in vitro* kinase assays with recombinant proteins; the substrate candidate approach. We felt such an approach would be somewhat cumbersome and an unlikely means to identify the target. Other techniques were discounted, such as the isolation of substrates by two-hybrid hybridisation, which were deemed to be potentially limited due to the transient or unstable nature of interactions, which in turn may mask potential candidates.

We wanted to apply a method that would isolate ATM and ATR kinase targets in the physiological context of egg extract, which would allow the entirety of *Xenopus* egg proteins to be screened as potential targets. We adopted and modified an expression screening method described by Lustig *et al.,* using a full length, normalised *Xenopus* laevis maternal cDNA library donated by Tony Hyman (Max Planck Institute of Molecular and Cellular Biology and Genetics, Dresden, Germany) (Lustig *et al.,* 1997). Lustig *et al.,* describe a functional assay that rapidly and systematically identifies cDNAs on the basis of protein biochemical activities or properties. This technique relies

on protein postmodifications, such as phosphorylation, which alter electrophoretic mobility. We adapted the screening procedure by introducing translated proteins into the biochemical setting of *Xenopus* egg extract with activated ATM and ATR, which would enable dependent DNA damage response interactions to occur with their natural partners and protein complexes.

A schematic illustration of the experimental procedure applied to screen cDNA expression library for ATM and ATR targets is shown in Figure 4.1a. In brief, pools of *Xenopus* plasmid cDNA under the control of the SP6 promoter were transcribed and translated in reticulate lysate Promega TnT system in the presence of [^{35}S]-methionine. Labelled lysates were mixed with *Xenopus* egg extracts supplemented with or without linear DNA (pA/pT) and run on a 10 % SDS-PAGE gel. Through this technique we scored translated proteins for changes in migration patterns in the presence of linear DNA addition compared to its absence. ATM and ATR activation or other DNA damage response kinases, modify proteins substrates by phosphorylation, leading to slower migrating forms. In performing the described screening experiments, SDS-PAGE gels and electrophoresis conditions were optimised to maximise the separation of translated proteins and enhance visibility of mobility shifts.

Using the assay described above, figure 4.1b shows examples of four cDNA pools (C, K, F and M) of labelled translated proteins containing different shifting clones (C9, F3, K11, M6 and M7). Both mitotic and interphase extracts were able to initiate phosphorylation of translated cDNAs to a similar level (data not shown), the assay in shown in figure 4.1b was conducted using interphase egg extract. The majority of translated clones showed no apparent gel shift in the presence of DNA damage. We observed a good overall representation of pooled clones amplified in standard *E. coli* strains, from which we identified on average, only one to three clones changed in gel mobility with ATM and ATR activation per 384 well plate.

The clones showing gel mobilitiy changes in Figure 4.2b were isolated by intersecting pools from rows and columns, cDNAs were then identified by DNA sequencing of both strands. Through sequencing we established: C9 as XCEP63; F3 as Gemmin coiled-coil containing protein (XGEMC1); K11 as *Xenopus* ortholog of cytoplasmic activation/proliferation-associated protein-1, Caprin-1 (XRNG-105); M6 as transcription factor Homobox-6 and M7 as **I**nterferon **r**egulatory **f**actor-**6** (XIRF-6). We

also ascertained from DNA sequencing analysis that the donated library was of a high quality and contained full-length cDNA inserts.

In combination with low frequencies of candidate 'hits', we were further reassured regarding the experimental set up as the data the obtained from the screening procedure indicates collectively a strong relevance to cell cycle regulation and/or checkpoint response networks. XGEMC1, Caprin-1 (XRNG-105) and XIRF-6 are particularly noteworthy examples identified in the screen. However, these ATM and ATR potential target candidates have not been previously described specifically in relation to mitotic process and no indications of involvement in centrosome-driven spindle assembly has yet been shown.

A) Schematic representation of experimental set up to identify ATM and ATR targets in *Xenopus* egg extract
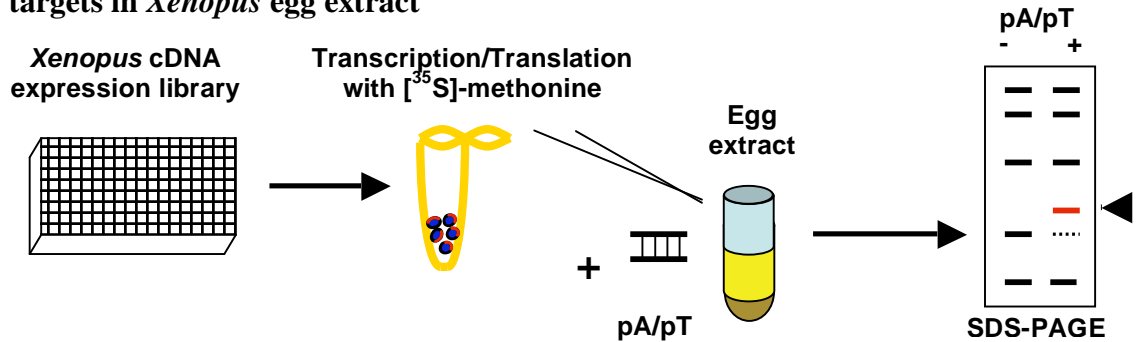
B) Autoradiographs of cDNA expression screening in *Xenopus* egg extract
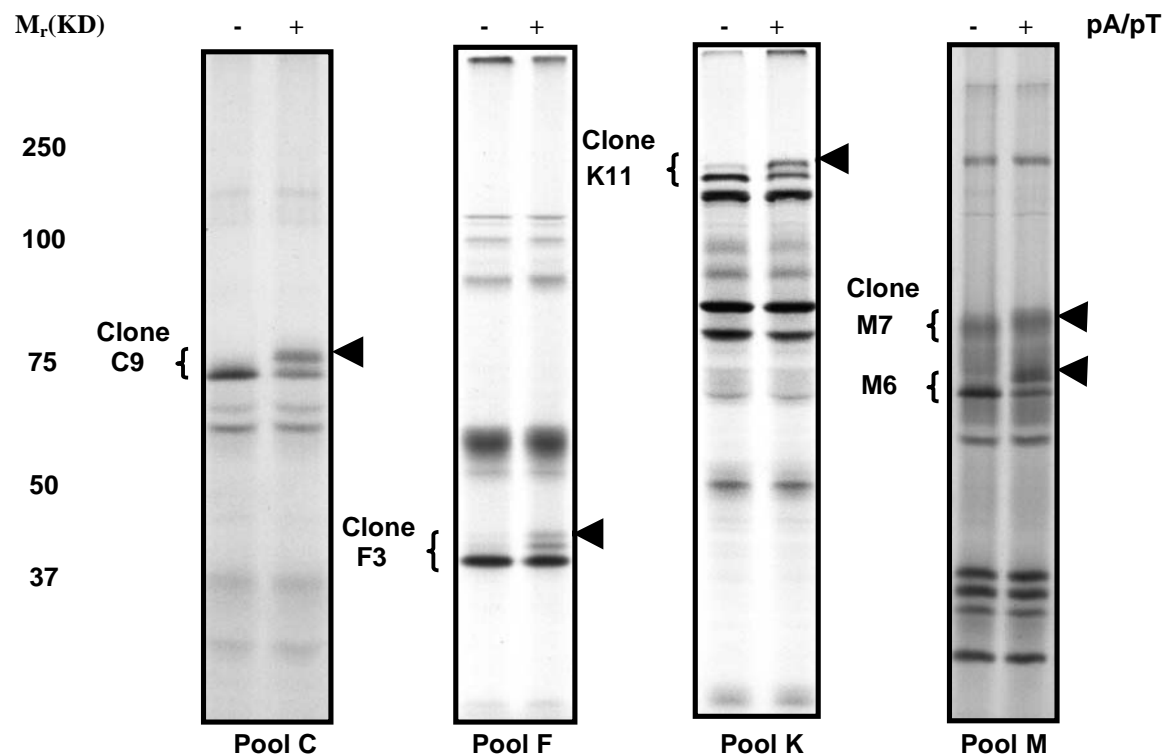
Figure 4.1 Small pool cDNA expression library screening for ATM and ATR substrates in *Xenopus* egg extract

(a) Schematic representation of screening protocol. Row and columns of cDNA library were pooled and then transcribed and translated in a reticulocyte lysate system (TNT, Promega) in the presence of $[^{35}S]$-methionine. Labelled proteins were exposed to interphase extracts treated with or without linear DNA (pA/pT). Samples were separate by electrophoresis on a SDS-PAGE gel and audioradiography films were analysed for shifts in migration patterns (band migration change shown in red and indicated by arrow). **(b)** Pools of cDNA library were transcribed and translated in 20 μl of TnT coupled Promega system containing $[^{35}S]$-methionine at 30 °C for 90 minutes. Interphase *Xenopus* egg extract was pretreated for 20 minutes at 23 °C with (+) or without (-) 50 ng/μl linear DNA (pA/pT). Labelled transcribed proteins (2 μl) were mixed with treated extracts 2 μl and incubated for a further 30 minutes at 23 °C. Samples were diluted in Bio-Rad sample buffer, boiled and separated by electrophoresis on a large 10 % SDS-PAGE gel. Gels then underwent audioradiography. Indicated are examples of pools: C, F, K and M showing shift in migration in the presence of pA/pT treatments of labeled proteins derived from clones C9, F3, K11, M6 and M7.

4.2   XCEP63 as an ATM and ATR target of interest

We described in the figure above the isolation of clones endoding potential ATM and ATR targets. The identified proteins beliefly mentioned, although verifying the cDNA expression screening approach, it does not imply any connection to centrosomes or relations specifically to mitotic processes. However, we did identify XCEP63, contained within pool C, isolated from clone C9 (GenBank accession number: FJ464988). Andersen *et al.* originally identified CEP63 in a proteomic analysis of the human centrosome and confirmed centrosomal localisation by expressing GFP construct in cells (Andersen *et al.,* 2003). At the time we isolated XCEP63, no CEP63 characterization studies had been published and consequently no function had been ascribed. The probable association to the centrosome distinguishes XCEP63, showing promise as a target of ATM and ATR that maybe linked to centrosome-driven spindle assembly.

In figure 4.2a, we show again XCEP63 translated protein molecular weight shift with introduction of pA/pT treatment. We determined the mobility shift of XCEP63 in the presence of pA/pT constituently in both interphase and mitotic egg extracts (data not shown). The prevention of XCEP63 gel mobility shift on caffeine addition is shown in figure 4.2a. Caffeine sensitivity indicates a dependency of XCEP63 gel mobility alteration on active ATM and ATR. These data confirm possible centrosomal XCEP63 targeting by ATM and ATR, raising interest in a possible role for XCEP63 in spindle assembly.

XCEP63 as a centrosome protein candidate was of high interest. We applied NCBI BLAST programs to analyze XCEP63 sequences. XCEP63 DNA and amino acid sequence is shown in Appendix one. Sequence analyses revealed XCEP63 is a coiled-coil protein that contains a large domain present in the SMC (**s**tructural **m**aintenance of **c**hromosomes) coiled coil protein superfamily of ABC-like ATPases, highly conserved from bacteria to humans (Hirano, 2005). XCEP63 SMC domain is depicted in Appendix two.

A) Audioradiograph of XCEP63 in *Xenopus* egg extract
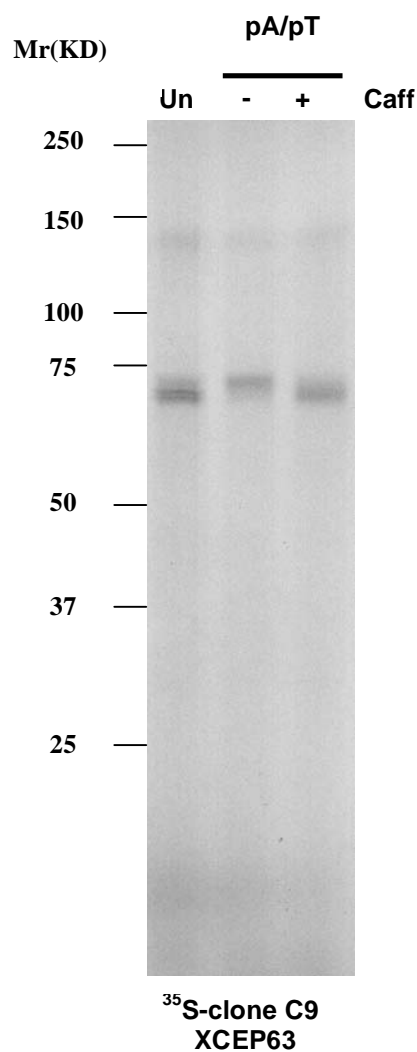
Figure 4.2 XCEP63 modification in the presence of active ATM and ATR in *Xenopus* egg extract

(**a**) Clone C9 plasmid cDNA encoding XCEP63 was transcribed and translated in the presence of [^{35}S]-methionine with Promega TnT system as previously decribed. Interphase extract was pretreated with (+pA/pT) and without (Un) 50 ng/µl of pA/pT in the absence (- Caff) or presence (+ Caff) of 2 mM caffeine for 20 minutes at 23 °C. Translated XCEP63 (2 µl) was mixed with treated extract (2 µl) and incubated for a further 30 minutes at 23 °C. Samples were suplemented with Bio-Rad sample buffer, boiled and underwent gel eletrophoresis on a large 10 % SDS-PAGE followed by audioradiography.

4.3 CEP63 conservation in vertebrates

Importantly for the significance of *Xenopus* CEP63 studies and the relevance of *Xenopus* CEP63 analyses to other species, we find that CEP63 is conserved among vertebrates. Figure 4.3a shows *Xenopus laevis* CEP63 amino acid sequence alignment with it's putative orthologs *Mus musculus (M.Musculus), Gallus gallus (G.gallus) and Homo sapiens (H.Sapiens).* CEP63 sequences were obtained from NCBI database and aligned using CLUSTALW multiple sequence alignment program. Textshade on the alignments shows identity highlighted in green, similarity in yellow and blue. The sequence alignment reveals CEP63 homology across species. All CEP63 orthologs carry the SMC domain architecture, shown by line mark within sequence alignment (figure 4.3). Isolated BLAST protein sequence comparison of *Xenopus* CEP63 aligned with human CEP63 indicates 38 % identity and 59 % similarity, verifying a significant level of homology. CEP63 conservation across species suggests CEP63 role is less likely to be evolutionarily redundant and its preservation indicates importance of functional purpose.

The commercially available gene expression profile of human CEP63 is shown in figure 4.3b. These data indicates CEP63 is expressed throughout the majority of tissues and suggests CEP63 plays a housekeeping role within all cells types. Of particular interest, expression levels are increased in highly replicating tissues such as the testis, which implies a potential importance of CEP63 function in cell proliferation.

A) Sequence alignment of XCEP63 and putative orthologes

```
M.Musculus   IEALLEGIQNRGHS------GGFLTSCEAELQELMKQIDIMVAHKKSEWEGQTHALETCLDIRDRELKALRSQLDMKHKEVGILHQQIEE
H.Sapiens    IEALLEGIQNRGHG------GGFLTSCEAELQELMKQIDIMVAHKKSEWEGRTHALETCLKIREQELKSLRSQLDVTHKEVGMLHQQVEE
G.gallus     IEALLEGMQRNGQGSLIPSSSGFLTSCEAELQELMKQIDIMVAHKKAEWEGQTQALEACLGVREQELSSARAALEEKHKEVGKLRQQLED
X.Laeis      IEALLQGLQRQDR------MGALQDSCEAELQELMKQIDIMLDHKRSQWEAETETMKTRLELKEQELNCALDREERLNQEVRRLRQQLIQ

             IEKTKQEMAMEYKEELLKLQEELSRLKRSYEKLQKKQLREFRGN-TKSFREDRSEIERLTGKIEEFRQKSLDWEKQRLIYQQQVSSLEAQ
             IEKIQEMTMEYKQELKKLHEELCILKRSYEKLQKKQMKEFRGN-TKNHREDRSEIERLTAKIEEFRQKSLDWEKQRLIYQQQVSSLEAQ
             IEAAKQDLVREYEQQLKKFQEELARLKRSYEKLQKKQLREAREEATKRQGDDQCEMSRLSRKLEEFRQKSLDWEKQRLLYQQQVASLEAQ
             IEEETQNKTTQYEAQLSGFKEELNRLKKSYEKVQKKHLRSEMKAKAE---EERSEVSRLTRRLEEFRQRSLDWEKQRLLYQQQLAGLEAQ

             IKALAEQSEIIQAQLANRKQKLESVELSSQSEIQHLNSKLERAKDTICANELEIERLNIRVNDLMGTNMTILQDHRQKEEKLRESEKLLE
             RKALAEQSEIIQAQLVNRKQKLESVELSSQSEIQHLSSKLERANDTICANELEIERLTMRVNDLVGTSMTVLQEQQQKEEKLRESEKLLE
             RKALAEQSELIQTQLASRKQILESVLASRSEIQHLTSKLERANDTICANELEVERLNMRVDDLTENNRMILEDQQRVAEELRQSKKMLE
             RKTLIEQTEMYQHQSHNRKQMLEQTSLVGRSELQNLSGQLHRANDSLCAKEEELETLKIQLR-------CAVEGQKRAEHETELSKQAVQ

             ALQEEQKELKASLQSQETFILEAKMQ-EKLQTTLK-AVGTQQSVE---RPLEDCQKERKYSSPGQGVLDNVLSQLDFSHSSEELLQAEVT
             ALQEEKRELKAALQSQENLIHEARIQKEKLQEKVK-ATNTQHAVEA-IRPREESLAEKKYTSQGQGDLDSVLSQLNFTHTSEDLLQAEVT
             VLQDEKMELRATLQSQEDFIDSSKLHQEQLQKELARVTETLHTKEILIKALEERLQEKQLSSPG---LEHILLQLDVAQEKEQHLQAEVT
             ALKEEKAELRATLQAHTEFLQGSRVQKHELLPEGYIRGSEVLRENNS-IRSVEERLQEMGQVG-GETEVEAIRSKLSVSRMNEHRLQAEVT

             RLEGSLESVSATCKQLSQELMEKYEELKRMEGHNNEYRTEIKKLKEQILQADQTYSSALEGMKMEISQLTRELHQRDITIASAKCSSSDM
             CLEGSLESVSATCKQLSQELMEKYEELKRMEAHNNEYKAEIKKLKEQILQGEQSYSSALEGMKMEISHLTQELHQRDITIASTKGSSSDM
             HLEDSLVSSNARCVQLSEELAESIKELQSMEEHRAESKVEIKKLKEQLSQAEQIHRGELEGMRKEILRTLQELHQRDITIASAGGSTSDL
             CLEDSVESVTSQCQLLAKELKGKEEYFHGVKEDHQKCLSENKKLKEQLSQAELTHKSVLDGMRKEISQLTQELHQRDIRMASSAG--IDW

             EKQLKAEMQKAEEKAVEHKEILSQLESLKLENHRLSETVMKLELGLHEAKEISLADLQENYIEALNKLVSENQQLQKDLMSTKSELEHAT
             EKRLRAEMQKAEDKAVEHKEILDQLESLKLENRHLSEMVMKLELGLHEAKEISLADLQENYIEALNKLVSENQQLQKDLMNTKSQLEIST
             EQRLRMEIERAERKAVEHRMILVQLETLKLENRHLSEMLEKVELGVLEGKDATLRALSEDYVVELNKLKSENQQLKKDLSEAKEKLELTT
             ERKIKAERQRAEREAAEHRMSLNALENLRQENCRLSELLQTQEP---------------DVAQALVNLEQANQRLQRELLQTQEKLELIA

             NMCKKKDGEIFNP--AHSRAAGFKNAELKPIHGQHRHDGIKTEQYKTGHHSPRG--QTLDSIDPVARG--PSPLSSHIS--PGSSTVSLP
             QMCKKQNDRIFKP--THSRTTEFKNTEFKPTHGQHRHDGIKTEHYKTDLHSPRG--QASDSINPHSRV--LSPLSPQIS--PCSSTRSLT
             QSQPEGTAQQLQSEEPEPRDVQHRPTQESQHKQDEQTEKIHHKPDKTTQHHQRWKIQPLPAEIPVAVIPEASVLPTQTSRKSCVESPTLA
             Q---RRESEIQN---------AVDSISQELLNKQEQELRIMQERLKVYEQEM----QTFRSQQDAASS--GSSLESIFS----EVWKEQA

             SNFLFEAHSLPSVLDINDVNFSDSLSDCMNDQEEFVSSGSLP-TSPLGSIATRFLEEEELRSHHILERLDAHIEELKRESEKTVRQFTAL
             SYSLCKTHSLPSALDTNEANFSDTMSESMNDQEEFISSCSLP-VSPLGSIATRFLEEEELRSHHILERLDAHIEELKRESEKTVRQFTAL
             AGALQGTDSLLLVLDDSKG-FPDATSRQSNHEQESVPLCPLF-TSSVGSVAARYLEEEELRSQHILECLDAHIEELKKESEKIVRHFGHQ
             TGSPISAASVDSAIEP---------------VEDLASSLPVPPTSPANAVASRFLQEEEQRSHELLQRLNAHIEELKQESQRTVEHFTQA

             V
             K
             E
             R
```

B) CEP63 gene expression profile

Figure 4.3 Homology of CEP63 in vertebrates and widespread human CEP63 gene expression

XCEP63 alignment with its putative orthologs in *M.Musculus, H.Sapiens and G.gallus* species. Amino acid sequence identity is highlighted in green, similarity in yellow and blue. The line mark shows the SMC domain. Sequences for CEP63 orthologs were obtained from NCBI databases and multiple alignment with CLUSTALW program. **(b)** Normalised Gene expression profile for human CEP63 generated by OriGene using OriGene's original Human "Major-Tissue" RapidScan (OriGene Technologies, www.origene.com).

4.4 Summary

The application of *Xenopus expression* cDNA library circumvented the downfalls of traditional techniques and enabled a high-throughput *in vitro* screening for DNA damage response factors. The developed screening assay showed a good level of specificity as relatively few translated proteins gel mobility's were modified in the presence of DNA damage mimicking conditions. Although considerable time was spent screening the cDNA library, we were very successful in identifying potential targets of DNA damage response kinases within the physiological framework of *Xenopus* egg extract. The potential targets identified include XCaprin-1, XGEMC1 and XIRF-6.

Within the realms of our research, we most interestingly identified novel XCEP63 protein containing an SMC domain. We were particularly encouraged by XCEP63' potential centrosome localisation. We showed that XCEP63 translated protein undergoes post-translational modification dependent on the presence of active ATM and ATR. Our interest in XCEP63 candidate rose when sequence analysis revealed CEP63 conservation across vertebrate species, suggesting CEP63' role may be of universal importance. CEP63' possible functional significance was also highlighted with commercial available data that shows human CEP63 is expressed in most cell types and highly expressed in replicating tissues. At this point, we believe we have compiled enough reasoning to warrant the continuation of XCEP63 investigations as a target of ATM and ATR in spindle assembly inhibition. We characterise XCEP63 and its function in the next chapter.

5   Chapter 5 Characterisation of XCEP63

In the previous chapter we describe the isolation of XCEP63 in a cDNA expression screen developed to identify ATM and ATR targets in *Xenopus* egg extract. It became clear that further XCEP63 investigations were warranted particularly as human CEP63 has been localized to the centrosome. XCEP63 has no ascribed function, with likely XCEP63 positioning at centrosomes it is possible XCEP63 could be the ATM and ATR centrosome target in spindle assembly defects. In this chapter we characterise XCEP63 and examine its function in spindle assembly.

5.1   XCEP63-GFP localisation at centrosomes

We began to characterise *Xenopus* CEP63 through protein localisation studies. For this purpose, we fused XCEP63 open reading frame (ORF) into green fluorescent protein (GFP) plasmid construct. XCEP63-GFP was transcribed and translated in reticulocyte lysate coupled system and added to *Xenopus* egg extract spindle assembly assays. Alternatively, we transfected XTC cells with XCEP63-GFP construct to confirm cellular localisation of XCEP63.

The XCEP63-GFP signal is seen at the spindles poles, where centrosomes are located in *Xenopus* egg extract spindle assembly (figure 5.1a). Furthermore, we also detected expressed XCEP63-GFP fusion protein co-localised with gamma tubulin (γ-tubulin) staining at the centrosomes in XTC cells (figure 5.1b). Thus, similarly to human CEP63, GFP tagged *Xenopus* protein localises to the centrosomes (Anderson *et al.,* 2003).

A) Fluorescent images of spindle assembly in *Xenopus* egg extract

MERGE

+ retic   **+ XCEP63-GFP retic**

Tubulin   **XCEP63-GFP**

B) Fluorescent images of XTC cells

MERGE

+ GFP plasmid   **+ XCEP63-GFP construct**

γ-Tubulin   **XCEP63- GFP**
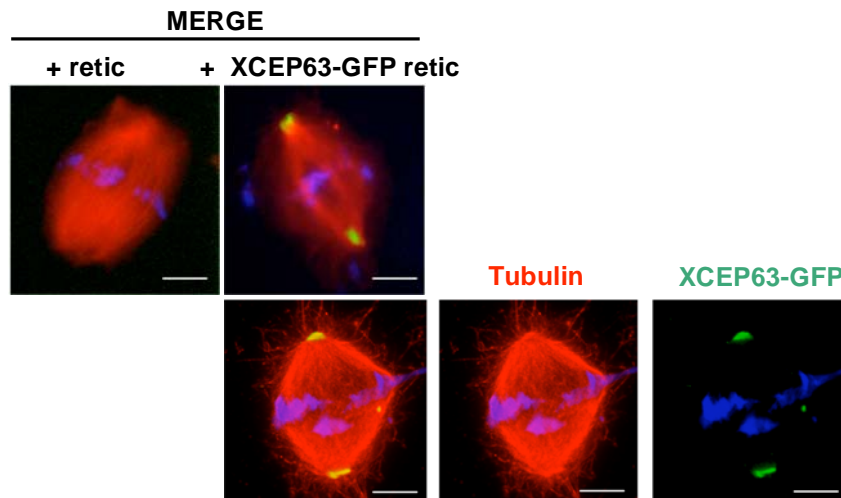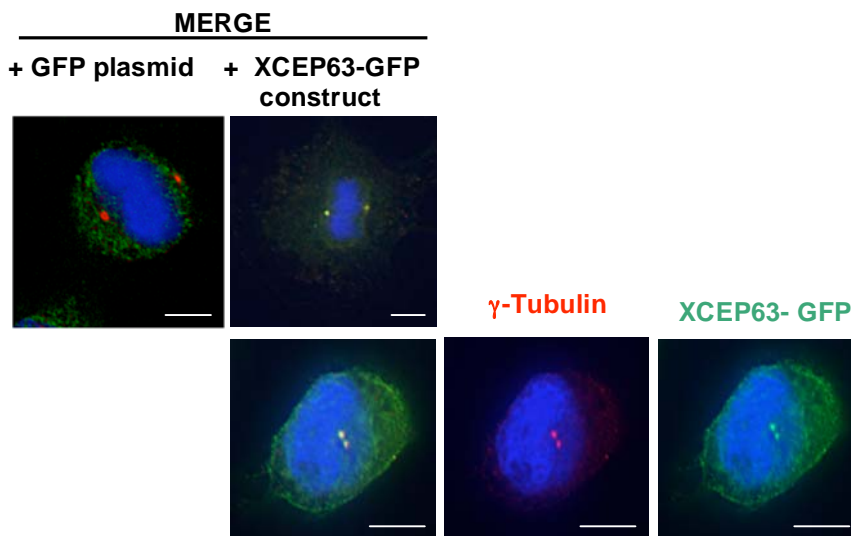
Figure 5.1 *In vitro* and *in vivo* XCEP63-GFP localisation to centrosomes

Representative images shown were acquired on a Deltavision microscope. Scale bar indicates 10 μm. **(a)** XCEP63-GFP fusion construct was transcribed and translated within Promega coupled reticulocyte lysate system as described previously. Spindles were formed in CSF egg extract with the addition of 1,000 sperm nuclei/μl, 50 μg/ml rhodamine tubulin in the presence of 1/5 retic or XCEP63-GFP reticulocyte lysates. Extract was incubated at 20 °C for 90 minutes, then diluted and formaldehyde fixed in BRB80 and spun onto coverslips through a glycerol cushion as described in material and methods. Immunofluorsecent was performed with antibody detecting GFP, shown in green. Microtubules are shown in red and DNA in blue (DAPI). **(b)** XTC cells were transfected in FUGENE6 reagent with empty GFP plasmid DNA or XCEP63-GFP construct DNA. Cells were harvested 24 hours after treatment and immunofluorescence was performed with antibodies recognizing GFP (GFP-XCEP63), shown in green, gamma-tubulin (γ-tubulin), shown in red and DNA was stained with DAPI, shown in blue.

5.2   Immunoblot detection of endogenous XCEP63

Up to this point we have evidence of XCEP63 localisation by using *in vitro* translated protein and an overexpressed XCEP63-GFP construct. It was also necessary to investigate the characteristics of endogenous XCEP63. We generated full-length recombinant 6xHisXCEP63 protein under denaturing conditions to be used in antibody production. Four rabbits were injected with recombinant XCEP63 protein following the standard protocol at Harlan UK (Harlan serum). We tested sera by immunoblot detection comparing pre-bleeds, interim bleeds and terminal bleeds (data not shown). Conditions were optimised for recognition of endogenous XCEP63 in immunoblot experiments. Figure 5.2a shows immunoblot detection with the selected rabbit polyclonal antibody recognising the presence of endogenous XCEP63 in *Xenopus* egg extract. XCEP63 antibodies detect a band corresponding to XCEP63 with a molecular weight of 71 kDa. Also, in figure 5.2a we determined endogenous XCEP63 antibody detection increased in proportion to amount of egg extract loaded. It is approximated within *Xenopus* egg extract that there is endogenous 50 nM XCEP63 (data not shown). To determine XCEP63 maintenance stability in *Xenopus* egg extract, we collected samples at 30 minute intervals across a two and half hour incubation time. In untreated egg extract XCEP63 was not degraded and remained stable (figure 5.2b).

Consistently, the antibody raised against 6xHisXCEP63 recognised a second cross-reacting band in *Xenopus* egg extract, indicated by asterisk in figure 5.2a and 5.2b. We determined this protein detection is non-specific band recognition, as the protein is retained in immunodepleted extracts indicated later in figure 5.5. We also show in figure 5.5 the detection of translated XCEP63 protein, confirming antibody recognition of band thought to be XCEP63 endogenous protein.

Immunoblot detections of XCEP63 in *Xenopus* egg extract

A)

M$_r$ (kD)

75 —

0.5   1   2

* XCEP63

µl of extract

B)

M$_r$ (kD)

75 —

0   30   60   90   120   150

* XCEP63

Minutes
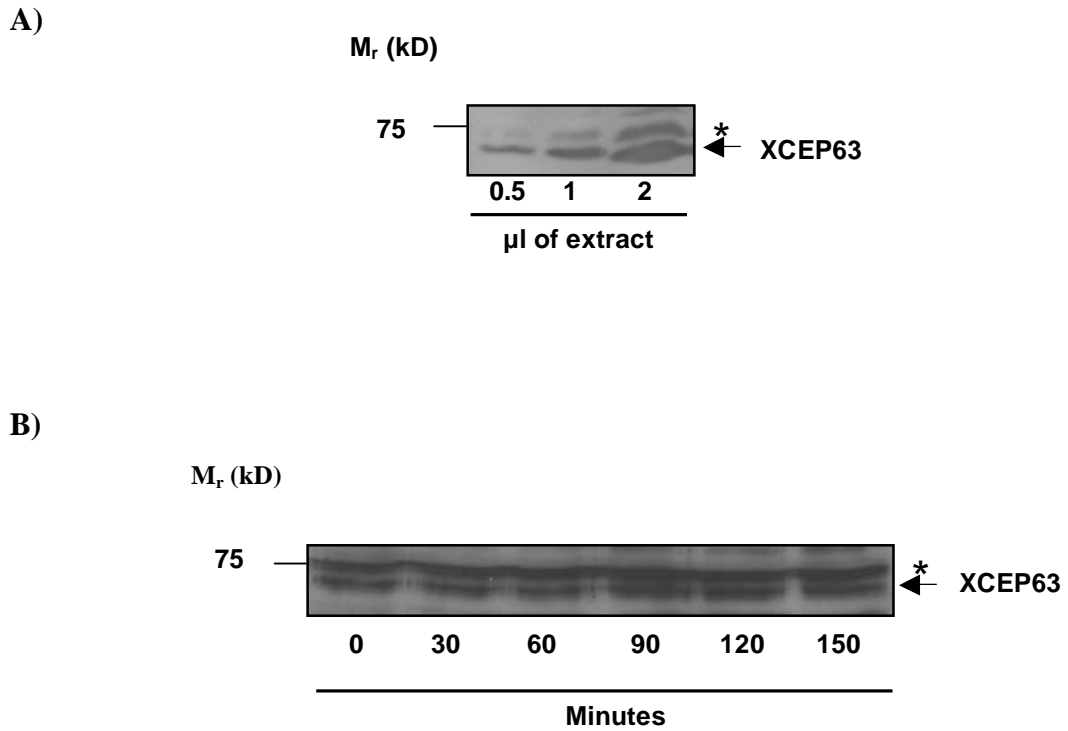
Figure 5.2 Antibody detection of stable endogenous XCEP63 in *Xenopus* egg extract

Shown are representative findings of immunoblot detections using polyclonal antibody serum raised against denatured 6xHisXCEP63 recombinant protein. **(a)** Increasing amounts of untreated CSF arrested *Xenopus* egg extract, 0.5, 1 and 2 µl were added to Bio-Rad sample buffer, boiled and then separated on a standard 10 % SDS-PAGE gel by electrophoresis. **(b)** Untreated egg extract was incubated at 20 ° C for 150 minutes, 2 µl were taken at indicated times. Samples underwent gel electrophoresis as above.

5.3 Immunofluorescence detection of endogenous XCEP63

We next used the four rabbits' XCEP63 antibodies to detect endogenous XCEP63 by immunofluorescence. We established the same antibody selected for immunoblots was also the most efficient in recognising XCEP63 in fluorescence studies. Some optimisation of immunoflorescence conditions were devised, including modifications to the blocking and washing procedures. In turn, we obtained proficient recognition of endogenous XCEP63 in *Xenopus* egg extract and *Xenopus* culture cells.

In figures 5.3a and 5.3b, we show endogenous XCEP53 co-localises with the poles of spindles assembled in *Xenopus* egg extracts and the centrosomes in XTC cells respectively. Taken together, these data strongly support XCEP63-GFP studies, which similarly determined XCEP63 centrosome association. In addition, the endogenous centrosome positioning of XCEP63 was found to be identical to the predetermined localisation of human CEP63 (Anderson *et al.,* 2003). In establishing CEP63 centrosome linkage between human and *Xenopus* we uncover another conservational aspect, in addition to previously described sequence similarities. Thus, it is possible that there may also be conservation of CEP63 function. Later on in this chapter in figure 5.8 we explore the possible XCEP63 involvement of XCEP63 centrosome-dependent spindle assembly on the basis that XCEP63 is appropriately compartmentalised to play a regulatory role.

A) Fluorescent images of spindle assembly in *Xenopus* egg extract

MERGE

Rabbit IgG **XCEP63** **PRIMARY ANTIBODY**

SPLIT

Tubulin **XCEP63**

B) Fluorescent images of XTC cells

MERGE

Rabbit IgG **XCEP63** **PRIMARY ANTIBODY**

SPLIT

γ-Tubulin **XCEP63**
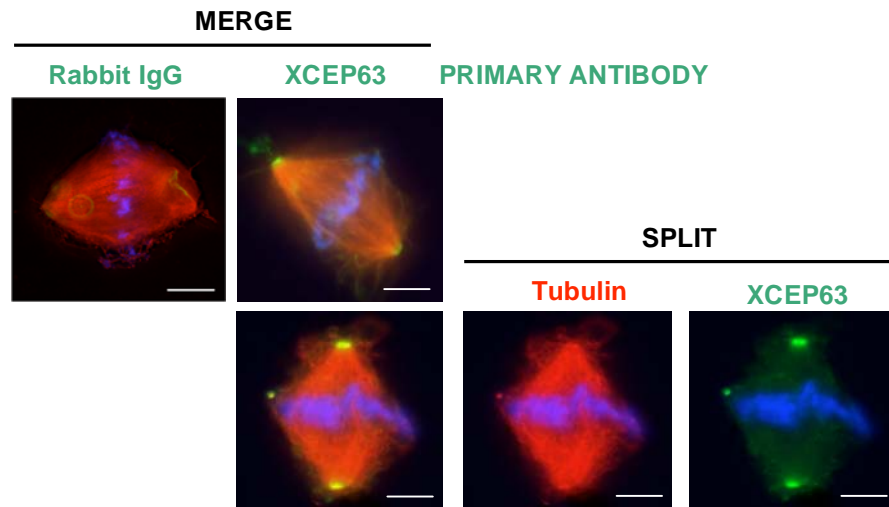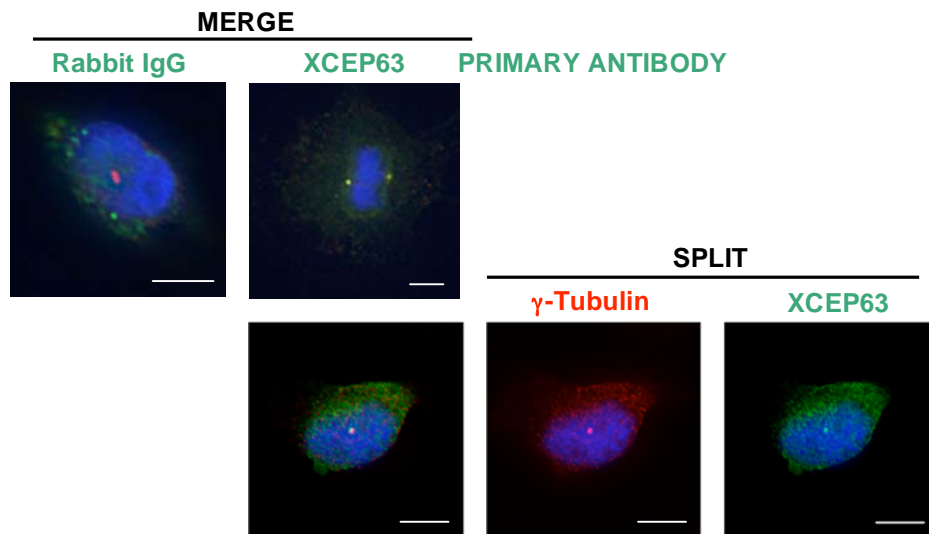
Figure 5.3 Immunoflorescence detection of endogenous XCEP63 in *Xenopus* egg extract and XTC cells

Images of fluorescence XCEP63 endogenous recognition are representative findings of three separate experiments. Images were acquired on a Deltavision microscope. Scale bars indicate 10 μm. **(a)** Spindles were assembled in CSF egg extracts supplemented with 1,000 sperm nuclei/μl and 50 μg/ml rhodamin tubulin. Extracts with incubated at 20 °C for 90 minutes, then diluted and formaldehyde fixed in BRB80 buffer and spun onto coverslips through a glycerol cushion as described in materials and methods. Immunofluorescence was performed as described in materials and methods, with antibodies recognising rabbit IgG or XCEP63 polyclonal antibody serum. XCEP63 is shown in green, microtubules are shown in red and DNA shown in blue (DAPI). **(b)** Asynchronous XTC cells were isolated on to coverslips as described above and then underwent immunoflorescence staining with antibodies recognising γ-tubulin and XCEP63. Centrosomes are shown in red, XCEP63 shown in green and DNA shown in blue (DAPI).

5.4 ATM and ATR phosphorylation of XCEP63 in *Xenopus* egg extract

We established in chapter four, reticulocyte lysate translated XCEP63 protein undergoes retardation in SDS-PAGE when ATM and ATR is activated in *Xenopus* egg extract. The XCEP63 gel migration shift was prevented in the presence of caffeine, thus attributing ATM and ATR activation to the observed XCEP63 alteration. We now questioned whether ATM and ATR activation similarly leads to gel mobility change of endogenous XCEP63 in *Xenopus* egg extract. The addition of pA/pT to *Xenopus* egg extracts prompted endogenous XCEP63 mobility retardation, as shown in figure 5.4a. We also show in figure 5.4a, when treated extracts were supplemented with caffeine and ATM inhibitor, the migration difference was somewhat lessened. These results suggest endogenous XCEP63 also undergoes at ATM and ATR dependent modification.

ATM and ATR are well-established DNA damage response signalling regulators, targeting network substrates through their kinase activity. ATM and ATR adaptation of XCEP63 is suggestive of a controlling phosphorylation event. We suspected phosphorylation of XCEP63 corresponds to the observed change in molecular weight. Thus, we tested the affects of phosphate removal by lambda phosphatase on XCEP63 gel migration patterns. Immunnoblot detection of XCEP63 in figure 5.4b, shows lambda phosphatase treatment eliminates the migration alteration. These data confirm that active ATM and ATR phosphorylates endogenous XCEP63. It is noteworthy that XCEP63 antibody recognises both non-phosphoylated and phosphorylated XCEP63 forms. In addition, the second band recognised by XCEP63 antibody does not show a gel migration shift with pA/pT treatment indicating again this protein detection is non-specific.

Interestingly, we observe a faster gel migrating form of untreated XCEP63 when exposed to lambda phosphatase. These data indicate a basal level of phosphorylation that is constitutively present on endogenous XCEP63 in *Xenopus* egg extract, which is removed by lambda phosphatase treatment. XCEP63 phosphorylation sites and levels are investigated in chapter six.

Immunoblot detections of XCEP63 in *Xenopus* egg extract

A)

M_r **(kD)**

B)

M_r **(kD)**
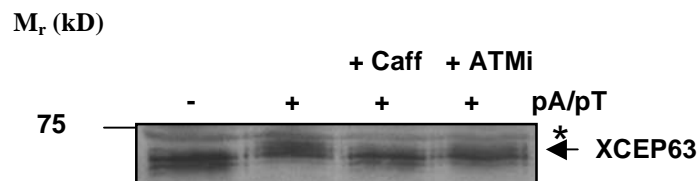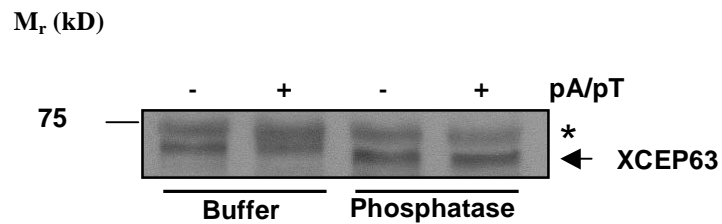
Figure 5.4 ATM and ATR dependent phosphorylation of endogenous XCEP63 in *Xenopus* egg extract

Immunoblot detection was performed with XCEP63 polyclonal antibodies. Data is representative of three separate experiments. * indicates nonspecific band. **(a)** CSF arrested egg extract was exposed to the presence (+) and absence (-) of 5 ng/μl of pA/pT, with and without 2 mM caffeine (Caff) or 20 uM Ku55933 (ATMi) for 30 minutes at 20 °C. Extracts (1μl) were mixed with Bio-Rad sample buffer, boiled and then underwent electrophoresis on a standard 10 % SDS-PAGE gel. **(b)** CSF egg extract was untreated and treated with 5 ng/μl pA/pT for 30 minutes at 20 °C. Extracts (2 μl) were exposed to Lambda phosphatase buffer alone (Buffer) or 2 μl Lambda phosphatase (Phosphatase) in 50 μl reaction volume for 30 minutes at 30 °C. Samples were separated as above.

5.5 Immunodepletion of endogenous XCEP63 from *Xenopus* egg extract

We set up an experiment that would enable investigations into the physiological relevance of XCEP63 function. *Xenopus* egg extract, as a cell free biochemical system, allows specific proteins to be depleted by antibodies. Immunodepletion of *Xenopus* egg extract is a useful tool in establishing protein roles. Furthermore, in this system recombinant protein can be added back, which should reverse the effects found in the absence of protein and provide confirmation of protein function.

We were able to achieve efficient antibody depletion of XCEP63 protein in *Xenopus* egg extract after minimal optimisation of conditions. In figure 5.5, we show XCEP63 antibody dramatically depletes XCEP63 protein from *Xenopus* egg extract. Immunoblot detection with the same XCEP63 antibody shows the presence of XCEP63 in untreated and mock depleted extract, which is not detectable in immunodepleted extracts. As previously mentioned, we confirm band marked with an asterisk is a non-specific protein detection, remaining unaffected from mock to immunodepleted egg extracts. The inclusion of translated XCEP63 protein in this immunoblot confirms antibody recognition of XCEP63.

As previously mentioned, *Xenopus* egg extract immunodepletion of proteins a very powerful technique, however the efficacy of depletion rarely meets 100 %. The maximal reduction of XCEP63 levels is imperative, as later experiments demands efficient XCEP63 knock down to determine the effects of protein absence. For this reason, we also performed a second antibody incubation to ensure the highest possible depletion of XCEP63 from extracts (figure 5.5).
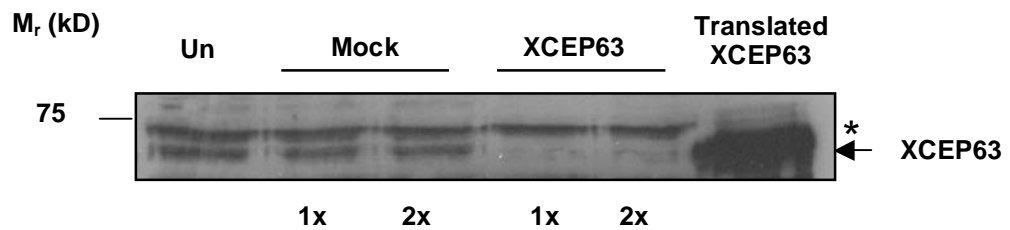
Figure 5.5 Immunodepletion of endogenous XCEP63 in *Xenopus* egg extracts

Xenopus eggs extracts were untreated (Un), mock depleted (mock) or XCEP63 immunodepleted (XCEP63). sepharose protein A beads were coupled with no antibody (mock) or 6xHisXCEP63 antibody overnight at 4 °C with rotation. 20 μl of extract was incubated once (1x) or twice (2x) with pre-bound beads at 4 °C for one hour with rotation. Extract was removed from beads and 1 μl of samples were separated on a standard small 10 % SDS-PAGE gel by electrophoresis and then underwent immunoblot detection with the same XCEP63 antibody. * indicates non-specific band. Immunoblot results shown are representative of all experiments based on XCEP63 immunodepletions.

5.6   The absence of XCEP63 functional role in interphase *Xenopus* egg extract

Previously, in chapter four figure 4.2, we mentioned XCEP63 undergoes ATM and ATR dependent gel migration shift in both interphase and mitotic *Xenopus* egg extracts. We were keen to ascertain whether XCEP63 functions specifically within processes of interphase or mitosis and to determine the physiological relevance of the phosphorylation.

To characterise the role of XCEP63 in interphase, we monitored DNA replication in the absence of XCEP63, with and without ATM and ATR induction. Quantification of DNA replication in XCEP63 depleted extract is shown in figure 5.6. The recorded levels of DNA replication were normalised to 100 % DNA replication in untreated extract. These data indicate that DNA replication is unaffected by the absence of XCEP63 protein. The XCEP63 immunodepleted sample shows a similarly high level of DNA replication as untreated or mock-depleted extracts. As expected, chromosomal breakage by *EcoRI* treatment led to an approximately 75 % reduction in DNA replication, a reduction which was prevented by the addition of caffeine. XCEP63 protein depletion did not mitigate on the low percentage of DNA replication found in the presence of *EcoRI* nor affect the rescue observed on caffeine addition.

In conclusion, we can argue that XCEP63 does not influence DNA replication regulation. We also can state that XCEP63 phosphorylation holds no direct functioning role in DNA damage hindrance of DNA replication progression within interphase egg extract. These results may imply a redundancy in XCEP63 function in interphase, or alternatively promiscuous activity of ATM and ATR. Further to this, these findings encourage the notion that XCEP63 may have a restricted role within mitosis.
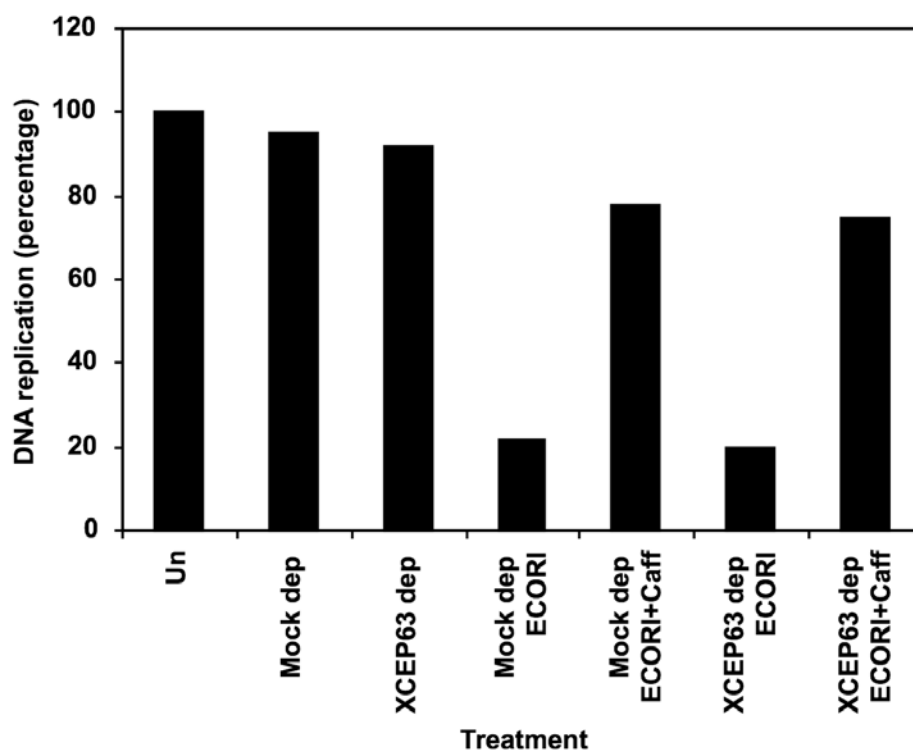
Figure 5.6 XCEP63 lacks interphase function in *Xenopus* egg extract

Interphase *Xenopus* extract was untreated (Un), or incubated twice with mock depleted (mock) or XCEP63 immunodepleted (XCEP63) pre-prepared sepharose beads, as described previously. Extracts were supplemented with 2,000 nuclei/µl and 10 µCi of [α^{32}P]-dATP in the absence and presence of 0.1 U/µl *EcoRI* or 0.1 U/µl *EcoRI* and 3 mM caffeine. After a two hour incubation at 20 °C, reactions were stopped with stop buffer and incubated at 37 °C for one hour. DNA was isolated by phenol-chloroform-ethanol extraction, run on agarose gels, and then proceeded to phosphoimaging monitoring. The percentage of DNA replication reported in the graph shows the quantification of radioactivity incorporation measured on a phosphoimager. Data shown is representative and shows typical findings of three separate experiments.

5.7   Purification of recombinant XCEP63-MBP protein

In the previous figure the data showed that XCEP63 function does not impact DNA replication in interphase egg extract (figure 5.6). We now investigated the possible role of XCEP63 within the context of mitosis.

One possibility is that spindle morphological changes may occur from the absence of XCEP63. For this purpose, we required recombinant protein to reconstitute spindle assays to substantiate any findings. The 6xHisXCEP63 recombinant protein used for antibody production was purified under denaturing conditions, but add back extract experiments demand correctly folded protein in a biologically active form. We selected the protein tag, maltose binding protein (MBP), which unlike many partner fusions has a reputation for solubility enhancement and reasonable yields of protein (Kapust and Waugh, 1999).

We inserted the XCEP63 ORF DNA into a PMAL construct and optimised expression parameters (data not shown). We obtained soluble XCEP63-MBP recombinant protein with protocol including the following modification: lowering of IPTG inductions levels, reduction of expression temperature to 25 °C and shortened the expression time to five hours. A Coomassie Blue stained gel of purified MBP and XCEP63-MBP recombinant proteins is shown in figure 5.7a. As expected, higher yields of soluble MBP recombinant protein control were obtained in comparison to XCEP63-MBP. Consequently, we concentrated pools of eluted XCEP63-MBP recombinant protein for further experiments.

We next asked whether recombinant XCEP63-MBP protein was correctly formed into its active conformation. We exposed XCEP63-MBP to *Xenopus* egg extract in the presence of ATM and ATR induction and monitored for changes in electrophoretic mobility compared to the absence of treatment. As shown in figure 5.7b, XCEP63-MBP underwent the signature ATM and ATR dependent gel migration alteration. These data suggest that the purified recombinant protein is active, retaining its potential biological function and is not hindered by the attachment to fusion partner, MBP.

We performed a further check on recombinant protein by illustrating again the phosphorylation modification. Recombinant XCEP63-MBP was shown to be highly

radio-labelled by [γ-^{32}P]-ATP in the presence of induced ATM and ATR, as illustrated in figure 5.7c autoradiograph. These data also confirm the XCEP63-MBP phosphorylation modification observed on endogenous protein in figure 5.4b. As previously thought, low levels of basal phosphorylation are apparent, indicated by comparatively very low levels of radio-labelled XCEP63-MBP in the absence of ATM and ATR triggering pA/pT treatment.

A) Coomassie Blue stain of purified MBP and XCEP63-MBP recombinant protein

M_r (kD)

MBP XCEP63
-MBP

100 —

75 —

50 —
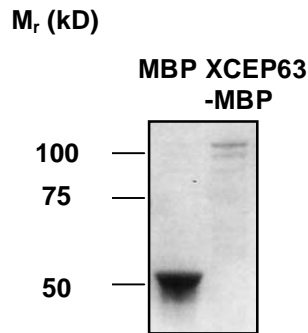
B) SYPRO® Ruby stain of XCEP63-MBP in *Xenopus* egg extract

M_r (kD)

MBP   XCEP63
       -MBP

100 —   ← XCEP63-MBP

75 —

50 —   ← MBP

\- + - +   pA/pT

C) Autoradiograph of XCEP63 in *Xenopus* egg extract

M_r (kD)

MBP   XCEP63
       -MBP

                ← XCEP63-MBP
100 —

75 —

50 —   ← MBP
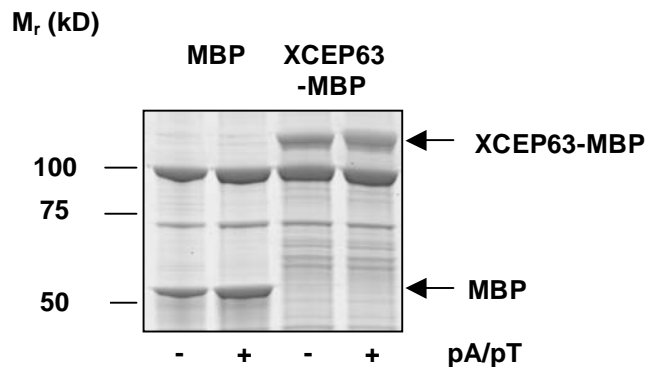
\- + - +   pA/pT
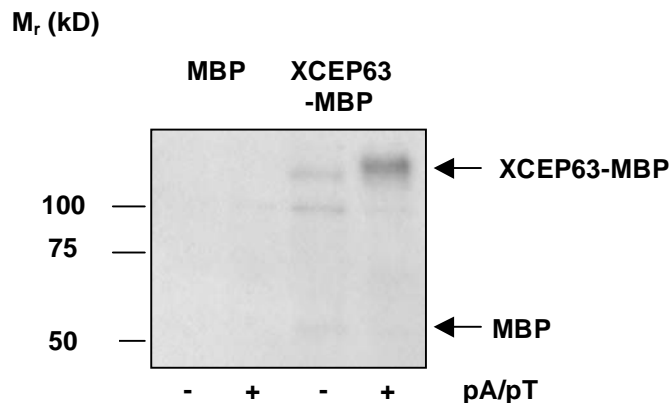
Figure 5.7 Purified biologically active recombinant XCEP63-MPB fusion protein

(a) As described in more detail in materials and methods, XCEP63 DNA was inserted into pMAL–c2X, a MBP tag plasmid construct. Both XCEP63-MBP fusion and MBP plasmid without insert were expressed in *E. coli* and then proceeded to be purified through amylose beads coupling and detachment protocol. Purified proteins were separated on a standard 10 % SDS-PAGE gel by electrophoresis and then proceeded to Coomassie Blue staining. (b) Recombinant proteins, MBP and XCEP63-MBP (5 μg) were pre-coupled to amylose beads then incubated for one hour at 20 °C with CSF arrested *Xenopus* egg extract in the absence and presence of 5 ng/μl pA/pT. Beads were boiled in Bio-Rad sample buffer, then samples were separated on a medium Bio-rad precast 4-12 % bis-tris PAGE gel proceeded to SYPRO® Ruby staining. (c) Recombinant proteins, MBP and XCEP63-MBP (5 μg) underwent treatments as above in the presence of $[\gamma\text{-}^{32}P]$-ATP. Samples were separated on a large standard 10 % SDS-PAGE gel and proceeded to autoradiography.

5.8   XCEP63 functions in *Xenopus* egg extract spindle assembly

To detect the function of XCEP63 in mitosis, we applied immunodepletion and reconstitution with XCEP63-MBP to the spindle assembly assays in *Xenopus* egg extracts. Figure 5.8a shows spindle assembly in the absence of XCEP63 is perturbed. Without XCEP63, spindles are lacking in pole orientation and DNA is dispersed. However, in reconstituting depleted samples with recombinant XCEP63 protein, spindle formation is rescued to that of untreated or mock depleted extracts. We also show that microtubule polymerisation and overall aster formation appears normal, remaining unaffected by knock down of XCEP63 (figure 5.8a, aster panel). The quantification of spindle structures is shown in figure 5.8b. These data show in the absence of XCEP63 normal spindle assembly is almost completely abolished with an approximate 8-fold reduction in spindle formation compared mock depleted extract. Furthermore, in the XCEP63 depleted extracts aberrant spindles structures are prevalent. Particularly apparent are the heightened numbers of asters present in the absence of XCEP63 compared to control extracts. This increase in aster frequency suggests XCEP63 has a role in a pathway involved in aster maturation into spindles. Quantification of spindle structures in the presence of recombinant XCEP63-MBP reconstitution suggests XCEP63 is required in normal spindle assembly. Reconstitution of XCEP63 in depleted extracts overcomes spindle defects and normal spindle formation returns to levels of control extracts.

Taken together, experimental data illustrates the absence of XCEP63 has a striking inhibitory affect on normal spindle assembly in *Xenopus* egg extract. XCEP63 importance in regulating normal spindle formation was confirmed when defective spindle formation was rescued with XCEP63 protein reconstitution. In establishing XCEP63 functioning in centrosome-driven spindle assembly, we were encouraged to explore whether XCEP63 spindle assembly regulation may be affected by phosphorylation modification by active ATM and ATR.

A) Fluorescent images of spindle assembly in *Xenopus* egg extract
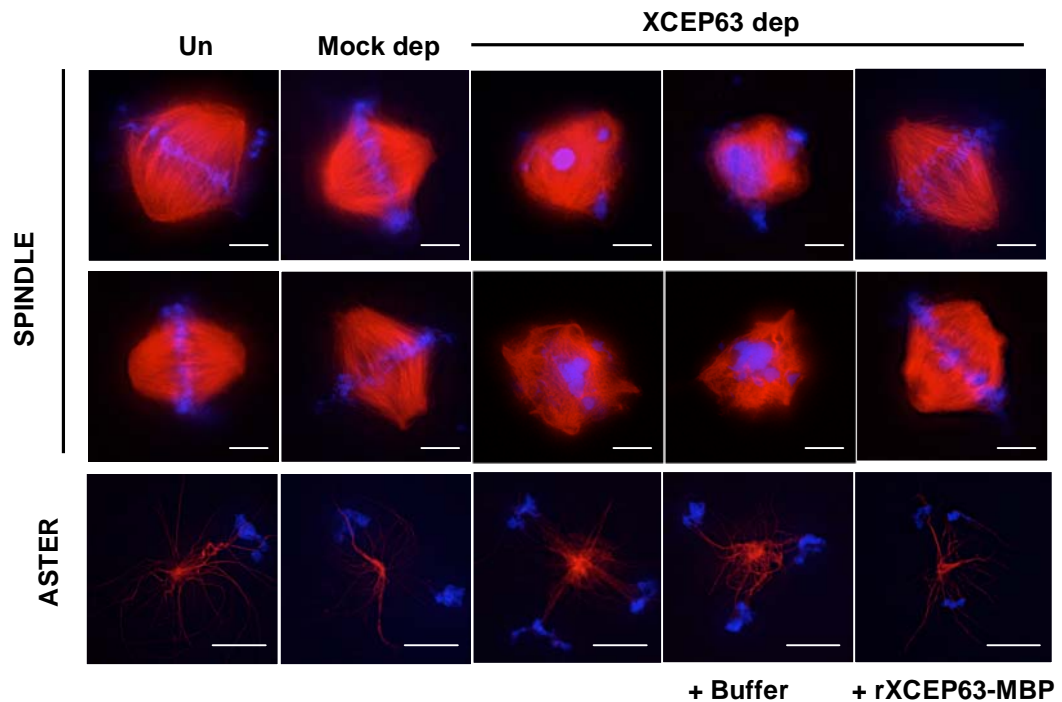
B) Quantification of spindle assembly structures
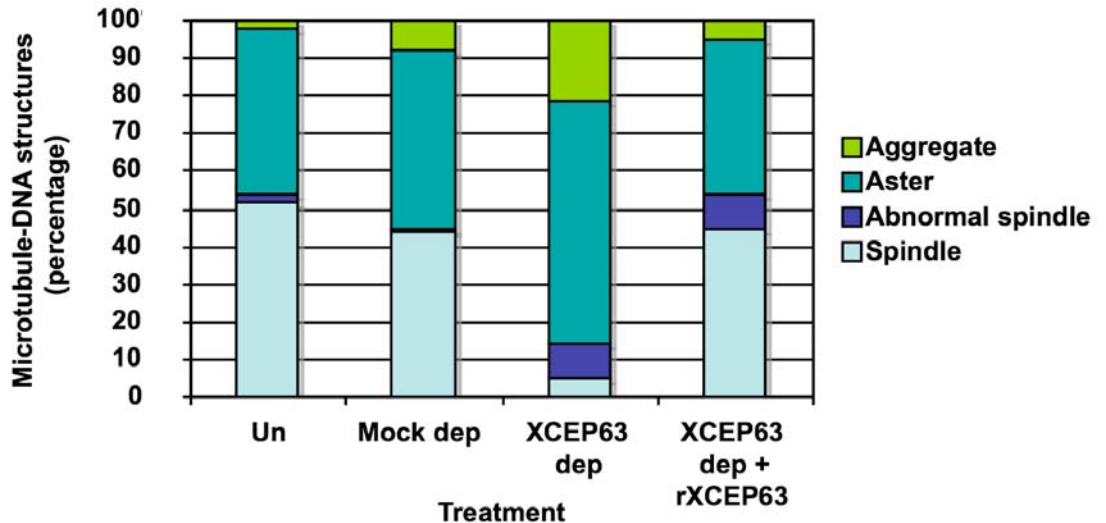
Figure 5.8 XCEP63 is required for spindle assembly in *Xenopus* egg extract

CSF extract was untreated (Un), mock depleted (Mock dep) or XCEP63 immunodepleted (XCEP63 dep), supplemented with buffer (Buffer) or 50 ng/µl recombinant XCEP63 (rXCEP63-MBP). Spindles were formed with 1,000 sperm nuclei/µl and addition of 50 µg/ml rhodamine tubulin, Extracts were incubated at 20 °C for 90 minutes and isolated onto coverslips as described in material and methods. Data shown is representative and shows typical findings of three separate experiments. **(a)** Images of spindles and asters were acquired on a Deltavision microscope, microtubules are shown red and DNA in blue (DAPI). Scale bar indicates 10 µm. **(b)** Quantification of DNA associated microtubule structures obtained under the conditions indicated above. Microtubule structures were qualified as: spindles, asters, abnormal spindles and aggregates. Percentages shown are relative to 100 structures were counted for each treatment.

5.9   ATM and ATR activation displaces XCEP63 centrosome localisation

In the last section, we determined that XCEP63 has a function within the pathway of centrosome dependent spindle assembly. If XCEP63 phosphorylation by ATM and ATR has a physiological relevance we would expect to observe a change in XCEP63 localisation and/or activity. Here, we wished to establish whether phosphorylation might result in an alteration in the previously determined centrosome localisation of endogenous XCEP63. We attempted this by performing a series of immuofluoresence analyses with previously used XCEP63 antibody, which we showed in figure 5.4 detects both non-phosphorylated and phosphorylated forms of XCEP63.

We first assessed the localisation of XCEP63 in *Xenopus* egg extract spindle formation in the absence and presence of activated ATM and ATR. Fluorescent images in figure 5.9a show XCEP63 positioning at the centrosomes of spindles assembled in extract lacking ATM and ATR induction, confirming figure 5.3 data. In the presence of ATM and ATR activation XCEP63 immunofluorescent detection shows a striking dispersion of XCEP63 throughout the ATM and ATR induced abnormal spindle structures. Whilst spindle assembly rescued by caffeine indicate an absence of XCEP63 staining diffusion, caffeine inhibition of ATM and ATR activation shows a preservation of XCEP63 centrosome localisation. The dramatic diffusion of XCEP63 away from centrosomes was confirmed by immunoflorescence observations in XTC cells. In figure 5.9b, we show XCEP63 displacement away from γ-tubulin centrosome staining in the presence of ATM and ATR activation by camptothecin treatment. Whereas XCEP63 co-localises with γ-tubulin staining of centrosomes in untreated cells and treated cells supplemented with caffeine.

Taken together, figure 5.9a and 5.9b data can be interpreted to mean that ATM and ATR phosphorylation of XCEP63 provokes XCEP63 displacement away from centrosomes. Whereas, in the absence of ATM and ATR triggering conditions, XCEP63 in non-phosphorylated form only localises to centrosomes. However, XCEP63 antibodies recognise both XCEP63 forms and therefore we need to confirm these findings with antibodies that only recognise phosphorylated XCEP63.

A) Fluorescent images of spindle assembly in *Xenopus* egg extract

Un   *EcoRI*   *EcoRI* +Caff

XCEP63

B) Fluorescent images of XTC cells

Un   CPT   CPT+Caff

XCEP63

γ-Tubulin
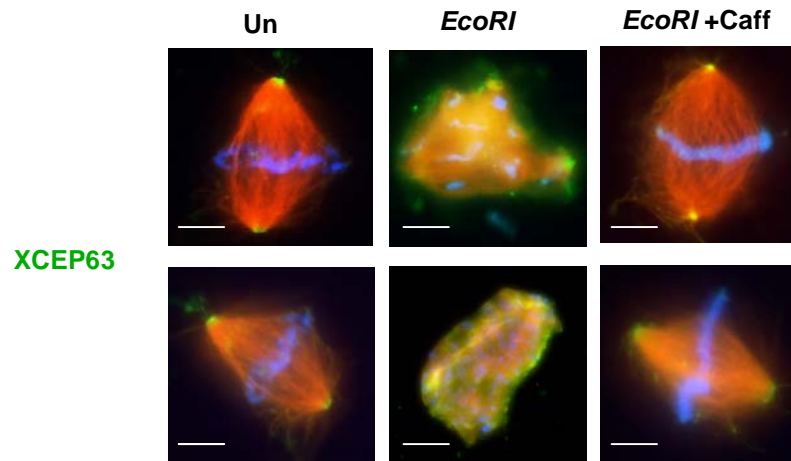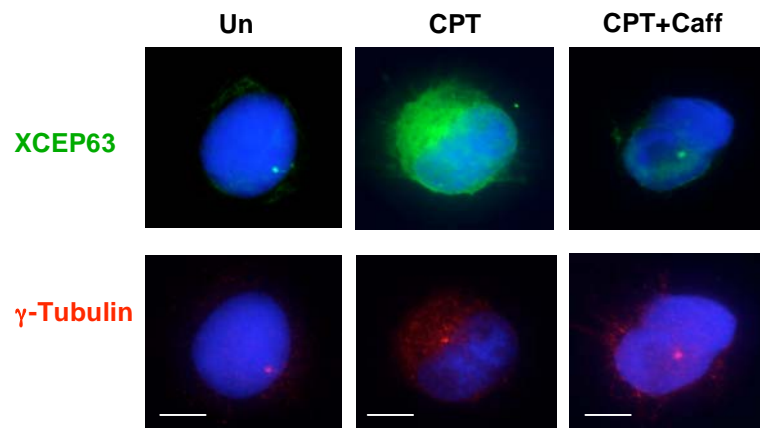
Figure 5.9 ATM and ATR dependent XCEP63 diffusion away from centrosomes in *Xenopus* egg extract and XTC cells

Images were acquired on a Deltavision microscope and are representative of three separate experiments. Scale bar indicates 10 μm. **(a)** Spindles were formed in CSF egg extract with the addition of 1,000 sperm nuclei/μl. Extracts were treated with CSF-XB buffer (Un) or 0.25 U/μl *EcoRI* (*EcoRI*) with and without 2 mM caffeine (*EcoRI* + Caff). Samples were incubated at 20 °C for 90 minutes, then fixed and spun onto coverslips as described in material and methods. Immunofluorescence was performed with antibodies recognizing XCEP63 and α-tubulin. XCEP63 is shown in green, microtubules are shown in red and DNA is shown in blue. **(b)** XTC cells were untreated (Un), treated with 400 nM camptothecin (CPT) or 400 nM camptothecin and 5 mM caffeine (CPT + Caff), cells were collected four hours incubation. Alternatively, XTC were untreated (Un) or treated with 10 Gy of Ionising Radiation (IR) in the absence and presence of 5 mM caffeine (IR + Caff), cells were collected 30 minutes after exposures. XTC cells underwent immunofluorescence with antibodies detecting XCEP63, shown in green and γ-tubulin, shown in red. DNA was stained with DAPI, shown in blue.

5.10 Summary

This chapter describes the characterisation of XCEP63, a protein up to this point with no ascribed function in any of the conserved vertebrate orthologes. Initial XCEP63-GFP investigations showed XCEP63 is localised to centrosomes both in cells and spindles assembled in *Xenopus* egg extract (figure 5.1). The indications that XCEP63 is a centrosome protein promoted the continuation of studies into endogenous XCEP63. We obtained polyclonal antibodies with efficient recognition of XCEP63 and through immuoblot detection we verified the presence of endogenous XCEP63 in *Xenopus* egg extract (figure 5.2). XCEP63 antibody also detected endogenous XCEP63 immunoflorescently, confirming co-localisation with centrosomes in both cells and in spindles assembled in *Xenopus* egg extract (figure 5.3). In continuing studies we verified endogenous XCEP63 undergoes a gel migration change dependent on ATM and ATR activation (figure 5.4a). Through treatment of extracts with lambda phosphatase we established ATM and ATR phosphorylates XCEP63 (figure 5.4b). In addition, we showed purified recombinant protein was also highly phosphorylated by active ATM and ATR in extract (figure 5.7). Collectively, data suggests that XCEP63 is indeed targeted by active ATM and ATR.

Within *Xenopus* egg extract system we were able to achieve efficient immunodepletion of XCEP63, which allowed studies into XCEP63 function (figure 5.5). We established no apparent role of XCEP63 or XCEP63 phosphorylation in the process of DNA replication (figure 5.6). It remains unclear why XCEP63 undergoes ATM and ATR phosphorylation in interphase extract. Instead, we have uncovered XCEP63 functions within mitosis. We found in the absence of XCEP63 spindle assembly was inhibited (figure 5.8). XCEP63 role in the formation of normal spindle was confirmed when reconstitution of XCEP63 recombinant protein restored spindle assembly. The outcomes of theses experiments elucidate XCEP63 as an essential factor in regulation of centrosome-driven spindle assembly.

Finally, we showed the displacement of XCEP63 centrosome localisation dependent on active ATM and ATR (figure 5.9). Immunofluorescent evidence from cells and *Xenopus* egg extract spindle assembly suggests that XCEP63 phosphorylation by active ATM and ATR affects XCEP63 protein behaviour. Although we can only speculate at this point, phosphorylation by ATM and ATR may de-localise XCEP63 away from

centrosomes, which may in turn lead to the disruption of XCEP63 role in regulating spindle assembly.

Within this chapter, we have not been able to determine whether XCEP63 is the ATM and ATR target involved in perturbation of centrosome-driven spindle assembly. The progression of XCEP63 functional analyses is limited without establishing the site of XCEP63 phosphorylation. Therefore, we continue in the next chapter by isolating the ATM and ATR phosphorylation position on XCEP63.

6 Chapter 6 Identification of XCEP63 phosphorylation site

In order to proceed with studies into the functional role of ATM and ATR XCEP63 modification in spindle assembly, we needed to identify the XCEP63 phosphorylation site. In isolating the XCEP63 target site we would be able to generate experimental aids, such as phospho-specific antibodies and recombinant XCEP63 non-phosphorylatable mutant protein.

We established, in the previous chapter, XCEP63 undergoes a phosphorylation modification in the presence of activated ATM and ATR in *Xenopus* egg extract (chapter five, figure 5.4a and 5.4b). Data collected also shows a stringent XCEP63 phosphorylation caffeine sensitivity, suggesting that both ATM and ATR separately or together could be responsible for the modification. We could argue that ATM is in part responsible for the phosphorylation event on XCEP63, as we have shown ATM inhibitor reduces XCEP63 phosphorylation (chapter five, figure 5.4a). Moreover, DNA damage reactions undertaken typically provoke ATM responses. However, as we discussed in chapter one (section 1.3), ATM and ATR phosphorylate a complex network of proteins with no clear demarcations, high numbers of common substrates and extensive pathway cross-overs (Abraham, 2001; Sancar *et al.,* 2004). Due to the present incomplete understanding of DNA damage response occurrence in mitosis, we are unable to discount the possibility that double strand break DNA damage is processed by and undergoes repair in a manner similar to other cell phase mechanisms that may employ ATR reactions (Hurley and Bunz, 2007; Jazayeri *et al.,* 2006). To date ATM and ATR substrate targets have been shown to have similar substrate specificity. In most reported cases the amino acid sequence serine-glutamine (**S**er-**G**ln, SQ) and threonine-glutamine (**T**hr-**G**ln, TQ) is a minimal essential requirement for ATM and ATR phosphorylation (Abraham, 2001; Kim *et al.,* 1999; Matsuoka *et al.,* 2007). However, in this chapter, we make the discovery that ATM and ATR potentially recognises serine-leucine-glutamate (Ser-Leu-Glu, SLE) motif, phosphorylating serine 560 of XCEP63.

6.1   XCEP63 mutations of ATM and ATR candidate phosphorylation sites

As a first step in finding the phosphorylation site, we performed a very crude phosphate radiolabelling assay on a spotted peptide array (data not shown). Peptide array data failed to highlight the putative phosphorylated region. Similarities in spot intensity patterns between samples suggested insufficient experimental sensitivity to allow the differentiation from basal levels of phosphorylation. Alternatively, the lack of signal may be due to ATM and ATR targeting dependency on XCEP63 protein conformation. Because the XCEP63 peptide array provided inconclusive information we concentrated our efforts to a more standard approach of phosphorylation identification by mutation of consensus sites SQ and TQ motifs. In figure 6.1a, we show XCEP63 amino acid sequence on which ATM and ATR potential phosphorylation sites are highlighted in red. Through site directed mutagenesis, we eliminated possible phosphorylation sites by exchanging nucleotide(s) within the XCEP63 DNA sequence that encode for amino acids, serines (S) and threonines (T), to non-phosphorylatable alanine (A). The XCEP63 DNA mutants were transcribed and translated within the Promega reticulate lysate system labelled with [^{35}S]-methioine and then exposed to *Xenopus* egg extract in the absence or presence of pA/pT, ATM and ATR activation treatment. Autoradiographs of mutants separated by SDS-PAGE were analysed for changes in gel migration in the presence of ATM and ATR activation. Identification of a correct XCEP63 converted phosphorylation site would be represented by eradication of the signature gel shift.

We spent a considerable amount of time generating and testing XCEP63 SQ/TQ candidates mutants indicated in figure 6.1a in order to uncover the corresponding ATM/ATR phosphorylation site. Representative autoradiograph results of XCEP63 mutants are shown in figure 6.1b (panel one). S41 and T471 XCEP63 alanine mutants showed no difference in gel migration in the presence of ATM and ATR activation to that of wild type XCEP63. Similarly, the remaining 11 mutants showed no alterations on alanine substitution (data not shown). We then changed tactics and combined mutations, due to the possibility that the absence of a primary phosphorylation target site may lead to phosphorylation of a secondary site, or alternatively that ATM and ATR may phosphorylate more than one site. A representative autoradiograph of the SQ/TQ alanine multiple mutations is shown in figure 6.1b (panel two) and still we determined no change in migration pattern compared to wild type. Although particularly puzzling, all combinations of SQ/TQ conversions tested were found to be negative for

imposing an effect on ATM and ATR mediated phosphorylation. On discounting all S/TQ candidate sites present on XCEP63, we considered XCEP63 may hold an alternative or novel ATM/ATR target sequence. There is some evidence that suggests the residue prerequisite of ATM/ATR kinase substrate recognition is glutamate at position N+1 and this provides enrichment of serine and threonine phosphorylations (Kim *et al.,* 1999; Matsuoka *et al.,* 2007). With this in mind and since we were unable to identify a standard ATM and ATR phosphorylation site, we reasoned that we had some rational to test phosphorylation of serine-glutamate (Ser-Glu, SE) and threonine-glutamate (Thr-Glu, TE) motif sites. SE and TE sites are indicated on the XCEP63 amino acid sequence in figure 6.1a, labelled in green. We again applied the previously described site directed mutagenesis screening technique. In the autoradiograph in figure 6.1c, we show a typical SE/TE XCEP63 mutation of S/T to alanine exemplifying here conversions of S135 and S202. These findings are representative of all SE/TE containing mutants, all showing a lack in phosphorylation alterations of the electrophoretic mobility. We combined many of the sites and similarly established no effect on gel migration in the presence of ATM and ATR activation (data not shown).

In conclusion, we were unable to identify the ATM and ATR dependent phosphorylation site through candidate or speculative site directed mutagenesis. Consequently, no further efforts were made with this approach and we realised we needed to focus on a different means in order to find the XCEP63 modification site(s).

A) XCEP63 amino acid sequence

```
1                                                    S41      50
     MEALLQGLQRQDRMGALQDSCEAELQELMKQIDIMLDHKRSQWEAETETM
51                                        T89    T94     100
     KTRLELKEQELNCALDREERLNQEVRRLRQQLIQQEEETQNKTTQYEAQL
101              S124         S135                       150
     SGFKEELNRLKKSYEKVQKKHLRSEMKAKAEEERSEVSRLTRRLEEFRQR
151                                                      200
     SLDWEKQRLLYQQQLAGLEAQRKTLIEQTEMYQHQSHNRKQMLEQTSLVG
201   S202                                      T246     250
     RSELQNLSGQLHRANDSLCAKEEELETLKIQLRCAVEGQKRAEHETELSK
251                           T271              S292     300
     QAVQALKEEKAELRATLQAHTEFLQGSRVQKHELLPEGYRGSEVLRENNS
301                T318                                  350
     IRSVEERLQEMGQVGGETEVEAIRSKLSVSRMNEHRLQAEVTCLEDSVES
351     S353                        S381        S391     400
     VTSQCQLLAKELKGKEEYFHGVKEDHQKCLSENKKLKGQLSQAELTHKSV
401        S409 T412                                     450
     LDGMRKEISQLTQELHQRDIRMASSAGIDWERKIKAERQRAEREAAEHRM
451              S466   T471                    T497     500
     SLNALENLRQENCRLSELLQTQEPDVAQALVNLEQANQRLQRELLQTQEK
501        S510         S520                     S550    550
     LELIAQRRESEIQNAVDSISQELLNKQEQELRIMQERLKVYEQEMQTFRS
551                          S566                        600
     QQDAASSGSSLESIFSEVWKEQATGSPISAASVDSAIEPVEDLASSLPVP
601                                     S638      T646   649
     PTSPANAVASRFLQEEEQRSHELLQRLNAHIEELKQESQRTVEHFTQAR
```

B) Autoradiograph of SQ/TQ XCEP63-A mutants in *Xenopus* egg extract
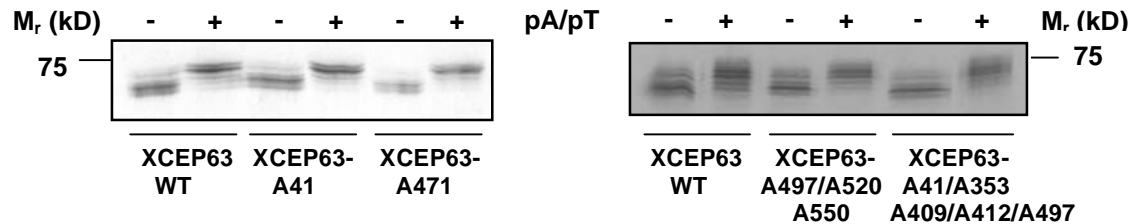
C) Autoradiograph of SE XCEP63-A mutants in *Xenopus* egg extract
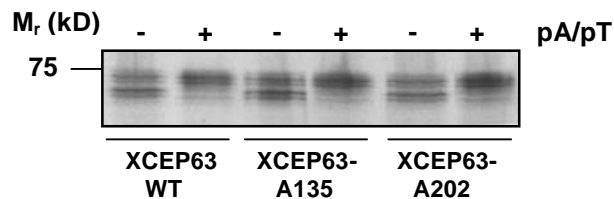
Figure 6.1 XCEP63 alanine mutants of candidate and speculative ATM and ATR phosphorylation sites in *Xenopus* egg extract

(a) XCEP63 amino acid sequence, ATM and ATR candidate SQ/TQ motifs are labelled in red and speculative ATM and ATR SE/TE motifs are labelled in green. Corresponding serine and threonine amino acid numbers are also shown. (b) XCEP63 alanine mutants were incorporated by site directed mutagenesis within the original C9 XCEP63 cDNA plasmid. XCEP63-A mutants were transcribed and translated in the presence of [35S]-methionine within Promega reticulocyte lysate system. Translated XCEP63 proteins were incubated for 30 minutes at 20 °C with CSF egg extract which had been pretreated for 20 minutes at 20 °C with (+) or without (-) linear DNA (pA/pT). Samples were separated on a standard large 10 % SDS-PAGE by gel electrophoresis and proceeded to audioradiography. Autoradiograph in panel one shows wild type XCEP63 (WT) along side SQ/TQ XCEP63-A S41 and S471 mutants. Autoradiograph in panel two shows wild type XCEP63 (WT) along side SQ/TQ XCEP63-A combined mutants S497/S520/S550 and S41/S353/S409/S412/S497. (c) The same technique was performed as above. Autoradiograph shows wild type XCEP63 (WT) along side SE XCEP63-A S135 and S202 mutants.

6.2 Mass Spectrometry identification of XCEP63 phosphorylation sites

At this point we decided to employ Mass Spectrometry analysis. We prepared recombinant MBP and XCEP63-MBP protein for Mass Spectrometry examination by exposing protein to mitotic *Xenopus* egg extracts in the absence and presence of pA/pT oligos, which induce ATM and ATR activation. Figure 6.2a shows SDS-PAGE separation of exposed recombinant proteins, stained with SYPRO® Ruby. Mass Spectrometry analysis on samples was undertaken by Alessandro Vindigni and Martin Hampel, at ICGEB (International Centre for Genetic Engineering and Biotechnology) in Italy and Christof Lenz, at Applied Biosystems in Germany.

Investigators prepared gel pieces by performing a trypsin digest followed by reversed phase-C18 chromatography separation. Samples were applied to 4000 Q TRAP hybrid triple quadrupole/linear ion trap Mass Spectrometer. Initially, two types of LC/MS/MS analyses were performed. Firstly, a regular LC/MS/MS (Liquid Chromatography/Tandem Mass Spectrometry) procedure was undertaken at high sequence coverage to determine peptide identities. Secondly, LC/MS/MS analysis to selectively identify phosphorylated peptides, consisting of a Precursor Ion Scan for m/z 79 followed by polarity switching ion trap experiments (Williamson *et al.,* 2006). The combined results obtained showed unequivocally the presence of three phosphorylated peptides. The peptides isolated were, SQQDAASSGSSLESIFSEVWK, GQLSQAELTHK and EQATGSPISAASVDSAIEPVEDLASSLPVPPTSPANAVASR. The Mass Spectrometry specialists also found in the presence of ATM and ATR activation an additional 252 Dalton possible post-modification on peptide EQATGSPISAASVDSAIEPVEDLASSLPVPPTSPANAVASR, in the position highlighted in green on table one shown below, but unfortunately the analysers could not explain this addition. Also featured within table one, are the assigned peptide numbers, the mass to charge ratios (*m/z*) of the phospho-peptides, the phosphorylation positions within peptide sequences and the corresponding XCEP63 serine amino acid number. The isolated peptide positions are marked within figure 6.2b XCEP63 amino acid sequence and the contained serine phosphorylation sites are labelled accordingly.

Peptide number assigned	*m/z*	Peptide amino acid sequences	XCEP63 amino acid position
1	1162.12^{2}	SQQDAASSGSpSLESIFSEVWK	S560
2	646.30^{2+}	GQLpSQAELTHK	S391
3	1441.2^{3+}	EQATGSPISAASVDSAIEPVEDLASSLPVPPTpSPA NAVAS(252)R	S603

Table 2 Summary of phosphorylated peptides isolated by Mass Spectrometry

Within the table are the phosphorylated peptides identified in Mass Spectrometry analysis along with their established mass to charge ratios (*m/z*). Peptides isolated were assigned numbers 1-3 as indicated. Sites of phosphorylation are marked with a p shown in red within the isolated peptide amino acid sequences. Corresponding XCEP63 amino acid sequence positions of serine phosphorylations are shown. The site of 252 Da sized unknown addition is indicated in green on peptide three.

Interestingly, the signals for phosphorylation were observed in both the absence and presence of active ATM and ATR. This information is in agreement with previous indications that a basal level of phosphorylation is present under untreated circumstances (chapter five, figures 5.4 and 5.7). In light of the phospho-peptide representation in the absence and the presence of ATM and ATR induction, the groups applied another type of LC/MS/MS analysis to confirm phospho-peptide identifications and obtain semiquantitative information about the phosphorylation levels. A series of **m**ultiple **r**eaction **m**onitoring (MRM) traces followed by product ion trap spectra were performed (Cox *et al.,* 2005; Unwin *et al.,* 2005). Multiple reaction monitoring LC/MS/MS analysis outcomes confirmed previously identified sites of phosphorylation. MRM traces were then integrated and compared to establish the relative amounts of phosphorylated peptides in untreated and treated XCEP63-MBP samples. Ratios 0.17, 0.91 and 1.02 were determined for phospho-peptides one, two and three respectively. These data indicates peptides one and two undergo increased phosphorylation in the presence of active ATM and ATR, whilst peptide three shows equal phosphorylation to that in the absence of ATM and ATR induction. In particular, ratio information shows the highest phosphorylation level is achieved on peptide one. In conclusion, quantification data suggests a heightened phosphorylation status of peptide one in ATM and ATR activated sample. Due to this we show analysis data mentioned above in more detail in the next figure, specifically for peptide one.

A) SYPRO® Ruby stain of MBP and XCEP63-MBP in *Xenopus* egg extract

B) XCEP63 amino acid sequence


```
1                                                    50
    MEALLQGLQRQDRMGALQDSCEAELQELMKQIDIMLDHKRSQWEAETETM
51                                                   100
    KTRLELKEQELNCALDREERLNQEVRRLRQQLIQQEEETQNKTTQYEAQL
101                                                  150
    SGFKEELNRLKKSYEKVQKKHLRSEMKAKAEEERSEVSRLTRRLEEFRQR
151                                                  200
    SLDWEKQRLLYQQQLAGLEAQRKTLIEQTEMYQHQSHNRKQMLEQTSLVG
201                                                  250
    RSELQNLSGQLHRANDSLCAKEEELETLKIQLRCAVEGQKRAEHETELSK
251                                                  300
    QAVQALKEEKAELRATLQAHTEFLQGSRVQKHELLPEGYRGSEVLRENNS
301                                                  350
    IRSVEERLQEMGQVGGETEVEAIRSKLSVSRMNEHRLQAEVTCLEDSVES
351                                           S391    400
    VTSQCQLLAKELKGKEEYFHGVKEDHQKCLSENKKLKGQLSQAELTHKSV
401                                                  450
    LDGMRKEISQLTQELHQRDIRMASSAGIDWERKIKAERQRAEREAAEHRM
451                                                  500
    SLNALENLRQENCRLSELLQTQEPDVAQALVNLEQANQRLQRELLQTQEK
501                                                  550
    LELIAQRRESEIQNAVDSISQELLNKQEQELRIMQERLKVYEQEMQTFRS
551          S560                                    600
    QQDAASSGSSLESIFSEVWK EQATGSPISAASVDSAIEPVEDLASSLPVP
601      S603                                        649
    PTSPANAVASRFLQEEEQRSHELLQRLNAHIEELKQESQRTVEHFTQAR
```

Figure 6.2 Mass spectrometry identification of XCEP63 phosphorylation sites

(a) Recombinant MBP and XCEP63-MBP protein were incubated in egg extract treated with or without pA/pT for one hour at 23 ºC. MBP-XCEP63 was purified using amylose resin and separated by SDS-PAGE electrophoresis and subsequently stained with SYPRO® Ruby stain. Gel slices containing MBP-XCEP63 were subjected to Mass Spectrometry analysis. **(b)** XCEP63 amino acid protein sequence with phosphopeptides in bold and marked by lines. Corresponding phoshorylated serines are labelled, highlighted in red.

6.3 Mass Spectrometry identification of potential ATM and ATR of XCEP63 phosphorylation site at serine 560

As described in the previous section, peptide one SQQDAASSGSpSLESIFSEVWK identified by Mass Spectrometry is likely to contain the main site of XCEP63 phosphorylation by ATM and ATR. Here we show in more detail the Mass Spectrometry data of XCEP63 phosphorylation at site serine 560. In figure 6.3a panel one, we show the LC/MS/MS product ion spectrums in the absence of pA/pT treatment, SQQDAASSGSSLESIFSEVWK peptide was observed at m/z 1122.0^{2+} at a retention time of 30.9 minutes. In figure 6.3b panel two we show LC/MS/MS Product Ion Spectrum in the presence of pA/pT treatment, SQQDAASSGSSLESIFSEVWK peptide was observed at m/z 1162.12 + at a retention time of 32.0 min. These data confirmed the phosphorylation at serine 560, SQQDAASSGSpSLESIFSEVWK on peptide was determined through Y ions undergoing serial neutral loss of phosphoric acid at 98 Daltons down to ion position Y11.

In figure 6.3b, top and bottom panels we show Multiple Reaction Monitoring traces for the *m/z* peptide transition, 1162.1>795.4 observed in the absence and the presence of pA/pT treatment respectively. Heighten intensity levels observed at a retention time of 32.0 minutes clearly implicate a prevalence of phosphorylation at serine 560 in the ATM and ATR activated sample compared to untreated sample. As previously mentioned the comparison of Multiple Reaction Monitoring traces revealed a ratio of 0.17 phosphorylation amount on peptide one between untreated and treated XCEP63. In conclusion, quantification data suggests a heightened phosphorylation status of serine 560 in ATM and ATR activated sample, which most likely can be attributed to XCEP63 gel migration shift.

A) Product Ion Spectrums of XCEP63 SQQDAASSGSSLESIFSEVWK peptide
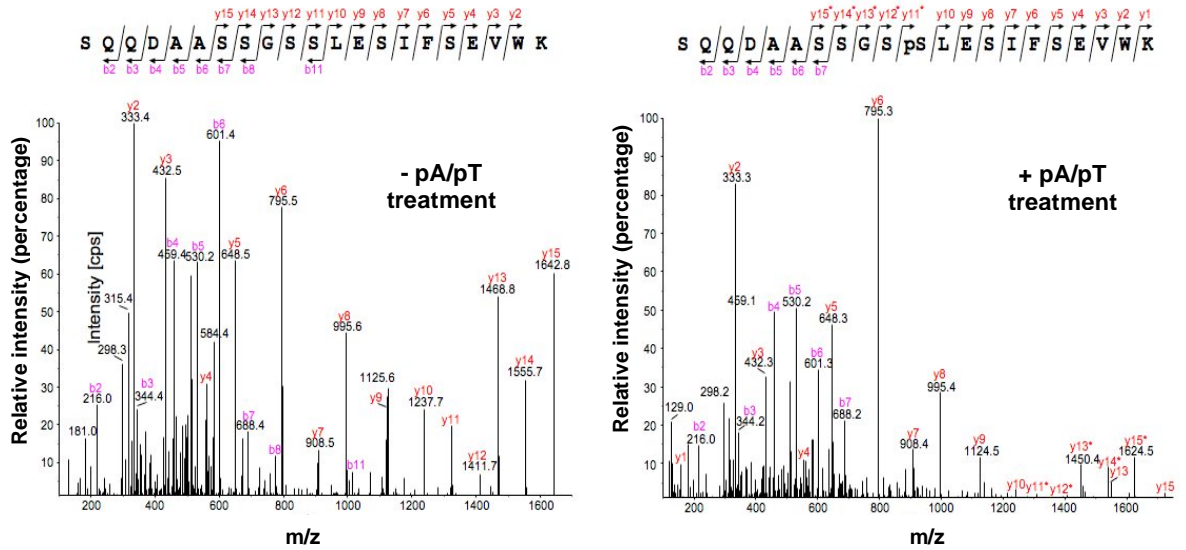
B) Multiple reaction monitoring (MRM) traces of XCEP63 SQQDAASSGSSLESIFSEVWK peptide
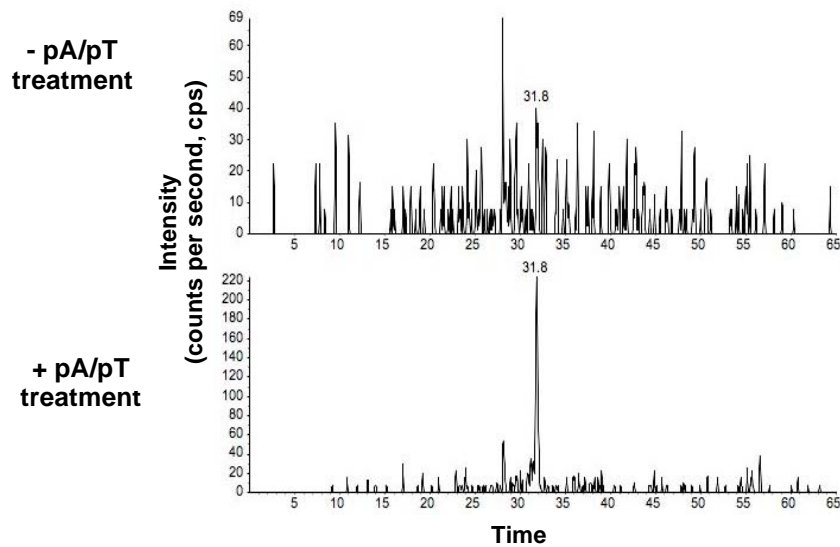
Figure 6.3 Mass Spectrometry analyses of SQQDAASSGSSLESIFSEVWK peptide phosphorylation

(a) Product Ion Spectrum of the doubly charged non-phosphorylated peptide, SQQDAASSGSSLESIFSEVWK observed in the sample containing XCEP63-MBP isolated from egg extract treated with no pA/pT at m/z 1122.0^{2+} with a retention time of 30.9 min. Product Ion Spectrum of the doubly charged phosphorylated peptide, SQQDAASSGSpSLESIFSEVWK observed in the sample containing XCEP63 isolated from egg extract treated with pA/pT at m/z 1162.12+ with a retention time of 32.0 min. Y ions marked with an asterisk have undergone neutral loss of 98 Da, indicating the loss of phosphoric acid. Y ions down to y11 exhibit this neutral loss, indicating that S560 is indeed a site of phosphorylation. (b) Multiple reaction monitoring (MRM) traces observed in XCEP63 – pA/pT (top) and XCEP63 + pA/pT (bottom) for the transition m/z 1162.1>795.4 specific for the phosphopeptide sequence SQQDAASSGSpSLESIFSEVWK. Integration of the traces revealed a phosphopeptide ratio of 0.17 between samples - and + pA/pT.

163

6.4 Confirmation of XCEP63 serine 560 phosphorylation site

We set out to verify the Mass Spectrometry analysis findings by converting serines to alanines at XCEP63 amino acid sites: 560 (peptide one), 391 (peptide two) and 603 (peptide three). Similarly to the rationale of candidate phosphorylation studies in figure 6.1, we tested site directed XCEP63-S560A mutants singly and in combination in *Xenopus* egg extract with and without ATM and ATR activation. Again, we assessed alterations in ATM and ATR dependent gel mobility of XCEP63-S560A mutant compared to XCEP63 wild type using autoradiography.

In figure 6.4a, we show autoradiographs of XCEP63 mutant shift assays. We observe that combinations of S391 and S603 double mutations and S560 single mutant gel mobilities are comparative to XCEP63 wild type in the absence of ATM and ATR activation. But in the absence of ATM and ATR activation XCEP63 containing a combination of all three serine conversions shows an increase in gel migration. These observations can be explained by a likely suppression of XCEP63 lower levels of constituent phosphorylation modifications. In agreement with Mass Spectrometry MRM trace phosphorylation ratios (figure 6.2), these data suggests S560, S391 and S603 attribute to a basal level of phoshorylation present on XCEP63 protein within *Xenopus* egg extract.

We show in figure 6.4a, XCEP63 serine 560 site mutation alone specifically abolishes XCEP63 gel mobility change in the presence of active ATM and ATR. We repeated the shift assay in isolation to check that serine 560 is indeed the site ATM and ATR phosphorylates XCEP63. Figure 6.4b autoradiograph clearly shows XCEP63 serine 560 mutation prevents ATM and ATR signature gel migration change. These data confirm serine 560 is the site at which active ATM and ATR phosphorylates XCEP63.

Autoradiographs of XCEP63-A mutants in *Xenopus* egg extract

A)

B)
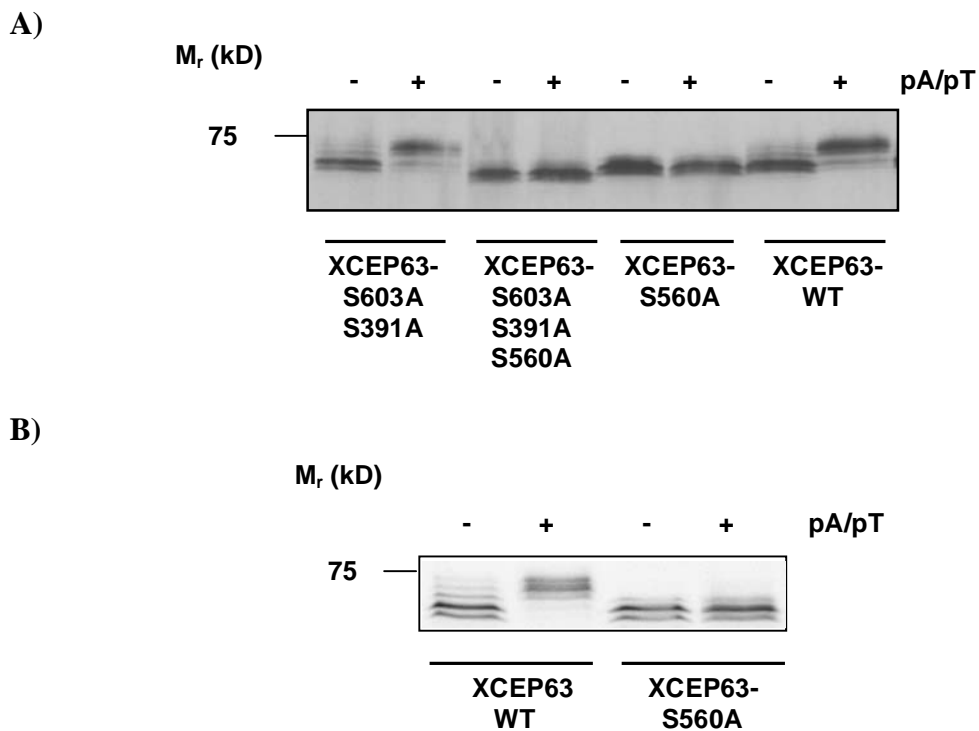
Figure 6.4 ATM and ATR phosphorylates XCEP63 at serine 560

XCEP63 (WT), XCEP63 S603A/S391A/S560A combined serine mutant and single XCEP63 S560A mutant were transcribed and translated in the presence of [^{35}S]-methionine in promega reticulate lysate coupled system. Transcribed proteins were exposed for 30 minutes at 20 °C to CSF arrested egg extract, pretreated for 20 minutes at 20 °C with (+) or without (-) linear DNA (pA/pT). Samples were separated by SDS-PAGE electrophoresis and then underwent audioradiography. **(b)** XCEP63 (WT) and single XCEP63-S560A mutant experiment was performed in isolation as above.

6.5   Summary

In this chapter we describe the phosphorylation modifications present on XCEP63-MBP recombinant protein. Initially, Mass Spectrometry analysis identified three sites of phosphorylation on XCEP63 in the absence and presence of ATM and ATR activation. Gel mobility analysis of site directed mutants verified preliminary Mass Spectrometry data. Combined serine 560, 139 and 603 XCEP63 alanine mutations show faster gel mobility to that of wild type protein in the absence of ATM and ATR inducing treatment. The collective evidence suggests XCEP63 is constituently phosphorylated at a low level in the presence of untreated *Xenopus* extract.

Furthermore, sophisticated Mass Spectrometry methods generated semi–quantitative information on the phosphorylation sites in untreated and treated XCEP63 samples (figure 6.2). Through integration of Mass Spectrometry MRM traces, the peptide containing serine 560 was isolated with a heightened phosphorylation ratio of 0.17 with regard to the absence and presence of treatment (figure 6.3). By testing of XCEP63 serine 560 conversion to alanine alone, we established the signature ATM and ATR gel migration change was abolished (figure 6.4). We therefore attribute XCEP63 ATM and ATR phosphorylation site to serine 560.

In the light of this finding it was not surprising that we were unsuccessful in our initial XCEP63 phosphorylation search attempts by site directed mutagenesis screening of ATM/ATR candidate SQ/TQ sites and speculative SE/TE sites. In ascertaining ATM and ATR phosphorylation at serine 560, we uncovered a novel ATM and ATR recognition motif of Ser-Leu-Glu (SLE) potentially present in other substrates. Previous ATM and ATR substrate studies described putative recognition site of SQ/TQ(E) motifs (Kim *et al.,* 1999; Matsuoka *et al.,* 2007). Although SLE phosphorylation motif requires further confirmation, in the case of XCEP63 we have potentially disregarded for this particular target the requirement for SQ/TQ(E) motif. In the next chapter we characterise ATM and ATR phosphorylation of XCEP63 at serine 560 and distinguish any XCEP63 functional changes in regulating spindle assembly.

7 Chapter 7 Characterisation of XCEP63 phosphorylation

In earlier characterisations, we ascribed to XCEP63 a role in regulating normal spindle assembly. We ascertained that in the absence of XCEP6 spindle assembly was perturbed. Furthermore, immuofluorescence data showed that XCEP63 diffuses away from centrosomes in the presence of active ATM and ATR. This dispersion of XCEP63 suggests its modification changes the behaviour of the protein. In order to characterise the physiological relevance of XCEP63 adaptation in spindle assembly, we undertook the identification of XCEP63 phosphorylation site. Strong evidence indicates XCEP63 phosphorylation by ATM and ATR at serine 560. In this chapter, we first confirm the isolated phosphorylation site on XCEP63. We then aimed to differentiate between non-modified and modified XCEP63 positioning in relation to the centrosomes. Finally, we wished to address XCEP63 role in centrosome-driven spindle assembly defects in the presence of ATM and ATR.

7.1 XCEP63 serine 560 phosphorylation in the presence of activated ATM and ATR in *Xenopus* egg extract

We sought to confirm XCEP63 serine 560 phosphorylation by active ATM and ATR. For this purpose, we required phospho-specific antibodies. Eight rabbits were injected with XCEP63 peptide antigen conjugated to KHL containing phosphorylated serine 560. Polyclonal antibodies were generated at Harlan UK using their extended standard protocol. Collected production sera were affinity purified against the same phosphorylated peptide and then with equivalent non-phosphorylated peptide. Purified antibodies and pre-bleed sera were tested and compared in immunoblot detections of *Xenopus* egg extract treatments (data not shown). The purified antibodies with the most stringent XCEP63 serine 560 phosphorylation recognition were selected for further experiments. Serine 560 phospho-specific immunoblot detections are shown in figure 7.1a and 7.1b. Blots of *Xenopus* egg extract reactions show strong band detection upon ATM and ATR activation treatments. Phospho-specific antibodies recognize both recombinant XCEP63-MBP protein and endogenous XCEP63 in the presence of ATM and ATR activating conditions, pA/pT or *EcoRI* with sperm nuclei. Very faint XCEP63

immuoblot detections are apparent in the absence of ATM and ATR activation. These data suggests a very low basal level of XCEP63 phosphorylation at serine 560 in comparison to the large increase observed in the presence of active ATM and ATR.

We continued by verifying the phosphorylation specificity of XCEP63 serine 560 polyclonal antibodies. We show complete eradication of XCEP63 immunoblot band detection observed in ATM and ATR active samples when treated with lambda phosphatase (figure 7.1c). The removal of XCEP63 phosphates by lambda phosphatase in the presence of ATM and ATR activation directly confirms that these phospho-specific antibodies are detecting only phosphorylated XCEP63. We confirm through these immunoblot detections with phospho-specific antibodies that ATM and ATR activating treatment dramatically increases phosphorylation levels of XCEP63 at serine 560.

Immunoblot detection of XCEP63 phosphorylation of endogenous and added recombinant protein in *Xenopus* egg extract

A)

eXCEP63

rXCEP63-MBP

B)

eXCEP63

rXCEP63-MBP

C)
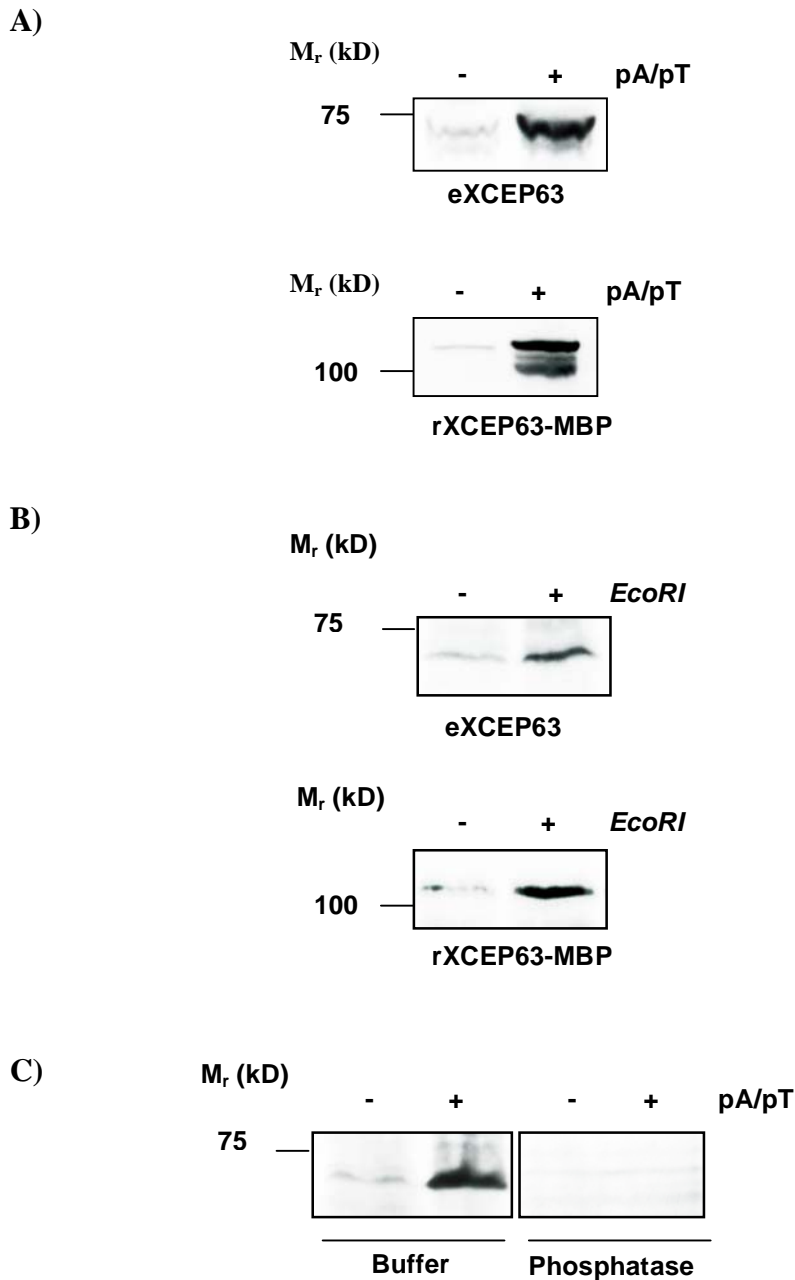
Figure 7.1 Immunoblot detection of serine 560 phosphorylation in the presence of ATM and ATR activation

All samples were separated by electrophoresis on standard 10 % SDS-PAGE gels. Immunoblot detections were performed with XCEP63 phospho serine 560 polyclonal antibodies Immunoblot detections show endogenous XCEP63 (eXCEP63) and recombinant XCEP63-MBP (rXCEP63-MBP). **(a)** CSF arrested *Xenopus* egg extract was incubated in the absence (-) and presence (+) 50 ng/µl pA/pT supplemented with 50 ng/µl XCEP63-MBP recombinant protein for 30 minutes at 20 °C. **(b)** CSF arrested *Xenopus* egg extract supplemented with 1,000 sperm nuclei/µl and 50 ng/µl recombinant XCEP63-MBP protein in the presence (+) or absence (-) of 0.25 U/µl *EcoRI*. Extracts were incubated for 30 minutes at 20 °C. **(c)** CSF arrested egg extracts were treated in the absence (-) and presence (+) of pA/pT linear DNA for 30 minutes at 20 °C. 2 µl of extracts were exposed to 2 µl lambda phosphatase (phosphatase) or lambda phosphatase buffer (Buffer) for 30 minutes at 30 °C.

7.2 XCEP63 serine 560 phosphorylation dependent on active ATM and ATR in *Xenopus* egg extract

We continued by attempting to confirm that the phosphorylation of XCEP63 at serine 560 corresponds directly to active ATM and ATR. We prevented ATM and ATR activity by chemical inhibition and monitored the levels of XCEP63 serine 560 phosphorylation by immunoblot detection. Figure 7.2a shows immunoblot detection of XCEP63 serine 560 phosphorylation diminished with caffeine or ATM inhibitor additions in the presence of pA/pT treatment.

Interestingly, in figure 7.2b, the immunoblot shows that XCEP63 serine 560 phosphorylation by ATM and ATR occurs within five minutes of activating treatment in *Xenopus* egg extract. In addition, we establish XCEP63 phosphorylation is consistently caffeine sensitive. Again, data suggests XCEP63 modification dependency on active ATM and ATR. We also show in figure 7.2b, the maintenance of XCEP63 serine 560 phosphorylation across the time of incubation, suggesting XCEP63 modification is stable. Furthermore, phosphorylation at serine 560 shows no indications of rendering XCEP63 susceptible to degradation.

Here, we have compiled evidence to suggest we have indeed isolated the correct site on which ATM and ATR modifies XCEP63. Overall, findings imply ATM and ATR targeting of centrosome protein, XCEP63, in a constant manner, thus indicating a possible importance of XCEP63 role in mitotic DNA damage responses.

Immunoblot detections of XCEP63 phosphorylation in *Xenopus* egg extract

A)

M_r (kD)

Caff   ATMi

75 —

-       +   +   +   pA/pT

B)

M_r (kD)

pA/pT

-       -   +   -   +   -   +   -   +   Caff

75 —

5   10   20   30   minutes
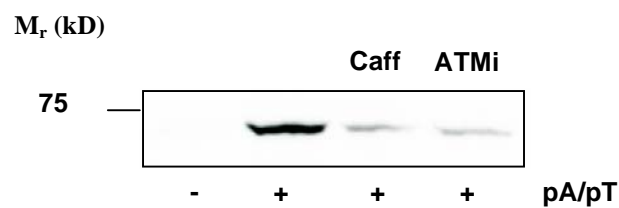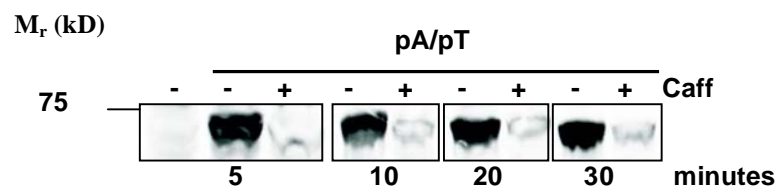
Figure 7.2 Serine 560 phosphorylation of XCEP63 by active ATM and ATR

Immunoblot detections were performed using antibodies recognizing XCEP63 phosphorylated serine 560. Typical detections are shown of two separate experiments. **(a)** CSF egg extract was treated in the absence (-) and presence (+) of 50 ng/µl linear DNA (pA/pT) with 2 mM caffeine (Caff) or 20 µM Ku55933 (ATMi). Samples underwent gel electrophoresis on a standard 10 % SDS-PAGE gel. **(b)** CSF arrested egg extract was treated with 50 ng/µl linear DNA (+) and without (-) pA/pT and 2 mM caffeine (Caff). Samples were collected at indicated incubation times after linear DNA addition. Samples were run on a medium pre-cast Bio-Rad 4-12 % Bis/Tris acrylamide gel.

7.3 XCEP63 serine 560 peptide phosphorylation by ATM and ATR kinases

At this point we decided to perform *in vitro* kinase assays to verify ATM and ATR phosphorylation of XCEP63 at serine 560. We applied phosphorylatable peptides containing XCEP63 serine 560 and non-phosphorylatable peptides containing serine to alanine mutation to reactions containing ATM or ATR kinases. We measured outcomes of reactions by monitoring radioactive phosphate incorporation. Quantification of *in vitro* assays are shown in figure 7.3. We found serine 560 peptide undergoes phosphorylation modification by ATM or ATR kinases. We observed the radioactive phosphate labelling increases by approximately 4-fold in the presence of ATM and over 3-fold with ATR addition in comparison to levels of incorporation in the absence of kinase activity. Thus, these data indicate a lower level of radioactive phosphate addition on serine 560 peptide in the presence of ATR compared to ATM in an *in vitro* assay. We suspect that ATM may preferentially targets and modifies XCEP63 although we have no data to show this is the case in *Xenopus* egg extract.

These data unveil in a non-physiological *in vitro* context that ATM and ATR specifically phosphorylates serine 560 containing XCEP63 peptide. These data, taken with the similar *Xenopus* egg extract experimental findings establish that XCEP63 serine 560 phosphorylation is dependent on ATM and ATR activity. The XCEP63 modification at serine 560 is linked directly to ATM/ATR kinase activities. Therefore, we can discount the possibilities of XCEP63 phosphorylation by alternative DNA damage kinases, for example, DNA-PK or downstream ATM/ATR factors, such as Chk1 or Chk2. Furthermore, we confirm the identification of the novel ATM and ATR SLE recognition motif.
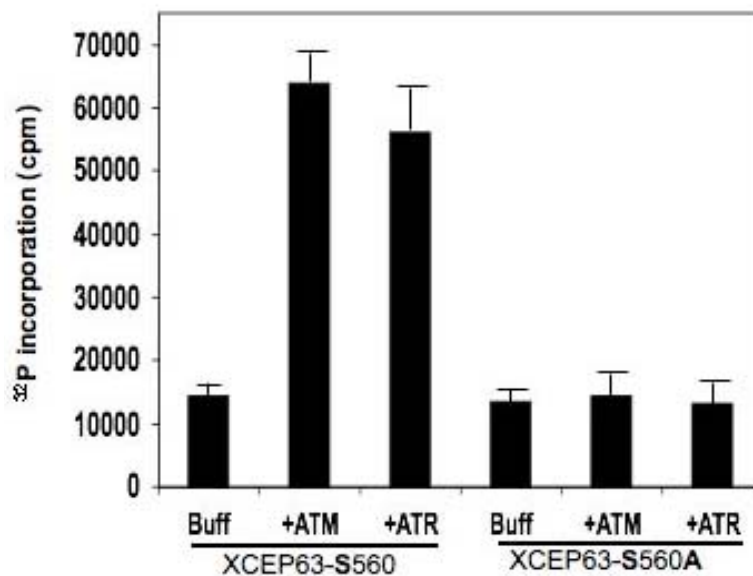
Figure 7.3 *In vitro* ATM and ATR phosphorylation of XCEP63 serine 560 containing peptide

XCEP63 50 mer peptides containing central serine 560 (XCEP63-S560) or substituted alanine 560 (XCEP63-S560A) were added at 0.5 mg/ml to 20 μl EB kinase buffer in the presence of 1 μl of [γ^{32}P]-ATP (10 mCi/μl). Samples were further supplemented without and with donated recombinant Flag-ATM (+ATM) or recombinant Flag-ATR (+ATR) proteins and then incubated at 30 °C for 20 minutes. Kinase reactions were spotted onto phosphocellulose filter paper and processed to be measured by a scintillation counter, as described in material and methods. The average of three independent experiments of radioactivity incorporation is reported in the graph. Error bars indicate standard deviation (s.d.).

7.4 Displacement of phosphorylated XCEP63 away from centrosome localisation

Previously in chapter five, figure 5.9, XCEP63 immunofluorescence detection experiments indicated XCEP63 dispersion away from centrosomes which is dependent on the presence of ATM and ATR activation. These characterisation studies uncovered a potential activity change in modified XCEP63. We continued to investigate phosphorylated XCEP63 positioning in both *Xenopus* egg extract spindle assembly and in cells. We aimed to determine any behaviour alteration caused by ATM and ATR modification by assessing XCEP63 localisation by immunofluorescence.

Immunofluorescent images of XCEP63 serine 560 phosphorylated protein detections in *Xenopus* egg extract spindle formation and XTC cells are shown in figures 7.4a and 7.4b respectively. We find undetectable immunofluorescence staining with serine 560 phospho-specific antibodies in both untreated and caffeine treated spindle assembly extracts. Likewise, immunofluorescent images of tissue culture cells show no visible detection of modified XCEP63 in samples that were untreated and in the two treatments supplemented with caffeine. Thus, immunofluorsecent images of untreated and caffeine inhibition of ATM and ATR triggering treatments show no modified XCEP63 localisation at centrosomes.

As we expected from previous immunoblot studies, we determine XCEP63 serine 560 phosphorylation is present at disguishable levels dependent on ATM and ATR induction. We establish XCEP63 phosphorylated protein does not reside at centrosomes in *Xenopus* egg extract. Figure 7.4a shows phosphorylation by ATM and ATR disperses XCEP63 localisation throughout defective spindle structures. Furthermore in XTC cell we observe XCEP63 serine 560 phosphorylated protein diffusion by ATM and ATR activating treatment, camptothecin (CPT) (figure 7.4b). In XTC cells, displacement of XCEP63 phosphorylated protein immunofluorescence indicates no residual staining co-localising with centrosomes.

In light of these XCEP63 studies, we can conclude that ATM and ATR dependent phosphorylation of XCEP63 changes centrosome positioning. These findings are indicative of a physiological behaviour alteration in modified XCEP63.

A) Fluorescent images of spindle assembly in *Xenopus* egg extract
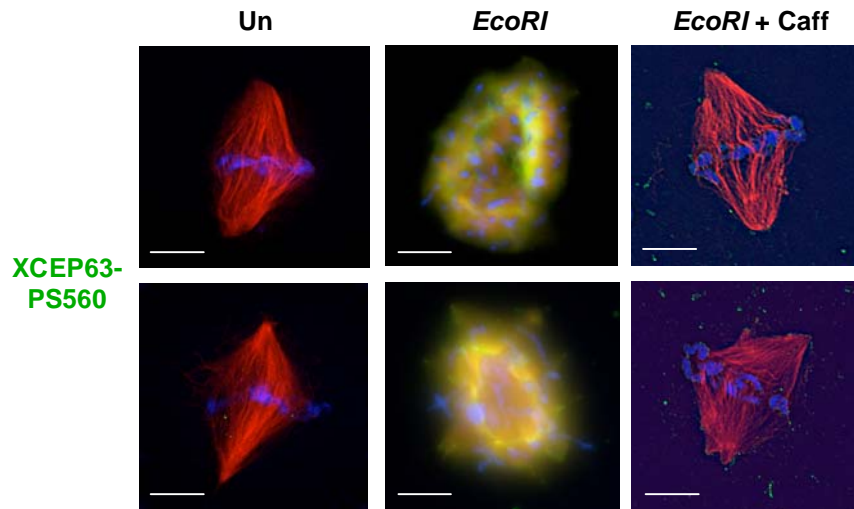
B) Fluorescent images of XTC cells
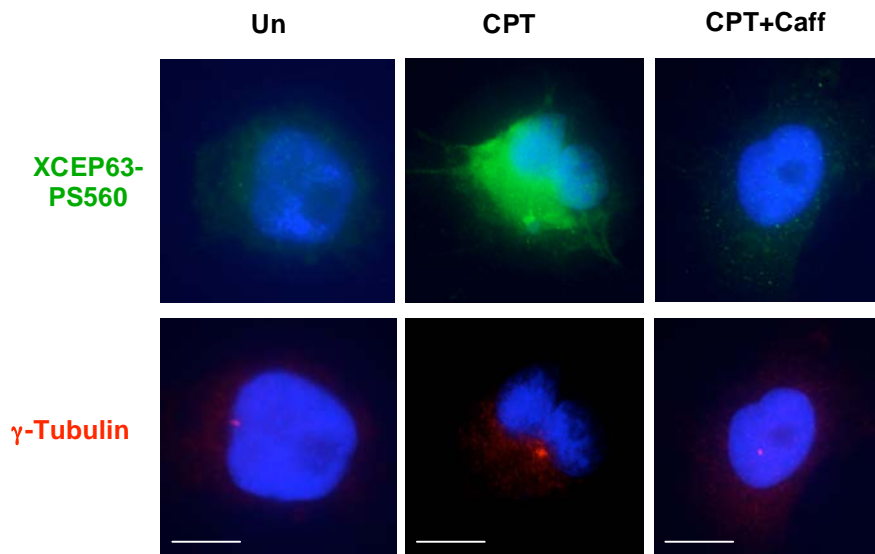
Figure 7.4 Absence of phosphorylated XCEP63 protein at centrosomes in *Xenopus* egg extract and XTC cells

Images were acquired on a Deltavision microscope and are representative of three independent experiments. Scale bar indicates 10 µm. **(a)** Spindles were formed in CSF egg extract with the addition of 1,000 sperm nuclei/µl. Extracts were treated with CSF-XB buffer (Un) extract or 0.25 U/µl *EcoRI* (*EcoRI*) with and without 2 mM caffeine (*EcoRI* + Caff). Samples were incubated at 20 °C for 90 minutes, then formaldehyde fixed and spun onto coverslips as described in material and methods. Immunofluorescence was performed with antibodies recognizing phosphorylated XCEP63 at serine 560 and α-tubulin. XCEP63-S560 is shown in green, microtubules are shown in red and DNA is shown in blue. **(b)** XTC cells were untreated (Un), treated with 400 nM camptothecin (CPT) or 400 nM camptothecin and 5 mM caffeine (CPT + Caff), cells were collected after four hours. XTC cells underwent immunofluorescence with antibodies detecting XCEP63-S560, shown in green and γ-tubulin, shown in red. DNA was stained with DAPI, shown in blue.

7.5   Purification of non-phosphorylatable recombinant XCEP63 alanine 560 mutant protein

At this point we wished to move forward with XCEP63 phosphorylation characterisation in the context of spindle assembly. We aimed to determine whether ATM and ATR phosphorylation of XCEP63 is the mechanism by which ATM and ATR dependent defects in spindle assembly occur. In order to provide a definitive answer to this question experiments required XCEP63 recombinant protein containing alanine conversion of serine 560 ATM and ATR phosphorylation site. We therefore needed to purify XCEP63-MBP alanine 560 recombinant protein (S560A).

We applied previously used techniques in producing recombinant XCEP63-MBP protein. In figure 7.5a we show the gel of purified XCEP63-MBP S560A mutant along side previously purified XCEP63-MBP wild type recombinant protein (chapter five, figure 5.7). We show XCEP63-MBP S560A and XCEP63-MBP wild type recombinant proteins have similar gel migrations.

In figure 7.5b, we show XCEP63-S560A mutant recombinant protein exposure to *Xenopus* egg extract. XCEP63-S560A does not exemplify XCEP63 wild type signature shift in gel migration in the presence of ATM and ATR. In resolving the absence of the typical XCEP63 gel mobility alteration, these data indicate XCEP63-S560A mutant recombinant protein phosphorylation is prevented. These findings are in consistent with previous data in establishing ATM and ATR phosphorylation targeting at serine 560 site. In obtaining recombinant non-phosphorylatable XCEP63-S560A, we had a reagent to distinguish ATM and ATR phosphorylation effects on XCEP63 spindle assembly regulation function.

A) Commassie Blue staining of XCEP63 recombinant proteins
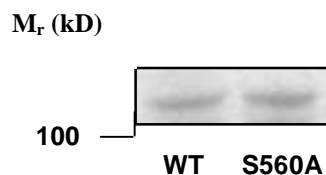
B) SYPRO® Ruby staining of XCEP63 recombinant proteins in *Xenopus* egg extract
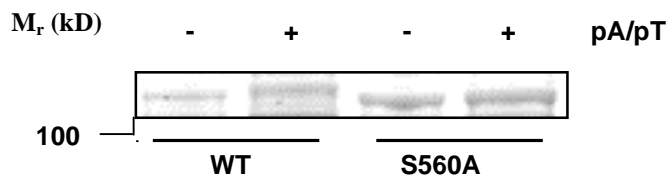
Figure 7.5 Purified XCEP63-S560A mutant recombinant protein is not phosphorylated in the presence of active ATM and ATR in *Xenopus* egg extract

(a) XCEP63 DNA pMAL–c2X, a MBP tag plasmid was altered by site directed mutagenesis incorporating alanine conversion of serine 560 site. XCEP63- MBP S560A mutated DNA was expressed in *E. coli* and the protein was purified through amylose beads as described in materials and methods. XCEP63 wild type (WT) and newly purified XCEP63-S560A proteins were separated on a standard 10 % SDS-PAGE gel by electrophoresis and then Coomassie Blue stained. **(b)** Recombinant proteins, XCEP63-MBP (WT) and XCEP63-S560A (S560A) were pre-coupled to amylose beads then incubated for one hour at 20 °C with CSF *Xenopus* egg extract in the absence and presence of 5 ng/µl pA/pT. Beads were boiled in Bio-Rad sample buffer and then samples were separated on a standard 10 % SDS-PAGE gel by electrophoresis and processed by SYPRO® Ruby staining.

7.6 ATM and ATR phosphorylation of XCEP63 inhibits spindle assembly in *Xenopus* egg extract

We previously established XCEP63 is a factor required in assembly of spindles with correct spatial orientation (chapter five, figure 5.8). Interestingly, abnormal spindle assembly morphology, in the absence of XCEP63, resembled spindle defects found in ATM and ATR activated extracts (chapter three, figures 3.4-3.7). We propose that non-modified centrosome XCEP63 regulates spindle assembly, a mechanism that is inactivated by ATM and ATR targeting. To examine this hypothesis we used XCEP63-S560A mutant recombinant protein. We set up XCEP63 immunodepleted spindle assembly assays in the presence of ATM and ATR activation, supplemented with wild type or mutant XCEP63. If XCEP63 modification does lead to spindle assembly abnormalities, we would expect to observe spindle formation rescue with the introduction of non-phosphorylatable XCEP63-S560A.

Fluorescent images in figure 7.6a show *Xenopus* egg extract spindle assembly in depleted extract in the presence of *EcoRI* with reconstitution of wild type XCEP63 and mutant XCEP63-S560A. Similar spindle organisation irregularities are present in ATM and ATR activated extract without endogenous XCEP63 protein and in extract with excess wild type XCEP63. As we proposed, we observed rescue of normal spindle formation with addition of excess non-phosphorylatable XCEP63-S560A mutant protein to ATM and ATR induced extract. Therefore, these data clearly indicate that XCEP63 regulation of spindle assembly is preserved when phosphorylation of added XCEP63 is prevented.

Experimental quantification of DNA microtubule structures is shown in figure 7.6b. In comparing *EcoRI* treatment alone with XCEP63 wild type introduction, there is a doubling in number of normal spindle assembly. However, we similarly observe high levels of aggregate DNA structures in both treatments. Wild type XCEP63 data indicates a very partial recovery effect on spindle assembly. This phenomenon is most probably due to an excess of XCEP63 protein compared to normal physiological levels of endogenous XCEP63. A slight rise in normal spindle assembly possibly illustrates that increasing XCEP63 abundance slightly overcomes ATM and ATR spindle assembly inhibitory affect. Most prominently, quantification data shows ATM and ATR spindle assembly defects correspond directly to XCEP63 modification. On addition of XCEP63-S560A mutant, we see normal spindle assembly similar to levels of untreated

extracts in the absence of ATM and ATR activating treatment. We observe an approximate 8-fold recovery in spindle formation with reconstitution of XCEP63-S560A mutant compared to activated ATM and ATR extract. Wild type XCEP63 retains the serine 560 ATM and ATR modification site, whereas XCEP63-S560A is unable to undergo active ATM and ATR targeting. These data suggest again, XCEP63 modification disrupts XCEP63 regulation in spindle organisation, whilst non-modified XCEP63 maintains a role in normal spindle array formation.

We can conclude from these experiments that XCEP63 serine 560 site is required for ATM and ATR targeting in defective spindle assembly. Consequently, ATM and ATR modification of XCEP63 inhibits regulatory function in spindle formation. We have determined that XCEP63 is a central mechanism by which ATM and ATR perturbs spindle assembly.

A) Fluorescent images of spindle assembly in *Xenopus* egg extract
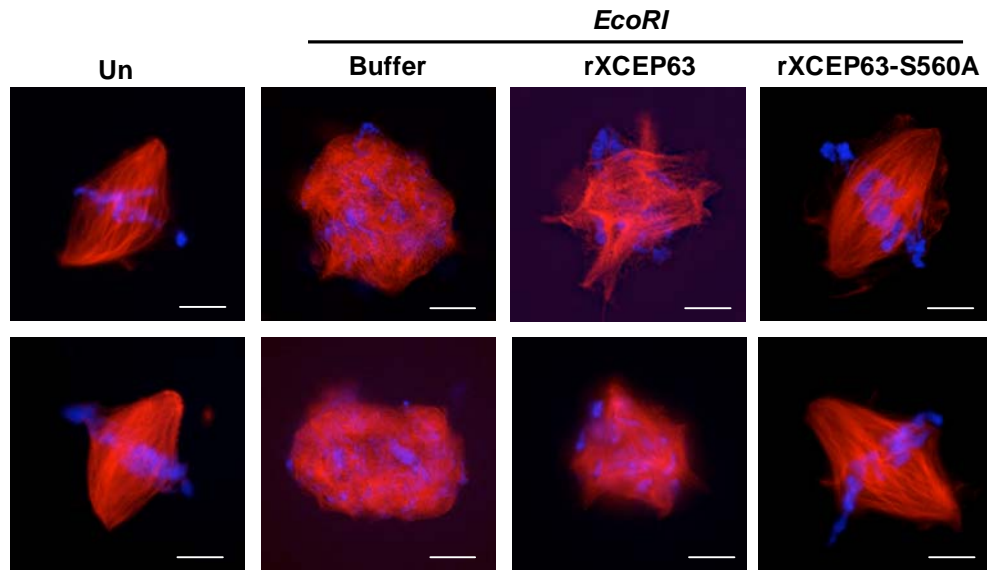
B) Quantification of spindle assembly structures
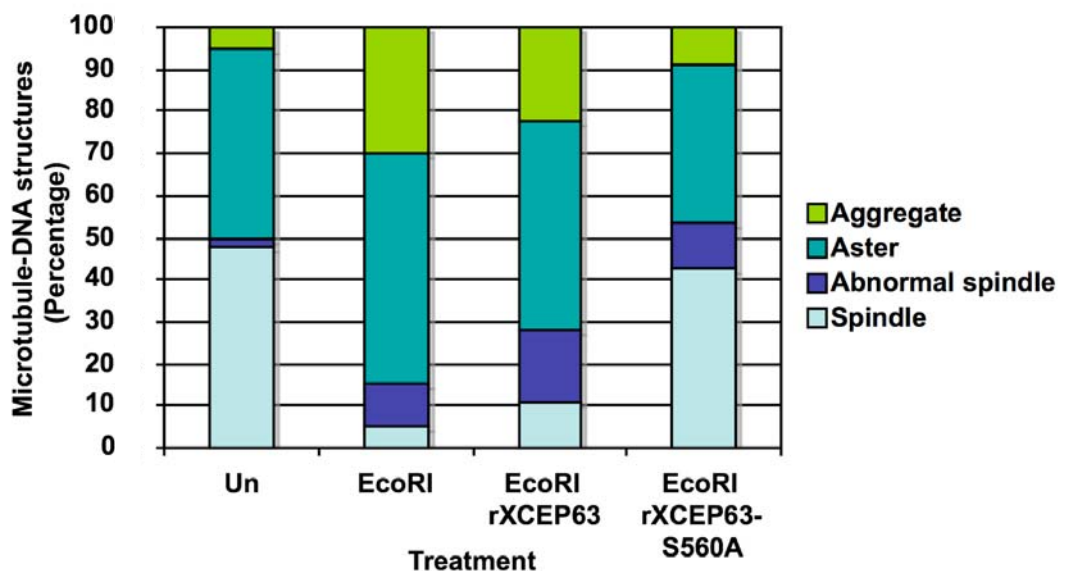
Figure 7.6 XCEP63-S560A protein reconstitution abolishes perturbed spindle formation in the presence of ATM and ATR activation in *Xenopus* egg extract

(a) XCEP63 was immunodepleted from CSF egg extract as previously described by two sequential incubations with 6xHisXCEP63 whole protein antibodies pre-bound in sepharose protein A beads. Spindles were assembled in untreated non-immunodepleted extract (Un) and immunnodepleted extract with 1,000 nuclei/μl and 50 μg/ml rhodamine tubulin. Immunodepleted extracts were treated with 0.2 U/μl of *EcoRI* (*EcoRI*) and further supplemented with recombinant protein buffer (Buffer), 50 ng/μl recombinant wild type XCEP63 –MBP protein (rXCEP63) or 50 ng/μl recombinant serine 560 to alanine mutant XCEP63-MBP protein (rXCEP63-S560A). Samples were incubated at 20 °C for 90 minutes, then formaldehyde fixed and spun onto polylysine coverslips through a glycerol cushion as described in material and methods. Microtubules are shown in red and DNA was stained with DAPI, shown in blue. Images shown were acquired on a Deltavision microscope and representative findings of three separate experiments. (b) Quantification of DNA associated microtubule structures obtained under the conditions indicated above. Microtubule structures were categories as: spindles, abnormal spindles, asters and aggregates Percentages shown are relative to 100 structures counted for each treatment. Data is representative and shows typical findings of three independent experiments.

7.7 Modified XCEP63 localisation alterations correspond to spindle assembly defects in *Xenopus* egg extract

We finalised the XCEP63 characterisation studies by determining localisation of mutant XCEP63-S560A on recovered spindle assembly. In ascertaining the position of XCEP63 in spindle formation in the presence of ATM and ATR, we can outline XCEP63 mechanism in spindle defects. We propose that phosphorylated XCEP63 diffusion prevents XCEP63 function in regulating spindle assembly at the centrosomes.

We performed spindle assembly in *Xenopus* egg extract as in figure 7.6. We used whole protein XCEP63 antibodies used in chapter five, recognising both non-modifed and modified XCEP63 forms for immunofluorescent detection of the proteins. Figure 7.7 shows the presence of XCEP63 at the spindle poles of untreated extracts and the absence of XCEP63 staining in XCEP63 immunodepleted aberrant spindle structures. Unsurprisingly, we find XCEP63 wild type dispersed throughout defective spindle structures. ATM and ATR phosphorylation of XCEP63 wild type protein occurs on retained serine 560 modification site. Finally, we observe that added recombinant XCEP63-S560A, in the presence of ATM and ATR, localises specifically to the poles of rescued normal spindle assemblies. XCEP63 mutant, non-modifiable protein remains positioned at the centrosomes.

In conclusion, these data tie XCEP63 centrosome localisation with the absence of XCEP63 serine 560 ATM and ATR phosphorylation. Furthermore, these data suggest centrosome positioning is required for XCEP63 to fulfil its role in normal spindle array assembly.

EcoRI

| Un | Buffer | rXCEP63 | rXCEP63-S560A |
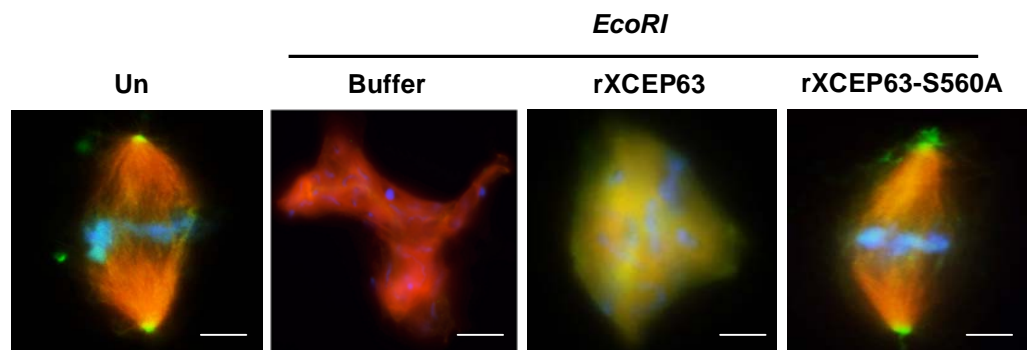
Figure 7.7 XCEP63-S560A, non-phosphorylatable protein in the presence of active ATM and ATR localises to poles of rescued spindles assembly in *Xenopus* egg extract

Extract was left untreated (Un) or underwent two sequential rounds of XCEP63 immuodepletion. XCEP63 depleted extracts were supplemented with *EcoRI* (*EcoRI*) in the presence of recombinant protein buffer (Buffer), 50 ng/µl recombinant wild type XCEP63 (rXCEP63) protein or 50 ng/µl recombinant alanine 560 mutant protein (rXCEP63-S560A). Spindles were formed with the addition of 1,000 sperm nuclei/µl at 20 °C for 90 minutes. Samples were diluted, then formaldehyde fixed in BRB80 solutions, and spun onto polylisine coverslips through a glycerol cushion as described in material and methods. Immunofluorence was performed with antibodies recognizing α-tubulin and XCEP63. Microtubules are shown in red and XCEP63 is shown in green. DNA was stained with DAPI, shown in blue. Analysis was undertaken on a Deltavision microscopy and images presented are representative of three separate experiments.

7.8 Summary

In this chapter we have strong evidence that shows XCEP63 undergoes ATM and ATR phosphorylation at serine 560. In more detail, immunoblot detections with XCEP63 serine 560 phospho antibody recognised XCEP63 phosphorylation specifically at serine 560 site in the presence of active ATM and ATR in *Xenopus* egg extracts (figures 7.1 and 7.2). These findings were confirmed by undertaking *in vitro* ATM and ATR kinase assays with peptides containing XCEP63 serine or alanine 560 (figure 7.3). We established serine 560 peptide was phoshorylated by both ATM and ATR, whereas alanine mutant peptide indicated an absence of phosphate addition by either kinases. In isolating ATM and ATR reactions, we disregarded the possibility XCEP63 phosphorylation by alternative DNA damage response kinases. Furthermore, we showed that active ATM and ATR did not phosphorylate XCEP63 recombinant protein containing serine 560 conversion to alanine in *Xenopus* egg extract (figure 7.5b). In turn, we have validated ATM and ATR novel SLE recognition motif on XCEP63.

Previously, we showed XCPE63 localisation at centrosomes and potential dispersion of XCEP63 away from centrosomes in the presence of activated ATM and ATR (chapter five, figures 5.3 and 5.9). The continuation of these investigations in figure 7.4 established a lack of inflorescence staining with serine 560 phospho-specific XCEP63 antibody in both *Xenopus* egg extract and XTC cells in the absence of active ATM and ATR. As expected, we found phosphorylated XCEP63 dispersion in the presence of induced ATM and ATR. Interestingly, immunofluorescence data showed no staining of phosphorylated XCEP63 at centrosomes. Theses data allowed the distinction of localisation differences between non-phosphorylated XCEP63 and phosphorylated XCEP63.

We established that ATM and ATR phosphorylation at serine 560 disrupts XCEP63' regulation role in centrosome-driven spindle assembly leading to the formation of abnormal spindles (figure 7.6). We showed in the presence of activated ATM and ATR the reconstitution of non-phosphorylatable XCEP63-S560A mutant protein strikingly recovered spindle assembly at centrosomes (figure 7.7). These findings indicated that normal spindle assembly relies on XCEP63 regulation function at centrosomes. Furthermore, data suggests that ATM and ATR dependent checkpoint targeting disrupts

XCEP63 function at centrosomes, the likely mechanism by which spindle assembly is inactivated.

8   Chapter 8 Discussion

ATM and ATR checkpoints have been extensively shown to prevent cell cycle progression up to the point of mitosis onset (Sancar *et al.,* 2004). Prior to this study, DNA damage responses within the setting of mitosis were poorly understood. In this thesis, we have investigated ATM and ATR DNA damage responses during mitosis using *Xenopus laevis* as a model system. We have established a novel ATM and ATR dependent checkpoint that inactivates spindle assembly by targeting centrosomal protein XCEP63 (Smith *et al.,* 2009). XCEP63 shows potential as a tumour suppressor protein, which safeguards the genome against mitotic DNA damage by blocking normal spindle assembly.

8.1   ATM and ATR activation during mitosis inhibits normal spindle assembly

In this body of research, we approached investigations in most part by manipulating the biochemical system provided by crushed *Xenopus* eggs. The use of *Xenopus* egg extracts has enabled insightful investigations into ATM and ATR key roles in activating G1/S, S phase and G2/M checkpoints recapitulated by the introduction of reagents that mimic DNA damage (Garner and Costanzo, 2009). These checkpoints support the process of DNA damage repair by modulating DNA replication onset, progression of DNA replication or entry into mitosis (Sancar *et al.,* 2004).

Although the time cells are in M phase is very short compared to other cell cycle phases, DNA damage could still occur. Genotoxic stresses resulting from endogenous and/or exogenous sources could have detrimental consequences at the critical stage of genetic transference to daughter cells. As described in chapter one (section 1.5) mitotic DNA damage checkpoint responses have remained under dispute, mainly due to mixed and contradictory published data. In general, it is thought that ATM and ATR dependent pathways most likely exist which impact on mitosis progression. It should be noted that a particular problem encountered by researchers is that the mitosis in the cell cycle is short in duration. For this reason, investigations have relied on microtubule depolymerising treatments to synchronize and arrest cells in mitosis, methods that could potentially influence findings.

Previous uses of the *Xenopus* egg extract cell free system have enabled valuable studies into cell cycle progression. We exploited this capability of *Xenopus* egg extract in order to investigate the effects of ATM and ATR signalling responses on mitotic processes. In these studies, we have demonstrated that mitotic *Xenopus* egg extract also recapitulates DNA damage responses. In chapter three, we demonstrated the mitotic induction of ATM and ATR in response to linear DNA molecules and in response to chromatin breakages by treatment of *EcoRI* restriction endonuclese together with sperm nuclei (chapter three, figures 3.1 and 3.2). This research revealed that DSBs either created by restriction enzyme or alternative treatment by DNA damage inducing or mimicking agents led to defects in spindle assembly in *Xenopus* egg extract (chapter three, figures 3.4-3.7). Spindle defects were also found in cells treated with IR (chapter three, figure 3.8). In the presence of activated ATM and ATR, we observed spindles lacking in polar orientation and large aggregated microtubule structures with DNA dispersed throughout. Interestingly, we recorded an increased number of structurally normal asters dependent on ATM and ATR activation in *Xenopus* egg extract (chapter three, figure 3.4). The defects in spindle assembly were found to be dependent on ATM and ATR signalling activation, as they were reversible by caffeine inhibition (chapter three, figure 3.4-3.8). The combined evidence from these experiments suggests that active ATM and ATR target an early event in spindle formation, deregulating operations from aster maturation to organised spindle array. These data also attribute spindle assembly abnormalities directly to ATM and ATR signalling.

8.2 The search for the ATM and ATR dependent spindle assembly inactivation factor

In order to establish the spindle assembly inhibition mechanism initiated by ATM and ATR, we monitored Cdk1 and Plx1 kinase activities in the presence of mitotic DNA damage (chapter three, figure 3.9). We established that activated ATM and ATR signalling had no affect on Cdk1 or Plx1 activities in egg extracts progressing through mitosis or in the process of mitotic exit (chapter three, figures 3.9). Furthermore, in establishing that the addition of excess Plx1 to *Xenopus* egg extract was unable to overcome spindle assembly defects confirmed the independence of ATM and ATR signalling from Plx1 spindle assembly function (chapter three, figure 3.10).

Consequently Cdk1-CyclinB and Plx1 factors were eliminated as downstream ATM and ATR checkpoint targets.

Cdk1 (-Cyclin B) and Plx1 activities are sustained within the Cdc25 amplification loop, which reaches a peak in mitosis (Hoffmann *et al.,* 1993; Kumagai and Dunphy 1996; Abrieu *et al.,*1998; Qian *et al.,* 1998). As we established by monitoring Cdk1 and Plx1, both kinase activities were unaffected by ATM and ATR activation. This suggests checkpoint induction has no inhibitory affect on Cdc25 dependent amplification loop once at heightened levels during mitosis (chapter three, figures 3.8-3.10). We believe that the resistance of mitotic kinases to ATM and ATR dependent down-regulation once mitosis has been fully established prevents premature exit of mitosis in the presence of DNA damage. However, we have not defined in this thesis the mechanism behind the resistance to DNA damage during mitosis. Although it seems reasonable that in maintaining mitotic state and prevention of mitosis exit could be a mechanism by which cell division in the presence of damaged DNA is controlled.

We also discounted RCC1 and Ran-GTP spindle assembly factors as targets of ATM and ATR. In the presence of ATM and ATR activation there was no effect on RCC1 chromatin association in *Xenopus* egg extract (chapter 3, figure 3.11) If RCC1 binding was affected by ATM and ATR activation this would have potentially altered the RCC1 generation of localised Ran-GTP/Ran-GDP gradient required for spindle assembly (Carazo-Salas *et al.,* 1999; Carazo-Salas *et al.,* 2001). Ran-GTP, which promotes microtubules nucleation was found not to be targeted in ATM and ATR dependent spindle assembly inactivation, as the addition of constitutively active Ran-GTP in excess was unable to rescue spindle formation abnormalities in egg extract (chapter three, figure 3.12).

We made great advances in studying the formation of anastral spindles (chapter three, figure 3.13). We established that chromatin-coated beads the platform on which anastral self assemble induce ATM and ATR activity. Anastral spindles form in *Xenopus* egg extract in the absence of sperm nuclei whose basal body carries a centriole that matures into a centrosome (Heald *et al.,* 1996). Heald *et al.,* determined that centrosomes are not a necessary requirement for spindle assembly, however when present they act as dominant microtubule organisation centres (Heald *et al.,* 1997). The distinctions of normal anastral spindles assembly in the presence of active ATM and ATR provided the

focus for an ATM and ATR target within a centrosomes-dependent spindle assembly pathway (Khodjakov and Rieder, 2001). The lack of an active ATM and ATR physiological effect on anastral spindle assembly suggests that in acentrosomal plant cells and meiotic cells may not have this checkpoint. The question arises, how do cells dependent on spindle self-assembly respond to the occurrence of mitotic DNA damage? It is possible that an alternative mechanism may exist to prevent these cells progressing to cell division with unchecked chromosomal breakages.

8.3 ATM and ATR substrates identified during adapted cDNA expression library screening in *Xenopus* egg extract

The cDNA small pool expression screening procedure developed to identify ATM and ATR checkpoint target(s) potentially involved in regulation of centrosome-driven spindle assembly was found to be highly effective, with a low 'hits' rate suggesting a less likely occurrence of false positives. A number of other interesting ATM and ATR potential substrates asides XCEP63 were also isolated, some of which have been associated with cell cycle control. These factors included XGEMC1, Caprin-1 and IRF-6 (chapter four, figure 4.1).

XGEMC1 (Geminin coiled-coil containing protein) identified from the cDNA expression library screen as a target of DNA damage responses, created a new research field. To date, experimental evidence indicates XGEMC1 is a novel protein required for initiation of chromosomal DNA replication (thesis of Alessia Balestrini, Genomic Stability Laboratory, Clare Hall Laboratories). Interestingly, data indicates that XGEMC1 interacts with Cdc45. Cdc45 loading is essential for the assembly of replication machinery, which is dependent on S-phase promoting Cdk2-Cyclin E activity (Mimura and Takisawa, 1998). Investigations show that in the absence of functional XGEMC1 Cdc45 chromosome loading onto replication origins is prevented and DNA replication is inhibited. In addition, XGEMC1 shows a direct role in the DNA replication checkpoint by association with and phosphorylation by Cdk2-Cyclin E. As described in chapter one (section 1.4) Cdk2-Cyclin E activity is also a downstream target of ATM/ATR DNA damage G1/S and S phase checkpoints (Sancar *et al.,* 2004). It is possible that DNA damage checkpoints may also affect Cdk2-Cyclin E interaction

with XGEMC1, which then potentially could prevent DNA replication by dissociating XGEMC1 and Cdc45.

Caprin-1 (cytoplasmic activation/proliferation-associated protein-1), also isolated from the cDNA screening for ATM and ATR targets, is a factor of great interest in cell cycle regulation. Interestingly, Caprin-1 is a conserved protein exhibiting RNA binding protein properties (Grill *et al.,* 2004). Caprin-1 is expressed in most tissue types. Its expression is increased on entry into cell cycle and decreased on cell division completion (Grill *et al.,* 2004). Wang *et al.,* showed that the absence of Caprin-1 retards cell phase progression from G1 to S and defined Caprin-1 as an essential factor in normal cell proliferation (Wang *et al.,* 2005). Studies undertaken by Solomon, *et al.* showed that Caprin-1 binds with another RNA binding protein, Ras**G**AP SH**3**-domain **b**inding **p**rotein-**1** (G3BP-1) (Solomon *et al.,* 2007). Caprin-1/G3BP-1 complex was shown to co-localize with microtubule associated "stress granules" (Solomon *et al.,* 2007). Stalled pre-initiation translation complexes induce formation of stress granules in cells, a consequence of various stress imposing conditions such as UV irradiation. Subsequently, mRNAs are recruited to these stress induced structures, where they are monitored and then sorted for translation or degradation (Anderson and Kedersha, 2002; Anderson and Kedersha, 2009).

Interestingly, Solomon *et al.* unveiled selective binding of c-Myc and Cyclin D2 mRNAs to Caprin-1 (Solomon *et al.,* 2007). As described in chapter one (section 1.4), in the cell phase transition from G1 to S, c-Myc has an important regulatory function and Cyclin D2 is the regulatory subunit of Cdk4/6 activity (Bouchard *et al.,* 1999; Perez-Roger *et al.,* 1999; Matsushime *et al.,* 1992; Meyerson and Harlow, 1996; Sherr, 1993; Ekholm and Reed, 2000). The role of Caprin-1 direct binding to c-Myc and Cyclin-D2 RNA transcripts is unknown, this binding may promote or repress translation, determine stability, localization and/or associated proteins (Palacios and Johnston, 2001). It is proposed that Caprin-1, through binding of c-Myc and Cyclin-D2 mRNA, is involved in G1/S transition regulation (Grill *et al.,* 2004). In cDNA expression screening, we determined a possible Caprin-1 modification in the presence of active DNA damage responses. DNA damage induces a modification that may impose an effect on Caprin-1 mRNAs binding and/or the effect Caprin-1' possible regulation role in cell proliferation.

Transcription factor, XIRF-6 (**I**nterferon **r**egulatory **f**actor-**6**) was also isolated in the cDNA expression screening for ATM and ATR targets. IRF-6 mutations have been identified in developmental defect conditions, Van der Woude syndrome and popliteal pterygium syndrome (Kondo *et al.,* 2002). These congenital disorders are distinguished by an epidermal hyperproliferation deficient in terminal differentiation, resulting in tissue fissions such as cleft lip and palate. Richardson *et al.,* established IRF-6 as a central factor in epidermal proliferation-differentiation switching (Richardson *et al.,* 2006). Investigations performed by Bailey *et al.,* revealed IRF-6 phosphorylation aided interaction with tumor suppressor protein, Maspin (**ma**mmary **s**erine **p**rotease **in**hibitor) in breast epithelial cells (Bailey *et al.,* 2005; Zhou *et al.,* 1994). It has also been shown that early cell cycle dependent phosphorylation events regulate IRF-6 expression by targeting IRF-6 for degradation. Baliey *et al.,* hypothesize that accumulation of non-phosphorylated IRF-6/Maspin coordinates cell cycle exit into G0 phase and therefore may regulate cellular differentiation (Bailey *et al.,* 2008; Bailey and Hedrix, 2008). Further involvement of IRF-6 in cell cycle control function were revealed by Richardson *et al.,* research findings that indicated a potential IRF-6 interaction with Stratfin (Sfn/14-3-3σ) gene, a regulator of Cdk1-Cyclin B1 activity (Richardson *et al.,* 2006). In most breast cancers, IRF-6 (as well as Maspin) is found to be absent or at low levels (Bailey *et al.,* 2005). Bailey *et al.,* postulates a promotion of breast transformations through the loss of IRF-6 interaction with Maspin, thought to lead to the deregulation of proliferation and differentiation controls (Bailey *et al.,* 2005). Although not proven, IRF-6 shows some properties of a tumor suppressor. Within the cDNA screening undertaken in this study we isolated IRF-6 as a transcription factor potentially modified in the presence of active DNA damage responses. This possible DNA damage induced modification could have an effect on IRF-6 functioning in control of the cell cycle.

We have shown that the application of cDNA expression library screening in *Xenopus* egg extract is a very powerful technique, particularly successful when compared to more traditional approaches of identifying kinase substrates. *Xenopus* egg extract contains an abundance of proteins allowing physiological interactions that otherwise may have been missed in isolated *in vitro* kinase assays. cDNA expression screening in *Xenopus* egg extract has the potential to be developed further and to identify more substrates of ATM and ATR or other DNA damage response kinases. As mentioned previously, most importantly we identified XCEP63 from the cDNA expression

screening. Without this screening assay it is very unlikely that we would have isolated ATM and ATR centrosomal substrate candidate XCEP63 with no ascribed function.

8.4 Screening candidate, centrosomal protein XCEP63 regulates spindle assembly

The background research into CEP63 revealed a coiled-coil structural domain that is a common feature of centrosome proteins. To date, the vast majority of the proteins identified by the human centrosome study undertaken by Anderson *et al.,* have no defined functions (Anderson *et al.,* 2003). On analysis of CEP63 DNA sequence we found that it has a conserved domain resembling SMC architecture (chapter four, figure 4.3 and appendix 2). SMC proteins are ABC-like ATPases, which typically associate with chromatin and contain a central coiled-coil and a dimerisation region. Examples of SMC heterodimers complexes include SMC1/SMC3 (cohesin) and SMC2/SMC4 (condensin), which are essential in sister chromatid attachment and chromosome assembly/segregation respectively (Losada and Hirano, 2005; Haering, and Nasmyth. 2003; Hirano, 2005). SMC protein functions have been strongly implicated in DNA damage responses and DNA repair processes. It has been shown that cohesin, SMC5/SMC6 and Rad50 (another SMC protein) all localize to sites of DSBs, directing homologous recombination DNA repair and inducing S phase checkpoint (Lehmann, 2005; Kim *et al.,* 2002; Yazdi *et al.,* 2002; Kitagawa *et al.,* 2004; Harvey *et al.,* 2004). In XCEP63 characterisation studies we were unable to detect XCEP63 chromatin binding capacity in interphase or in mitotic egg extracts (data not shown). Many reports have revealed that SMC proteins tend to have multiple and diverse functions. Interestingly, cytoplasmic SMC1 protein of the cohesin complex, was found to localise to centrosomes (Gregson *et al.,* 2001; Guan *et al.,* 2008; Kong *et al.,* 2009). In vertebrates a cohesin function was shown to be necessary in aster assembly and required in microtubule spindle organisation (Kong *et al.,* 2009). Cohesin has been shown to interact with NuMa prior to mitosis, it is hypothesized that NuMa transports cohesin to spindle poles in a dynein dependent manner (Gregson *et al.,* 2001; Kong *et al.,* 2009; Merdes *et al.,* 2000).

As shown in chapter five, figures 5.1 and 5.3 XCEP63 localisation to the centrosome was confirmed by GFP and endogenous XCEP63 immunofluorescence analyses. We

were satisfied that XCEP63 is a true centrosomal protein as it co-localised with gamma-tubulin staining in a manner similar to that of the previously determined human CEP63 (Anderson *et al.,* 2003). The centrosomal position of XCEP63 was a good indication of a potential involvement in spindle assembly. In further XCEP63 characterisation studies, we showed that XCEP63 function is essential in regulating centrosome-driven normal spindle assembly (chapter five, figure 5.8). The immunodepletion of XCEP63 from *Xenopus* egg extracts led to the formation of DNA associated microtubule aggregates. Importantly, in the absence of XCEP63, spindle assembly was inhibited as demonstrated by an increase in aster numbers, whereas aster morphology was normal. By establishing that spindle assembly is restored by reconstitution with recombinant XCEP63, we reasoned that XCEP63 protein functions directly in the assembly of normal spindle arrays and not via an interacting partner. The outcome of these characterisation investigations is to show that XCEP63 centrosome dependent regulation of spindle arrays most probably contributes to the organisation of chromosomes and potentially aids their correct segregation into daughter cells.

Unfortunately, we were unable to determine the mechanism by which XCEP63 functions regulate spindle assembly. Since asters formed normally in XCEP63 depleted extracts, this suggests that XCEP63 function does not relate specifically to microtubule polymerisation or to an integral centrosome structure component. It has been hypothesised that cohesin functions in spindle assembly through SMC domain dependent bundling and stabilisation of fibres, albeit microtubules instead of chromatin fibres (Kong *et al.,* 2009). The probable functional importance of the SMC domain within XCEP63 is supported by the fact that it is maintained across vertebrate species. Furthermore, it remains intact in the identified alternatively spliced transcript variants of human CEP63 (NCBI database). It is possible that the function of XCEP63 in regulating normal spindle organisation may relate to its contained SMC domain.

8.5   XCEP63 basal level phosphorylations and the identification of ATM and ATR target site

Mass Spectrometry analysis pinpointed the XCEP63 ATM and ATR phosphorylation site to serine 560 (chapter six, figures 6.2-6.4), which was later confirmed by a series of phospho-specific antibody immunodetections (chapter seven, figure 7.1). We verified

by using an XCEP63 peptide in *in vitro* kinase reactions that ATM and ATR directly phosphorylates serine 560 (chapter seven, figure 7.3). It was not surprising that previous attempts had failed to identify the XCEP63 phosphorylation site through residue mutation and screening of potential ATM and ATR consensus motif sites (chapter six, figure 6.1). XCEP63 phosphorylation at serine 560 specifies that ATM and ATR recognises a novel SLE motif, although the presence of glutamate (E) within the motif is in line with previous general scheme of S/TQE (Kim *et al.,* 1999; Matsuoka *et al.,* 2007). In XCEP63 case residue glutamate adjacency may similarly enrich phosphorylation. The identification of this novel motif is of great interest to the ATM and ATR research field. This potentially opens an exciting new direction in ATM and ATR substrate studies. It is possible that other ATM and ATR targets with the SLE recognition motif may exist. Also, in establishing one novel ATM and ATR phosphorylation site it is conceivable that there may be more alternative motifs.

We considered the significance of the basal level of phosphorylation present on XCEP63 at serine 560 in the absence of ATM and ATR activation that was highlighted by Mass Spectrometry data (chapter 6, figure 6.2). It is possible that the low levels of XCEP63 phosphorylation at serine 560 could possibly represent an artefact of the assay conditions i.e. the *Xenopus* egg extract. Basal phosphorylation may be attributed to localised and minimal ATM and ATR induction, perhaps corresponding to the physical stress incurred during extract preparations. However, in previous spindle assembly isolation from non-treated extracts, with likely low level of XCEP63 phosphorylation at serine 560, we showed no noticeable widespread affects on spindle assembly regulation in *Xenopus* egg extract (chapter three, figure 3.4). It is probable that XCEP63 phosphorylation at basal levels does not alter overall XCEP63 role in spindle assembly.

Another line of investigations provided by XCEP63 Mass Spectrometry analysis is the unidentified modification of 252 Da molecular weight assigned to XCEP63 Carboxyl terminus (chapter six, figure 6.2). Although outside the scope of this thesis, it is very intriguing what this modification is and whether it is a required element in XCEP63 function or perhaps for partner or structural interactions.

8.6   ATM and ATR inhibition of XCEP63 regulatory role in spindle assembly

In chapter seven, we determined that XCEP63 serine 560 phosphorylation by ATM and ATR coincided with the delocalisation of XCEP63 away from centrosomes (chapter seven, figures 7.4). We hypothesise that this displacement is reliant on a serine 560 phosphorylation threshold above that of basal phosphorylation levels, which is dependent on active ATM and ATR targeting. We observed that in the presence of DNA damage, XCEP63 phosphorylation and XCEP63 delocalisation also coincided with spindle assembly abnormalities. These findings were verified following reconstitution of depleted extract with XCEP63-S560A non-phosphorylatable recombinant protein which remained localised to centrosomes of normal spindles unaffected by active ATM and ATR (chapter seven, figures 7.6 and 7.7).   In this manner, we established that XCEP63 is the major target of ATM and ATR checkpoint. From the experimental evidence, we posit that XCEP63 spindle assembly regulation function is inactivated as a consequence of ATM and ATR serine 560 phosphorylation. This suggested localisation dependency of XCEP63 spindle assembly regulation is required for functioning of centrosomes as dominant centres of microtubule organisation.

ATM and ATR targeting of spindle assembly regulation is in agreement with the theory that centrosomes are a "command centre for cellular control" for mitotic events (Doxsey, 2001; Doxsey *et al.,* 2005; Reider *et al.,* 2001; Löffler *et al.,* 2006). These studies show that ATM and ATR target centrosomes which influences the progression of mitotic events, in which ATM/ATR control of centrosome-driven spindle assembly factor XCEP63 seems to be critical. An increasing number of reports also discuss the potential compartmentalisation of proteins in the context of DNA damage responses (Lukas *et al.,* 2004; Löffer *et al.,* 2006). Centrosomes are becoming key structures of interest, containing an abundance of mitotic control and DNA damage response factors (Takada *et al.,* 2003; Löffer *et al.,* 2006; Jackman *et al.,* 2003; Golsteyn *et al.,* 1995; Tsvetkov *et al.,* 2003). This thesis shows evidence correlating with previous investigations in other systems, in which centrosomes were inactivated as the end-result of DNA damage induced pathways in mitosis (Sibon *et al.,* 2000; Sibon, 2003; Takada *et al.,* 2003; Löffer *et al.,* 2006). Furthermore, it is possible that the control of CEP63 centrosome function by ATM and ATR could potentially participate in preventing

genomic instability and cellular transformations, in which centrosomes role has been proven (Basto *et al.,* 2008).

There is published evidence to suggest that ATM and ATR are localised to centrosomes in mitosis (Shen *et al.,* 2006; Zhang *et al.,* 2007). Considering the ATM and ATR are nuclear, the question arises how do they phosphorylate centrosomal CEP63 in the presence of mitotic DNA damage? However, there are many non-nuclear ATM and ATR substrates that have been identified (Matsuoka *et al.,* 2007). Although we were able to verify ATM/ATR phosphorylation of XCEP63 peptide *in vitro*, we were unable to show a direct interaction with ATM and ATR kinases in egg extract. This could be attributed to a fast rate of association and disassociation. We were notified by Óscar Fernández-Capetillo, group leader of the Genomic Instability at the Spanish National Cancer Center (CNIO), that two-hybrid screening of ATM revealed a consistent CEP63 interaction in the C terminal ATM kinase region (unpublished communication). This substantiates the data on XCEP63 direct phosphorlylation by ATM/ATR, but also encourages the possibility that ATM CEP63 spindle assembly inactivation pathway may exist in other species due to this conserved interaction. However, as XCEP63 phosphorylation site of serine 560 is not conserved in vertebrates it raises the question of whether CEP63 phosphorylation is a universal ATM and ATR DNA damage response kinases regulated checkpoint mechanism.

The mechanism behind XCEP63 delocalisation still remains unknown. Although we have shown that XCEP63 participates directly in spindle assembly regulation, the displacement of XCEP63 from centrosomes may disrupt XCEP63 association with a centrosomal binding partner, which in turn could contribute to the inactivation of spindle assembly. However, this would most likely be secondary to XCEP63 functional importance in normal spindle assembly at the centrosome, as was shown when the addition of non-phosphorylatable XCEP63 recombinant protein rescued normal spindle assembly. It is noteworthy that centrosomes in cells remained intact when XCEP63 was delocalised in the presence of active ATM and ATR (chapter seven, figure 7.4). We therefore can eliminate the requirement for centrosome localised XCEP63 in the scaffolding of the centrosome structure. If XCEP63 is necessary for maintaining centrosomes we might expect to observe disruption such as centrosome fragmentation.

In efforts to extend our understanding of XCEP63 actions, extensive work was undertaken to identify XCEP63 interactions with other cellular factors, which may facilitate XCEP63 spindle assembly regulatory function. We used many experimental approaches in our attempts to identify XCEP63 binding partners. These investigations included pull-down experiments with recombinant XCEP63 and immunoprecipitation with phospho-specific and whole XCEP63 antibodies (data not shown). Despite extensive assays, including Mass Spectrometry, no conclusive data was obtained. However, it is worth mentioning that there was some evidence to suggest that non-phsophorylated and also phosphorylated XCEP63 protein is associated with gamma tubulin. This preliminary data suggests that XCEP63 may have a microtubule-binding site through which XCEP63 directly binds to spindle fibres. In contrast, as many cenrosomal protein are transported towards the centrosomes via actions of motor proteins, XCEP63 could also be transported in this manner and this could be prevented by phosphorylation. We had some inconsistent results that also indicated a possible interaction with dynein and/or dynactin, which suggested that XCEP63 may bind to an alternative matrix in order to be transported. However, we were unable to show whether these potential weak interactions were specific or whether they changed with XCEP63 phosphorylation status. An alternative mechanism could be possible in which phosphorylated XCEP63 may 'piggy-back' a protein that is being transported away from centrosomes. At this stage this question remains open.

Interestingly, published data determined that human DISC1 (**D**isrupted-**I**n-**Sc**hizophrenia **1**, gene mutations of which are associated with hereditary schizophrenia) potentially interacts with CEP63 (Morris *et al.,* 2003). DISC1 is localised to centrosomes and its interaction with dynein has been shown to be necessary in maintaining dynein at centrosomes in normal spindle assembly (Morris *et al.,* 2003; Kamiya *et al.,* 2005). Therefore, it is possible that CEP63 interaction with DISC1 may be important in dynein function in centrosome-dependent spindle assembly. Moreover, another study has revealed that DISC1 may have a role in specifically regulating neuronal progenitor cell proliferation (Mao *et al.,* 2009). As many DNA damage pathway defects often exemplify impaired brain development, this DISC1 connection is fitting as a potential element in this ATM and ATR dependent pathway (Frappart and Mckinnon, 2006). Due to the absence of commercially available *Xenopus* cross-reacting DISC1 antibodies, we were unable to validate a XCEP63-DISC1 interaction and

therefore we were unable to determine its significance in the context of spindle assembly regulation. This question therefore remains speculative.

8.7 Supporting findings from avian CEP63 research

Although not presented in this thesis, CEP63 avain orthologue investigations were undertaken in collaboration with Donniphat Dejsusphong from Kyoto University Graduate School of Medicine, Japan. Investigations using genetically modifiable DT40 chicken cells were performed to establish whether CEP63 has similar mitotic functions in another vertebrate species (Smith *et al.,* 2009). Studies in the most part used DT40 GCEP63 knock out cells (GCEP63$^{-/-}$) generated by target inactivation of the GCEP63 gene locus (Zachos *et al.,* 2007). Interestingly, cell cycle and cell proliferation analyses of GCEP63$^{-/-}$ cells indicated an increase in G2/M cell population, impaired cell duplication and raised levels in apoptosis. Investigations into the effects of CEP63 knock out in mitotic cells revealed an accumulation of cells in prophase and the formation of various aberrant and multipolar spindle structures with irregularities in chromosome segregation and microtubule attachment. The slow mitotic progression of GCEP63$^{-/-}$ cells was attributed to spindle assembly delay combined with spindle assembly defects. Similarly to the *Xenopus* findings, GCEP63$^{-/-}$ data illustrated a CEP63 functional role in early mitosis. GCEP63$^{-/-}$ spindle assembly aberrancies were in accordance with the spindle formation inhibition found in *Xenopus* egg extract lacking XCEP63 protein. However, in contrast in GCEP63$^{-/-}$ cells spindle assembly eventually recovered. It was proposed that factors crucial to spindle assembly recapitulation in GCEP63 knock out cells are absent from *Xenopus* egg extract, which are retained in a mitotic arrest. It was postulated that GCEP63$^{-/-}$ spindle recovery possibly involves spindle pole rearrangement reliant on microtubule self-reorganisation mechanisms or on a mitotic progression event (Khodjakov *et al.,* 2000).

The effects of chromosomal breakage on GCEP63 positioning verified XCEP63 delocalisation findings (chapter five, figure 5.9 and chapter seven, figures 7.4 and 7.7). Immunofluorescent data indicated GCEP63-GFP displacement away from centrosomes was dependent on ATM and ATR induction. Importantly, the treatment of cells with camptothecin showed an immediate displacement of CEP63 from centrosomes, suggesting the delocalisation was not caused by centrosome amplification that requires

longer treatment incubations (Matsumoto and Maller, 2002; Dodson *et al.,* 2004). Investigations into the effects of ATM and ATR activating treatment on GCEP63$^{+/+}$ and GCEP63$^{-/-}$ cells in mitosis unveiled a transient mitotic delay in wild type cells that was absent in knock out cells. In agreement with *Xenopus* data, spindle assembly abnormalities observed in wild type DT40 cells were rescued with caffeine addition, suggesting spindle formation defects reliance on active ATM and ATR. Also in alignment with XCEP63, GCEP63 data also showed a caffeine sensitive DNA damage induced phosphorylation adaptation. However, *Xenopus* serine 560 ATM and ATR phosphorylation site is not conserved on GCEP63. ATM and ATR kinases may not phosphorylate GCEP63 and therefore it is possible that alternative DNA damage kinases such as Chk1 or Chk2 may target avain CEP63 spindle assembly function. From avian studies, CEP63 function in regulating of spindle assembly shows preservation between *Xenopus laevis* and *Gallus gallus*, however we have not ascertained whether this distribution holds in other species.

8.8   Proposed model of ATM and ATR checkpoint spindle assembly inactivation

The mitotic ATM and ATR checkpoint mechanism described in the model in figure 8.1 potentially prevents the transference of damaged genetic information to daughter cells via centrosomes. This checkpoint may provide an alternative means of detecting DSB DNA damage when other mechanisms such as the G2/M transition checkpoint preventing mitosis entry have failed. It has been shown in *S.cerevisiae* that cells can enter mitosis with un-repaired chromosomal breakages originating from S phase (Sandell and Zakian, 1993; Toczyski *et al.,* 1997; Lee *et al.,* 2000). Although not fully characterised this DSB adaptation pathway, which enables cells to overcome the G2/M checkpoint was only thought to exist in unicellular organisms. However, there is evidence in pluricellular organisms that checkpoint responses are also terminated after a period of arrest, which leads to the recovery of cell cycle progression in the presence of DNA damage (Andreassen *et al.,* 2003; Yoo *et al.,* 2004; Syljuåsen, 2007) Recently, it has been determined in checkpoint proficient cells that have defects in DSB DNA repair enter into mitosis with a low number of chromosomal breakages (Deckbar *et al.,* 2007; Krempler *et al.,* 2007). It has been proposed that the G2/M checkpoint may have a low sensitivity and that DNA DSBs can escape this damage surveillance mechanism (Löbrich and Jeggo, 2007). For this reason, it is possible that another monitoring

checkpoint pathway, such as ATM/ATR-CEP63 may recognise un-repaired DSBs before cell division is completed. Such a pathway therefore could be the cell's "safety net" in detecting chromosomal breakages and prevent unequal segregation of DNA to daughter cells.

In figure 8.1 we show a model for chromatin breakage induced ATM and ATR mediated checkpoint control of centrosome dependent spindle assembly. This pathway inactivates early mitosis stages without affecting major mitotic kinase Cdk1 or Plx1 activities. Instead, active ATM and ATR phosphorylates CEP63 and displaces CEP63 centrosome position. CEP63 localisation disruption inactivates CEP63 regulation role, which in turn inhibits normal spindle assembly. Consequently, this pathway of spindle assembly inactivation leads to a transient delay in mitosis progression, possibly induced by activating indirectly the spindle assembly checkpoint (SAC) or alternatively may in turn result in cell death. The transient mitosis arrest depicted in the model was highlighted in analysis of DT40 cells with chromatin breakage (Smith *et al.,* 2009). It is possible that this ATM/ATR dependent CEP63 checkpoint disrupts spindle assembly, which leads to mitotic progression delay that allows DNA damage repair to take place. Alternatively, persistent DNA damage may prolong ATM/ATR-CEP63 pathway activation, which may lead to cell death.
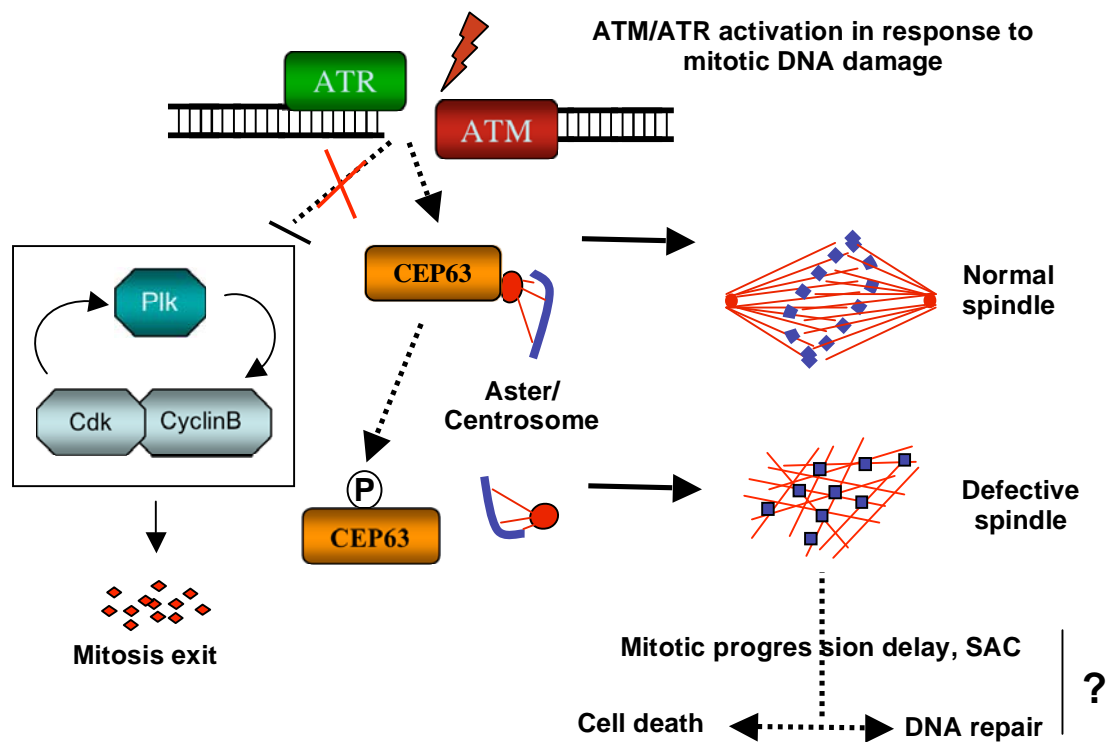
Figure 8.1. A symmetric representation of the proposed model devised for ATM and ATR dependent regulation of spindle assembly

ATM and ATR target CEP63 regulatory spindle assembly function in the presence of chromatin breakages. ATM and ATR phosphorylation of CEP63 leads to the delocalisation of CEP63 away from the centrosomes, a mechanism of inhibiting CEP63 regulation in assembly of organised spindles. The resulting defective spindles cause a mitotic progression delay by activation of SAC most likely leading to cell death. Adapted from Smith *et al.,* 2009 (Smith *et al.,* 2009).

8.9 Potential downstream events and effects on the mitotic ATM and ATR checkpoint inactivation of spindle assembly

To account for previous research in detecting inconsistencies DNA damage induced mitotic arrest, it is probable that the response to chromosomal breakages varies depending timing and extent (Morrison and Rieder, 2004). It is also likely that a threshold level of DNA damage is required to provoke an effect. Cellular responses to DNA damage under different condition may be further complex due to the contribution of non-centrosomal chromatin dependent spindle assembly pathways (or cells with compromised centrosome function), as we demonstrated ATM/ATR resistance in the absence of centrosomes (chapter three, figure 3.13). The complexity and heterogenous effects of treatments with mitotic inhibitors was highlighted in a recent study that was performed with various cell lines, which exemplified differences in mitotic fates across cell populations and between individual cells within a population (Gascoigne and Taylor, 2008). The endpoints recorded included mitotic arrest, DNA endoreduplication and apoptosis (Gascoigne and Taylor, 2008). Much of the past research into mitotic DNA damage was performed using more traditional population-based experiments analysed by methods such as flow-cytometry. In light of Gascoigne and Taylor's publication describing the complexity of cellular responses to anti-mitotic agents, previous studies perhaps need revisiting with more sensitive automated time-lapse light microscopy. Such an application of monitoring DNA damage effects will facilitate a clearer understanding of the responses during mitosis.

In utilising *Xenopus* egg extract cell-free system in this investigation we have gained great understanding into the effects of mitotic DNA damage and the potential mechanism that prevents the segregation of damaged chromosomes. The evidence provided by CEP63 *Xenopus* and *Gallus* experiments suggests that DNA damage results in a delay in mitosis progression (Smith *et al.,* 2009). The halt in mitosis progression provoked by DNA damage does not resemble that of durable metaphase arrest described by Skoufias *et al.,* in response to DNA decatenation (Skoufias *et al.,* 2004). A less stringent mitotic delay suggests indirect activation of SAC checkpoint. Interestingly, Brown and Costanzo following up the research presented in this thesis showed the presence of DNA damage induced upstream SAC factors in *Xenopus* egg extract, suggesting the convergence of this XCEP63 checkpoint pathway (Brown and Costanzo, 2009). Although, the common theory is that DSB DNA damage at kinetochore regions

activates the spindle assembly checkpoint, this study suggests an independence of SAC activation to the disruption of kinetochores. However, this was not verified and therefore there could be unattached kinetochores due to the disruption of spindle assembly by active ATM/ATR. These preliminary findings are in agreement with a study in yeast in which ATM/ATR activation of SAC was shown to be independent of kinetochores status (Kim and Burke, 2008). These findings collectively substantiate the link between DNA damage checkpoint and indirect SAC activation. Furthermore, the regulation of mitosis progression by ATM and ATR dependent CEP63 pathway may support repair of mitotic damaged DNA.

The possibility of DNA damage repair of mitotic chromatin remains undetermined and is either presumed unlikely or inefficient compared to that in S phase. The main consideration is that the mitotic DNA is highly condensed and therefore inaccessible to repair factors. However, a mechanism may exist in mitosis similar to that illustrated on heterochromatin where ATM locally relaxes DNA to allow repair processes to proceed (Goodarzi et al., 2008). In the event of damage, potentially ATM dependent signalling promotes remodelling and de-condensation of chromatin allowing the accessibility of DNA repair complexes to the site of damage. However, in the circumstances where there are higher levels of chromosome breakages or the presence of un-repaired DNA damage it is probable that sustained ATM and ATR checkpoint inactivation of spindle assembly may lead to mitotic catastrophe that prevents survival of cells with persistent DNA damage.

Importantly, these studies have substantiated further the link between centrosomes and genomic stability. The ATM/ATR CEP63 checkpoint pathway could sense and respond to double strand breaks (DSBs) and in turn might prevent genomic instability and the dangerous outcomes of the loss of genetic information. It is quite possible that ATM and ATR checkpoint control over XCEP63 regulation factor in spindle assembly could avoid the transference of these genomic defects to the next generation of cells. Potentially, such un-repaired lesions in mitosis could contribute to the development of cellular transformations. The conservation of CEP63 across species suggests that this DNA damage checkpoint response that inactivates spindle assembly may have retained its function through evolution.

In cancer cells, centrosomes are often altered in quantity, structure and/or defective in function. Such phenomena in cancer cells may be adopted to evade this ATM and ATR dependent CEP63 checkpoint pathway in response to damaged DNA. Cells with centrosome abnormalities may be impaired in this mitotic DNA damage checkpoint and consequently cells survive with damaged chromosomes, which could potentially jeopardise the genome. However, reports have described DNA damage activated pathways that result in the amplification of centrosomes, which in turn contribute to the elimination of cells with DNA damage (Hut *et al.,* 2003; Takada *et al.,* 2003). Centrosome supernumeracy is most likely attributed to centrosome or centriole fragmentation, which leads to the formation of multipolar spindles. In this situation normal cells are unable to undergo cytokenesis and do not survive. It is possible that this is an alternative mechanism of maintaining genomic stability in mitosis to that which we have described in this investigation.

A study undertaken by Buim *et al.,* describes a down-regulation of human CEP63 transcript in invasive bladder tumours (Buim *et al.,* 2005). These findings implicate CEP63 protein aberrancies in potentially contributing to tumorgenesis. Although not confirmed normal CEP63 functioning may prevent the genomic instability that is strongly associated with aggressive cancers. Individuals with congenital defects in CEP63 spindle assembly regulation pathways have not been identified as yet, it would be probable that they may suffer from brain developmental problems and would most likely be highly susceptibility to developing cancers. It is likely that the complete loss of CEP63 gene function would be lethal to embryos.

8.10   Future directions of XCEP63 research

In these studies we have made great progress in characterising XCEP63 and we have gained much understanding of XCEP63' role within the novel ATM and ATR dependent checkpoint inactivation of spindle assembly. However, there are still many aspects of XCEP63 that remain undefined and many questions that are unanswered, particularly in reference to the biochemical activities of XCEP63 pathway. In order to further understand XCEP63 role further, assays are required to dissect XCEP63 function at the centrosomes and how XCEP63 controls spindle assembly. It would be interesting to determine whether XCEP63 is localised to particular centrosomal

structure(s). Further studies are required to determine whether XCEP63 interacts with other factors, which may aid or inhibit XCEP63 function. More experiments are also needed in order to ascertain specifically the effects XCEP63 phosphorylation event on its function in regulating spindle assembly. Although there is some previous evidence to suggest that ATM and ATR, predominantly nuclear proteins are localised to centrosomes in mitosis, this process still remains quite unclear and requires further investigation into how ATM and ATR phosphorylates XCEP63. It is also important to establish the mechanism by which XCEP63 is delocalised away from centrosomes.

It is possible that as XCEP63 contains an SMC domain, that CEP63 may have alternative functions, which we have not found in this investigation. XCEP63 may also hold a role during interphase, perhaps with an involvement in interphase centrosome structural duplication or assembly. As many ATM and ATR checkpoint are not dependent on one substrate, it is very possible that there may be more targets of this novel ATM and ATR mitotic checkpoint. Although there has been one screening of cancers published that reveal irregularities in CEP63 expression, it is necessary to determine whether CEP63 is also deregulated in other cancer cells and whether their affect cell cycle progression is affected. For this purpose, commercially available antibody will soon be available, production which was provoked by the publication of these studies (Smith *et al.,* 2009).

References

Abraham, R.T. (2001) Cell cycle checkpoint signaling through the ATM and ATR kinases. Genes Dev 15, 2177-2196.

Abrieu, A., Brassac, T., Galas, S., Fisher, D., Labbe, J.C., and Doree, M. (1998) The Polo-like kinase Plx1 is a component of the MPF amplification loop at the G2/M-phase transition of the cell cycle in Xenopus eggs. J Cell Sci 111 (Pt 12), 1751-1757.

Adams, K.E., Medhurst, A.L., Dart, D.A., and Lakin, N.D. (2006) Recruitment of ATR to sites of ionising radiation-induced DNA damage requires ATM and components of the MRN protein complex. Oncogene 25, 3894-3904.

Agami, R., and Bernards, R. (2000) Distinct initiation and maintenance mechanisms cooperate to induce G1 cell cycle arrest in response to DNA damage. Cell 102, 55-66.

Alderton, G.K., Joenje, H., Varon, R., Borglum, A.D., Jeggo, P.A., and O'Driscoll, M. (2004) Seckel syndrome exhibits cellular features demonstrating defects in the ATR-signalling pathway. Hum Mol Genet 13, 3127-3138.

Andersen, J.S., Wilkinson, C.J., Mayor, T., Mortensen, P., Nigg, E.A., and Mann, M. (2003) Proteomic characterization of the human centrosome by protein correlation profiling. Nature 426, 570-574.

Anderson, C.W., Baum, P.R., and Gesteland, R.F. (1973) Processing of adenovirus 2-induced proteins. J Virol 12, 241-252.

Anderson, P., and Kedersha, N. (2002) Stressful initiations. J Cell Sci 115, 3227-3234.

Anderson, P., and Kedersha, N. (2009) RNA granules: post-transcriptional and epigenetic modulators of gene expression. Nat Rev Mol Cell Biol 10, 430-436.

Andreassen, P.R., Lohez, O.D., and Margolis, R.L. (2003) G2 and spindle assembly checkpoint adaptation, and tetraploidy arrest: implications for intrinsic and chemically induced genomic instability. Mutat Res 532, 245-253.

Araki, M., Wharton, R.P., Tang, Z., Yu, H., and Asano, M. (2003) Degradation of origin recognition complex large subunit by the anaphase-promoting complex in Drosophila. Embo J 22, 6115-6126.

Ashcroft, M., and Vousden, K.H. (1999) Regulation of p53 stability. Oncogene 18, 7637-7643.

Ausubel, F.M.B., R Kingston, R. E. Moore, D. D. Seidman, J. G. Smith, J. A. Struhl, K. . (1991) Current protocols in molecular biology. John Wiley and Sons Inc, New York.

Bailey, C.M., Abbott, D.E., Margaryan, N.V., Khalkhali-Ellis, Z., and Hendrix, M.J. (2008) Interferon regulatory factor 6 promotes cell cycle arrest and is regulated by the proteasome in a cell cycle-dependent manner. Mol Cell Biol 28, 2235-2243.

Bailey, C.M., and Hendrix, M.J. (2008) IRF6 in development and disease: a mediator of quiescence and differentiation. Cell Cycle 7, 1925-1930.

Bailey, C.M., Khalkhali-Ellis, Z., Kondo, S., Margaryan, N.V., Seftor, R.E., Wheaton, W.W., Amir, S., Pins, M.R., Schutte, B.C., and Hendrix, M.J. (2005) Mammary serine protease inhibitor (Maspin) binds directly to interferon regulatory factor 6: identification of a novel serpin partnership. J Biol Chem 280, 34210-34217.

Bakkenist, C.J., and Kastan, M.B. (2003) DNA damage activates ATM through intermolecular autophosphorylation and dimer dissociation. Nature 421, 499-506.

Baldino, F., Jr., Chesselet, M.F., and Lewis, M.E. (1989) High-resolution in situ hybridization histochemistry. Methods Enzymol 168, 761-777.

Banin, S., Moyal, L., Shieh, S., Taya, Y., Anderson, C.W., Chessa, L., Smorodinsky, N.I., Prives, C., Reiss, Y., Shiloh, Y., and Ziv, Y. (1998) Enhanced phosphorylation of p53 by ATM in response to DNA damage. Science 281, 1674-1677.

Barr, A.R., and Gergely, F. (2007) Aurora-A: the maker and breaker of spindle poles. J Cell Sci 120, 2987-2996.

Barr, F.A., and Gruneberg, U. (2007) Cytokinesis: placing and making the final cut. Cell 131, 847-860.

Barr, F.A., Sillje, H.H., and Nigg, E.A. (2004) Polo-like kinases and the orchestration of cell division. Nat Rev Mol Cell Biol 5, 429-440.

Bartolini, F., and Gundersen, G.G. (2006) Generation of noncentrosomal microtubule arrays. J Cell Sci 119, 4155-4163.

Basto, R., Brunk, K., Vinadogrova, T., Peel, N., Franz, A., Khodjakov, A., and Raff, J.W. (2008) Centrosome amplification can initiate tumorigenesis in flies. Cell 133, 1032-1042.

Beamish, H., Williams, R., Chen, P., and Lavin, M.F. (1996) Defect in multiple cell cycle checkpoints in ataxia-telangiectasia postirradiation. J Biol Chem 271, 20486-20493.

Bekker-Jensen, S., Lukas, C., Kitagawa, R., Melander, F., Kastan, M.B., Bartek, J., and Lukas, J. (2006) Spatial organization of the mammalian genome surveillance machinery in response to DNA strand breaks. J Cell Biol 173, 195-206.

Bell, S.P., and Dutta, A. (2002) DNA replication in eukaryotic cells. Annu Rev Biochem 71, 333-374.

Belmont, L.D., Hyman, A.A., Sawin, K.E., and Mitchison, T.J. (1990) Real-time visualization of cell cycle-dependent changes in microtubule dynamics in cytoplasmic extracts. Cell 62, 579-589.

Bischoff, F.R., Klebe, C., Kretschmer, J., Wittinghofer, A., and Ponstingl, H. (1994) RanGAP1 induces GTPase activity of nuclear Ras-related Ran. Proc Natl Acad Sci U S A 91, 2587-2591.

Bischoff, F.R., Krebber, H., Smirnova, E., Dong, W., and Ponstingl, H. (1995) Co-activation of RanGTPase and inhibition of GTP dissociation by Ran-GTP binding protein RanBP1. Embo J 14, 705-715.

Bischoff, F.R., and Ponstingl, H. (1991) Catalysis of guanine nucleotide exchange on Ran by the mitotic regulator RCC1. Nature 354, 80-82.

Bischoff, F.R., and Ponstingl, H. (1991) Mitotic regulator protein RCC1 is complexed with a nuclear ras-related polypeptide. Proc Natl Acad Sci U S A 88, 10830-10834.

Blangy, A., Arnaud, L., and Nigg, E.A. (1997) Phosphorylation by p34cdc2 protein kinase regulates binding of the kinesin-related motor HsEg5 to the dynactin subunit p150. J Biol Chem 272, 19418-19424.

Blasina, A., Price, B.D., Turenne, G.A., and McGowan, C.H. (1999) Caffeine inhibits the checkpoint kinase ATM. Curr Biol 9, 1135-1138.

Blow, J.J., Dilworth, S.M., Dingwall, C., Mills, A.D., and Laskey, R.A. (1987) Chromosome replication in cell-free systems from Xenopus eggs. Philos Trans R Soc Lond B Biol Sci 317, 483-494.

Blow, J.J., and Laskey, R.A. (1986) Initiation of DNA replication in nuclei and purified DNA by a cell-free extract of Xenopus eggs. Cell 47, 577-587.

Blow, J.J., and Laskey, R.A. (1988) A role for the nuclear envelope in controlling DNA replication within the cell cycle. Nature 332, 546-548.

Bork, P., Hofmann, K., Bucher, P., Neuwald, A.F., Altschul, S.F., and Koonin, E.V. (1997) A superfamily of conserved domains in DNA damage-responsive cell cycle checkpoint proteins. Faseb J 11, 68-76.

Bouchard, C., Thieke, K., Maier, A., Saffrich, R., Hanley-Hyde, J., Ansorge, W., Reed, S., Sicinski, P., Bartek, J., and Eilers, M. (1999) Direct induction of cyclin D2 by Myc contributes to cell cycle progression and sequestration of p27. Embo J 18, 5321-5333.

Bourke, E., Dodson, H., Merdes, A., Cuffe, L., Zachos, G., Walker, M., Gillespie, D., and Morrison, C.G. (2007) DNA damage induces Chk1-dependent centrosome amplification. EMBO Rep 8, 603-609.

Branzei, D., and Foiani, M. (2005) The DNA damage response during DNA replication. Curr Opin Cell Biol 17, 568-575.

Broderick, R., and Nasheuer, H.P. (2009) Regulation of Cdc45 in the cell cycle and after DNA damage. Biochem Soc Trans 37, 926-930.

Brown, E.J., and Baltimore, D. (2000) ATR disruption leads to chromosomal fragmentation and early embryonic lethality. Genes Dev 14, 397-402.

Brown, N., and Costanzo, V. (2009) An ATM and ATR dependent pathway targeting centrosome dependent spindle assembly. Cell Cycle 8, 1997-2001.

Budde, P.P., Kumagai, A., Dunphy, W.G., and Heald, R. (2001) Regulation of Op18 during spindle assembly in Xenopus egg extracts. J Cell Biol 153, 149-158.

Buim, M.E., Soares, F.A., Sarkis, A.S., and Nagai, M.A. (2005) The transcripts of SFRP1,CEP63 and EIF4G2 genes are frequently downregulated in transitional cell carcinomas of the bladder. Oncology 69, 445-454.

Bunz, F., Dutriaux, A., Lengauer, C., Waldman, T., Zhou, S., Brown, J.P., Sedivy, J.M., Kinzler, K.W., and Vogelstein, B. (1998) Requirement for p53 and p21 to sustain G2 arrest after DNA damage. Science 282, 1497-1501.

Cahill, D.P., Lengauer, C., Yu, J., Riggins, G.J., Willson, J.K., Markowitz, S.D., Kinzler, K.W., and Vogelstein, B. (1998) Mutations of mitotic checkpoint genes in human cancers. Nature 392, 300-303.

Canman, C.E., Lim, D.S., Cimprich, K.A., Taya, Y., Tamai, K., Sakaguchi, K., Appella, E., Kastan, M.B., and Siliciano, J.D. (1998) Activation of the ATM kinase by ionizing radiation and phosphorylation of p53. Science 281, 1677-1679.

Capasso, H., Palermo, C., Wan, S., Rao, H., John, U.P., O'Connell, M.J., and Walworth, N.C. (2002) Phosphorylation activates Chk1 and is required for checkpoint-mediated cell cycle arrest. J Cell Sci 115, 4555-4564.

Carazo-Salas, R.E., Gruss, O.J., Mattaj, I.W., and Karsenti, E. (2001) Ran-GTP coordinates regulation of microtubule nucleation and dynamics during mitotic-spindle assembly. Nat Cell Biol 3, 228-234.

Carazo-Salas, R.E., Guarguaglini, G., Gruss, O.J., Segref, A., Karsenti, E., and Mattaj, I.W. (1999) Generation of GTP-bound Ran by RCC1 is required for chromatin-induced mitotic spindle formation. Nature 400, 178-181.

Carlson, J.G. (1950) Effects of radiation on mitosis. J Cell Physiol Suppl 35, 89-101.

Casenghi, M., Meraldi, P., Weinhart, U., Duncan, P.I., Korner, R., and Nigg, E.A. (2003) Polo-like kinase 1 regulates Nlp, a centrosome protein involved in microtubule nucleation. Dev Cell 5, 113-125.

Cazales, M., Schmitt, E., Montembault, E., Dozier, C., Prigent, C., and Ducommun, B. (2005) CDC25B phosphorylation by Aurora-A occurs at the G2/M transition and is inhibited by DNA damage. Cell Cycle 4, 1233-1238.

Celeste, A., Fernandez-Capetillo, O., Kruhlak, M.J., Pilch, D.R., Staudt, D.W., Lee, A., Bonner, R.F., Bonner, W.M., and Nussenzweig, A. (2003) Histone H2AX phosphorylation is dispensable for the initial recognition of DNA breaks. Nat Cell Biol 5, 675-679.

Cha, R.S., and Kleckner, N. (2002) ATR homolog Mec1 promotes fork progression, thus averting breaks in replication slow zones. Science 297, 602-606.

Chan, T.A., Hermeking, H., Lengauer, C., Kinzler, K.W., and Vogelstein, B. (1999) 14-3-3Sigma is required to prevent mitotic catastrophe after DNA damage. Nature 401, 616-620.

Chaturvedi, P., Eng, W.K., Zhu, Y., Mattern, M.R., Mishra, R., Hurle, M.R., Zhang, X., Annan, R.S., Lu, Q., Faucette, L.F., Scott, G.F., Li, X., Carr, S.A., Johnson, R.K., Winkler, J.D., and Zhou, B.B. (1999) Mammalian Chk2 is a downstream effector of the ATM-dependent DNA damage checkpoint pathway. Oncogene 18, 4047-4054.

Cheeseman, I.M., and Desai, A. (2008) Molecular architecture of the kinetochore-microtubule interface. Nat Rev Mol Cell Biol 9, 33-46.

Chi, Y.H., and Jeang, K.T. (2007) Aneuploidy and cancer. J Cell Biochem 102, 531-538.

Choi, E., and Lee, H. (2008) Chromosome damage in mitosis induces BubR1 activation and prometaphase arrest. FEBS Lett 582, 1700-1706.

Chow, J.P., Siu, W.Y., Fung, T.K., Chan, W.M., Lau, A., Arooz, T., Ng, C.P., Yamashita, K., and Poon, R.Y. (2003) DNA damage during the spindle-assembly checkpoint degrades CDC25A, inhibits cyclin-CDC2 complexes, and reverses cells to interphase. Mol Biol Cell 14, 3989-4002.

Ciciarello, M., Mangiacasale, R., and Lavia, P. (2007) Spatial control of mitosis by the GTPase Ran. Cell Mol Life Sci 64, 1891-1914.

Cimprich, K.A., and Cortez, D. (2008) ATR: an essential regulator of genome integrity. Nat Rev Mol Cell Biol 9, 616-627.

Cimprich, K.A., Shin, T.B., Keith, C.T., and Schreiber, S.L. (1996) cDNA cloning and gene mapping of a candidate human cell cycle checkpoint protein. Proc Natl Acad Sci U S A 93, 2850-2855.

Cliby, W.A., Lewis, K.A., Lilly, K.K., and Kaufmann, S.H. (2002) S phase and G2 arrests induced by topoisomerase I poisons are dependent on ATR kinase function. J Biol Chem 277, 1599-1606.

Compton, D.A. (1998) Focusing on spindle poles. J Cell Sci 111 (Pt 11), 1477-1481.

Cortez, D., Guntuku, S., Qin, J., and Elledge, S.J. (2001) ATR and ATRIP: partners in checkpoint signaling. Science 294, 1713-1716.

Cortez, D., Wang, Y., Qin, J., and Elledge, S.J. (1999) Requirement of ATM-dependent phosphorylation of brca1 in the DNA damage response to double-strand breaks. Science 286, 1162-1166.

Costanzo, V., Paull, T., Gottesman, M., and Gautier, J. (2004) Mre11 assembles linear DNA fragments into DNA damage signaling complexes. PLoS Biol 2, E110.

Costanzo, V., Robertson, K., Bibikova, M., Kim, E., Grieco, D., Gottesman, M., Carroll, D., and Gautier, J. (2001) Mre11 protein complex prevents double-strand break accumulation during chromosomal DNA replication. Mol Cell 8, 137-147.

Costanzo, V., Robertson, K., and Gautier, J. (2004) Xenopus cell-free extracts to study the DNA damage response. Methods Mol Biol 280, 213-227.

Costanzo, V., Robertson, K., Ying, C.Y., Kim, E., Avvedimento, E., Gottesman, M., Grieco, D., and Gautier, J. (2000) Reconstitution of an ATM-dependent checkpoint that inhibits chromosomal DNA replication following DNA damage. Mol Cell 6, 649-659.

Costanzo, V., Shechter, D., Lupardus, P.J., Cimprich, K.A., Gottesman, M., and Gautier, J. (2003) An ATR- and Cdc7-dependent DNA damage checkpoint that inhibits initiation of DNA replication. Mol Cell 11, 203-213.

Cox, D.M., Zhong, F., Du, M., Duchoslav, E., Sakuma, T., and McDermott, J.C. (2005) Multiple reaction monitoring as a method for identifying protein posttranslational modifications. J Biomol Tech 16, 83-90.

Crasta, K., Huang, P., Morgan, G., Winey, M., and Surana, U. (2006) Cdk1 regulates centrosome separation by restraining proteolysis of microtubule-associated proteins. Embo J 25, 2551-2563.

Crasta, K., and Surana, U. (2006) Disjunction of conjoined twins: Cdk1, Cdh1 and separation of centrosomes. Cell Div 1, 12.

Cuadrado, M., Martinez-Pastor, B., Murga, M., Toledo, L.I., Gutierrez-Martinez, P., Lopez, E., and Fernandez-Capetillo, O. (2006) ATM regulates ATR chromatin loading in response to DNA double-strand breaks. J Exp Med 203, 297-303.

Damelin, M., and Bestor, T.H. (2007) The decatenation checkpoint. Br J Cancer 96, 201-205.

Dasso, M., and Newport, J.W. (1990) Completion of DNA replication is monitored by a feedback system that controls the initiation of mitosis in vitro: studies in Xenopus. Cell 61, 811-823.

Deckbar, D., Birraux, J., Krempler, A., Tchouandong, L., Beucher, A., Walker, S., Stiff, T., Jeggo, P., and Lobrich, M. (2007) Chromosome breakage after G2 checkpoint release. J Cell Biol 176, 749-755.

den Elzen, N., and Pines, J. (2001) Cyclin A is destroyed in prometaphase and can delay chromosome alignment and anaphase. J Cell Biol 153, 121-136.

Desai, A., and Mitchison, T.J. (1997) Microtubule polymerization dynamics. Annu Rev Cell Dev Biol 13, 83-117.

Desai, A., Murray, A., Mitchison, T.J., and Walczak, C.E. (1999) The use of Xenopus egg extracts to study mitotic spindle assembly and function in vitro. Methods Cell Biol 61, 385-412.

Dewar, H., Tanaka, K., Nasmyth, K., and Tanaka, T.U. (2004) Tension between two kinetochores suffices for their bi-orientation on the mitotic spindle. Nature 428, 93-97.

Diehl, J.A., Cheng, M., Roussel, M.F., and Sherr, C.J. (1998) Glycogen synthase kinase-3beta regulates cyclin D1 proteolysis and subcellular localization. Genes Dev 12, 3499-3511.

Diehl, J.A., Zindy, F., and Sherr, C.J. (1997) Inhibition of cyclin D1 phosphorylation on threonine-286 prevents its rapid degradation via the ubiquitin-proteasome pathway. Genes Dev 11, 957-972.

do Carmo Avides, M., Tavares, A., and Glover, D.M. (2001) Polo kinase and Asp are needed to promote the mitotic organizing activity of centrosomes. Nat Cell Biol 3, 421-424.

Dodson, H., Bourke, E., Jeffers, L.J., Vagnarelli, P., Sonoda, E., Takeda, S., Earnshaw, W.C., Merdes, A., and Morrison, C. (2004) Centrosome amplification induced by DNA damage occurs during a prolonged G2 phase and involves ATM. Embo J 23, 3864-3873.

Dowdy, S.F., Hinds, P.W., Louie, K., Reed, S.I., Arnold, A., and Weinberg, R.A. (1993) Physical interaction of the retinoblastoma protein with human D cyclins. Cell 73, 499-511.

Doxsey, S., McCollum, D., and Theurkauf, W. (2005) Centrosomes in cellular regulation. Annu Rev Cell Dev Biol 21, 411-434.

Doxsey, S.J. (2001) Centrosomes as command centres for cellular control. Nat Cell Biol 3, E105-108.

Doxsey, S.J., Stein, P., Evans, L., Calarco, P.D., and Kirschner, M. (1994) Pericentrin, a highly conserved centrosome protein involved in microtubule organization. Cell 76, 639-650.

Dunphy, W.G. (1994) The decision to enter mitosis. Trends Cell Biol 4, 202-207.

Dynlacht, B.D., Flores, O., Lees, J.A., and Harlow, E. (1994) Differential regulation of E2F transactivation by cyclin/cdk2 complexes. Genes Dev 8, 1772-1786.

Dynlacht, B.D., Moberg, K., Lees, J.A., Harlow, E., and Zhu, L. (1997) Specific regulation of E2F family members by cyclin-dependent kinases. Mol Cell Biol 17, 3867-3875.

Edwards, R.J., Bentley, N.J., and Carr, A.M. (1999) A Rad3-Rad26 complex responds to DNA damage independently of other checkpoint proteins. Nat Cell Biol 1, 393-398.

Ekholm, S.V., and Reed, S.I. (2000) Regulation of G(1) cyclin-dependent kinases in the mammalian cell cycle. Curr Opin Cell Biol 12, 676-684.

Evans, L., Mitchison, T., and Kirschner, M. (1985) Influence of the centrosome on the structure of nucleated microtubules. J Cell Biol 100, 1185-1191.

Ewen, M.E., Sluss, H.K., Sherr, C.J., Matsushime, H., Kato, J., and Livingston, D.M. (1993) Functional interactions of the retinoblastoma protein with mammalian D-type cyclins. Cell 73, 487-497.

Falck, J., Mailand, N., Syljuasen, R.G., Bartek, J., and Lukas, J. (2001) The ATM-Chk2-Cdc25A checkpoint pathway guards against radioresistant DNA synthesis. Nature 410, 842-847.

Fang, G., Yu, H., and Kirschner, M.W. (1998) Direct binding of CDC20 protein family members activates the anaphase-promoting complex in mitosis and G1. Mol Cell 2, 163-171.

Fang, Y., Liu, T., Wang, X., Yang, Y.M., Deng, H., Kunicki, J., Traganos, F., Darzynkiewicz, Z., Lu, L., and Dai, W. (2006) BubR1 is involved in regulation of DNA damage responses. Oncogene 25, 3598-3605.

Feng, Y., Hodge, D.R., Palmieri, G., Chase, D.L., Longo, D.L., and Ferris, D.K. (1999) Association of polo-like kinase with alpha-, beta- and gamma-tubulins in a stable complex. Biochem J 339 (Pt 2), 435-442.

Fesquet, D., Labbe, J.C., Derancourt, J., Capony, J.P., Galas, S., Girard, F., Lorca, T., Shuttleworth, J., Doree, M., and Cavadore, J.C. (1993) The MO15 gene encodes the catalytic subunit of a protein kinase that activates cdc2 and other cyclin-dependent kinases (CDKs) through phosphorylation of Thr161 and its homologues. Embo J 12, 3111-3121.

Fisher, R.P., and Morgan, D.O. (1994) A novel cyclin associates with MO15/CDK7 to form the CDK-activating kinase. Cell 78, 713-724.

Fornace, A.J., Jr., and Little, J.B. (1980) Normal repair of DNA single-strand breaks in patients with ataxia telangiectasia. Biochim Biophys Acta 607, 432-437.

Frappart, P. O., and McKinnon, P. J. (2006) Ataxia-telangiectasia and related diseases. Neuromolecular Med 8, 95-511.

Fourest-Lieuvin, A., Peris, L., Gache, V., Garcia-Saez, I., Juillan-Binard, C., Lantez, V., and Job, D. (2006) Microtubule regulation in mitosis: tubulin phosphorylation by the cyclin-dependent kinase Cdk1. Mol Biol Cell 17, 1041-1050.

Friedel, A.M., Pike, B.L., and Gasser, S.M. (2009) ATR/Mec1: coordinating fork stability and repair. Curr Opin Cell Biol 21, 237-244.

Fukasawa, K. (2007) Oncogenes and tumour suppressors take on centrosomes. Nat Rev Cancer 7, 911-924.

Gadde, S., and Heald, R. (2004) Mechanisms and molecules of the mitotic spindle. Curr Biol 14, R797-805.

Garber, P.M., and Rine, J. (2002) Overlapping roles of the spindle assembly and DNA damage checkpoints in the cell-cycle response to altered chromosomes in Saccharomyces cerevisiae. Genetics 161, 521-534.

Garner, E., and Costanzo, V. (2009) Studying the DNA damage response using in vitro model systems. DNA Repair (Amst) 8, 1025-1037.

Gascoigne, K.E., and Taylor, S.S. (2008) Cancer cells display profound intra- and interline variation following prolonged exposure to antimitotic drugs. Cancer Cell 14, 111-122.

Gautier, J., Minshull, J., Lohka, M., Glotzer, M., Hunt, T., and Maller, J.L. (1990) Cyclin is a component of maturation-promoting factor from Xenopus. Cell 60, 487-494.

Geley, S., Kramer, E., Gieffers, C., Gannon, J., Peters, J.M., and Hunt, T. (2001) Anaphase-promoting complex/cyclosome-dependent proteolysis of human cyclin A starts at the beginning of mitosis and is not subject to the spindle assembly checkpoint. J Cell Biol 153, 137-148.

Girard, F., Strausfeld, U., Fernandez, A., and Lamb, N.J. (1991) Cyclin A is required for the onset of DNA replication in mammalian fibroblasts. Cell 67, 1169-1179.

Glotzer, M., Murray, A.W., and Kirschner, M.W. (1991) Cyclin is degraded by the ubiquitin pathway. Nature 349, 132-138.

Golan, A., Yudkovsky, Y., and Hershko, A. (2002) The cyclin-ubiquitin ligase activity of cyclosome/APC is jointly activated by protein kinases Cdk1-cyclin B and Plk. J Biol Chem 277, 15552-15557.

Golsteyn, R.M., Mundt, K.E., Fry, A.M., and Nigg, E.A. (1995) Cell cycle regulation of the activity and subcellular localization of Plk1, a human protein kinase implicated in mitotic spindle function. J Cell Biol 129, 1617-1628.

Goodarzi, A.A., Noon, A.T., Deckbar, D., Ziv, Y., Shiloh, Y., Lobrich, M., and Jeggo, P.A. (2008) ATM signaling facilitates repair of DNA double-strand breaks associated with heterochromatin. Mol Cell 31, 167-177.

Gottlieb, T.M., and Jackson, S.P. (1993) The DNA-dependent protein kinase: requirement for DNA ends and association with Ku antigen. Cell 72, 131-142.

Gould, K.L., and Nurse, P. (1989) Tyrosine phosphorylation of the fission yeast cdc2+ protein kinase regulates entry into mitosis. Nature 342, 39-45.

Grandi, P., Eltsov, M., Nielsen, I., and Raska, I. (2001) DNA double-strand breaks induce formation of RP-A/Ku foci on in vitro reconstituted Xenopus sperm nuclei. J Cell Sci 114, 3345-3357.

Gregson, H.C., Schmiesing, J.A., Kim, J.S., Kobayashi, T., Zhou, S., and Yokomori, K. (2001) A potential role for human cohesin in mitotic spindle aster assembly. J Biol Chem 276, 47575-47582.

Griffith, E., Walker, S., Martin, C.A., Vagnarelli, P., Stiff, T., Vernay, B., Al Sanna, N., Saggar, A., Hamel, B., Earnshaw, W.C., Jeggo, P.A., Jackson, A.P., and O'Driscoll, M. (2008) Mutations in pericentrin cause Seckel syndrome with defective ATR-dependent DNA damage signaling. Nat Genet 40, 232-236.

Grill, B., Wilson, G.M., Zhang, K.X., Wang, B., Doyonnas, R., Quadroni, M., and Schrader, J.W. (2004) Activation/division of lymphocytes results in increased levels of cytoplasmic activation/proliferation-associated protein-1: prototype of a new family of proteins. J Immunol 172, 2389-2400.

Gruss, O.J., Carazo-Salas, R.E., Schatz, C.A., Guarguaglini, G., Kast, J., Wilm, M., Le Bot, N., Vernos, I., Karsenti, E., and Mattaj, I.W. (2001) Ran induces spindle assembly by reversing the inhibitory effect of importin alpha on TPX2 activity. Cell 104, 83-93.

Guan, J., Ekwurtzel, E., Kvist, U., and Yuan, L. (2008) Cohesin protein SMC1 is a centrosomal protein. Biochem Biophys Res Commun 372, 761-764.

Guertin, D.A., Trautmann, S., and McCollum, D. (2002) Cytokinesis in eukaryotes. Microbiol Mol Biol Rev 66, 155-178.

Guo, Y., Harwalkar, J., Stacey, D.W., and Hitomi, M. (2005) Destabilization of cyclin D1 message plays a critical role in cell cycle exit upon mitogen withdrawal. Oncogene 24, 1032-1042.

Guo, Z., and Dunphy, W.G. (2000) Response of Xenopus Cds1 in cell-free extracts to DNA templates with double-stranded ends. Mol Biol Cell 11, 1535-1546.

Guo, Z., Kumagai, A., Wang, S.X., and Dunphy, W.G. (2000) Requirement for Atr in phosphorylation of Chk1 and cell cycle regulation in response to DNA replication blocks and UV-damaged DNA in Xenopus egg extracts. Genes Dev 14, 2745-2756.

Haber, J.E. (2000) Partners and pathwaysrepairing a double-strand break. Trends Genet 16, 259-264.

Haering, C.H., and Nasmyth, K. (2003) Building and breaking bridges between sister chromatids. Bioessays 25, 1178-1191.

Hagting, A., Den Elzen, N., Vodermaier, H.C., Waizenegger, I.C., Peters, J.M., and Pines, J. (2002) Human securin proteolysis is controlled by the spindle checkpoint and reveals when the APC/C switches from activation by Cdc20 to Cdh1. J Cell Biol 157, 1125-1137.

Hagting, A., Jackman, M., Simpson, K., and Pines, J. (1999) Translocation of cyclin B1 to the nucleus at prophase requires a phosphorylation-dependent nuclear import signal. Curr Biol 9, 680-689.

Harbour, J.W., and Dean, D.C. (2000) The Rb/E2F pathway: expanding roles and emerging paradigms. Genes Dev 14, 2393-2409.

Harlow, E.L., D. (1988) Antibodies: A Laboratory Manual Cold Spring Harbor Laboratory Press, New York.

Harper, J.W., Adami, G.R., Wei, N., Keyomarsi, K., and Elledge, S.J. (1993) The p21 Cdk-interacting protein Cip1 is a potent inhibitor of G1 cyclin-dependent kinases. Cell 75, 805-816.

Hartwell, L.H., and Weinert, T.A. (1989) Checkpoints: controls that ensure the order of cell cycle events. Science 246, 629-634.

Harvey, S.H., Sheedy, D.M., Cuddihy, A.R., and O'Connell, M.J. (2004) Coordination of DNA damage responses via the Smc5/Smc6 complex. Mol Cell Biol 24, 662-674.

Hauf, S., Cole, R.W., LaTerra, S., Zimmer, C., Schnapp, G., Walter, R., Heckel, A., van Meel, J., Rieder, C.L., and Peters, J.M. (2003) The small molecule Hesperadin reveals a role for Aurora B in correcting kinetochore-microtubule attachment and in maintaining the spindle assembly checkpoint. J Cell Biol 161, 281-294.

Hauf, S., Waizenegger, I.C., and Peters, J.M. (2001) Cohesin cleavage by separase required for anaphase and cytokinesis in human cells. Science 293, 1320-1323.

Hayden, J.H., Bowser, S.S., and Rieder, C.L. (1990) Kinetochores capture astral microtubules during chromosome attachment to the mitotic spindle: direct visualization in live newt lung cells. J Cell Biol 111, 1039-1045.

Heald, R., Tournebize, R., Blank, T., Sandaltzopoulos, R., Becker, P., Hyman, A., and Karsenti, E. (1996) Self-organization of microtubules into bipolar spindles around artificial chromosomes in Xenopus egg extracts. Nature 382, 420-425.

Heald, R., Tournebize, R., Habermann, A., Karsenti, E., and Hyman, A. (1997) Spindle assembly in Xenopus egg extracts: respective roles of centrosomes and microtubule self-organization. J Cell Biol 138, 615-628.

Heald, R., and Walczak, C.E. (1999) Microtubule-based motor function in mitosis. Curr Opin Struct Biol 9, 268-274.

Heffernan, T.P., Simpson, D.A., Frank, A.R., Heinloth, A.N., Paules, R.S., Cordeiro-Stone, M., and Kaufmann, W.K. (2002) An ATR- and Chk1-dependent S checkpoint inhibits replicon initiation following UVC-induced DNA damage. Mol Cell Biol 22, 8552-8561.

Hekmat-Nejad, M., You, Z., Yee, M.C., Newport, J.W., and Cimprich, K.A. (2000) Xenopus ATR is a replication-dependent chromatin-binding protein required for the DNA replication checkpoint. Curr Biol 10, 1565-1573.

Hetzer, M., Gruss, O.J., and Mattaj, I.W. (2002) The Ran GTPase as a marker of chromosome position in spindle formation and nuclear envelope assembly. Nat Cell Biol 4, E177-184.

Hickson, I., Zhao, Y., Richardson, C.J., Green, S.J., Martin, N.M., Orr, A.I., Reaper, P.M., Jackson, S.P., Curtin, N.J., and Smith, G.C. (2004) Identification and characterization of a novel and specific inhibitor of the ataxia-telangiectasia mutated kinase ATM. Cancer Res 64, 9152-9159.

Hinchcliffe, E.H., and Sluder, G. (2001) "It takes two to tango": understanding how centrosome duplication is regulated throughout the cell cycle. Genes Dev 15, 1167-1181.

Hirano, T. (2005) SMC proteins and chromosome mechanics: from bacteria to humans. Philos Trans R Soc Lond B Biol Sci 360, 507-514.

Hirano, T. (2005) Condensins: organizing and segregating the genome. Curr Biol 15, R265-275.

Hirao, A., Kong, Y.Y., Matsuoka, S., Wakeham, A., Ruland, J., Yoshida, H., Liu, D., Elledge, S.J., and Mak, T.W. (2000) DNA damage-induced activation of p53 by the checkpoint kinase Chk2. Science 287, 1824-1827.

Hitomi, M., Yang, K., Stacey, A.W., and Stacey, D.W. (2008) Phosphorylation of cyclin D1 regulated by ATM or ATR controls cell cycle progression. Mol Cell Biol 28, 5478-5493.

Hoffmann, I., Clarke, P.R., Marcote, M.J., Karsenti, E., and Draetta, G. (1993) Phosphorylation and activation of human cdc25-C by cdc2--cyclin B and its involvement in the self-amplification of MPF at mitosis. Embo J 12, 53-63.

Howell, B.J., McEwen, B.F., Canman, J.C., Hoffman, D.B., Farrar, E.M., Rieder, C.L., and Salmon, E.D. (2001) Cytoplasmic dynein/dynactin drives kinetochore protein transport to the spindle poles and has a role in mitotic spindle checkpoint inactivation. J Cell Biol 155, 1159-1172.

Hoyt, M.A., Totis, L., and Roberts, B.T. (1991) S. cerevisiae genes required for cell cycle arrest in response to loss of microtubule function. Cell 66, 507-517.

Hsu, L.C., and White, R.L. (1998) BRCA1 is associated with the centrosome during mitosis. Proc Natl Acad Sci U S A 95, 12983-12988.

Huang, X., Tran, T., Zhang, L., Hatcher, R., and Zhang, P. (2005) DNA damage-induced mitotic catastrophe is mediated by the Chk1-dependent mitotic exit DNA damage checkpoint. Proc Natl Acad Sci U S A 102, 1065-1070.

Hurley, P.J., and Bunz, F. (2007) ATM and ATR: components of an integrated circuit. Cell Cycle 6, 414-417.

Hut, H.M., Lemstra, W., Blaauw, E.H., Van Cappellen, G.W., Kampinga, H.H., and Sibon, O.C. (2003) Centrosomes split in the presence of impaired DNA integrity during mitosis. Mol Biol Cell 14, 1993-2004.

Izumi, T., and Maller, J.L. (1993) Elimination of cdc2 phosphorylation sites in the cdc25 phosphatase blocks initiation of M-phase. Mol Biol Cell 4, 1337-1350.

Jackman, M., Lindon, C., Nigg, E.A., and Pines, J. (2003) Active cyclin B1-Cdk1 first appears on centrosomes in prophase. Nat Cell Biol 5, 143-148.

Jang, Y.J., Ji, J.H., Choi, Y.C., Ryu, C.J., and Ko, S.Y. (2007) Regulation of Polo-like kinase 1 by DNA damage in mitosis. Inhibition of mitotic PLK-1 by protein phosphatase 2A. J Biol Chem 282, 2473-2482.

Jason, J.M., and Gelfand, E.W. (1979) Diagnostic considerations in ataxia-telangiectasia. Arch Dis Child 54, 682-686.

Jazayeri, A., Falck, J., Lukas, C., Bartek, J., Smith, G.C., Lukas, J., and Jackson, S.P. (2006) ATM- and cell cycle-dependent regulation of ATR in response to DNA double-strand breaks. Nat Cell Biol 8, 37-45.

Jin, P., Gu, Y., and Morgan, D.O. (1996) Role of inhibitory CDC2 phosphorylation in radiation-induced G2 arrest in human cells. J Cell Biol 134, 963-970.

Job, D., Valiron, O., and Oakley, B. (2003) Microtubule nucleation. Curr Opin Cell Biol 15, 111-117.

Jones, R.E., Chapman, J.R., Puligilla, C., Murray, J.M., Car, A.M., Ford, C.C., and Lindsay, H.D. (2003) XRad17 is required for the activation of XChk1 but not XCds1 during checkpoint signaling in Xenopus. Mol Biol Cell 14, 3898-3910.

Jordan, M.A., Thrower, D., and Wilson, L. (1992) Effects of vinblastine, podophyllotoxin and nocodazole on mitotic spindles. Implications for the role of microtubule dynamics in mitosis. J Cell Sci 102 (Pt 3), 401-416.

Kais, Z., and Parvin, J.D. (2008) Regulation of centrosomes by the BRCA1-dependent ubiquitin ligase. Cancer Biol Ther 7, 1540-1543.

Kalab, P., Weis, K., and Heald, R. (2002) Visualization of a Ran-GTP gradient in interphase and mitotic Xenopus egg extracts. Science 295, 2452-2456.

Kamiya, A., Kubo, K., Tomoda, T., Takaki, M., Youn, R., Ozeki, Y., Sawamura, N., Park, U., Kudo, C., Okawa, M., Ross, C.A., Hatten, M.E., Nakajima, K., and Sawa, A. (2005) A schizophrenia-associated mutation of DISC1 perturbs cerebral cortex development. Nat Cell Biol 7, 1167-1178.

Kapoor, T.M., Lampson, M.A., Hergert, P., Cameron, L., Cimini, D., Salmon, E.D., McEwen, B.F., and Khodjakov, A. (2006) Chromosomes can congress to the metaphase plate before biorientation. Science 311, 388-391.

Kapust, R.B., and Waugh, D.S. (1999) Escherichia coli maltose-binding protein is uncommonly effective at promoting the solubility of polypeptides to which it is fused. Protein Sci 8, 1668-1674.

Karsenti, E., and Vernos, I. (2001) The mitotic spindle: a self-made machine. Science 294, 543-547.

Kastan, M.B., and Bartek, J. (2004) Cell-cycle checkpoints and cancer. Nature 432, 316-323.

Kastan, M.B., Zhan, Q., el-Deiry, W.S., Carrier, F., Jacks, T., Walsh, W.V., Plunkett, B.S., Vogelstein, B., and Fornace, A.J., Jr. (1992) A mammalian cell cycle checkpoint pathway utilizing p53 and GADD45 is defective in ataxia-telangiectasia. Cell 71, 587-597.

Khodjakov, A., Cole, R.W., Oakley, B.R., and Rieder, C.L. (2000) Centrosome-independent mitotic spindle formation in vertebrates. Curr Biol 10, 59-67.

Khodjakov, A., and Rieder, C.L. (2001) Centrosomes enhance the fidelity of cytokinesis in vertebrates and are required for cell cycle progression. J Cell Biol 153, 237-242.

Kim, E.M., and Burke, D.J. (2008) DNA damage activates the SAC in an ATM/ATR-dependent manner, independently of the kinetochore. PLoS Genet 4, e1000015.

Kim, S.T., Lim, D.S., Canman, C.E., and Kastan, M.B. (1999) Substrate specificities and identification of putative substrates of ATM kinase family members. J Biol Chem 274, 37538-37543.

Kim, S.T., Xu, B., and Kastan, M.B. (2002) Involvement of the cohesin protein, Smc1, in Atm-dependent and independent responses to DNA damage. Genes Dev 16, 560-570.

King, J.M., Hays, T.S., and Nicklas, R.B. (2000) Dynein is a transient kinetochore component whose binding is regulated by microtubule attachment, not tension. J Cell Biol 151, 739-748.

King, R.W., Deshaies, R.J., Peters, J.M., and Kirschner, M.W. (1996) How proteolysis drives the cell cycle. Science 274, 1652-1659.

Kitagawa, R., Bakkenist, C.J., McKinnon, P.J., and Kastan, M.B. (2004) Phosphorylation of SMC1 is a critical downstream event in the ATM-NBS1-BRCA1 pathway. Genes Dev 18, 1423-1438.

Kobayashi, H., Stewart, E., Poon, R., Adamczewski, J.P., Gannon, J., and Hunt, T. (1992) Identification of the domains in cyclin A required for binding to, and activation of, p34cdc2 and p32cdk2 protein kinase subunits. Mol Biol Cell 3, 1279-1294.

Koff, A., Cross, F., Fisher, A., Schumacher, J., Leguellec, K., Philippe, M., and Roberts, J.M. (1991) Human cyclin E, a new cyclin that interacts with two members of the CDC2 gene family. Cell 66, 1217-1228.

Koff, A., Giordano, A., Desai, D., Yamashita, K., Harper, J.W., Elledge, S., Nishimoto, T., Morgan, D.O., Franza, B.R., and Roberts, J.M. (1992) Formation and activation of a cyclin E-cdk2 complex during the G1 phase of the human cell cycle. Science 257, 1689-1694.

Kojis, T.L., Gatti, R.A., and Sparkes, R.S. (1991) The cytogenetics of ataxia telangiectasia. Cancer Genet Cytogenet 56, 143-156.

Kondo, S., Schutte, B.C., Richardson, R.J., Bjork, B.C., Knight, A.S., Watanabe, Y., Howard, E., de Lima, R.L., Daack-Hirsch, S., Sander, A., McDonald-McGinn, D.M., Zackai, E.H., Lammer, E.J., Aylsworth, A.S., Ardinger, H.H., Lidral, A.C., Pober, B.R., Moreno, L., Arcos-Burgos, M., Valencia, C., Houdayer, C., Bahuau, M., Moretti-Ferreira, D., Richieri-Costa, A., Dixon, M.J., and Murray, J.C. (2002) Mutations in IRF6 cause Van der Woude and popliteal pterygium syndromes. Nat Genet 32, 285-289.

Kong, X., Ball, A.R., Sonoda, E., Feng, J., Takeda, S., Fukagawa, T., Yen, T.J., and Yokomori, K. (2009) Cohesin Associates with Spindle Poles in a Mitosis-specific Manner and Functions in Spindle Assembly in Vertebrate Cells. Mol Biol Cell 20, 1289-1301.

Kops, G.J., Weaver, B.A., and Cleveland, D.W. (2005) On the road to cancer: aneuploidy and the mitotic checkpoint. Nat Rev Cancer 5, 773-785.

Kraft, C., Herzog, F., Gieffers, C., Mechtler, K., Hagting, A., Pines, J., and Peters, J.M. (2003) Mitotic regulation of the human anaphase-promoting complex by phosphorylation. Embo J 22, 6598-6609.

Kramer, A., Lukas, J., and Bartek, J. (2004) Checking out the centrosome. Cell Cycle 3, 1390-1393.

Kramer, E.R., Gieffers, C., Holzl, G., Hengstschlager, M., and Peters, J.M. (1998) Activation of the human anaphase-promoting complex by proteins of the CDC20/Fizzy family. Curr Biol 8, 1207-1210.

Krek, W., Ewen, M.E., Shirodkar, S., Arany, Z., Kaelin, W.G., Jr., and Livingston, D.M. (1994) Negative regulation of the growth-promoting transcription factor E2F-1 by a stably bound cyclin A-dependent protein kinase. Cell 78, 161-172.

Krempler, A., Deckbar, D., Jeggo, P.A., and Lobrich, M. (2007) An imperfect G2M checkpoint contributes to chromosome instability following irradiation of S and G2 phase cells. Cell Cycle 6, 1682-1686.

Kuerbitz, S.J., Plunkett, B.S., Walsh, W.V., and Kastan, M.B. (1992) Wild-type p53 is a cell cycle checkpoint determinant following irradiation. Proc Natl Acad Sci U S A 89, 7491-7495.

Kumagai, A., and Dunphy, W.G. (1996) Purification and molecular cloning of Plx1, a Cdc25-regulatory kinase from Xenopus egg extracts. Science 273, 1377-1380.

Kumagai, A., and Dunphy, W.G. (2000) Claspin, a novel protein required for the activation of Chk1 during a DNA replication checkpoint response in Xenopus egg extracts. Mol Cell 6, 839-849.

Laemmli, U.K. (1970) Cleavage of structural proteins during the assembly of the head of bacteriophage T4. Nature 227, 680-685.

Lakin, N.D., and Jackson, S.P. (1999) Regulation of p53 in response to DNA damage. Oncogene 18, 7644-7655.

Lampson, M.A., Renduchitala, K., Khodjakov, A., and Kapoor, T.M. (2004) Correcting improper chromosome-spindle attachments during cell division. Nat Cell Biol 6, 232-237.

Lane, H.A., and Nigg, E.A. (1996) Antibody microinjection reveals an essential role for human polo-like kinase 1 (Plk1) in the functional maturation of mitotic centrosomes. J Cell Biol 135, 1701-1713.

Laskey, R.A. (1980) The use of intensifying screens or organic scintillators for visualizing radioactive molecules resolved by gel electrophoresis. Methods Enzymol 65, 363-371.

Laskey, R.A., Mills, A.D., and Morris, N.R. (1977) Assembly of SV40 chromatin in a cell-free system from Xenopus eggs. Cell 10, 237-243.

Laurencon, A., Purdy, A., Sekelsky, J., Hawley, R.S., and Su, T.T. (2003) Phenotypic analysis of separation-of-function alleles of MEI-41, Drosophila ATM/ATR. Genetics 164, 589-601.

Lavin, M.F., and Shiloh, Y. (1997) The genetic defect in ataxia-telangiectasia. Annu Rev Immunol 15, 177-202.

Lee, J., Kumagai, A., and Dunphy, W.G. (2003) Claspin, a Chk1-regulatory protein, monitors DNA replication on chromatin independently of RPA, ATR, and Rad17. Mol Cell 11, 329-340.

Lee, J.H., and Paull, T.T. (2004) Direct activation of the ATM protein kinase by the Mre11/Rad50/Nbs1 complex. Science 304, 93-96.

Lee, M.S., Ogg, S., Xu, M., Parker, L.L., Donoghue, D.J., Maller, J.L., and Piwnica-Worms, H. (1992) cdc25+ encodes a protein phosphatase that dephosphorylates p34cdc2. Mol Biol Cell 3, 73-84.

Lee, S.E., Pellicioli, A., Demeter, J., Vaze, M.P., Gasch, A.P., Malkova, A., Brown, P.O., Botstein, D., Stearns, T., Foiani, M., and Haber, J.E. (2000) Arrest, adaptation, and recovery following a chromosome double-strand break in Saccharomyces cerevisiae. Cold Spring Harb Symp Quant Biol 65, 303-314.

Lee, S.H., and Kim, C.H. (2002) DNA-dependent protein kinase complex: a multifunctional protein in DNA repair and damage checkpoint. Mol Cells 13, 159-166.

Lehmann, A.R. (2005) The role of SMC proteins in the responses to DNA damage. DNA Repair (Amst) 4, 309-314.

Lengauer, C., Kinzler, K.W., and Vogelstein, B. (1998) Genetic instabilities in human cancers. Nature 396, 643-649.

Li, J., Meyer, A.N., and Donoghue, D.J. (1997) Nuclear localization of cyclin B1 mediates its biological activity and is regulated by phosphorylation. Proc Natl Acad Sci U S A 94, 502-507.

Li, R., and Murray, A.W. (1991) Feedback control of mitosis in budding yeast. Cell 66, 519-531.

Liang, F., and Wang, Y. (2007) DNA damage checkpoints inhibit mitotic exit by two different mechanisms. Mol Cell Biol 27, 5067-5078.

Lim, D.S., Kim, S.T., Xu, B., Maser, R.S., Lin, J., Petrini, J.H., and Kastan, M.B. (2000) ATM phosphorylates p95/nbs1 in an S-phase checkpoint pathway. Nature 404, 613-617.

Lindon, C., and Pines, J. (2004) Ordered proteolysis in anaphase inactivates Plk1 to contribute to proper mitotic exit in human cells. J Cell Biol 164, 233-241.

Lindqvist, A., Kallstrom, H., Lundgren, A., Barsoum, E., and Rosenthal, C.K. (2005) Cdc25B cooperates with Cdc25A to induce mitosis but has a unique role in activating cyclin B1-Cdk1 at the centrosome. J Cell Biol 171, 35-45.

Lindqvist, A., van Zon, W., Karlsson Rosenthal, C., and Wolthuis, R.M. (2007) Cyclin B1-Cdk1 activation continues after centrosome separation to control mitotic progression. PLoS Biol 5, e123.

Lindsay, H.D., Whitaker, M.J., and Ford, C.C. (1995) Calcium requirements during mitotic cdc2 kinase activation and cyclin degradation in Xenopus egg extracts. J Cell Sci 108 (Pt 11), 3557-3568.

Liu, F., Stanton, J.J., Wu, Z., and Piwnica-Worms, H. (1997) The human Myt1 kinase preferentially phosphorylates Cdc2 on threonine 14 and localizes to the endoplasmic reticulum and Golgi complex. Mol Cell Biol 17, 571-583.

Liu, J., and Maller, J.L. (2005) Xenopus Polo-like kinase Plx1: a multifunctional mitotic kinase. Oncogene 24, 238-247.

Liu, Q., Guntuku, S., Cui, X.S., Matsuoka, S., Cortez, D., Tamai, K., Luo, G., Carattini-Rivera, S., DeMayo, F., Bradley, A., Donehower, L.A., and Elledge, S.J. (2000) Chk1 is an essential kinase that is regulated by Atr and required for the G(2)/M DNA damage checkpoint. Genes Dev 14, 1448-1459.

Lobrich, M., and Jeggo, P.A. (2007) The impact of a negligent G2/M checkpoint on genomic instability and cancer induction. Nat Rev Cancer 7, 861-869.

Loffler, H., Bochtler, T., Fritz, B., Tews, B., Ho, A.D., Lukas, J., Bartek, J., and Kramer, A. (2007) DNA damage-induced accumulation of centrosomal Chk1 contributes to its checkpoint function. Cell Cycle 6, 2541-2548.

Loffler, H., Lukas, J., Bartek, J., and Kramer, A. (2006) Structure meets function--centrosomes, genome maintenance and the DNA damage response. Exp Cell Res 312, 2633-2640.

Lohka, M.J., and Maller, J.L. (1985) Induction of nuclear envelope breakdown, chromosome condensation, and spindle formation in cell-free extracts. J Cell Biol 101, 518-523.

Lohka, M.J., and Masui, Y. (1983) Formation in vitro of sperm pronuclei and mitotic chromosomes induced by amphibian ooplasmic components. Science 220, 719-721.

Longhese, M.P., Foiani, M., Muzi-Falconi, M., Lucchini, G., and Plevani, P. (1998) DNA damage checkpoint in budding yeast. Embo J 17, 5525-5528.

Lorca, T., Cruzalegui, F.H., Fesquet, D., Cavadore, J.C., Mery, J., Means, A., and Doree, M. (1993) Calmodulin-dependent protein kinase II mediates inactivation of MPF and CSF upon fertilization of Xenopus eggs. Nature 366, 270-273.

Losada, A., and Hirano, T. (2005) Dynamic molecular linkers of the genome: the first decade of SMC proteins. Genes Dev 19, 1269-1287.

Lukas, J., Lukas, C., and Bartek, J. (2004) Mammalian cell cycle checkpoints: signalling pathways and their organization in space and time. DNA Repair (Amst) 3, 997-1007.

Lustig, K.D., Stukenberg, P.T., McGarry, T.J., King, R.W., Cryns, V.L., Mead, P.E., Zon, L.I., Yuan, J., and Kirschner, M.W. (1997) Small pool expression screening: identification of genes involved in cell cycle control, apoptosis, and early development. Methods Enzymol 283, 83-99.

Maddox, P., Desai, A., Oegema, K., Mitchison, T.J., and Salmon, E.D. (2002) Poleward microtubule flux is a major component of spindle dynamics and anaphase a in mitotic Drosophila embryos. Curr Biol 12, 1670-1674.

Mailand, N., Bekker-Jensen, S., Bartek, J., and Lukas, J. (2006) Destruction of Claspin by SCFbetaTrCP restrains Chk1 activation and facilitates recovery from genotoxic stress. Mol Cell 23, 307-318.

Mailand, N., Falck, J., Lukas, C., Syljuasen, R.G., Welcker, M., Bartek, J., and Lukas, J. (2000) Rapid destruction of human Cdc25A in response to DNA damage. Science 288, 1425-1429.

Majewski, F., and Goecke, T. (1982) Studies of microcephalic primordial dwarfism I: approach to a delineation of the Seckel syndrome. Am J Med Genet 12, 7-21.

Maller, J.L., Schwab, M.S., Gross, S.D., Taieb, F.E., Roberts, B.T., and Tunquist, B.J. (2002) The mechanism of CSF arrest in vertebrate oocytes. Mol Cell Endocrinol 187, 173-178.

Maniatis, T.F., E. F. Sambrook, J. . (1982) Molecular cloning : a laboratory manual Cold Spring Harbor Laboratory Press, New York.

Mao, Y., Desai, A., and Cleveland, D.W. (2005) Microtubule capture by CENP-E silences BubR1-dependent mitotic checkpoint signaling. J Cell Biol 170, 873-880.

Mao, Y., Ge, X., Frank, C.L., Madison, J.M., Koehler, A.N., Doud, M.K., Tassa, C., Berry, E.M., Soda, T., Singh, K.K., Biechele, T., Petryshen, T.L., Moon, R.T., Haggarty, S.J., and Tsai, L.H. (2009) Disrupted in schizophrenia 1 regulates neuronal progenitor proliferation via modulation of GSK3beta/beta-catenin signaling. Cell 136, 1017-1031.

Masui, Y., and Markert, C.L. (1971) Cytoplasmic control of nuclear behavior during meiotic maturation of frog oocytes. J Exp Zool 177, 129-145.

Matsumoto, Y., and Maller, J.L. (2002) Calcium, calmodulin, and CaMKII requirement for initiation of centrosome duplication in Xenopus egg extracts. Science 295, 499-502.

Matsuoka, S., Ballif, B.A., Smogorzewska, A., McDonald, E.R., 3rd, Hurov, K.E., Luo, J., Bakalarski, C.E., Zhao, Z., Solimini, N., Lerenthal, Y., Shiloh, Y., Gygi, S.P., and Elledge, S.J. (2007) ATM and ATR substrate analysis reveals extensive protein networks responsive to DNA damage. Science 316, 1160-1166.

Matsuoka, S., Huang, M., and Elledge, S.J. (1998) Linkage of ATM to cell cycle regulation by the Chk2 protein kinase. Science 282, 1893-1897.

Matsushime, H., Ewen, M.E., Strom, D.K., Kato, J.Y., Hanks, S.K., Roussel, M.F., and Sherr, C.J. (1992) Identification and properties of an atypical catalytic subunit (p34PSK-J3/cdk4) for mammalian D type G1 cyclins. Cell 71, 323-334.

Matsushime, H., Quelle, D.E., Shurtleff, S.A., Shibuya, M., Sherr, C.J., and Kato, J.Y. (1994) D-type cyclin-dependent kinase activity in mammalian cells. Mol Cell Biol 14, 2066-2076.

Matsushime, H., Roussel, M.F., Ashmun, R.A., and Sherr, C.J. (1991) Colony-stimulating factor 1 regulates novel cyclins during the G1 phase of the cell cycle. Cell 65, 701-713.

Matthies, H.J., McDonald, H.B., Goldstein, L.S., and Theurkauf, W.E. (1996) Anastral meiotic spindle morphogenesis: role of the non-claret disjunctional kinesin-like protein. J Cell Biol 134, 455-464.

McKim, K.S., and Hawley, R.S. (1995) Chromosomal control of meiotic cell division. Science 270, 1595-1601.

McSherry, T.D., and Mueller, P.R. (2004) Xenopus Cds1 is regulated by DNA-dependent protein kinase and ATR during the cell cycle checkpoint response to double-stranded DNA ends. Mol Cell Biol 24, 9968-9985.

Merdes, A., Heald, R., Samejima, K., Earnshaw, W.C., and Cleveland, D.W. (2000) Formation of spindle poles by dynein/dynactin-dependent transport of NuMA. J Cell Biol 149, 851-862.

Meyerson, M., and Harlow, E. (1994) Identification of G1 kinase activity for cdk6, a novel cyclin D partner. Mol Cell Biol 14, 2077-2086.

Mikhailov, A., Cole, R.W., and Rieder, C.L. (2002) DNA damage during mitosis in human cells delays the metaphase/anaphase transition via the spindle-assembly checkpoint. Curr Biol 12, 1797-1806.

Mimura, S., and Takisawa, H. (1998) Xenopus Cdc45-dependent loading of DNA polymerase alpha onto chromatin under the control of S-phase Cdk. Embo J 17, 5699-5707.

Mitchison, T.J. (1989) Polewards microtubule flux in the mitotic spindle: evidence from photoactivation of fluorescence. J Cell Biol 109, 637-652.

Mogensen, M.M., Malik, A., Piel, M., Bouckson-Castaing, V., and Bornens, M. (2000) Microtubule minus-end anchorage at centrosomal and non-centrosomal sites: the role of ninein. J Cell Sci 113 (Pt 17), 3013-3023.

Molinari, M., Mercurio, C., Dominguez, J., Goubin, F., and Draetta, G.F. (2000) Human Cdc25 A inactivation in response to S phase inhibition and its role in preventing premature mitosis. EMBO Rep 1, 71-79.

Morgan, D.O. (1997) Cyclin-dependent kinases: engines, clocks, and microprocessors. Annu Rev Cell Dev Biol 13, 261-291.

Moritz, M., Braunfeld, M.B., Guenebaut, V., Heuser, J., and Agard, D.A. (2000) Structure of the gamma-tubulin ring complex: a template for microtubule nucleation. Nat Cell Biol 2, 365-370.

Morris, J.A., Kandpal, G., Ma, L., and Austin, C.P. (2003) DISC1 (Disrupted-In-Schizophrenia 1) is a centrosome-associated protein that interacts with MAP1A, MIPT3, ATF4/5 and NUDEL: regulation and loss of interaction with mutation. Hum Mol Genet 12, 1591-1608.

Morrison, C., and Rieder, C.L. (2004) Chromosome damage and progression into and through mitosis in vertebrates. DNA Repair (Amst) 3, 1133-1139.

Mueller, P.R., Coleman, T.R., Kumagai, A., and Dunphy, W.G. (1995) Myt1: a membrane-associated inhibitory kinase that phosphorylates Cdc2 on both threonine-14 and tyrosine-15. Science 270, 86-90.

Murray, A.W. (1991) Cell cycle extracts. Methods Cell Biol 36, 581-605.

Murray, A.W. (1995) The genetics of cell cycle checkpoints. Curr Opin Genet Dev 5, 5-11.

Murray, A.W. (2004) Recycling the cell cycle: cyclins revisited. Cell 116, 221-234.

Murray, A.W., and Kirschner, M.W. (1989) Cyclin synthesis drives the early embryonic cell cycle. Nature 339, 275-280.

Murray, A.W., Solomon, M.J., and Kirschner, M.W. (1989) The role of cyclin synthesis and degradation in the control of maturation promoting factor activity. Nature 339, 280-286.

Musacchio, A., and Salmon, E.D. (2007) The spindle-assembly checkpoint in space and time. Nat Rev Mol Cell Biol 8, 379-393.

Nasmyth, K. (2002) Segregating sister genomes: the molecular biology of chromosome separation. Science 297, 559-565.

Nigg, E.A. (1996) Cyclin-dependent kinase 7: at the cross-roads of transcription, DNA repair and cell cycle control? Curr Opin Cell Biol 8, 312-317.

Niida, H., and Nakanishi, M. (2006) DNA damage checkpoints in mammals. Mutagenesis 21, 3-9.

Ninomiya-Tsuji, J., Nomoto, S., Yasuda, H., Reed, S.I., and Matsumoto, K. (1991) Cloning of a human cDNA encoding a CDC2-related kinase by complementation of a budding yeast cdc28 mutation. Proc Natl Acad Sci U S A 88, 9006-9010.

Nitiss, J.L. (2009) DNA topoisomerase II and its growing repertoire of biological functions. Nat Rev Cancer 9, 327-337.

Nogales, E. (2000) Structural insights into microtubule function. Annu Rev Biochem 69, 277-302.

Noton, E., and Diffley, J.F. (2000) CDK inactivation is the only essential function of the APC/C and the mitotic exit network proteins for origin resetting during mitosis. Mol Cell 5, 85-95.

Nurse, P. (1990) Universal control mechanism regulating onset of M-phase. Nature 344, 503-508.

Nyberg, K.A., Michelson, R.J., Putnam, C.W., and Weinert, T.A. (2002) Toward maintaining the genome: DNA damage and replication checkpoints. Annu Rev Genet 36, 617-656.

O'Driscoll, M., Ruiz-Perez, V.L., Woods, C.G., Jeggo, P.A., and Goodship, J.A. (2003) A splicing mutation affecting expression of ataxia-telangiectasia and Rad3-related protein (ATR) results in Seckel syndrome. Nat Genet 33, 497-501.

Onuki, Y., Rounds, D.E., Olson, R.S., and Berns, M.W. (1972) Laser microbeam irradiation of the juxtanucleolar region of prophase nucleolar chromosomes. Exp Cell Res 71, 132-144.

Oricchio, E., Saladino, C., Iacovelli, S., Soddu, S., and Cundari, E. (2006) ATM is activated by default in mitosis, localizes at centrosomes and monitors mitotic spindle integrity. Cell Cycle 5, 88-92.

Paciotti, V., Clerici, M., Lucchini, G., and Longhese, M.P. (2000) The checkpoint protein Ddc2, functionally related to S. pombe Rad26, interacts with Mec1 and is regulated by Mec1-dependent phosphorylation in budding yeast. Genes Dev 14, 2046-2059.

Pagano, M., Pepperkok, R., Verde, F., Ansorge, W., and Draetta, G. (1992) Cyclin A is required at two points in the human cell cycle. Embo J 11, 961-971.

Pagano, M., Theodoras, A.M., Tam, S.W., and Draetta, G.F. (1994) Cyclin D1-mediated inhibition of repair and replicative DNA synthesis in human fibroblasts. Genes Dev 8, 1627-1639.

Painter, R.B., and Young, B.R. (1980) Radiosensitivity in ataxia-telangiectasia: a new explanation. Proc Natl Acad Sci U S A 77, 7315-7317.

Palacios, I.M., and St Johnston, D. (2001) Getting the message across: the intracellular localization of mRNAs in higher eukaryotes. Annu Rev Cell Dev Biol 17, 569-614.

Pardee, A.B. (1989) G1 events and regulation of cell proliferation. Science 246, 603-608.

Parker, L.L., and Piwnica-Worms, H. (1992) Inactivation of the p34cdc2-cyclin B complex by the human WEE1 tyrosine kinase. Science 257, 1955-1957.

Paules, R.S., Levedakou, E.N., Wilson, S.J., Innes, C.L., Rhodes, N., Tlsty, T.D., Galloway, D.A., Donehower, L.A., Tainsky, M.A., and Kaufmann, W.K. (1995) Defective G2 checkpoint function in cells from individuals with familial cancer syndromes. Cancer Res 55, 1763-1773.

Paull, T.T., and Gellert, M. (1999) Nbs1 potentiates ATP-driven DNA unwinding and endonuclease cleavage by the Mre11/Rad50 complex. Genes Dev 13, 1276-1288.

Peng, C.Y., Graves, P.R., Thoma, R.S., Wu, Z., Shaw, A.S., and Piwnica-Worms, H. (1997) Mitotic and G2 checkpoint control: regulation of 14-3-3 protein binding by phosphorylation of Cdc25C on serine-216. Science 277, 1501-1505.

Perez-Roger, I., Kim, S.H., Griffiths, B., Sewing, A., and Land, H. (1999) Cyclins D1 and D2 mediate myc-induced proliferation via sequestration of p27(Kip1) and p21(Cip1). Embo J 18, 5310-5320.

Peschiaroli, A., Dorrello, N.V., Guardavaccaro, D., Venere, M., Halazonetis, T., Sherman, N.E., and Pagano, M. (2006) SCFbetaTrCP-mediated degradation of Claspin regulates recovery from the DNA replication checkpoint response. Mol Cell 23, 319-329.

Peters, J.M. (2002) The anaphase-promoting complex: proteolysis in mitosis and beyond. Mol Cell 9, 931-943.

Peters, J.M. (2006) The anaphase promoting complex/cyclosome: a machine designed to destroy. Nat Rev Mol Cell Biol 7, 644-656.

Petersen, B.O., Lukas, J., Sorensen, C.S., Bartek, J., and Helin, K. (1999) Phosphorylation of mammalian CDC6 by cyclin A/CDK2 regulates its subcellular localization. Embo J 18, 396-410.

Petersen, B.O., Wagener, C., Marinoni, F., Kramer, E.R., Melixetian, M., Lazzerini Denchi, E., Gieffers, C., Matteucci, C., Peters, J.M., and Helin, K. (2000) Cell cycle- and cell growth-regulated proteolysis of mammalian CDC6 is dependent on APC-CDH1. Genes Dev 14, 2330-2343.

Petrini, J.H., and Stracker, T.H. (2003) The cellular response to DNA double-strand breaks: defining the sensors and mediators. Trends Cell Biol 13, 458-462.

Pines, J. (2006) Mitosis: a matter of getting rid of the right protein at the right time. Trends Cell Biol 16, 55-63.

Planas-Silva, M.D., and Weinberg, R.A. (1997) The restriction point and control of cell proliferation. Curr Opin Cell Biol 9, 768-772.

Poon, R.Y., Yamashita, K., Adamczewski, J.P., Hunt, T., and Shuttleworth, J. (1993) The cdc2-related protein p40MO15 is the catalytic subunit of a protein kinase that can activate p33cdk2 and p34cdc2. Embo J 12, 3123-3132.

Potapova, T.A., Daum, J.R., Pittman, B.D., Hudson, J.R., Jones, T.N., Satinover, D.L., Stukenberg, P.T., and Gorbsky, G.J. (2006) The reversibility of mitotic exit in vertebrate cells. Nature 440, 954-958.

Prasanth, S.G., Mendez, J., Prasanth, K.V., and Stillman, B. (2004) Dynamics of pre-replication complex proteins during the cell division cycle. Philos Trans R Soc Lond B Biol Sci 359, 7-16.

Qian, Y.W., Erikson, E., Li, C., and Maller, J.L. (1998) Activated polo-like kinase Plx1 is required at multiple points during mitosis in Xenopus laevis. Mol Cell Biol 18, 4262-4271.

Quimby, B.B., and Dasso, M. (2003) The small GTPase Ran: interpreting the signs. Curr Opin Cell Biol 15, 338-344.

Rai, R., Phadnis, A., Haralkar, S., Badwe, R.A., Dai, H., Li, K., and Lin, S.Y. (2008) Differential regulation of centrosome integrity by DNA damage response proteins. Cell Cycle 7, 2225-2233.

Ramadan, K., Bruderer, R., Spiga, F.M., Popp, O., Baur, T., Gotta, M., and Meyer, H.H. (2007) Cdc48/p97 promotes reformation of the nucleus by extracting the kinase Aurora B from chromatin. Nature 450, 1258-1262.

Rao, P.N., and Johnson, R.T. (1970) Mammalian cell fusion: studies on the regulation of DNA synthesis and mitosis. Nature 225, 159-164.

Rape, M., and Kirschner, M.W. (2004) Autonomous regulation of the anaphase-promoting complex couples mitosis to S-phase entry. Nature 432, 588-595.

Rhind, N., and Russell, P. (2000) Chk1 and Cds1: linchpins of the DNA damage and replication checkpoint pathways. J Cell Sci 113 (Pt 22), 3889-3896.

Richardson, R.J., Dixon, J., Malhotra, S., Hardman, M.J., Knowles, L., Boot-Handford, R.P., Shore, P., Whitmarsh, A., and Dixon, M.J. (2006) Irf6 is a key determinant of the keratinocyte proliferation-differentiation switch. Nat Genet 38, 1329-1334.

Rieder, C.L., and Alexander, S.P. (1990) Kinetochores are transported poleward along a single astral microtubule during chromosome attachment to the spindle in newt lung cells. J Cell Biol 110, 81-95.

Rieder, C.L., and Cole, R.W. (1998) Entry into mitosis in vertebrate somatic cells is guarded by a chromosome damage checkpoint that reverses the cell cycle when triggered during early but not late prophase. J Cell Biol 142, 1013-1022.

Rieder, C.L., Faruki, S., and Khodjakov, A. (2001) The centrosome in vertebrates: more than a microtubule-organizing center. Trends Cell Biol 11, 413-419.

Rieder, C.L., and Salmon, E.D. (1994) Motile kinetochores and polar ejection forces dictate chromosome position on the vertebrate mitotic spindle. J Cell Biol 124, 223-233.

Rieder, C.L., and Salmon, E.D. (1998) The vertebrate cell kinetochore and its roles during mitosis. Trends Cell Biol 8, 310-318.

Robertson, K., Hensey, C., and Gautier, J. (1999) Isolation and characterization of Xenopus ATM (X-ATM): expression, localization, and complex formation during oogenesis and early development. Oncogene 18, 7070-7079.

Rogakou, E.P., Pilch, D.R., Orr, A.H., Ivanova, V.S., and Bonner, W.M. (1998) DNA double-stranded breaks induce histone H2AX phosphorylation on serine 139. J Biol Chem 273, 5858-5868.

Roninson, I.B., Broude, E.V., and Chang, B.D. (2001) If not apoptosis, then what? Treatment-induced senescence and mitotic catastrophe in tumor cells. Drug Resist Updat 4, 303-313.

Rowley, R., Phillips, E.N., and Schroeder, A.L. (1999) The effects of ionizing radiation on DNA synthesis in eukaryotic cells. Int J Radiat Biol 75, 267-283.

Royou, A., Macias, H., and Sullivan, W. (2005) The Drosophila Grp/Chk1 DNA damage checkpoint controls entry into anaphase. Curr Biol 15, 334-339.

Sambrook, J.F., E.F. Maniatis, T. (1989) Molecular cloning : a laboratory manual Cold Spring Harbor Laboratory Press, New York.

Sancar, A., Lindsey-Boltz, L.A., Unsal-Kacmaz, K., and Linn, S. (2004) Molecular mechanisms of mammalian DNA repair and the DNA damage checkpoints. Annu Rev Biochem 73, 39-85.

Sanchez, Y., Wong, C., Thoma, R.S., Richman, R., Wu, Z., Piwnica-Worms, H., and Elledge, S.J. (1997) Conservation of the Chk1 checkpoint pathway in mammals: linkage of DNA damage to Cdk regulation through Cdc25. Science 277, 1497-1501.

Sandell, L.L., and Zakian, V.A. (1993) Loss of a yeast telomere: arrest, recovery, and chromosome loss. Cell 75, 729-739.

Sarkaria, J.N., Busby, E.C., Tibbetts, R.S., Roos, P., Taya, Y., Karnitz, L.M., and Abraham, R.T. (1999) Inhibition of ATM and ATR kinase activities by the radiosensitizing agent, caffeine. Cancer Res 59, 4375-4382.

Savitsky, K., Bar-Shira, A., Gilad, S., Rotman, G., Ziv, Y., Vanagaite, L., Tagle, D.A., Smith, S., Uziel, T., Sfez, S., Ashkenazi, M., Pecker, I., Frydman, M., Harnik, R., Patanjali, S.R., Simmons, A., Clines, G.A., Sartiel, A., Gatti, R.A., Chessa, L., Sanal, O., Lavin, M.F., Jaspers, N.G., Taylor, A.M., Arlett, C.F., Miki, T., Weissman, S.M., Lovett, M., Collins, F.S., and Shiloh, Y. (1995) A single ataxia telangiectasia gene with a product similar to PI-3 kinase. Science 268, 1749-1753.

Sawin, K.E., and Mitchison, T.J. (1991) Mitotic spindle assembly by two different pathways in vitro. J Cell Biol 112, 925-940.

Schatten, H. (2008) The mammalian centrosome and its functional significance. Histochem Cell Biol 129, 667-686.

Schatten, H., Chakrabarti, A., and Hedrick, J. (1999) Centrosome and microtubule instability in aging Drosophila cells. J Cell Biochem 74, 229-241.

Schultz, L.B., Chehab, N.H., Malikzay, A., and Halazonetis, T.D. (2000) p53 binding protein 1 (53BP1) is an early participant in the cellular response to DNA double-strand breaks. J Cell Biol 151, 1381-1390.

Schwob, E., and Nasmyth, K. (1993) CLB5 and CLB6, a new pair of B cyclins involved in DNA replication in Saccharomyces cerevisiae. Genes Dev 7, 1160-1175.

Seo, G.J., Kim, S.E., Lee, Y.M., Lee, J.W., Lee, J.R., Hahn, M.J., and Kim, S.T. (2003) Determination of substrate specificity and putative substrates of Chk2 kinase. Biochem Biophys Res Commun 304, 339-343.

Seong, Y.S., Kamijo, K., Lee, J.S., Fernandez, E., Kuriyama, R., Miki, T., and Lee, K.S. (2002) A spindle checkpoint arrest and a cytokinesis failure by the dominant-negative polo-box domain of Plk1 in U-2 OS cells. J Biol Chem 277, 32282-32293.

Shechter, D., Costanzo, V., and Gautier, J. (2004) ATR and ATM regulate the timing of DNA replication origin firing. Nat Cell Biol 6, 648-655.

Shechter, D., Costanzo, V., and Gautier, J. (2004) Regulation of DNA replication by ATR: signaling in response to DNA intermediates. DNA Repair (Amst) 3, 901-908.

Shen, K., Wang, Y., Brooks, S.C., Raz, A., and Wang, Y.A. (2006) ATM is activated by mitotic stress and suppresses centrosome amplification in primary but not in tumor cells. J Cell Biochem 99, 1267-1274.

Sherr, C.J. (1993) Mammalian G1 cyclins. Cell 73, 1059-1065.

Sherr, C.J., and Roberts, J.M. (1999) CDK inhibitors: positive and negative regulators of G1-phase progression. Genes Dev 13, 1501-1512.

Shiloh, Y. (1997) Ataxia-telangiectasia and the Nijmegen breakage syndrome: related disorders but genes apart. Annu Rev Genet 31, 635-662.

Shiloh, Y. (2003) ATM and related protein kinases: safeguarding genome integrity. Nat Rev Cancer 3, 155-168.

Shinmura, K., Bennett, R.A., Tarapore, P., and Fukasawa, K. (2007) Direct evidence for the role of centrosomally localized p53 in the regulation of centrosome duplication. Oncogene 26, 2939-2944.

Sibon, O.C. (2003) Centrosomes as DNA damage regulators. Nat Genet 34, 6-7.

Sibon, O.C., Kelkar, A., Lemstra, W., and Theurkauf, W.E. (2000) DNA-replication/DNA-damage-dependent centrosome inactivation in Drosophila embryos. Nat Cell Biol 2, 90-95.

Sigrist, S., Jacobs, H., Stratmann, R., and Lehner, C.F. (1995) Exit from mitosis is regulated by Drosophila fizzy and the sequential destruction of cyclins A, B and B3. Embo J 14, 4827-4838.

Siu, W.Y., Lau, A., Arooz, T., Chow, J.P., Ho, H.T., and Poon, R.Y. (2004) Topoisomerase poisons differentially activate DNA damage checkpoints through ataxia-telangiectasia mutated-dependent and -independent mechanisms. Mol Cancer Ther 3, 621-632.

Skoufias, D.A., Lacroix, F.B., Andreassen, P.R., Wilson, L., and Margolis, R.L. (2004) Inhibition of DNA decatenation, but not DNA damage, arrests cells at metaphase. Mol Cell 15, 977-990.

Smith, E., Dejsuphong, D., Balestrini, A., Hampel, M., Lenz, C., Takeda, S., Vindigni, A., and Costanzo, V. (2009) An ATM- and ATR-dependent checkpoint inactivates spindle assembly by targeting CEP63. Nat Cell Biol 11, 278-285.

Smith, L., Liu, S.J., Goodrich, L., Jacobson, D., Degnin, C., Bentley, N., Carr, A., Flaggs, G., Keegan, K., Hoekstra, M., and Thayer, M.J. (1998) Duplication of ATR inhibits MyoD, induces aneuploidy and eliminates radiation-induced G1 arrest. Nat Genet 19, 39-46.

Smits, V.A., Klompmaker, R., Arnaud, L., Rijksen, G., Nigg, E.A., and Medema, R.H. (2000) Polo-like kinase-1 is a target of the DNA damage checkpoint. Nat Cell Biol 2, 672-676.

Smythe, C., and Newport, J.W. (1991) Systems for the study of nuclear assembly, DNA replication, and nuclear breakdown in Xenopus laevis egg extracts. Methods Cell Biol 35, 449-468.

Solomon, M.J., Harper, J.W., and Shuttleworth, J. (1993) CAK, the p34cdc2 activating kinase, contains a protein identical or closely related to p40MO15. Embo J 12, 3133-3142.

Solomon, S., Xu, Y., Wang, B., David, M.D., Schubert, P., Kennedy, D., and Schrader, J.W. (2007) Distinct structural features of caprin-1 mediate its interaction with G3BP-1 and its induction of phosphorylation of eukaryotic translation initiation factor 2alpha, entry to cytoplasmic stress granules, and selective interaction with a subset of mRNAs. Mol Cell Biol 27, 2324-2342.

Sorensen, C.S., Syljuasen, R.G., Lukas, J., and Bartek, J. (2004) ATR, Claspin and the Rad9-Rad1-Hus1 complex regulate Chk1 and Cdc25A in the absence of DNA damage. Cell Cycle 3, 941-945.

Stearns, T. (2001) Centrosome duplication. a centriolar pas de deux. Cell 105, 417-420.

Stewart, G.S., Wang, B., Bignell, C.R., Taylor, A.M., and Elledge, S.J. (2003) MDC1 is a mediator of the mammalian DNA damage checkpoint. Nature 421, 961-966.

Stiff, T., Walker, S.A., Cerosaletti, K., Goodarzi, A.A., Petermann, E., Concannon, P., O'Driscoll, M., and Jeggo, P.A. (2006) ATR-dependent phosphorylation and activation of ATM in response to UV treatment or replication fork stalling. Embo J 25, 5775-5782.

Su, T.T., and Jaklevic, B. (2001) DNA damage leads to a Cyclin A-dependent delay in metaphase-anaphase transition in the Drosophila gastrula. Curr Biol 11, 8-17.

Sudakin, V., Chan, G.K., and Yen, T.J. (2001) Checkpoint inhibition of the APC/C in HeLa cells is mediated by a complex of BUBR1, BUB3, CDC20, and MAD2. J Cell Biol 154, 925-936.

Sudakin, V., Ganoth, D., Dahan, A., Heller, H., Hershko, J., Luca, F.C., Ruderman, J.V., and Hershko, A. (1995) The cyclosome, a large complex containing cyclin-selective ubiquitin ligase activity, targets cyclins for destruction at the end of mitosis. Mol Biol Cell 6, 185-197.

Sullivan, M., and Morgan, D.O. (2007) Finishing mitosis, one step at a time. Nat Rev Mol Cell Biol 8, 894-903.

Sun, Q.Y., and Schatten, H. (2006) Role of NuMA in vertebrate cells: review of an intriguing multifunctional protein. Front Biosci 11, 1137-1146.

Sunkel, C.E., and Glover, D.M. (1988) polo, a mitotic mutant of Drosophila displaying abnormal spindle poles. J Cell Sci 89 (Pt 1), 25-38.

Syljuasen, R.G. (2007) Checkpoint adaptation in human cells. Oncogene 26, 5833-5839.

Takada, S., Kelkar, A., and Theurkauf, W.E. (2003) Drosophila checkpoint kinase 2 couples centrosome function and spindle assembly to genomic integrity. Cell 113, 87-99.

Takai, H., Tominaga, K., Motoyama, N., Minamishima, Y.A., Nagahama, H., Tsukiyama, T., Ikeda, K., Nakayama, K., Nakanishi, M., and Nakayama, K. (2000) Aberrant cell cycle checkpoint function and early embryonic death in Chk1(-/-) mice. Genes Dev 14, 1439-1447.

Takeda, D.Y., and Dutta, A. (2005) DNA replication and progression through S phase. Oncogene 24, 2827-2843.

Tanaka, K., Kitamura, E., Kitamura, Y., and Tanaka, T.U. (2007) Molecular mechanisms of microtubule-dependent kinetochore transport toward spindle poles. J Cell Biol 178, 269-281.

Tanaka, K., Mukae, N., Dewar, H., van Breugel, M., James, E.K., Prescott, A.R., Antony, C., and Tanaka, T.U. (2005) Molecular mechanisms of kinetochore capture by spindle microtubules. Nature 434, 987-994.

Tanaka, T.U., and Desai, A. (2008) Kinetochore-microtubule interactions: the means to the end. Curr Opin Cell Biol 20, 53-63.

Tanaka, T.U., Rachidi, N., Janke, C., Pereira, G., Galova, M., Schiebel, E., Stark, M.J., and Nasmyth, K. (2002) Evidence that the Ipl1-Sli15 (Aurora kinase-INCENP) complex promotes chromosome bi-orientation by altering kinetochore-spindle pole connections. Cell 108, 317-329.

Theurkauf, W.E., and Hawley, R.S. (1992) Meiotic spindle assembly in Drosophila females: behavior of nonexchange chromosomes and the effects of mutations in the nod kinesin-like protein. J Cell Biol 116, 1167-1180.

Tibbetts, R.S., Brumbaugh, K.M., Williams, J.M., Sarkaria, J.N., Cliby, W.A., Shieh, S.Y., Taya, Y., Prives, C., and Abraham, R.T. (1999) A role for ATR in the DNA damage-induced phosphorylation of p53. Genes Dev 13, 152-157.

Tibbetts, R.S., Cortez, D., Brumbaugh, K.M., Scully, R., Livingston, D., Elledge, S.J., and Abraham, R.T. (2000) Functional interactions between BRCA1 and the checkpoint kinase ATR during genotoxic stress. Genes Dev 14, 2989-3002.

Tinker-Kulberg, R.L., and Morgan, D.O. (1999) Pds1 and Esp1 control both anaphase and mitotic exit in normal cells and after DNA damage. Genes Dev 13, 1936-1949.

Toczyski, D.P., Galgoczy, D.J., and Hartwell, L.H. (1997) CDC5 and CKII control adaptation to the yeast DNA damage checkpoint. Cell 90, 1097-1106.

Towbin, H., Staehelin, T., and Gordon, J. (1979) Electrophoretic transfer of proteins from polyacrylamide gels to nitrocellulose sheets: procedure and some applications. Proc Natl Acad Sci U S A 76, 4350-4354.

Toyoshima-Morimoto, F., Taniguchi, E., Shinya, N., Iwamatsu, A., and Nishida, E. (2001) Polo-like kinase 1 phosphorylates cyclin B1 and targets it to the nucleus during prophase. Nature 410, 215-220.

Trenz, K., Errico, A., and Costanzo, V. (2008) Plx1 is required for chromosomal DNA replication under stressful conditions. Embo J 27, 876-885.

Trenz, K., Smith, E., Smith, S., and Costanzo, V. (2006) ATM and ATR promote Mre11 dependent restart of collapsed replication forks and prevent accumulation of DNA breaks. Embo J 25, 1764-1774.

Tritarelli, A., Oricchio, E., Ciciarello, M., Mangiacasale, R., Palena, A., Lavia, P., Soddu, S., and Cundari, E. (2004) p53 localization at centrosomes during mitosis and postmitotic checkpoint are ATM-dependent and require serine 15 phosphorylation. Molecular Biology of the Cell 15, 3751–3757.

Tsvetkov, L., Xu, X., Li, J., and Stern, D.F. (2003) Polo-like kinase 1 and Chk2 interact and co-localize to centrosomes and the midbody. J Biol Chem 278, 8468-8475.

Tulu, U.S., Rusan, N.M., and Wadsworth, P. (2003) Peripheral, non-centrosome-associated microtubules contribute to spindle formation in centrosome-containing cells. Curr Biol 13, 1894-1899.

Uhlmann, F., Lottspeich, F., and Nasmyth, K. (1999) Sister-chromatid separation at anaphase onset is promoted by cleavage of the cohesin subunit Scc1. Nature 400, 37-42.

Unsal-Kacmaz, K., Makhov, A.M., Griffith, J.D., and Sancar, A. (2002) Preferential binding of ATR protein to UV-damaged DNA. Proc Natl Acad Sci U S A 99, 6673-6678.

Unsal-Kacmaz, K., and Sancar, A. (2004) Quaternary structure of ATR and effects of ATRIP and replication protein A on its DNA binding and kinase activities. Mol Cell Biol 24, 1292-1300.

Unwin, R.D., Griffiths, J.R., Leverentz, M.K., Grallert, A., Hagan, I.M., and Whetton, A.D. (2005) Multiple reaction monitoring to identify sites of protein phosphorylation with high sensitivity. Mol Cell Proteomics 4, 1134-1144.

van den Bosch, M., Bree, R.T., and Lowndes, N.F. (2003) The MRN complex: coordinating and mediating the response to broken chromosomes. EMBO Rep 4, 844-849.

van Leuken, R., Clijsters, L., and Wolthuis, R. (2008) To cell cycle, swing the APC/C. Biochim Biophys Acta 1786, 49-59.

van Vugt, M.A., Bras, A., and Medema, R.H. (2004) Polo-like kinase-1 controls recovery from a G2 DNA damage-induced arrest in mammalian cells. Mol Cell 15, 799-811.

van Vugt, M.A., and Medema, R.H. (2005) Getting in and out of mitosis with Polo-like kinase-1. Oncogene 24, 2844-2859.

van Vugt, M.A., Smits, V.A., Klompmaker, R., and Medema, R.H. (2001) Inhibition of Polo-like kinase-1 by DNA damage occurs in an ATM- or ATR-dependent fashion. J Biol Chem 276, 41656-41660.

van Vugt, M.A., van de Weerdt, B.C., Vader, G., Janssen, H., Calafat, J., Klompmaker, R., Wolthuis, R.M., and Medema, R.H. (2004) Polo-like kinase-1 is required for bipolar spindle formation but is dispensable for anaphase promoting complex/Cdc20 activation and initiation of cytokinesis. J Biol Chem 279, 36841-36854.

Vasquez, R.J., Howell, B., Yvon, A.M., Wadsworth, P., and Cassimeris, L. (1997) Nanomolar concentrations of nocodazole alter microtubule dynamic instability in vivo and in vitro. Mol Biol Cell 8, 973-985.

Verde, F., Labbe, J.C., Doree, M., and Karsenti, E. (1990) Regulation of microtubule dynamics by cdc2 protein kinase in cell-free extracts of Xenopus eggs. Nature 343, 233-238.

Visintin, R., Prinz, S., and Amon, A. (1997) CDC20 and CDH1: a family of substrate-specific activators of APC-dependent proteolysis. Science 278, 460-463.

Walczak, C.E., Mitchison, T.J., and Desai, A. (1996) XKCM1: a Xenopus kinesin-related protein that regulates microtubule dynamics during mitotic spindle assembly. Cell 84, 37-47.

Walczak, C.E., Vernos, I., Mitchison, T.J., Karsenti, E., and Heald, R. (1998) A model for the proposed roles of different microtubule-based motor proteins in establishing spindle bipolarity. Curr Biol 8, 903-913.

Walter, J., and Newport, J. (2000) Initiation of eukaryotic DNA replication: origin unwinding and sequential chromatin association of Cdc45, RPA, and DNA polymerase alpha. Mol Cell 5, 617-627.

Wang, B., David, M.D., and Schrader, J.W. (2005) Absence of caprin-1 results in defects in cellular proliferation. J Immunol 175, 4274-4282.

Wang, B., Matsuoka, S., Carpenter, P.B., and Elledge, S.J. (2002) 53BP1, a mediator of the DNA damage checkpoint. Science 298, 1435-1438.

Wassmann, K., and Benezra, R. (2001) Mitotic checkpoints: from yeast to cancer. Curr Opin Genet Dev 11, 83-90.

Watanabe, N., Arai, H., Nishihara, Y., Taniguchi, M., Watanabe, N., Hunter, T., and Osada, H. (2004) M-phase kinases induce phospho-dependent ubiquitination of somatic Wee1 by SCFbeta-TrCP. Proc Natl Acad Sci U S A 101, 4419-4424.

Wiese, C., Wilde, A., Moore, M.S., Adam, S.A., Merdes, A., and Zheng, Y. (2001) Role of importin-beta in coupling Ran to downstream targets in microtubule assembly. Science 291, 653-656.

Williamson, B.L., Marchese, J., and Morrice, N.A. (2006) Automated identification and quantification of protein phosphorylation sites by LC/MS on a hybrid triple quadrupole linear ion trap mass spectrometer. Mol Cell Proteomics 5, 337-346.

Won, K.A., Xiong, Y., Beach, D., and Gilman, M.Z. (1992) Growth-regulated expression of D-type cyclin genes in human diploid fibroblasts. Proc Natl Acad Sci U S A 89, 9910-9914.

Woo, R.A., and Poon, R.Y. (2003) Cyclin-dependent kinases and S phase control in mammalian cells. Cell Cycle 2, 316-324.

Xia, G., Luo, X., Habu, T., Rizo, J., Matsumoto, T., and Yu, H. (2004) Conformation-specific binding of p31(comet) antagonizes the function of Mad2 in the spindle checkpoint. Embo J 23, 3133-3143.

Xiong, Y., Zhang, H., and Beach, D. (1992) D type cyclins associate with multiple protein kinases and the DNA replication and repair factor PCNA. Cell 71, 505-514.

Yamane, K., Wu, X., and Chen, J. (2002) A DNA damage-regulated BRCT-containing protein, TopBP1, is required for cell survival. Mol Cell Biol 22, 555-566.

Yang, M., Li, B., Tomchick, D.R., Machius, M., Rizo, J., Yu, H., and Luo, X. (2007) p31comet blocks Mad2 activation through structural mimicry. Cell 131, 744-755.

Yang, S.S., Yeh, E., Salmon, E.D., and Bloom, K. (1997) Identification of a mid-anaphase checkpoint in budding yeast. J Cell Biol 136, 345-354.

Yang, Z., Tulu, U.S., Wadsworth, P., and Rieder, C.L. (2007) Kinetochore dynein is required for chromosome motion and congression independent of the spindle checkpoint. Curr Biol 17, 973-980.

Yarden, R.I., Pardo-Reoyo, S., Sgagias, M., Cowan, K.H., and Brody, L.C. (2002) BRCA1 regulates the G2/M checkpoint by activating Chk1 kinase upon DNA damage. Nat Genet 30, 285-289.

Yarm, F.R. (2002) Plk phosphorylation regulates the microtubule-stabilizing protein TCTP. Mol Cell Biol 22, 6209-6221.

Yazdi, P.T., Wang, Y., Zhao, S., Patel, N., Lee, E.Y., and Qin, J. (2002) SMC1 is a downstream effector in the ATM/NBS1 branch of the human S-phase checkpoint. Genes Dev 16, 571-582.

Yoo, H.Y., Kumagai, A., Shevchenko, A., Shevchenko, A., and Dunphy, W.G. (2004) Adaptation of a DNA replication checkpoint response depends upon inactivation of Claspin by the Polo-like kinase. Cell 117, 575-588.

Yoo, H.Y., Kumagai, A., Shevchenko, A., Shevchenko, A., and Dunphy, W.G. (2007) Ataxia-telangiectasia mutated (ATM)-dependent activation of ATR occurs through phosphorylation of TopBP1 by ATM. J Biol Chem 282, 17501-17506.

Yoo, H.Y., Shevchenko, A., Shevchenko, A., and Dunphy, W.G. (2004) Mcm2 is a direct substrate of ATM and ATR during DNA damage and DNA replication checkpoint responses. J Biol Chem 279, 53353-53364.

Yu, H. (2002) Regulation of APC-Cdc20 by the spindle checkpoint. Curr Opin Cell Biol 14, 706-714.

Yuan, J., Eckerdt, F., Bereiter-Hahn, J., Kurunci-Csacsko, E., Kaufmann, M., and Strebhardt, K. (2002) Cooperative phosphorylation including the activity of polo-like kinase 1 regulates the subcellular localization of cyclin B1. Oncogene 21, 8282-8292.

Zachos, G., Black, E.J., Walker, M., Scott, M.T., Vagnarelli, P., Earnshaw, W.C., and Gillespie, D.A. (2007) Chk1 is required for spindle checkpoint function. Dev Cell 12, 247-260.

Zhang, S., Hemmerich, P., and Grosse, F. (2007) Centrosomal localization of DNA damage checkpoint proteins. J Cell Biochem 101, 451-465.

Zheng, Y., Wong, M.L., Alberts, B., and Mitchison, T. (1995) Nucleation of microtubule assembly by a gamma-tubulin-containing ring complex. Nature 378, 578-583.

Zhou, B.B., Chaturvedi, P., Spring, K., Scott, S.P., Johanson, R.A., Mishra, R., Mattern, M.R., Winkler, J.D., and Khanna, K.K. (2000) Caffeine abolishes the mammalian G(2)/M DNA damage checkpoint by inhibiting ataxia-telangiectasia-mutated kinase activity. J Biol Chem 275, 10342-10348.

Zhou, B.B., and Elledge, S.J. (2000) The DNA damage response: putting checkpoints in perspective. Nature 408, 433-439.

Zhou, J., Yao, J., and Joshi, H.C. (2002) Attachment and tension in the spindle assembly checkpoint. J Cell Sci 115, 3547-3555.

Zirkle, R.E. (1970) Ultraviolet-microbeam irradiation of newt-cell cytoplasm: spindle destruction, false anaphase, and delay of true anaphase. Radiat Res 41, 516-537.

Zou, L., and Elledge, S.J. (2003) Sensing DNA damage through ATRIP recognition of RPA-ssDNA complexes. Science 300, 1542-1548.

Zou, Z., Anisowicz, A., Hendrix, M.J., Thor, A., Neveu, M., Sheng, S., Rafidi, K., Seftor, E., and Sager, R. (1994) Maspin, a serpin with tumor-suppressing activity in human mammary epithelial cells. Science 263, 526-529.

Zunino, F., Gambetta, R., Di Marco, A., Velcich, A., Zaccara, A., Quadrifoglio, F., and Crescenzi, V. (1977) The interaction of adriamycin and its beta anomer with DNA. Biochim Biophys Acta 476, 38-46.

Appendix 1: XCEP63 DNA and translated amino acid sequences

```
1/1                          31/11                        61/21
|                            |                            |
ATG GAA GCT TTG TTA CAA GGG CTT CAA CGA CAA GAC AGA ATG GGG GCT TTG CAA GAT TCC TGT GAG GCT GAG CTG CAA GAA CTC ATG AAG
M   E   A   L   L   Q   G   L   Q   R   Q   D   R   M   G   A   L   Q   D   S   C   E   A   E   L   Q   E   L   M   K

91/31                        121/41                       151/51
|                            |                            |
CAG ATA GAC ATT ATG CTG GAT CAC AAG AGG TCA CAG TGG GAA GCA GAG ACA GAG ACA ATG AAG ACT CGT CTA GAG CTG AAA GAG CAG GAG
Q   I   D   I   M   L   D   H   K   R   S   Q   W   E   A   E   T   E   T   M   K   T   R   L   E   L   K   E   Q   E

181/61                       211/71                       241/81
|                            |                            |
CTG AAC TGT GCC CTG GAC AGA GAG GAG CGC TTG AAC CAG GAG GTT AGG AGA TTG AGA CAG CAG CTC ATA CAG CAG GAA GAA GAG ACT CAA
L   N   C   A   L   D   R   E   E   R   L   N   Q   E   V   R   R   L   R   Q   Q   L   I   Q   Q   E   E   E   T   Q

271/91                       301/101                      331/111
|                            |                            |
AAT AAG ACG ACA CAG TAT GAG GCT CAG CTA TCT GGC TTT AAG GAG GAG TTA AAC CGA TTG AAA AAA AGT TAC GAG AAA GTA CAG AAG AAG
N   K   T   T   Q   Y   E   A   Q   L   S   G   F   K   E   E   L   N   R   L   K   K   S   Y   E   K   V   Q   K   K

361/121                      391/131                      421/141
|                            |                            |
CAC CTG CGA TCA GAG ATG AAG GCT AAA GCA GAG GAG GAA AGA TCC GAG GTC AGC CGT CTG ACT CGC CGG TTA GAG GAA TTC CGT CAG AGA
H   L   R   S   E   M   K   A   K   A   E   E   E   R   S   E   V   S   R   L   T   R   R   L   E   E   F   R   Q   R

451/151                      481/161                      511/171
|                            |                            |
TCT TTG GAT TGG GAA AAG CAG CGT TTG TTG TAT CAG CAA CAA CTG GCT GGA CTT GAG GCA CAA CGC AAA ACG TTG ATT GAG CAG ACA GAA
S   L   D   W   E   K   Q   R   L   L   Y   Q   Q   Q   L   A   G   L   E   A   Q   R   K   T   L   I   E   Q   T   E

541/181                      571/191                      601/201
|                            |                            |
ATG TAC CAG CAT CAG TCA CAT AAT CGC AAG CAG ATG CTG GAG CAG ACA AGC CTA GTC GGC CGT TCT GAA CTT CAG AAC CTC AGT GGT CAG
M   Y   Q   H   Q   S   H   N   R   K   Q   M   L   E   Q   T   S   L   V   G   R   S   E   L   Q   N   L   S   G   Q

631/211                      661/221                      691/231
|                            |                            |
TTG CAT CGC GCC AAT GAC AGT CTC TGT GCT AAA GAA GAG GAA CTG GAG ACT CTG AAA ATT CAG CTG CGG TGT GCT GTT GAA GGG CAG AAG
L   H   R   A   N   D   S   L   C   A   K   E   E   E   L   E   T   L   K   I   Q   L   R   C   A   V   E   G   Q   K

721/241                      751/251                      781/261
|                            |                            |
CGG GCA GAA CAC GAA ACG GAG CTC TCA AAG CAA GCT GTT CAG GCA CTT AAG GAG GAG AAG GCT GAG CTA AGG GCC ACT TTG CAA GCT CAC
R   A   E   H   E   T   E   L   S   K   Q   A   V   Q   A   L   K   E   E   K   A   E   L   R   A   T   L   Q   A   H

811/271                      841/281                      871/291
|                            |                            |
ACA GAA TTT CTA CAG GGC TCC AGA GTA CAG AAA CAT GAG CTT CTG CCA GAA GGG TAC AGG GGG AGT GAG GTC CTA AGA GAA AAC AAC AGC
T   E   F   L   Q   G   S   R   V   Q   K   H   E   L   L   P   E   G   Y   R   G   S   E   V   L   R   E   N   N   S

901/301                      931/311                      961/321
|                            |                            |
ATC AGG TCT GTG GAG GAG CGA TTA CAG GAG ATG GGG CAA GTA GGA GGC GAG ACT GAA GTG GAG GCT ATA AGG TCT AAG CTG TCT GTC AGT
I   R   S   V   E   E   R   L   Q   E   M   G   Q   V   G   G   E   T   E   V   E   A   I   R   S   K   L   S   V   S

991/331                      1021/341                     1051/351
|                            |                            |
CGT ATG AAT GAA CAC AGG CTA CAG GCT GAG GTG ACC TGT TTG GAA GAC AGT GTT GAG TCT GTG ACA TCC CAG TGT CAA CTG CTG GCA AAG
R   M   N   E   H   R   L   Q   A   E   V   T   C   L   E   D   S   V   E   S   V   T   S   Q   C   Q   L   L   A   K

1081/361                     1111/371                     1141/381
|                            |                            |
GAG CTT AAA GGA AAG GAG GAA TAT TTC CAT GGG GTT AAA GAG GAC CAT CAA AAA TGC TTG TCT GAA AAT AAA AAG CTG AAA GGC CAG CTC
E   L   K   G   K   E   E   Y   F   H   G   V   K   E   D   H   Q   K   C   L   S   E   N   K   K   L   K   G   Q   L

1171/391                     1201/401                     1231/411
|                            |                            |
TCA CAG GCT GAG CTG ACC CAC AAG AGC GTG CTG GAT GGG ATG AGG AAG GAG ATC TCA CAG CTC ACT CAG GAG TTA CAC CAG AGA GAT ATC
S   Q   A   E   L   T   H   K   S   V   L   D   G   M   R   K   E   I   S   Q   L   T   Q   E   L   H   Q   R   D   I

1261/421                     1291/431                     1321/441
|                            |                            |
AGA ATG GCT TCC AGT GCA GGC ATC GAC TGG GAG AGG AAA ATT AAA GCC GAA CGG CAG AGG GCA GAG AGA GAG GCT GCA GAA CAC AGG ATG
R   M   A   S   S   A   G   I   D   W   E   R   K   I   K   A   E   R   Q   R   A   E   R   E   A   A   E   H   R   M

1351/451                     1381/461                     1411/471
|                            |                            |
TCT CTA AAT GCT CTG GAA AAC TTG AGG CAG GAG AAT TGC CGG TTA TCG GAA CTC CTT CAG ACG CAA GAG CCG GAT GTG GCG CAG GCA CTG
S   L   N   A   L   E   N   L   R   Q   E   N   C   R   L   S   E   L   L   Q   T   Q   E   P   D   V   A   Q   A   L

1441/481                     1471/491                     1501/501
|                            |                            |
GTT AAT TTG GAG CAG GCA AAT CAG AGG CTG CAG AGG GAG CTG CTA CAG ACA CAG GAG AAA CTG GAG CTG ATA GCG CAG AGA GGG GAG TCT
V   N   L   E   Q   A   N   Q   R   L   Q   R   E   L   L   Q   T   Q   E   K   L   E   L   I   A   Q   R   R   E   S

1531/511                     1561/521                     1591/531
|                            |                            |
GAA ATC CAG AAT GCA GTG GAT AGT ATA TCT CAA GAG CTG TTG AAT AAA CAG GAG CAG GAG CTG AGA ATA ATG CAG GAG AGG CTG AAG GTT
E   I   Q   N   A   V   D   S   I   S   Q   E   L   L   N   K   Q   E   Q   E   L   R   I   M   Q   E   R   L   K   V

1621/541                     1651/551                     1681/561
|                            |                            |
TAT GAG CAG GAG ATG CAG ACT TTT AGG TCC CAA CAA GAT GCA GCT TCA AGT GGA AGC TCA CTG GAG TCT ATA TTC TCT GAG GTT TGG AAA
Y   E   Q   E   M   Q   T   F   R   S   Q   Q   D   A   A   S   S   G   S   S   L   E   S   I   F   S   E   V   W   K

1711/571                     1741/581                     1771/591
|                            |                            |
GAA CAA GCT ACG GGT TCA CCA ATA TCT GCA GCA AGC GTG GAT TCC GCT ATT GAG CCA GTG GAG GAC CTT GCC TCT TCT CTG CCC GTT CCA
E   Q   A   T   G   S   P   I   S   A   A   S   V   D   S   A   I   E   P   V   E   D   L   A   S   S   L   P   V   P

1801/601                     1831/611                     1861/621
|                            |                            |
CCC ACC TCC CCA GCA AAT GCC GTA GCC TCA CGC TTC CTC CAG GAA GAG GAG CAG CGA TCA CAT GAA CTT TTG CAG CGA CTG AAT GCT CAC
P   T   S   P   A   N   A   V   A   S   R   F   L   Q   E   E   E   Q   R   S   H   E   L   L   Q   R   L   N   A   H

1891/631                     1921/641                     1951/651
|                            |                            |
ATA GAA GAG CTG AAG CAG GAA AGT CAG CGC ACC GTC GAG CAT TTC ACC CAA GCC AGG TAA CTC AGA GCA GGA CTT CAC AAC GAG CCC CAC
I   E   E   L   K   Q   E   S   Q   R   T   V   E   H   F   T   Q   A   R   *   L   R   A   G   L   H   N   E   P   H

1981/661                     2011/671                     2041/681
|                            |                            |
TTA GGA TGG TGG TGA ATT TCA CTG ATG TTA TAG CAA AGA TGT GAC TGT TGG ATA TTT CTT CCA CAT TCC TCT TAA TAA AAT TTC TCC AAG
L   G   W   W   *   I   S   L   M   L   *   Q   R   C   D   C   W   I   F   L   P   H   S   S   *   *   N   F   S   K

2071/691                     2101/701
|                            |
CTA CCT CTA AAT GTT GCA GTG CTG CCA AAG AAG AAA TGT TCT GCA CAT TT
L   P   L   N   V   A   V   L   P   K   K   K   C   S   A   H
```

Appendix 2: **XCEP63 reprentation of structure showning N-terminal SMC domain in yellow**